# The impact of *Candida albicans* phenotype on the oral microbiome

by

**Mark Craig Butcher**

Submitted in fulfilment of requirements for the

Degree of Doctor of Philosophy

School of Medicine, Dentistry and Nursing

College of Medical, Veterinary and Life Sciences

University of Glasgow

January 2025

# Abstract

*Candida albicans* is a prolific opportunistic pathogen and resides within the mucosa-associated microbiome in the human body. The presence of *Candida albicans* has commonly been reported as a potential indicator or risk factor in the development of caries in children and adults. Typically commensal in nature, it has also been well established that the development of pathogenicity in *Candida albicans* is driven by environmental factors which lead to its overabundance or phenotypic switching to a more pathogenic hyphal morphology. While this has been found to aid in adhesion to oral surfaces, both biological and inert, it also provides a substrate and environmental niche for other micro-organisms. In this study, we propose that alteration of *Candida* phenotype directly influences the microbial and cariogenic profile of a fixed model biofilms and complex, undefined biofilms.

Firstly, by employing a meta-analytic approach to examining relevant media related to the oral microbiome to synthesise findings which examine the influence of bacteria within the microbiome and the ability to predict onset or development of caries based on these findings. Following this, *C albicans* isolates with high and low biofilm phenotype were selected for co-aggregation assessment with other organisms of a previously published “caries” biofilm model and profiled based on biomass, metabolism, drug response and response to environmental stimuli such as sucrose. Saliva was pooled from 19 individuals and used as starter biofilm culture for *ex-vivo* experiments *ex-vivo* models were grown on bovine enamel and assessed for shifting microbial profile, acidogenesis and alteration of substrate when exposed to environmental stimuli. Additionally, Complex bacterial biofilms ± *Candida albicans* were formed over 5 days ± fluconazole (FLU) or amphotericin B (AMB), with

biofilms sampled every 24 h for 120 hrs. DNA was extracted with propidium monoazide to amplify live cell DNA. Microbiome analysis was performed using long read Nanopore sequencing.

Analysis of the literature containing 16S rRNA sequencing data relating to caries revealed insights into the collection, curation, and storage of sequencing data which highlighted a lack of standardisation in the field. In addition, though some significance was found between studies, it was determined that more data would be required to be able to reliably use microbiome data as a predictive tool for caries pathology. When screening isolates, *C albicans* was found to buffer pH profile of “caries” organisms in both dual and multi-species formats. Using sucrose as an environmental stimulus of multi-species biofilms resulted in both a shift in microbial distribution and a higher erosion profile in bovine enamel. Additionally, *Candida* was shown to influence the distribution of organism taxonomy in a complex saliva-derived *ex-vivo* model where it was also identified that environmental conditions such as media requirements, substrate development and challenge through oral hygiene regimen or antifungal exposure can also impact the oral microbiome. Overall, *Candida* was shown to provide a key role in the oral *in-vitro* microenvironment, in the context of caries, and in a strain-dependent manner, using *in-vitro* and *ex-vivo* methods. This has implications in both the application of strains of *C. albicans* in fixed models for testing of novel compounds and in applications of personalised healthcare where the ramifications of affecting these core organisms, via antimicrobial interventions, could have further, unexpected effects.

# *Table of Contents*

# List of Tables

# List of Figures

# Acknowledgments

I would like state my overwhelming gratitude to Professor Gordon Ramage, my initial supervisor on this project for his guidance and support throughout my studies at University of Glasgow through my Masters' and PhD projects. His input over these years was invaluable and I cannot understate his contribution in allowing me to make it to this point of my academic career.

I would like to thank Dr. Jason Brown for his continued support as an academic supervisor and as a friend. I would also like to thank Professor Emilie Combet who provided encouragement and support from afar during many phases of this projects' infancy.

My thanks, also, to Dr Christopher Delaney, whose input was integral to the completion of this study. Many aspects of this research would simply not have been possible without his influence and oversight.

I would like to also thank my industrial supervisors at Haleon, including Dave Bradshaw, Jon Pratten, Rob Howlin, and Ricarda Hawkins. Your encouragement and support over the last 4 years was very much appreciated.

A huge thank you to all the members of the Oral Sciences department at University of Glasgow, as well as many staff members at the Glasgow Dental Hospital and School.

Finally, most of all, thank you to my family and friends. This would have been impossible without you.

# Author’s declaration

I declare that the work described within this thesis, unless otherwise stated via acknowledgement or citation, has been carried out by myself, under the supervision of Dr. Jason Brown and Professor Emilie Combet-Aspray, and formerly Professor Gordon Ramage. I declare that, in whole or in part, this thesis has not been submitted for any other degree.

Mark Craig Butcher

# Abbreviations

| | |
|---|---|
| AHL | Lysis Buffer |
| AMB | Amphotericin B |
| AnO2 | Anaerobic |
| ANOVA | Analysis of Variables |
| APL2 | Lysis Buffer |
| ATCC | American Type Culture Collection |
| ATL | Tissue Lysis Buffer |
| AUC | Area Under the Curve |
| AW1 | Wash Buffer 1 |
| AW2 | Wash Buffer 2 |
| BB | Bead Beating |
| BHI | Brain Heart Infusion |
| BR | Broad Range |
| CAMP | Cyclic Adenosine Monophosphate |
| CBA | Columbia Blood Agar |
| CFE | Colony Forming Equivalent |
| CFU | Colony Forming Unit |
| CHD-FA | Carbohydrate-Derived Fulvic Acid |
| CLASI | Combinatorial Labelling and Spectral Imaging |
| CLR | Centred Log Ratio |
| CLRV | Chandra Lekha Ramalingam Veena |
| $CO_2$ | Carbon Dioxide |
| COPD | Chronic Obstructive Pulmonary Disease |
| CT | Cycle Threshold |

| | |
|---|---|
| CTRL | Control |
| CV | Crystal Violet |
| D0-5 | Days 0-5 |
| DE | Germany |
| DMFT | Decayed, Missing and Filled Teeth |
| DMSO | Dimethyl Sulfoxide |
| DNA | Deoxyribonuclease |
| DOI | Digital Object identifier |
| DSMZ | Deutsche Sammlung von Mikroorganismen und Zellkulturen GmbH |
| ECC | Early Childhood Caries |
| EDTA | Ethylenediaminetetraacetic acid |
| EFG1 | Enhanced Filamentous Growth Protein 1 |
| ENA | European Nucleotide Archive |
| EPS | Exopolymeric Substances |
| EtOH | Ethanol |
| FAA | Fastidious Anaerobic Agar |
| FFPE | Formalin-Fixed Paraffin Embedded |
| FISH | Fluorescent *In-Situ* Hybridization |
| FLU | Fluconazole |
| GSK | GlaxoSmithKline |
| HA | Hydroxyapatite |
| HAC | High-Accuracy Basecalling |
| HBF | High Biofilm Former |
| HCL | Hydrochloric Acid |
| HIV | Human Immunodeficiency Virus |

| | |
|---|---|
| HK | Knoop Hardness |
| HMDS | Hexamethyldisilizane |
| HMR | High Metabolic Rate |
| HOMD | Human Oral Microbiome Database |
| IBF | Intermediate Biofilm Former |
| ICU | Intensive Care Unit |
| ID | Identification |
| IL | Interleukin |
| IMR | Intermediate Metabolic Rate |
| IRG | Intermediate Rate of Growth |
| ITS | Internal Transcribed Spacer |
| KO | Kegg Orthology |
| LBF | Low Biofilm Former |
| LED | Light Emitting Diode |
| LMR | Low Metabolic Rate |
| LRG | Low Rate of Growth |
| MA | Microbiome Analyst |
| MAPK | Mitogen Active Protein Kinase |
| MCP-1 | Monocyte Chemoattractant Protein 1 |
| MIC | Minimum Inhibitory Concentration |
| MP | Masterpure® Complete DNA and RNA kit |
| MP-Y | Masterpure® Yeast DNA Extraction kit |
| MPC | Milk Protein Concentrate |
| MRS | DeMan, Rogosa, and Sharpe Media |
| MS | Mass Spectrometry |

| | |
|---|---|
| MTT | (3-(4,5-dimethylthiazol-2-yl)-2,5-diphenyltetrazolium bromide) |
| NA | Not Applicable |
| NaCl | Sodium Chloride |
| NC | Negative Control |
| NCBI | National Centre for Biotechnology Information |
| NCTC | National Collection of Type Cultures |
| ND | Not Disclosed |
| NEB | New England Bioscience |
| NGS | Next Generation Sequencing |
| NHS | National Health Service |
| NICU | Neonatal Intensive Care Unit |
| NMR | Nuclear Magnetic Resonance |
| NRG1 | Neuregulin 1 |
| OD | optical density |
| OMICs | Analysis of DNA, RNA, Proteins and Metabolites |
| OOR | Out of Range |
| OTUs | Operational Taxonomic Units |
| PBS | Phosphate Buffered Saline |
| PC | Positive Control |
| PCoA | Principal Coordinates Analysis |
| PCR | Polymerase Chain Reaction |
| PhiLR | Phylogenetic Isometric Log Ratio Transformation |
| PLI | Purelink™ Microbiome DNA Purification Kit |
| PMA | Propidium Monoazide |
| PMMA | Poly-Methyl Methacrylate |

| | |
|---|---|
| PMN | Polymorphonuclear |
| PVC | PolyVinyl Chloride |
| QIA | Qiagen DNEasy® Blood & Tissue Kit |
| QMB | QIAamp® DNA Microbiome Kit |
| qPCR | Quantitative polymerase chain reaction |
| RCT | Randomised Control Trial |
| ROC | Receiver operator curves |
| RPMI | Roswell Parks Memorial Institute |
| rRNA | Ribosomal Ribonucleic Acid |
| RT | Real-Time |
| SAB | Sabouraud's Dextrose Agar |
| SAL | Saliva Only |
| SAL_DNA | Saliva pool DNA |
| SCH | Schaedler's media |
| SDH | Social Determinants of Health |
| SEM | Scanning Electron Micrography |
| SLS | Scientific Laboratory Supplies |
| SMDI | Subgingival Microbial Dysbiosis Index |
| STORMS | Strengthening the Organization and Reporting of Microbiome Studies |
| T0-T5 | Timepoint 0-5 |
| TE | DNA Elution Buffer |
| THB | Todd Hewitt Broth |
| TLR | Toll-Like Receptor |
| TNF | Tumour Necrosis Factor |
| Tris | Tris(hydroxymethyl)aminomethane |

| | |
|---|---|
| TSB | Tryptone Soy Broth |
| UK | United Kingdom |
| USA | United States of America |
| UV | UltraViolet |
| WHO | World Health Organisation |
| XTT | (2,3-bis(2-methoxy-4-nitro-5-sulfo-phenyl)-2H-tetrazolium-5-carboxanilide) |
| YLDs | Years Lived with Disability |
| YPD | Yeast Peptone Dextrose |

# 1 Introduction

## List of Publications

This introduction section contains material written by the author adapted from the following published material:

Redfern, J., L. Tosheva, S. Malic, **M. Butcher**, G. Ramage, and J. Verran. 2022. 'The denture microbiome in health and disease: an exploration of a unique community', *Lett Appl Microbiol*, 75: 195-209.

Brown, J. L., W. Johnston, C. Delaney, B. Short, **M. C. Butcher**, T. Young, J. Butcher, M. Riggio, S. Culshaw, and G. Ramage. 2019. 'Polymicrobial oral biofilm models: simplifying the complex', *J Med Microbiol*, 68: 1573-84.

Ramage, Gordon, Bryn Short, Emily McKloud, Om Alkhir Alshanta, **Mark Butcher**, William McLean, and Jason L. Brown. 2022. 'Clinical Management of Fungal Biofilm Infections.' in Katharina Richter and Kasper Nørskov Kragh (eds.), *Antibiofilm Strategies: Current and Future Applications to Prevent, Control and Eradicate Biofilms* (Springer International Publishing: Cham).

## 1.1 Introduction

Clinically, *Candida* biofilms are an increasingly significant problem. These provide a safe sanctuary and act as reservoirs for persistent sources of infections. It is clear that yeast biofilms adversely impact the health of an increasing number of immunocompromised patients, with soaring economic impact. Among the pathogenic yeasts, *C. albicans*, a normal commensal of human mucosal surfaces and opportunistic pathogen in immunocompromised patients, is most frequently associated with biofilm formation (Douglas, 2003, Ramage et al., 2006). A range of biological and inert substrates can become colonized, either endogenously or exogenously, which develop into adherent biofilm structures from which cells can then detach and cause a range of pathologies. Implant-associated infections are inherently difficult to resolve and often result in the implant having to be physically removed from the patient and long-term antifungal therapy administered to control the infection. Depending on where this occurs in the body, can have significant consequences for the patient.

### *1.1.1 What are biofilms?*

Most microbiology investigations have traditionally focused upon free living (planktonic) cells in pure culture, resulting in the common perception that microorganisms are unicellular life forms. Nevertheless, Costerton and colleagues (1981) were among the first to link the surface attached growth state to microbial pathogenesis and human infection (Costerton et al., 1981). Extensive research has now revealed that a wide range of bacteria and fungi alternate between planktonic and surface attached multicellular communities, a growth modality that is commonly referred to as a biofilm. Within their natural ecosystems most microbes have been

shown to exist as attached communities of cells within an organized biofilm and not as planktonic organisms. In fact, it is estimated that up to 80% of all bacteria in the environment exist in sessile biofilm communities and over 65% of human microbial infections involve biofilms (Donlan, 2002, Penesyan et al., 2021). Biofilms are by definition highly structured, communities of microorganisms that are surface-associated, and/or attached to one another, enclosed within a self-produced protective extracellular matrix (Costerton et al., 1995). These can form in the natural environment as well as inside the human host, and can be considered as complex cities of microbes that cooperatively interact in an altruistic manner (Azevedo et al., 2021). The advantages to an organism of forming a biofilm include protection from the environment, resistance to physical and chemical removal of cells, metabolic cooperation and a community based regulation of gene expression (Jabra-Rizk et al., 2004, Mah and O'Toole, 2001, Uruén et al., 2020). In recent years there has been an increased appreciation of the role that microbial biofilms play in human medicine, particularly because microbes growing within biofilms (sessile cells) exhibit unique phenotypic characteristics compared to their planktonic counterpart cells, including increased resistance to antimicrobial agents and protection from host response (Dodson et al., 2022). Therefore, they pose a major problem to clinicians as the dose required to eradicate the biofilm can exceed the highest therapeutically attainable concentrations (Rasmussen and Givskov, 2006, Sharma et al., 2019). Figure 1-1, below, illustrates the variety of biofilm infections that are observed clinically *in-vivo* and the differing size and complexity of surface associated and aggregate phenotypes (Rumbaugh and Bjarnsholt, 2023). Moreover, the costs associated with biofilm infections are staggering in the health sector, between medical and oral health

accounting for over $430 billion, as outlined in Table 1-1 (Cámara et al., 2022). Some of the clinical and biological characteristics of yeast biofilms will now be addressed.

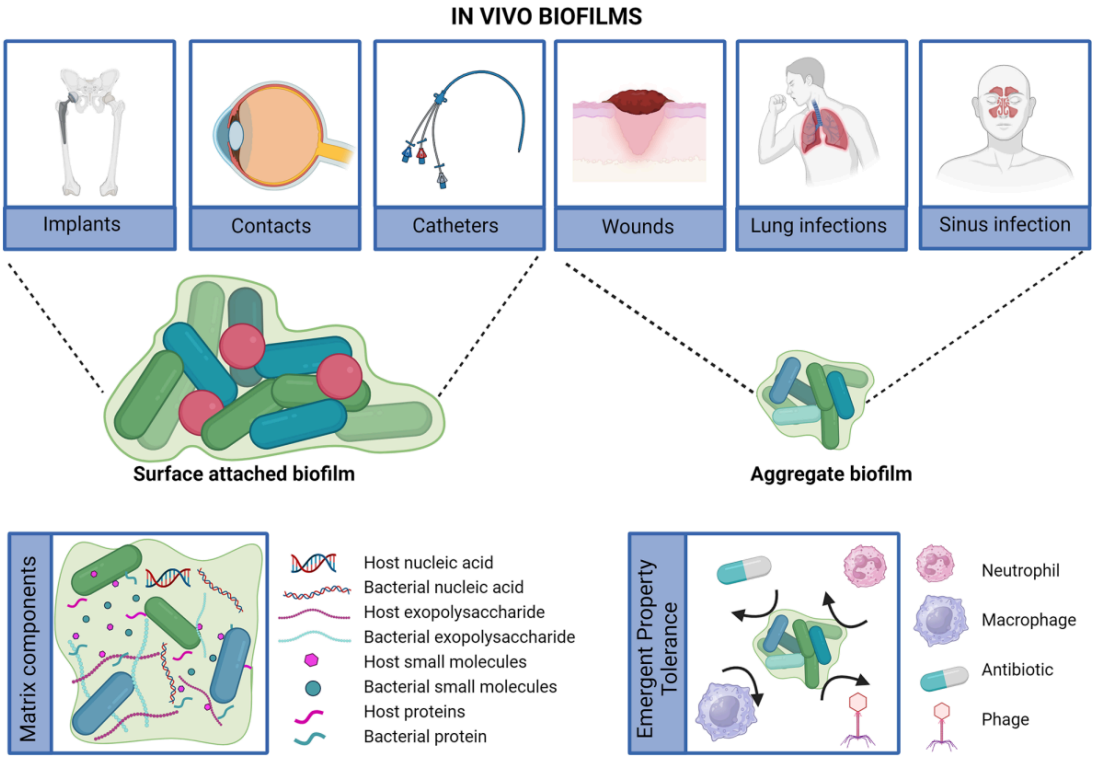


**Figure 1-1 - Biofilm development *in-vivo*.** Biofilms commonly display as surface-attached communities on contact points or as suspended aggregates which have grown or disseminated through tissue surfaces. In comparison to *in-vitro* biofilms, key extracellular components are derived from the host environment. These factors often drive key functionality related to antimicrobial tolerance. Adapted from (Rumbaugh and Bjarnsholt, 2023)

| Sector | Global ($bn) | Comment |
|---|---|---|
| **Medical and human health** | | |
| Wound healing | 281 | Biofilms form on wound surface and delay healing. |
| Cystic fibrosis | 7.5 | Mucus produced in the lungs of CF patients is colonised by pathogens. |
| Infective endocarditis | 16 | Biofilms in natural and artificial heart valves result in serious cardiac disease. |
| Chronic sinusitis | 24.4 | Often associated with secondary biofilm infections which are difficult to clear. |
| Ophthalmology | 0.759 | Surfaces in the eye are prone to biofilm infection. |
| Human antibiotics | 34.2 | Bacterial infections are often linked to biofilms and widely treated with antibiotics. |
| Central venous catheter bloodstream infection | 11.5 | Biofilms colonise catheters and can cause infection. |
| Catheter-associated urinary tract infection | 1 | Biofilms colonise catheters and can cause infection. |
| Prosthetic cardiac valves and pacemakers | 0.22 | Surfaces of surgically implanted devices may host biofilms and can only be treated by surgery. |
| Ventilator-associated pneumonia | 2.3 | Endotracheal tubes are prone to biofilm infections |
| Breast implants | 0.093 | Surfaces of breast implants can become infected with biofilms |
| Prosthetic joints | 7.8 | Surfaces of surgically implanted devices may host biofilms and can only be treated by surgery. |
| *Total medical and human health* | *386.8* | |
| **Personal care** | | |
| *Total personal care* | *91* | Personal care products control biofilms on skin and hair |
| **Oral care** | | |
| Human oral care | 47 | Tooth scale is a form of biofilm and central to oral health |
| Animal oral care | 1.85 | Increasing awareness of animal oral health |
| *Total oral care* | *48.9* | |

**Table 1-1 - Quantification of market sectors engaging with biofilm technologies - Summary of economic information. Table adapted from (Cámara et al., 2022)**

## 1.2 *Candida* biofilms

The importance of fungi in human health is a significant issue, so much so that their impact has now been fully recognised by the World Health Organisation (WHO) within their relatively recent publication of priority fungal pathogens (Fisher and Denning, 2023). Despite the lack of definitive data to demonstrate the burden of disease, some have estimated that over 1 billion people are affected by fungal disease, which in turns kills 1.5 million annually (Bongomin et al., 2017). Amongst these pathogens is *Candida albicans* that has been identified within the critical priority group. Indeed, tens of millions are affected by mucosal candidiasis, and an estimated further 750,000 people with systemic candidiasis, of which the latter has mortality rates of around 50% (Bongomin et al., 2017). These statistics highlight the critical importance that candidiasis has in human disease.Notably, one of the key contributing factors to this burden of health is the ability of *Candida* species to form an aggregative biofilm phenotype upon mucosal and hard surfaces, intimately attached to indwelling biomedical implants or as aggregates surrounding adjacent tissue to biomaterials (Ramage et al., 2006). Figure 1-2 illustrates the array of biofilm-mediated diseases associated with *Candida* biofilms. Biofilms may be present as mono-species consortia of yeast and hyphal cells embedded within polymeric matrix (Nett and Andes, 2020), but also as aggregates (or floccules) of cells (Sauer et al., 2022). More frequently they are co-associated with bacteria as interkingdom populations. Irrespective of their constituent parts, they are notably recalcitrant to antifungal agents, and this tolerance makes them a significant clinical issue (Ramage et al., 2022). This chapter aims to provide a detailed insight into the strides made in increasing our understanding of *Candida* within simple and complex biofilm consortia.

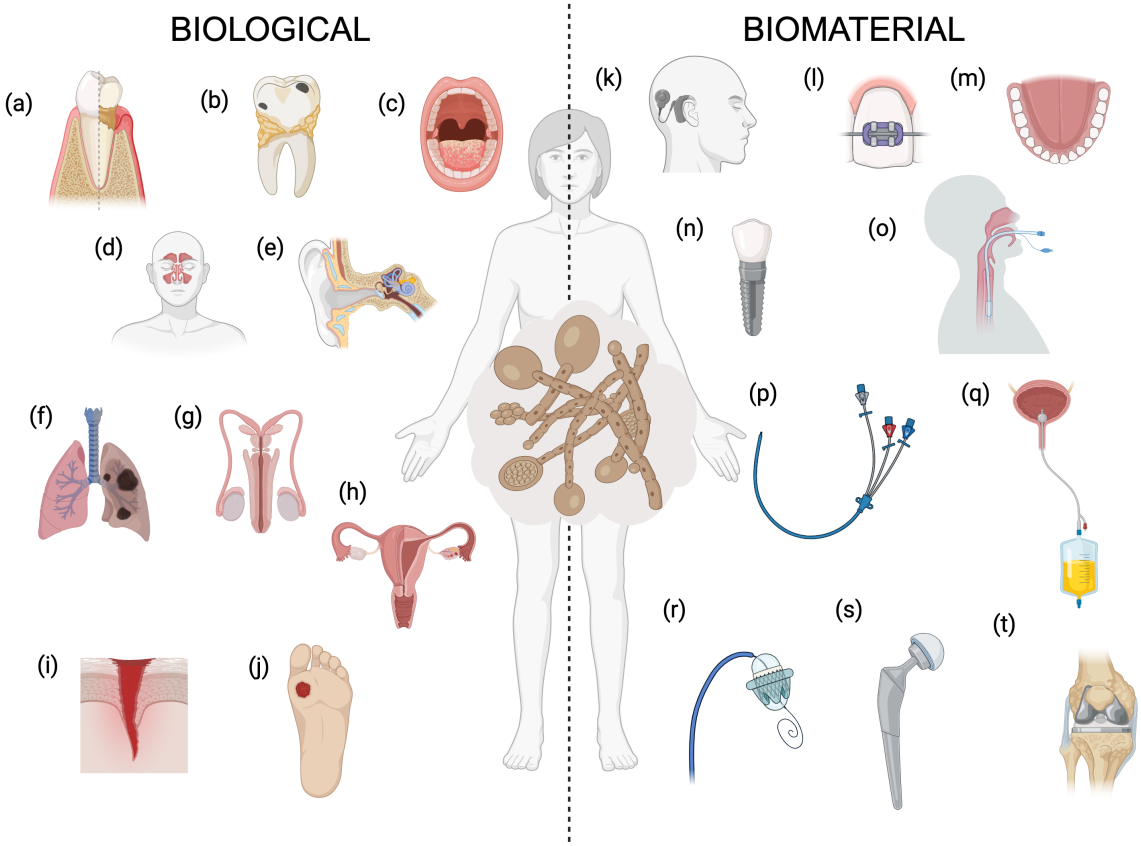


**Figure 1-2 - Overview of the different anatomical sites for Candida biofilm related infection associated with biological and artificial surfaces.** Biofilms form on both biological substrates including (a) gingival crevice [periodontitis], (b) enamel [caries], (c) oral mucosa and palate [oral candidosis], (d) sinuses [chronic rhinosinusitis], (e) auditory canal [otitis media], (f) respiratory tract [CF and COPD], (g) male genitourinary tract [prostatitis], (h) female genitourinary tract [vaginosis] (i) open wound [surgical site infection and trauma] (j) non-healing wound [diabetic foot ulcer] (k) cochlear implant [otitis externa] (l) orthodontic appliance [caries/gingivitis] (m) dentures [denture stomatitis/caries] (n) dental implant (implantitis] (o) endotracheal tube [pneumonia] (p) central venous catheter [septicaemia] (q) urinary catheter [bladder and renal infection] (r) heart valves [endocarditis] (s) hip prosthesis [implant failure/wound infection] (t) knee prosthesis [implant failure/wound infection]. Created with BioRender®.

### *1.2.1 Candida biofilm risk groups*

The mucosal barriers of the oral cavity, oropharynx, respiratory, gastrointestinal, and genitourinary tracts are all potential sites for the genus *Candida* to reside, colonise and potentially initiate pathogenesis. Alongside an exhaustive list of 'who's who' amongst the human microbiome (Manos, 2022), *Candida* species have the capacity to either co-aggregate, co-exist or be antagonised by bacteria in both yeast and hyphal forms. Notably, *Candida spp.* appear to preferentially interact as innocent bystanders in these relationships (Delaney et al., 2018).

Those at greatest risk from these infections are those with weakened immunity or those with underlying health issues (Richardson and Lass-Flörl, 2008). This includes chronic lung disease, HIV, cancer, diabetes, and many other serious diseases. Those critically ill patients in the ICU, those undergoing invasive procedures and those receiving immunosuppressants or broad-spectrum antibiotics are all high-risk groups. Patients within these groups will inevitably continue to expand, especially as the world population grows past 8 billion inhabitants in 2022. Patients undergoing treatment for cancer, including immunotherapy and chemotherapy, a patient population that continues to advance at pace and will undoubtedly lead to more within these risk groups. The consequence of this was laid bare during the COVID-19 pandemic, and the necessity to use immunotherapies and a range of supportive measures that result in co-morbid invasive fungal disease in this patient group (van Charante et al., 2022). The critical care environment coupled with severely ill patients provided the perfect storm for biofilm-related disease.

Biofilm-related infection plays an additional role in patients with any form of biomaterial, e.g. prosthetic heart valve, total hip arthroplasty, knee joint, presence of

an indwelling venous or urinary catheter, artificial lens, cochlear implants, etc (Ramage et al., 2006). Moreover, the risk of biofilm-related infection is increased in patients with wound-related trauma, which may be disease related (e.g. diabetic ulcers), or in the form of burns or trauma (Kalan and Grice, 2018). Biofilms can also exist outwith the patient, adhering to fomites and medical equipment around the clinical environment (Alfa, 2019). Collectively, this paints a particularly gloomy outlook for an ageing population who will increasingly rely on these medical interventions and be exposed to challenges brought about by innovative immunotherapies. Whilst the relative risks of biofilm-related infection remain stable, the increasing population profile means more and more patients will be exposed to these hard-to-treat infections. With a limited arsenal of antifungal agents available for clinical use, the successful management of these patients is challenging.

### *1.2.2 Candida biofilm developmental characteristics.*

The colonization of complex, adherent yeast populations on biological and innate surfaces, such as the oral mucosa or denture material substrates is commonplace for clinically relevant yeasts (Lemberg et al., 2022). Analogous to bacterial biofilms, yeast biofilms have defined developmental phases. Various groups have worked to develop suitable and robust models of yeast biofilm development (Gulati and Nobile, 2016, Nett and Andes, 2006). Although slight variations exist within individual models, such as the substrate, incubation time and growth media, the overall premise remains universal. These key stages include arrival at an appropriate substratum, adhesion, colonisation, polysaccharide production, biofilm maturation and dispersal (McCall et al., 2019). These phases of biofilm formation of *C. albicans* are illustrated in Figure 1-3, below. A wide variety of environmental factors contribute to the initial surface attachment of a microbe. These include the flow velocity of the surrounding medium

(urine, blood, saliva), pH, temperature, presence of antimicrobial agents, and presence of extracellular polymeric substances (Cavalheiro and Teixeira, 2018).

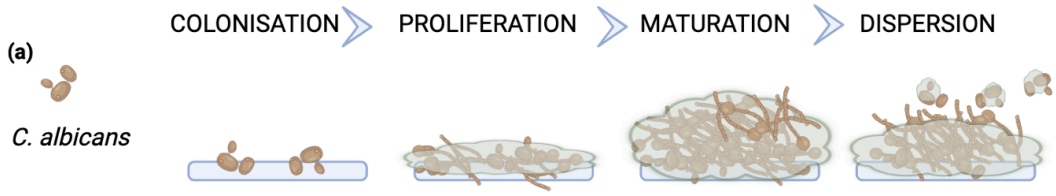


**Figure 1-3 - Schematic representation of the key phases of *Candida albicans* biofilm formation.** Colonisation – *C. albicans* cells **(a)** adhere to a surface and form a basal layer. Proliferation – cells multiply and form germ tubes. Maturation – germ tubes develop to hyphae and cells produce an extracellular matrix. Maturation – Cells disperse from the biofilm to continue the cycle elsewhere. Image created in Biorender®.

The most well-defined eukaryotic organism with regard to biofilm formation is the yeast *C. albicans.* Endogenous or exogenous *C. albicans* cells must firstly colonize a suitable substrate and quickly adhere to its surface. This initial attachment phase is mediated by both non-specific factors, including hydrophobicity of the cell surface and electrostatic forces as well as by specific adhesins on the surface of *C. albicans* that bind to ligands on the conditioning film (fibrinogen and fibronectin) (Talapko et al., 2021, Ponde et al., 2021). *Candida* species can also directly attach to one another or to bacterial organisms that have already colonized the biomaterial (Morales and Hogan, 2010, Gerós-Mesquita et al., 2020). After the initial attachment phase, growth ensues and microcolonies are formed, *C. albicans* then begins to multiply by budding, a filamentous scaffolding is produced and the initial deposition of extracellular matrix material occurs and subsequent biofilm development follows (Gulati and Nobile, 2016). Filamentous growth, although not strictly essential for biofilm formation *per se*, strengthens the entire structure and provides protection and adhesion sites for the budding yeast cells (Ramage et al., 2005). Microscopical analysis has demonstrated that *C. albicans* biofilm formation could be separated into three distinct developmental phases: Early (0 to 11 hours), intermediate (12 to 30 hours) and maturation (38 to 72 hours) (Gulati and Nobile, 2016). Following initial adhesion by blastospores, microcolonies of budding yeast are detected in the 3$^{rd}$ and 4$^{th}$ hour, with pseudo-hyphae and true hyphae being present at four hours and eight hours, respectively (Mukaremera et al., 2017). Microcolonies are later conjoined by hyphal extensions, leading towards a confluent monolayer (intermediate phase). This phase is made distinct by the development of an opaque film covering the fungal microcolonies made of predominantly non-cellular material. The cloudy appearance is due to the extracellular material, composed of predominantly cell-wall-like polysaccharides

(Cavalheiro and Teixeira, 2018). Yeast cells make up the basal layer, while filamentous cells compose the structural framework (Desai and Mitchell, 2015). In the maturation phase the quantity of this extracellular material increases in a time dependant manner until the microbial communities are entirely enclosed to form a mature biofilm (Gulati and Nobile, 2016). It has been shown that the exopolymeric substance (EPS) consists of proteins, chitins, DNA and β-1,3 glucan carbohydrates (Gientka et al., 2016). It covers the biofilm, and it is thought to act as a protective barrier by preventing penetration of host immune factors, antifungals, and impeding physical disruption of underlying cells.

Confocal laser scanning microscopy has shown mature *C. albicans* biofilms to be complex 3-D structures that can range from anything between 50 to 350 μm thick, depending on the model (Ramage et al., 2001b, Lanni et al., 2020, Lagree et al., 2018). Images obtained from scanning electron microscopy (SEM) have shown a mature *C. albicans* biofilms consist of yeasts, pseudo-hyphal forms and true hyphae. *C. glabrata* biofilms tend to be sparse and consist of clumps, whereas *C. albicans* biofilms are dense and heterogeneous, characterized by different morphological forms. *C. glabrata* appears to use *C. albicans* as a scaffold to maintain biofilm integrity (Staniszewska et al., 2013). Overall, it is proposed that the architecture of biofilms is highly ordered to enable the perfusion of nutrients and expulsion of waste products. Mature biofilms exhibit spatial heterogeneity with microcolonies and water channels being present. These features are common to both bacterial and fungal biofilms (Evans et al., 2023, Quan et al., 2022, Wang et al., 2024). This complexity is governed by defined genetic pathways.

The shift to a biofilm mode of growth is a complex, highly orchestrated and intricately regulated process at the molecular level, with many signalling processes that drive biofilm growth in pathogenic fungi. This has been an area of intense investigation for approximately two decades now, with the majority of studies on *C. albicans*, the archetypical biofilm-forming fungus. Initial studies highlighted the importance of morphogenetic transitions, adhesive interactions, and quorum sensing in the development of *C. albicans* biofilms (Nobile and Mitchell, 2006, Karine Marcomini and Negri, 2023). The MAP kinase Mkc1 is activated by contact with a number of surfaces and may represent a key regulator during the initial adherence phase (Correia et al., 2019). Pioneering research by the Mitchell group began to unravel the roles of individual genes and proteins in biofilm formation and maintenance, identifying key transcription factors and adhesins involved in the process. For instance, *C. albicans* mutants lacking the transcription factors Efg1 and Tec1 fail to form biofilms due to their inability to undergo filamentation (Araújo et al., 2022, Panariello et al., 2017). Bcr1 has also been identified as a crucial regulator of biofilm formation, as it controls the expression of several hyphal adhesins, including the complementary Als3 and Hwp1, which provide structural cohesion to the biofilm (McCall et al., 2019). Simultaneously, various research groups employed transcriptomic techniques to compare global gene expression patterns in *C. albicans* biofilms and their planktonic counterparts, underscoring the role of metabolism in biofilm growth. Landmark studies by Nobile and colleagues identified a core network of nine interwoven transcriptional regulators—Bcr1, Brg1, Efg1, Ndt80, Rob1, Tec1, Flo8, Gal4, and Rfx2—essential for normal biofilm formation (Nobile et al., 2012, Fox et al., 2015). These regulators collectively control the expression of approximately one thousand genes, representing about 15% of the *C. albicans* genome.

### *1.2.3 Pathogenesis of Candida biofilms*

The high density of cells present within a biofilm represents a challenge to the host through direct and indirect interaction of the sessile cells and associated products, which ultimately lead to inflammation and pathology. Certain individuals suffer from denture stomatitis because the denture provides a reservoir for the heterogeneous yeast biofilm, which subsequently induces inflammation of the oral mucosa. It has been shown that both *Candida* biofilm diversity and quantity can contribute to high level inflammation (Li et al., 2022). Limited information is available on the role of the host immune response in relation to biofilm formation. However, it was shown that the epithelial surfaces can be protected from the development of mucosal infections through a TLR4-mediated protective mechanism, which is PMN-dependent (Naglik et al., 2011). One of the few papers to directly investigate biofilm immunology in any detail reported that upon exposure to *C. albicans* biofilms adherent human peripheral blood mononuclear cells secreted significant amounts of IL-1β, IL-10 and MCP-1 compared to planktonic yeast cells (Bhardwaj et al., 2020, Cangui-Panchi et al., 2023). Biofilm matrices are thought to play a key role in protecting microbial biofilms from host immune responses. For example, increased phagocytosis and killing of staphylococcal biofilms has been reported for knock-out strains missing polysaccharide intercellular adhesion, which is a main constituent of staphylococcal biofilms (Kuipers et al., 2016). Antibodies are also thought to fail to penetrate biofilms due to the coating of biofilms by matrix material.

### *1.2.4 Candida biofilm model systems*

Historically, a wide range of biofilm model systems have been developed to study yeasts *in-vitro*. Many factors affect *in-vitro* yeast biofilm formation, including strain,

species and substrate specificity, and the role of conditioning film and bacterial competitors (Adam et al., 2002, Ramage et al., 2001b, Thein et al., 2006). However, the primary function of many of these models is to investigate biofilm developmental properties and their susceptibility to antimicrobial agents.

An early fungal biofilm model involved adherent populations of *Candida sp*. developing on catheter discs (Hawser and Douglas, 1994). Static biofilm growth was quantified using dry weight measurements, tetrazolium salt (MTT) reduction assays and incorporation of [$^{3}$H] leucine, of which the latter two methods showed excellent correlation to the dry weight of the biofilm. Six different species of *Candida* were investigated for their ability to form biofilms. *C. albicans* showed superior biofilm formation compared to *C. parapsilosis* and *C. glabrata* on catheter material. Latex material produced the best biofilm, followed by PVC and polyurethane. Biofilm formation on silicone was found to be more variable, with the surface topography and hydrophobicity differing between the two types of catheter discs (Hawser and Douglas, 1994). A biofilm model for *C. albicans* has been reported using polymethyl-methacrylate strips (Chandra et al., 2001a), where total biofilm biomass (dry weight) and the metabolic activity of cells (XTT reduction assay) of *C. albicans* cells were determined using this model system. The authors found that inoculum size, adherence time, incubation time, and exposure to carbohydrate (especially glucose) and saliva all influenced biofilm development of *C. albicans* within this model system. In this denture biofilm model *C. albicans* was found to be significantly more resistant to a range of antifungals compared to planktonic cells (Chandra et al., 2001b).

Traditionally, most models for the formation of microbial biofilms are cumbersome, requiring expert handling, longer processing times and the use of specialized

equipment not generally available in a regular microbiology laboratory. Moreover, these complex and technically demanding biofilm models are generally not amenable to high throughput screening since relatively few equivalent biofilms can be produced at the same time. Ramage and colleagues were the first to describe a standardized high throughput 96 well microtiter plate model for the formation of *C. albicans* biofilms (Pierce et al., 2008, Ramage et al., 2001a). This model has now been adopted by a number of other groups to evaluate various experimental parameters of biofilm formation (Ramage et al., 2001a, Thein et al., 2007, Tumbarello et al., 2007). The XTT (2,3-bis(2-methoxy-4-nitro-5-sulfo-phenyl)-2H-tetrazolium-5-carboxanilide) reduction assay is based on initial candidal adhesion and antifungal drug susceptibility studies (Hawser, 1996, Tellier et al., 1992). This methodology was found to be rapid and highly reproducible, and particularly amenable for biofilm susceptibility testing against a range of current antifungal agents (Ramage et al., 2002, Ramage et al., 2001b). This colorimetric assay is non-invasive and non-destructive, requiring minimal post-processing of samples as compared to other alternative methods (such as viable cell counts). Using this technique multiple microtiter plates can be processed simultaneously without compromising accuracy, and is important due to its utility for testing of biofilms which are inherently more resistant to antifungal therapy compared to their free-floating planktonic cell counterparts (Pierce et al., 2008, Ramage and Lopez-Ribot, 2005). Whereas the assay is useful for antifungal testing to evaluate the effects of the drug on a sessile population in comparison to an untreated control, metabolic variability between different isolates makes its usefulness in quantifying biofilm development limited, and, despite its significant impact in the field, caution should therefore be taken when interpreting the data obtained from this metabolic assay (Ramage, 2016).

The presence of flowing liquid over the biofilm can increase the amount of matrix formed compared to statically developed sessile populations (Khu et al., 2023). Therefore, flow systems have been utilized by many researchers to model biofilm development (Tournu and Van Dijck, 2012, McCall and Edgerton, 2017). A 'seed and feed' modified Robin's device has been described, which permits multiple biofilms to be formed under constant flow conditions (Ramage et al., 2008). The production of polymeric material was increased under flow conditions, with the architecture of the resultant biofilms altered with respect to water channels, porosity, topography and thickness compared to biofilms grown statically. Conversely, recent studies have shown that shear flow can reduce the biofilm thickness whilst increasing overall cellular density (Kurz et al., 2022). This highlights the intrinsic variability in biofilm flow systems modelling. For flow systems, although perhaps more representative of certain physiological conditions, limitations to this type of apparatus are evident. These include their poor availability and accessibility to many laboratories, difficulty in implementation, and their limited utility to high throughput screening.

The majority of yeast biofilm research to date is carried out *in-vitro*, but it has proved important to validate laboratory-based models with those formed *in-vivo*, which has revealed structures with equivalent architecture (Vyas et al., 2022, Guzmán-Soto et al., 2021, Nett and D, 2015). With conditions encountered *in situ* distinctive from those *in-vitro* it is practically impossible to reproduce all the environmental permutations experienced by the biofilm, particularly the host-pathogen relationship in relation to the host immune response system (Nett and Andes, 2006). Indeed, two key specific yeast biofilm models have been developed within animal hosts. The first model, described by Schinabeck and coworkers, was developed on central venous catheters within New

Zealand white rabbits for *C. albicans* biofilms to investigate antifungal lock therapy (Schinabeck et al., 2004). Similarly, Andes and coworkers described a central venous catheter biofilm model using rats (Andes et al., 2004). Both groups noted a similar time course of biofilm formation over 24 h and confirmed the presence of a multilayered structure with extracellular matrix using microscopy. These models are critically important, as whether *in-vitro* or *in-vivo* are important for testing and developing new antifungal agents, which are primarily focused on planktonic cells.

### *1.2.5 Antifungal considerations*

The traditional clinical management of oral fungal infections involves the use of topical and systemic antifungals. In oropharyngeal candidiasis, identification and removal of local and systemic predisposing factors is paramount if feasible. Oral candidiasis is usually successfully managed with topical azoles and polyenes in the form of oral suspensions, lozenges, gels, creams and ointment. Nystatin is usually effective for treatment of oral candidiasis. Amphotericin and miconazole can also be used, both of which elicit positive fungicidal effects (Farah et al., 2010). Refractory and recurrent infections usually require the use of systemic antifungals such as ketoconazole, fluconazole and itraconazole and amphotericin in conjunction with topical agents to control the infection (Epstein and Polsky, 1998). Despite treatment with antifungal, recurrence of oral candidiasis is not uncommon (Rautemaa and Ramage, 2011). Recurrent infection can be due to incorrect diagnosis, inability to identify or treat underlying factors or inappropriate drug selection, or simply that the infection is biofilm-based and therefore intrinsically tolerant (Darwazeh and Darwazeh, 2014). Systemic antifungals are mainly used for the treatment of deep mycoses and drug selection depends on the severity of the infection and may require surgical debridement. Amphotericin B, caspofungin, voriconazole, itraconazole, miconazole, ketoconazole

and fluconazole are the most commonly used systemic agents for deep fungal infections (Santosh et al., 2021). Recurrent or refractory infections are not uncommon and usually require the use of systemic antifungals, such as fluconazole, itraconazole, ketoconazole, and AMB in conjunction with topical agents to control the infection (Epstein and Polsky, 1998). Antifungal resistance remains a serious concern with classical azole therapy, so drug combinations may overcome drug resistance. With β-1,3-D-glucan of fungi being an ideal drug target, combining drugs that act on this essential cell wall component will potentially help in resolving antifungal resistance. Oral ibrexafungerp (SCY-078) is a semisynthetic potent β-1,3-D-glucan synthase inhibitor, shown to be effective against *C. albicans*, C. *parapsilosis, C. tropicalis* and *C. auris* (Scorneaux et al., 2017, Wiederhold et al., 2021).

## 1.3 *Candida* biofilms in the oral cavity

Oral fungal infections, or “oral mycoses”, are broadly categorized as candidal and non-candidal fungal infections, or as superficial and deep mycoses (Santosh et al., 2021). Oral candidiasis (candidosis) is the most frequently reported oral fungal infection. This form of superficial mycoses is a result of the overgrowth of *Candida* species; mainly *Candida albicans.* Other non *albicans* species, *Candida parapsilosis, Candida krusei, Candida stellatoidea, Candida tropicalis, Candida glabrata, Candida guilliermondii,* and *Candida dubliniensis* are also contributed to oral candidiasis to a lesser extent. The diagnosis of oral candidiasis is usually based on the cytological/histopathological examinations and clinical presentation of the infection (Rautemaa and Ramage, 2011). As *C. albicans* is a typical commensal of the oral microbiome, in the majority of healthy individuals, oral samples with a positive culture for *Candida* species with absence of clinical manifestation are diagnostically inconclusive.

Candidal infections of the oral cavity are mainly opportunistic in nature, and frequently co-aggregate with microbial species in the form of biofilms on biological and inert substrates, or as aggregates within saliva. Within the oral environment these yeasts coalesce upon mucosal surfaces an give the clinical appearance of thick white plaques. Microscopically, these appear as mixtures of yeasts and hyphae intertwined and covered thoroughly by a glucans matrix, a substance shared by the genus (Dominguez et al., 2018). Moreover, this glue-like material supports architecture and tolerance within an interkingdom biofilm (Kim et al., 2018b). Studies from the Ramage laboratory have shown that *Candida* species play an important role in these biofilms as resilient cells within interkingdom biofilms, but that bacteria occupy the biofilms by up to 2 logs greater than yeasts (Delaney et al., 2019). This has an impact for the consideration for therapeutic control, though it is clear that frequent daily denture cleansing extra-orally is the most effective preventative strategy (Ramage et al., 2019).

Other prevalent oral chronic biofilm diseases in humans are dental caries and periodontal diseases, both of which are considered primarily bacterial driven diseases (Casamassimo et al., 2009, Nazir et al., 2020). However, the role of yeasts within these diseases often overlooked and widely disregarded despite their presence in saliva. Elevated levels of *Candida* species have been detected in children with caries (Raja et al., 2010b), though whether they are directly associated with dental caries remains unconfirmed (Sridhar et al., 2020). Their presence may be indicative of disease rather than directly causality (Fechney et al., 2019a). Similar detection rates have been reported in patients with periodontal diseases, much higher than in healthy patients, and shown to correlate with disease severity (Canabarro et al., 2013, Urzúa et al., 2008, Peters et al., 2017). This is somewhat confirmed in what limited data exists

within a recent systematic review from 21 available studies (Suresh Unniachan et al., 2020). Taken together, and until proved otherwise, it would appear that we observe elevated of *Candida* levels in these biofilm diseases as a consequence of microbial dysbiosis and host derived factors, though we cannot exclude their indirect effects contributing to pathological processes (Delaney et al., 2018). Indeed, we know that key periodontal pathogens are pathogenically primed on encountering *C. albicans* (Sztukowska et al., 2018). It is unclear whether this higher abundance has a direct role in disease causation, or it is simply a consequence of bacterial dysbiosis and environmental change that favours fungal growth. There is a significant growth of studies investigating synergism and antagonism amongst these interkingdom diseases to define the importance of *Candida* in the oral cavity , so the increasing use of newer molecular tools begins to define a clearer idea of the role that fungi play in these seemingly bacterial centric infections. The first ever mycobiome study by Ghannoum (2010) and colleagues reported over 101 separate species from 21 individuals, though whether these fungi play defined roles remains to be ascertained (Ghannoum et al., 2010b).

### *1.3.1 Interkingdom biofilms in the oral cavity*

Our understanding of how dental plaque composition relates to oral health and disease has also changed over time. For example, hypotheses such as the “specific plaque hypothesis” (Loesche, 1976), “non-specific plaque hypothesis” (Theilade, 1986), “ecological plaque hypothesis” (Marsh, 1994) and “keystone pathogen hypothesis” (Hajishengallis et al., 2012) were all developed over the past 50 years. Throughout time, these hypotheses have set the foundations of future oral microbiological research, ultimately contributing to our current understanding of the complex nature behind microbial disease onset and progression in the oral cavity. Approximately 700

bacterial species or phylotypes (Aas et al., 2005) and more than 100 fungal species (Peters et al., 2017) have been identified in the oral cavity. It is estimated that overall species numbers may well exceed 1000, although many of these are uncultivated (Jenkinson, 2011). There is significant diversity in the oral microbiome, varying greatly from person to person. For example, only 100-200 bacterial species are thought to be found in the oral cavity of any given individual (Paster et al., 2006). Despite this diversity, the concept of microbial “complexes” of microorganisms has emerged, which demonstrates a shift in biofilm colonisation from health to disease, such as in the development of periodontal diseases (Socransky et al., 1998, Haffajee et al., 2008). Notably, the presence or contribution of *Candida* species is often ignored in the development of our understanding of oral disease, which has hampered progress in the field. Recently, OMICs approaches (e.g., genomics, transcriptomics, proteomics and metabolomics) have enhanced our understanding of microbial interactions in the oral cavity, and it is now possible to identify all microbial species that colonise our mouths (Jenkinson, 2011, Dewhirst et al., 2010). The OMICs platforms provide the power to investigate complex systems in unprecedented detail, and these have been used to examine biofilms in human diseases and in animal models of disease.

### *1.3.2 The microbiome in dental caries*

Oral caries is considered one of the most common, non-transmissible diseases worldwide (Zhang et al., 2022b). Importantly, despite enhanced understanding and awareness from oral healthcare providers, the prevalence of caries has remained relatively static over the last 25 years (Zhang et al., 2022b). Much of this may be represented by considering caries as a multifactorial disease which can be heavily influenced by socio-economic, environmental, and genetic factors (Menon et al.,

2022). However, the microbial activity which drives the disease cannot be understated. As indicated previously, the capacity for organism attachment and adherence can be heavily influenced by the site of adhesion. Clear differences can be found when considering studies which examine oral microbiome samples from both hard and soft tissue (Siddiqui et al., 2023).

Classically, samples would be derived from carious lesions or samples of dental plaque to identify associated organisms (Martin et al., 2002, Marsh et al., 2016) and identified using classical culture methods. In this way, bacteria such as *Streptococcus mutans*, *Veillonella dispar* and *Lactobacillus* species became commonly associated with dental caries (Tanner et al., 2018, Struzycka, 2014). Alongside these, *Candida albicans* was often identified as having a synergistic or symbiotic relationship with *Streptococcus* species (Sridhar et al., 2020). Given the capacity of these organisms to form robust biofilms, it has been indicated that they can be important in caries initiation (Kim et al., 2017b, Lu et al., 2023). Indeed, systematic reviews, such as those conducted by Xiao et al., in 2018, have indicated that the identification of *Candida albicans* can be associated with a 5-fold increase in the odds of children having or developing early childhood caries (Xiao et al., 2018). Despite these findings, however, the role of *C. albicans* as a pathogen in oral caries is often questioned (Willems et al., 2016). As the accessibility of new techniques for examining and assessing the oral microbiome, such as next generation sequencing, have developed, the role of single organisms in disease development has become much more complex (Radaic and Kapila, 2021). Indeed, the complexity of dysbiosis in oral caries, such as that outlined by Baker et al., in 2021, highlights the role of organisms such as *Prevotella,* and even the presence of the Epstein-Barr virus (EBV) as having an ecological influence on the development of oral caries (Baker et al., 2021). As with other oral pathologies, the role

of the microbiome and the interaction of organisms beyond the bacterial can be crucial in developing our understanding of disease development.

### *1.3.3 Denture related diseases*

The complexity of polymicrobial biofilms is particularly important when considering denture induced oral diseases, which may typically be associated with inflammation of the oral mucosa. However, as adults are more likely to retain their natural dentition, then partial dentures are increasingly common. This can create a perfect storm where inert material adjacent to healthy enamel can lead to adult-onset caries and gingival inflammation. As dentures are not sterile and are used at the body-external environment interface, they are readily colonised by microorganisms (Olms et al., 2018). The oral environment differs between the dentate and edentate mouth: the tooth is replaced by an inert removable prosthesis; the fitting surface of the denture provides a unique protected environment; the gumline is absent in complete denture wearers, and the natural dentition that abuts a partial denture is particularly prone to caries and gum disease (Zlatarić et al., 2002). The microbiology in these different scenarios is varied and should be considered separately.

As with natural dentition, a denture surface once placed in the mouth, becomes coated with an ‘acquired pellicle’ of salivary glycoproteins (including salivary amylase, albumin, mucin and lysozyme) and immunoglobulins (Marsh et al., 2016, Edgerton and Levine, 1992, Chawhuaveang et al., 2021). The profile of the acquired pellicle on the enamel and denture is not consistent and can change depending on the location of the dental arch (Ventura et al., 2017). The pellicle composition might vary, and

influence the identity of primary colonisers, though initial colonization may not necessarily differ between a range of dental materials (Mukai et al., 2020).

In the oral cavity, primary colonisers of hard/enamel surfaces include Gram positive *Streptococcus* spp. (*S. gordonii, S. mitis, S. oralis, S. sanguinis, S. mutans, and S. parasanguinis*), and other species including *Rothia* spp., *Neisseria* spp., *Veillonella* spp., *Abiotrophia* spp., *Gemella* spp. and *Granullicatella* spp. (Theilade et al., 1983, Yitzhaki et al., 2018, Aas et al., 2005). Secondary colonisers can adhere to and co-aggregate with primary colonising microbes, which if adhered to a denture can form complex denture plaque communities (Coulthwaite and Verran, 2007, Jenkinson, 2011). Despite the prevalence of bacteria in denture plaque, the most commonly studied microorganism is the yeast *C. albicans* (Gleiznys et al., 2015, Verran, 1998, Ramage et al., 2004), and to a lesser extent other *Candida* species such as *C. glabrata* (Zomorodian et al., 2011, Coco et al., 2008), *C. famata, C. dubliniensis* and *C. tropicalis* (Gauch et al., 2018, Zomorodian et al., 2011).

The interest in *Candida* in denture plaque derives from its association with denture stomatitis, a term which describes inflammation of the epithelial surfaces in contact with the denture, particularly the maxillary denture (Salerno et al., 2011). *Candida* spp. are well-known secondary colonisers of denture plaque, with data suggesting *C. albicans* can co-aggregate with *Streptococcus* spp. and result in biofilm on saliva-coated surfaces (Bamford et al., 2009). The yeast is found primarily on the fitting surface of the maxillary denture. The enclosed environment, the presence of pre-existing plaque, the protective nature of the surface topography and the acidogenic nature of the plaque have all been proposed as factors which enhance survival (Verran, 1988). It is has also been demonstrated recently that *C. albicans* acts as a

'keystone' commensal within relevant oral biofilm model systems, with the suggestion that the larger physical nature of this dimorphic yeast makes it capable of creating physical and chemical micro-environments that supporting smaller bacteria and obligate anaerobes (Janus et al., 2016, Young et al., 2020).

### *1.3.4 Culture based studies*

Culture based studies of denture plaque have shown that it is a diverse microbial biofilm, structurally similar to dental plaque (Walter and Frank, 1985, Budtz-Jørgensen, 1981), with a similar microbial composition (Nikawa et al., 1998), but with elevated levels of yeasts (primarily *Candida* spp.), *Lactobacillus* spp., streptococci and staphylococci (Marsh et al., 1992, Theilade and Budtz-Jørgensen, 1988). These elevated levels have been shown to be particularly notable in cases of denture stomatitis (Theilade and Budtz-Jørgensen, 1988), and have been found to increase with the increase in age of the denture (Budtz Jorgensen, 1974, Theilade et al., 1983, Mizugai et al.). Although *Candida* spp. are of particular concern in denture wearers due to their strong association with denture stomatitis, their reported proportion in denture plaque in comparison to bacterial isolates is relatively low (Theilade and Budtz-Jørgensen, 1988). Whilst such investigations have been able to inform on microorganisms associated with dentures, classic microbiological techniques are not able to culture all microorganisms onto agar. First described by Staley and Konopka (1985), the 'Great Plate Count Anomaly' describes the phenomenon that the majority of microorganisms are non-culturable on agar, limiting the ability to discover the true microbial community of an environment – particularly one so complex as plaque - if only reliant on culture-based techniques.

### *1.3.5 Non-culture-based studies*

The denture microflora is composed of a wide range of both prokaryotic and eukaryotic microorganisms, but predictably not all are culturable. Contemporary molecular biology techniques that do not rely on culturing have gained momentum in the study of denture-related plaque. Amplicon sequencing is one such technique, whereby specific genes (16S, 18S and ITS for bacterial, fungal and microbial eukaryotes respectively), which are present in all but unique for each species, are sequenced and analysed using computer-based bioinformatics. Quantitative polymerase chain reaction (qPCR) analyses is also widely used, which measures the amount of a specific gene (usually the 16S rRNA gene for bacteria, or 18S or internal transcribed region [ITS] for fungi) in a sample without the need to sequence. Using these approaches, it is estimated that the oral microbiome contains over 700 species of bacteria (Deo and Deshmukh, 2019, Verma et al., 2018). Whilst such studies specifically looking at dentures are limited compared to the wider oral cavity, they nevertheless provide a more accurate picture of the microbial population of a denture, and how this might be associated with other factors such as disease state.

Campos (2008) was the first to use a pre-next generation sequencing approach (16S rDNA cloning) (Campos et al., 2008). Here, over 82 different bacterial species were identified, of which 29 were exclusive to disease and 26 to healthy denture wearers alongside *Candida* sp. in both. The first microbiome study was performed by the Ramage laboratory, where it was shown that bacteria from the taxa Bacilli and Actinobacteria were most abundant on the mucosa and denture of 130 patients, with *Lactobacillus spp.* showing a positive correlation in those with higher quantities of *Candida* spp. (O'Donnell et al., 2016). Despite no significant difference in overall microbiology between the dentures of healthy versus inflamed mouths, a follow up

study by these authors using qPCR it was found that dentures could be a reservoir for respiratory pathogens, including *Streptococcus pneumoniae*, *Pseudomonas aeruginosa*, *Haemophilus influenzae B*, *Streptococcus pyogenes* and *Moraxella catarrhalis*, (O'Donnell et al., 2016). In a smaller study Shi et al. (2016) reported the genus *Actinomyces* was most pervasive on both dentures and remaining teeth, followed by *Streptococcus*, *Veillonella*, *Capnocytophaga*, *Neisseria*, *Prevotella*, and *Corynebacterium*, independent of the surface or health status, while the microbiome of dentures from stomatitis patients was more diverse than dentures belonging to healthy patients. As reported using culture techniques, *Candida* is present as part of the denture microbiome (Campos et al., 2008). In a study analysing 82 Dutch denture-wearers, high *Candida* loads were associated with the bacterial class Bacilli, negatively associated with bacterial classes Fusobacteria, Flavobacteria, and Bacteroidia, and were generally less diverse and dominated by streptococci (Kraneveld et al., 2012). Whilst such studies are useful and provide data on the potential relationship between denture stomatitis, the literature is limited, lacking many large study populations/sample sizes, and making generalisation difficult. Together, these and other studies demonstrate that denture-based microbiomes are not dissimilar to dental plaque (Redfern et al., 2022). These studies have started to provide a greater insight into the diversity of bacteria that occupy these substrates, alongside *Candida* spp.

### *1.3.6 Dentures and biofilm: denture plaque*

Physiologically, a positive relationship exists between the oral microflora and the host. Oral microorganisms naturally thrive in areas with limited saliva dynamics in and around the teeth and areas between the teeth and gingival crevice; in addition to the surfaces of a denture. Microorganisms are found in complex communities on the

denture attached to the denture surface or to other cells whilst embedded in extracellular polymeric substance (EPS) (Gendreau and Loewy, 2011). It is widely agreed in the literature that microorganisms displaying this biofilm phenotype are physically difficult to remove (Sharma et al., 2019). Although the phenomenon of biofilm formation is similar for denture and dental plaque, the specific environment between the denture and the roof of the mouth has been shown to be microbially distinct (O'Donnell et al., 2015b).

As interest in denture stomatitis increased during the 1980s, studies on the attachment of *C. albicans* to denture PMMA and silicone began (Samaranayake and MacFarlane, 1980, Rodger et al., 2010, Pereira-Cenci et al., 2008). The yeast readily attached to the surface, with retention being enhanced by increased surface roughness (Verran et al., 2014, Verran and Maryan, 1997, Jackson et al., 2014), lowered pH (Verran et al., 1991) and other factors. *In-vitro*, studies on the interactions occurring between *C. albicans* and *Streptococcus mutans* are common (Baena-Monroy et al., 2005, Zhou et al., 2018, Falsetta et al., 2014). Initially this might seem counter-intuitive, because *S. mutans* is best known for its role in dental caries (Hamada et al., 1984), and it may not be the most common streptococcus present in denture plaque, with *S. sanguinis* historically recovered more often (Carlsson et al., 1969). However, the highly acidogenic and aciduric nature the environment generated by *S. mutans* would likely prove beneficial for yeast proliferation. These basic studies exploring co-aggregation and antagonistic behaviours have fuelled an exploration of interkingdom interactions (Delaney et al., 2019).

More complex studies on denture plaque models have been carried out, for example using a denture plaque microcosm (Coulthwaite and Verran, 2007, Coulthwaite and

Verran, 2008, Brown et al., 2022b), and biofilm models, used to assess the impact of putative antimicrobial/antibiofilm agents (Brown et al., 2022b, Sherry et al., 2016). In line with Marsh's 'Ecological Plaque Hypothesis' (Marsh, 1994), it has been proposed that denture stomatitis arises from a shift in the plaque microbiology away from health due to external changes such as increased plaque acidogenicity and increased plaque quantity (Verran, 1998) – and perhaps diversity (Marsh, 1994). Thus, both control of plaque quantity and management of specific aspects of the microcosm might enable progress towards maintenance if a healthy denture plaque, which in turn could minimise the impact on dental caries. Having the ability to study and model complex polymicrobial biofilms is therefore an essential requirement to improving our understanding of these communities and finding new therapeutic strategies to control them.

## 1.4 Oral biofilm modelling

Our fascination with oral microbial plaque was a catalyst for the use of artificial cultures to generate "biofilms" under appropriate controlled conditions (e.g., under shear force and constant flow). For example, using a chemostat flow system allows for the growth of planktonic cultures and biofilms through a regular supply of fresh medium, continuously pumped through the system, with spent growth medium being removed at a similar rate. Pioneering work by Marsh who instigated the use of the chemostat in oral microbiology, measured the growth rate of 1-2 bacterial species or undefined plaque samples in nutrient-excess or limited media (Marsh et al., 1982, Marsh et al., 1983), then later defined mixed-species containing a complex consortium of anaerobic microorganisms, such as *Fusobacteria*, *Actinomyces*, *Veillonella*, *Neisseria* and *Bacteroides* species under standardised conditions. Whilst reductionist in nature, these studies were some of the first to piece together interactions between different

species which relatively reflected *in-vivo* plaque, and subsequently led to the formulation of the “ecological plaque hypothesis” (Marsh, 1994). Of note at the time, the works of McKee et al (McKee et al., 1985), McDermid et al (McDermid et al., 1986) and Bradshaw et al (Bradshaw et al., 1989) all demonstrated that mixed-species cultures were influenced by carbohydrate availability, and subsequent shifts in pH between meals. These flow-through models also allowed for minimum inhibitory concentration (MIC) testing of anti-microbials such as triclosan, chlorhexidine, xylitol and fluoride against mixed-species biofilms. An advantage being that the compounds could be pulsed through the system using MIC or sub-MIC levels or dosed appropriately to give a constant final concentration. This meant that the effects of such compounds could be assessed either directly on bacterial species, or indirectly, if inhibition of one species impacting on the growth of another, thus altering the homeostasis of the biofilm. Indeed, it was shown that *S. mutans*, *Lactobacillus casei* and *Veillonella dispar* (carbohydrate-fermenting, acid-tolerant bacterial species) predominate a mixed-species biofilm in environments of carbohydrate excess, and subsequent acidic pH, whilst treatment with sodium fluoride reduced the acid production, thus stabilising the biofilm and allowing other bacterial species to flourish (Marsh, 1991). Similar mechanisms were proposed for pathogens associated with periodontal disease, where it was demonstrated that anaerobic bacteria such as *P. gingivalis* and *Fusobacterium nucleatum* could only survive aerobic environments when grown in communities containing oxygen-consuming bacteria (Bradshaw et al., 1996, Bradshaw, 1997, Bradshaw et al., 1998). Based on these observations, Marsh proposed the “ecological plaque hypothesis”, which assumed that an imbalance in the composition of the oral biofilm due to environmental factors (carbohydrate accessibility

and pH in dental caries), and nutrient availability (oxygen levels and redox potential in PD) can result in the enrichment of disease-associated pathogens (Marsh, 1994).

### *1.4.1 Static biofilm models*

Static biofilm models are another important system in the field of oral microbiology. These models exploited a relatively simple method of producing biofilms to perform high-throughput antimicrobial susceptibility testing and phenotypic screening of mutant libraries to assess the importance of certain genes in biofilm formation (Thrower et al., 1997, Wright et al., 1997, Loo et al., 2000). Oral biofilms were grown on either plastic, glass, hydroxyapatite (HA) coated-substrates, directly in the bottom of different sized microtiter plates, or on inverted pegs placed into specific media with inoculum (Figure 1-4B). One major advantage of these static models is that multi-species biofilms can be grown in large quantities, an improvement of chemostat flow systems which were restricted to producing no more than a few biofilms at any given time. More recently, high-throughput techniques for oral biofilm cultivation have been developed, e.g., microfluidics for miniaturising biofilm culture and characterisation (Kim et al., 2012, Nance et al., 2013, Samarian et al., 2014) and impedance-based technology for real time monitoring of biofilm growth (Mira et al., 2019) (Figure 1-4C). However, these new techniques are expensive and therefore batch methods for growing biofilms in microtiter plates are arguably the preferred choice for most research groups given the cost attached to generating such models. Additionally, these high-throughput approaches serve as ideal models employed by industry, which seek robust, minimalistic biofilm platforms that can be used as definitive test-beds for standardised biofilm testing (Malone et al., 2017, Coenye et al., 2018). Advantages and disadvantages of the continuous flow models, static biofilm systems and current

high-throughput modern-day options utilising new technology are discussed in greater depth below in Figure 1-4.

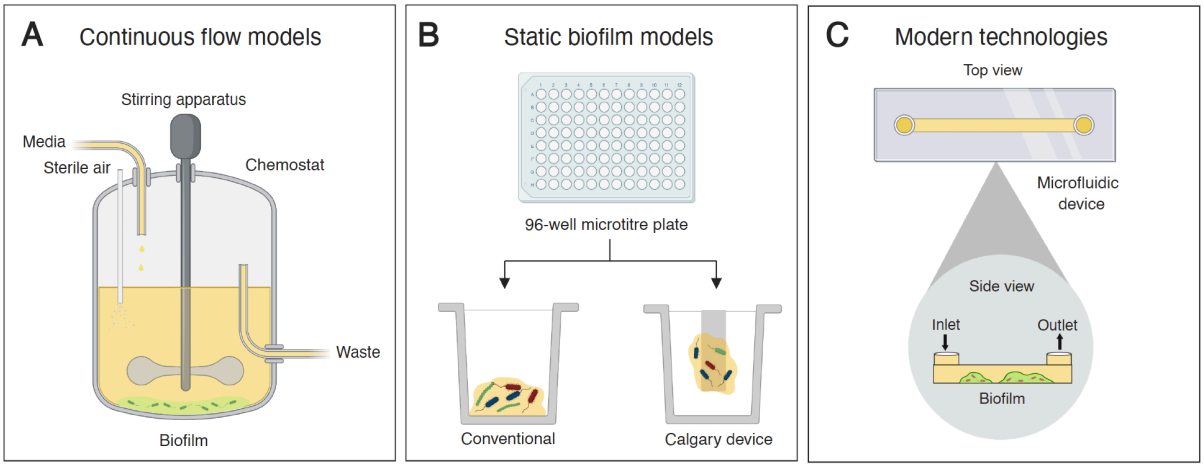


**Figure 1-4 - Models used to grow oral biofilms.** Early work focused on the use of continuous flow systems such as the chemostat model which offered the advantage of a regular supply of fresh medium whilst maintaining a constant media volume (**A**). However, such models were hindered by low-throughput, leading to the development of high-throughput static biofilm models (**B**). Since development, static biofilms have become the most ubiquitously used models in oral research and encompass the conventional model; where biofilms are grown in microtiter plates, and the Calgary device; where biofilms are grown on pegs attached to the surface of lids. As the field of biofilm research continues to grow, novel systems have been employed to incorporate the advantages of continuous flow and static models. One such model is the microfluidic device, which uses microchannels to combine continuous media flow with high-throughput screening potential (**C**). Image created with Biorender® and adapted from (Brown et al., 2019)

| Model | Description | Advantages | Disadvantages |
|---|---|---|---|
| **Continuous flow models** | | | |
| Chemostat | A bioreactor system with a continuous inflow of fresh media and sterile air; waste media is removed at the same rate to maintain a constant culture volume. Biofilms form within the culture chamber. | Suitable for growth of large biofilms.<br>Continuous flow of fresh media.<br>Allows for control of the external environment which can influence biofilm growth. | Low throughput.<br>Requires specialized equipment.<br>Large quantity of material lost if contaminated.<br>No direct access to biofilms.<br>Prone to contamination. |
| Flow cell | Slides containing suitable substrata that allow biofilms to form within small channels under a constant flow of media. Spent media is removed. | Allows for direct visualization of biofilm growth stages.<br>Optimized for microscopy.<br>Compatible with a range of substrata.<br>Continuous flow of fresh media. | Low throughput.<br>Requires specialized equipment.<br>No direct access to biofilms.<br>Prone to contamination. |
| Constant-depth film fermenter | Coupons are suspended from the lid via a suitable coupon holder. Fresh media is pumped through the reactor, with continuous mixing. Biofilms form on the surface of coupons. | Commercially available.<br>Continuous flow of fresh media.<br>Allows for direct access to biofilms.<br>Can alter shear stress. | Low throughput.<br>Requires specialized equipment.<br>Expensive.<br>Prone to contamination. |
| **Static models** | | | |
| Microtitre plate | Media containing bacteria is placed into microtitre plate. Biofilms form on the bottom of wells, or on suitable substrates placed in each well. Media can be replaced through pipetting. | High throughput.<br>Inexpensive.<br>No specialized equipment required.<br>Microtitre plates with varying well sizes can be used to better suit the desired assay. | Biofilms not grown under continuous flow.<br>Prone to sedimentation.<br>Multiple plates required for continuous timepoint assays.<br>Labour-intensive. |
| Calgary device | Media containing bacteria is placed into 96-well microtitre plates. Pegs suspended from lids are placed into wells, allowing for biofilm formation on their surface. | High throughput.<br>Allows for easy manipulation of culture media.<br>Requires active attachment of bacteria as opposed to sedimentation. | More expensive than simple microtitre plates.<br>Multiple plates required for continuous timepoint assays.<br>Prone to contamination.<br>Labour-intensive. |
| **Modern technologies** | | | |
| Microfluidics (e.g. BioFlux microfluidic devices) | Small microfluidic chips contain channels etched into a suitable substrate (glass, silicon, plastic). which are connected through inlets and outlets. Media is pumped through channels, allowing for micro-biofilm formation. | High throughput.<br>Can be designed to mimic specific environments.<br>Suitable for antimicrobial susceptibility testing.<br>Allows for analysis of different stages of biofilm growth. | Expensive.<br>Requires specialized equipment for preparation and analysis.<br>Clogging may occur in micro-channels. |
| Impedance-based technology (e.g. XCELLigence real-time monitoring system) | Media containing bacteria are placed into microtitre E-plates with gold electrodes on the plate floor. Electron impedence is used to monitor several factors such as biofilm growth and cell morphology. Cell index values are directly related to biofilm maturation. | High throughput.<br>Allows for real-time monitoring of biofilm growth.<br>Suitable for antimicrobial susceptibility testing.<br>Can allow for direct access to the biofilm. | Expensive.<br>Requires specialized equipment for preparation and analysis.<br>Prone to sedimentation.<br>Gold electrodes can be fragile and easily damaged. |

**Table 1-2 - Advantages and disadvantages of current oral biofilm methodologies.** The table depicts the current methodologies used by research groups for growth of oral biofilm models including continuous flow systems, static models and current modern options utilising new technology. A description of the models, advantages and disadvantages are highlighted for each methodology. Adapted from (Brown et al., 2019).

Over the past 2 decades, many research groups began to utilise high-throughput static systems to develop their own multi-species biofilms from a defined number of microorganisms. The increase in commercially available real-time quantitative polymerase chain reaction (RT-qPCR) machines makes this possible, meaning oral biofilm models could be grown to precise composition (Figure 1-5A). Previously, compositional analysis was largely restricted to using selective and differential media for identification of different microbial species grown in multi-species biofilms. Currently, the use of genus- or species-specific primers in conjunction with microscopic technology means that biofilms can be repeatedly grown with reproducible composition and architecture (Kommerein et al., 2017). In addition, it is now possible to discriminate between viable or dead microbial species in biofilms using RT-qPCR methods. In 2011, Loozen et al (Loozen et al., 2011) described a protocol using a DNA intercalating substance called propidium monoazide to identify the proportion of dead *S. mutans*, *Prevotella intermedia* and *Aggregatibacter actinomycetemcomitans* cells in heat-killed mono-cultures. Since development, this method has become an important tool in assessing the effectiveness of antimicrobials and other actives on oral biofilms (Yasunaga et al., 2013, Sherry et al., 2016).

### *1.4.2 Imaging biofilms*

Microscopy techniques have advanced in recent years; light, fluorescent and electron microscopic technology are now common methodologies for imaging oral biofilms in most laboratories (Figure 1-5C). In addition, these methods, in particularly fluorescent microscopy, have been adapted for more unique investigations in oral biofilm research. For example, a ratiometric pH-sensitive dye called C-SNARF-4 has been applied to oral biofilms to monitor changes in pH in the biofilm landscape (Schlafer et al., 2011). A five-species early dental plaque biofilm containing four *Streptococcus* species and *A. naeslundii* was grown in the presence and absence of artificial saliva containing 0.4% glucose, and pH gradients in the extracellular matrix monitored fluorescently. Regions within the biofilm with higher cell density correlated with lower pH values (Schlafer et al., 2011). Fluorescent *in situ* hybridization (FISH), has also been used to image oral biofilms sampled directly from volunteers, or grown *in-vitro*. Thurnheer, Gmur and Guggenheim (2004) were the first to combine FISH and CLSI to stain six species of bacteria and fungi within *in-vitro*-grown oral biofilms (Thurnheer et al., 2004). All six microbial species were identified using fluorescently labelled 16S or 18S rRNA-targeted oligonucleotides, with biofilms containing *S. oralis*, *Streptococcus sobrinus*, *Veillonella dispar*, *F. nucleatum*, *Actinomyces naeslundii* and *C. albicans* visualised. It is now possible to use additional combinations of fluorophores to identify tens of bacterial species in dental plaque. Valm and colleagues (2011) elegantly described a “proof of concept” imaging technique which combines fluorescent labelling coupled with spectral image acquisition and analysis to identify 15 different oral taxa in dispersed dental plaque (Valm et al., 2011). The technology, which is known as Combinatorial Labelling and Spectral Imaging (CLASI-FISH), has scope to distinguish between 120 different fluorescently-labelled microorganisms in a single image (Valm

et al., 2016). This was used to visualise the “biogeography of the human oral microbiome” in intact dental plaque (Mark Welch et al., 2016).

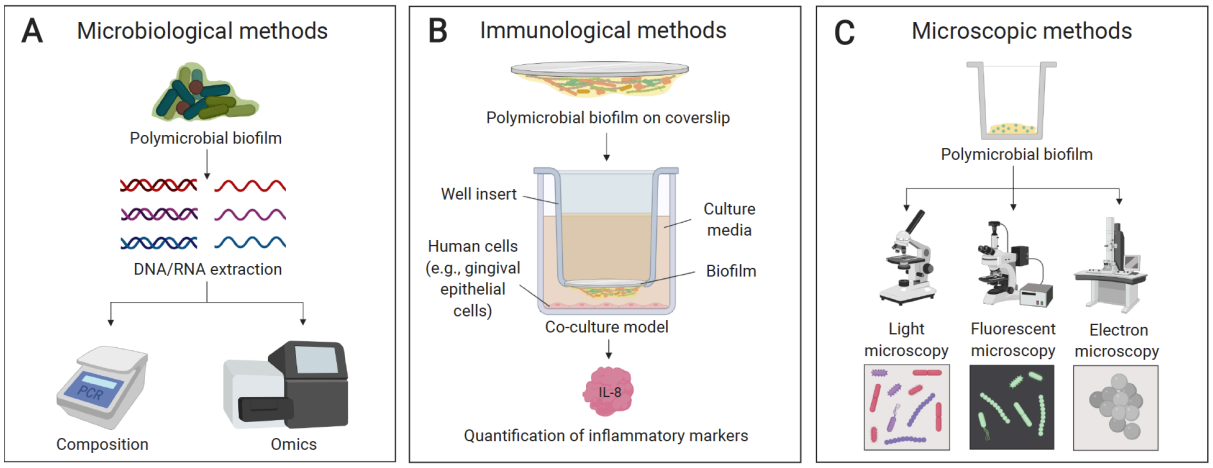


**Figure 1-5 - Key investigative methodologies for oral biofilms.** Oral biofilm research seeks to investigate outputs associated with 3 key domains: Microbiological, Immunological, and Visual. Quantitative analysis through PCR of organism DNA or RNA seeks to gain insight into distribution of organisms or key transcriptional outputs (**A**). Co-culture with relevant cell lines seeks to inform the immunological mechanisms associated with inflammatory biomarkers associated with immune response to biofilm systems (**B**). Microscopy is key in underpinning these outputs through visual interpretation of biofilm growth and development as well as response to treatment outcomes in qualitative and quantitative measures (**C**). Created with Biorender® and adapted from (Brown et al., 2019).

### *1.4.3 Technological advances*

Throughout the last 20 years, the use of high throughput technologies has become routine to support biological discoveries and drive hypotheses. OMICs approaches have enabled researchers to view the genomics, transcripts, metabolites and proteins of oral biofilm models in a “holistic” manner. Microbiome analysis by shotgun sequencing or 16S amplicon sequencing has become one of the most widely used technologies and bioinformatic techniques in the microbiologist’s toolbox. Within the last 10 years there has been an increase in microbiome studies due to the cost of the sequencing technologies decreasing and the availability of analysis pipelines and packages increasing (Minich et al., 2018, McMurdie and Holmes, 2013, Dhariwal et al., 2017). The microbiome has been studied in caries, PD, denture stomatitis, peri-implantitis among several other oral diseases (Kirst et al., 2015, Tanner et al., 2018, O'Donnell et al., 2015b, Apatzidou et al., 2017). These studies have allowed for the greater in-depth characterisation of distinct microbial community shifts within the oral cavity, also accounting for uncultivated organisms. Large-scale molecular techniques such as microbiome sequencing have allowed for the identification of species, as well as species-species interactions and environment-species interactions previously undeterminable with conventional techniques. Analysis of the sub-gingival plaque microbiome has revealed that disease associated organisms may extend far beyond the previously identified ‘Red-complex’. Of note, organisms such as *Filifactor alocis* and *Prevotella denticola* have been consistently found to be higher in diseased sites (Perez-Chaparro et al., 2014, Chen et al., 2018, Griffen et al., 2012). These types of analysis has led to the re-evaluation of individual pathogens driving a disease state, and it is now hypothesised that “ecotypes” and/or whole microbial communities may drive dysbiosis and pathogenesis (Zaura et al., 2017, Marsh and Zaura, 2017).

The sequencing of messenger RNA for studying transcriptomics is a powerful tool to gain insight into how an organism is reacting to and adapted to its environment. This can give us clues and hypotheses about how microorganisms interact in a complex biofilm environment. For example, the use of RNA-Seq has helped in our understanding of species-species adhesion and virulence mechanisms between *C. albicans* and *P. gingivalis* (Sztukowska et al., 2018), and synergistic relationships in *C. albicans* and *S. mutans* biofilms (He et al., 2017). Transcriptomic studies have also been indispensable in understanding disease pathogenesis, drug resistance mechanisms and community dynamics with regard to oral biofilm research in recent years (Frias-Lopez and Duran-Pinedo, 2012, Benitez-Paez et al., 2014).

Similarly, Mass Spectrometry (MS) and Nuclear Magnetic Resonance (NMR) have allowed for snapshot profiling of metabolic and protein expression for the identification of signatures in oral biofilms. Metabolomics enables the identification and relative quantification of all the metabolites in a biological system. Metabolomic pathways and biofilm regulatory mechanisms are discernible with these technologies (Takahashi et al., 2012). They offer the potential to identify signatures associated with disease progression. This was highlighted in a 2015 pilot study which validated the use of metabolomics by Gas Chromatography–MS in identifying metabolic profiles between cariogenic and disease-free oral biofilms (Zandona et al., 2015). Advancements have also been made in oral microbial studies which allow for the correlation of the metabolome with shifts in the oral microbiome (Zaura et al., 2017). These studies further our understanding of bacterial communities with different ecological states with more specialised function, which the authors of the 2017 study (Zaura et al., 2017) suggest could highlight specific metabolic function of communities which could indicate dysbiosis. In the coming years, it is likely that the use of OMICs approaches

in investigating microbial-host interactions will continue to grow. It is important that these techniques should be utilised in conjunction with laboratory science, in order to identify mechanistic pathways by which oral pathogens facilitate disease onset and progression.

## 1.5 Concluding remarks

This introductory review has highlighted how our understanding of oral microbiology at any given time has resulted in relevant robust biofilm models, often simple to start with, but developing complexity over time. There is a notable lack of appreciation of pathogenic yeasts in many of these model systems, yet it has been demonstrated how important these microorganisms are to oral and systemic health. *In-vitro* biofilm models have also enhanced our knowledge of the simple and complex microbial interactions in the oral cavity, and recent OMICs analyses imply that no oral biofilm model is ideal. Indeed, it is simply impossible to replicate exact microbial-microbial or microbial-host interactions *in-vitro*. Nonetheless, understanding how a few organisms interact together in biofilms, and how they respond to antimicrobials, aids our view of dynamic microbial interactions. We should not lose sight of the importance of hypothesis-driven research when creating or using these models, and not simply rely on ‘big data’ to shape our ideas and become more speculative in our outlook. As with all approaches, OMICs techniques are not devoid of disadvantages.

## 1.6 Hypothesis and aims

This thesis hypothesises that *Candida albicans* is an important and under-recognised member of the oral microbiome. Primarily considered a yeast associated with denture disease, its role in caries and gingival inflammation are not fully appreciated or

considered. It is the primary aim of this dissertation to explore its role in human oral diseases using a combination of systematic reviewing and investigational *in-vitro* modelling in complex communities. The specific aims are as follows:

1. Undertake a systematic metanalysis of caries microbiome studies to assess the predictive value of the bacterial microbiome alone
2. Develop simple models of cariogenic plaque, including *C. albicans*
3. Develop complex undefine models of cariogenic plaque, including *C. albicans* etc

# 2 Meta-analysis of caries microbiome studies.

# List of Publications

This section has been submitted under the University of Glasgow code of practice for thesis submission by alternative format. The work has been reformatted in-keeping with thesis formatting guidelines and is an adaptation of the following published article (Butcher et al., 2022):

**Butcher MC**, Short B, Veena CLR, Bradshaw D, Pratten JR, McLean W, Shaban SMA, Ramage G, Delaney C. Meta-analysis of caries microbiome studies can improve upon disease prediction outcomes. APMIS. 2022 Dec;130(12):763-777. doi: 10.1111/apm.13272. Epub 2022 Sep 20. PMID: 36050830; PMCID: PMC9825849.

## 2.1 Introduction

Home to approximately 700 species of bacteria, the oral cavity is a complex and diverse environment and the development of oral diseases such as dental caries is closely related to the oral microbiome (Deo and Deshmukh, 2019, Chen et al., 2020, Struzycka, 2014). Dental caries is one of the most common infectious diseases worldwide (Vos et al., 2012). The fundamental principle driving the onset and progression of dental caries stems from frequent carbohydrate intake, that causes dental plaque bacteria to produce acid, which in turn lowers the pH of the oral cavity, resulting in demineralisation of the tooth surface (Abou Neel et al., 2016). Previously thought to be primarily caused by *Streptococcus mutans,* theories about the aetiology of dental caries have developed in parallel with developments in culture-independent techniques, and it is now considered a result of a dysbiotic oral microbiome (Zhan, 2018, Tanner et al., 2018, Radaic and Kapila, 2021). There remains some debate regarding the composition of the oral microbiome in caries when compared to healthy subjects, with some reporting little to no changes, whereas others state there is a shift in microbial diversity and an enrichment of pathogenic genera (Zheng et al., 2017). Additionally, we recognise a fundamental gap in knowledge in relation to the interaction of more than just bacterial organisms in the oral cavity with regards to fungal species which are well documented in terms of oral dysbiosis (Akpan and Morgan, 2002, Ghannoum et al., 2010a, Bandara et al., 2019)

The popularity of next generation sequencing (NGS) studies has risen hand in hand with accessibility and advances in associated technologies. This has resulted in an increase in the number of microbiome related studies. With this, our knowledge concerning complex areas of disease biology, such as microbiome and transcriptome, have developed rapidly in recent years. This has meant that many conditions are now

hypothesised to arise because of a shift away from what is typically considered a ‘healthy’ microbiome, resulting in a more ‘dysbiotic’ community (Kilian et al., 2016). However, with the ever-increasing quantities of data that are produced from Omics studies, we are now confronted with the dilemma of how these results can be accurately and appropriately combined to enable researchers to investigate and interrogate ‘the bigger picture’ (Hasin et al., 2017, Chen et al., 2022). Indeed, the lack of standardisation regarding data uploading and availability can produce difficulties in terms of methodological reproducibility and unintentional introduction of bias (Mirzayi et al., 2021, Langille et al., 2018). In particular, major differences in platform and sequencing region introduce high levels of variation from study to study. Despite the large number of microbiome data described within the literature, previous meta-analysis attempts, such as those carried out in the gut have found only a small subset of studies to have available or appropriate data for re-analysis (Duvallet et al., 2017, Bisanz et al., 2019).

By employing a meta-analytic approach, we now have the unique opportunity to synthesise findings while addressing issues that often occur in microbiome studies such as small cohort sizes. This approach allows researchers to combine datasets and findings to identify consistencies and trends across studies, therefore helping develop our understanding of disease biology (Duvallet et al., 2017).

## 2.2 Hypothesis & Aims

Herein we aimed to describe a reproducible, standardised, pipeline for the downloading, processing, combination, and analysis of publicly available microbiome datasets that can be applied to a myriad of health conditions. Additionally, we sought to assess the rigour of this data in the context of oral caries as a tool for pathological identification of disease state. Finally, we aimed to observe trends in how microbiome samples are collected, treated, stored, extracted and sequenced, to gain a better understanding of how these processes may differ across studies and locations. This highlights the inconsistencies in the study design of caries microbiome studies such as choice of DNA extraction kit, 16S target region and sample preparation, which can have a considerable impact on study findings.

## 2.3 Methodology

### *2.3.1 Study Design*

As outlined in Figure 2-1**,** below, we aimed to obtain and assess publicly available datasets for caries-related microbiome research and assess that data based on a 5-point access scale. From this, we were able to collect and combine analysis outputs from respective studies, filter them based on our own parameters, and observe trends in outputs with the intent to connect those trends to the onset or progression of caries. This approach allowed for detailed examination of study-to-study conditions and differences as well as highlighted areas where microbiome research, in the field of caries, may be of limited emphasis. This also highlighted the need for a standardised approach to sample acquisition when considering study design as well as producing a reliable metric for the identification of cariogenic samples.

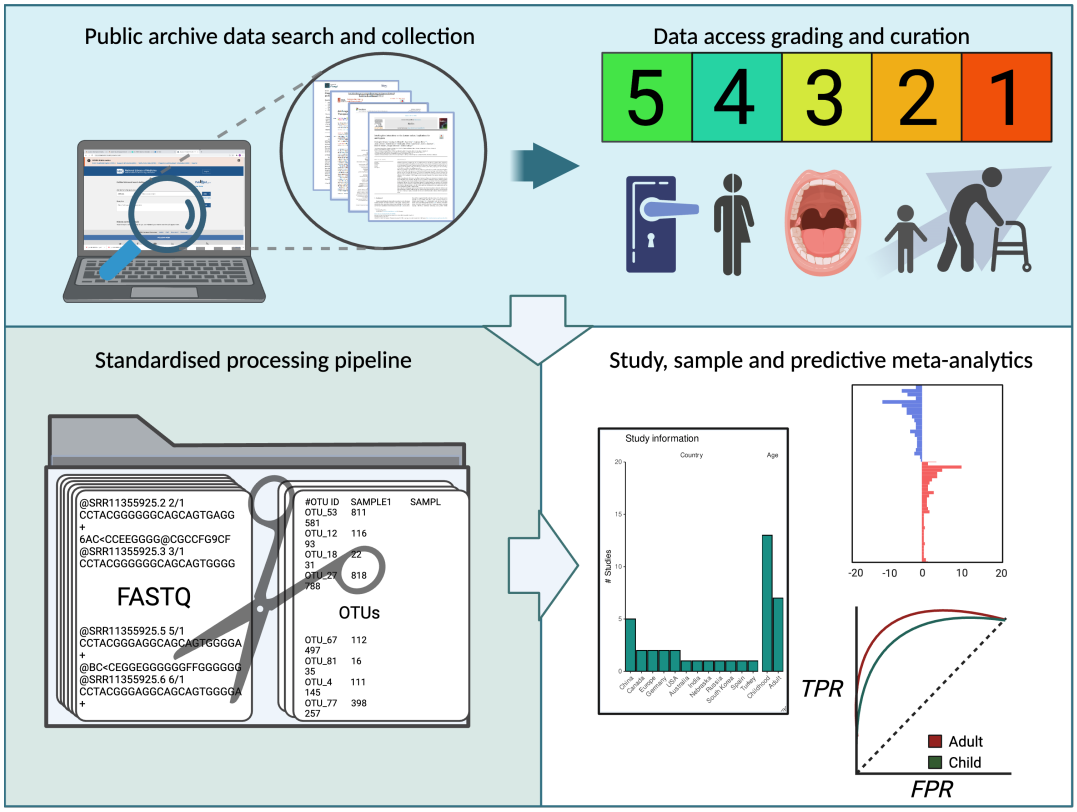


**Figure 2-1 - Graphical representation of study design and approach.** The study intent was to collect, curate, assess and leverage publicly available sequencing data related to 16S rRNA sequencing in the context of oral caries. The data was graded using a newly developed system to assess for data availability, meta-data availability and the ease of mapping data to samples as well as potential inclusion. Once assessed, study data were processed and analysed in combination to determine if 16S microbiome data in the context of oral caries could be used to predict disease progression and outcome. Created with Biorender.com®.

### *2.3.2 Search criteria, Study criteria, and data scoring*

Studies were collected by using keyword searches on PubMed. Search results were filtered to exclude any study published before 2012 to coincide with the advancement of Illumina sequencing platforms providing more time effective access to microbiome analysis after this point (Shokralla et al., 2012). Remaining studies were exported to the reference manager EndNote (version X8). Search terms used aimed to firstly select for microbiome and NGS studies, and then additional search terms were added using the "AND" function to further narrow search results down to those performed on the oral cavity, specifically related to dental caries.

Search results used are shown below:

((microb* OR bacteri* OR archea* OR fung* OR mycob*) AND (structure OR composition OR diversity OR community) AND (sequencing OR metabarcoding OR amplicon OR metagenom* OR 16S OR "ITS")) AND (("dental caries" OR "dental cavities" OR "tooth decay" OR "tooth demineralization" OR "carious dentin" OR "carious teeth" OR "caries" OR cariogenic))

Once obtained, studies were collected and scored for data access based on the criteria questions outlined in Figure 2-2, below.

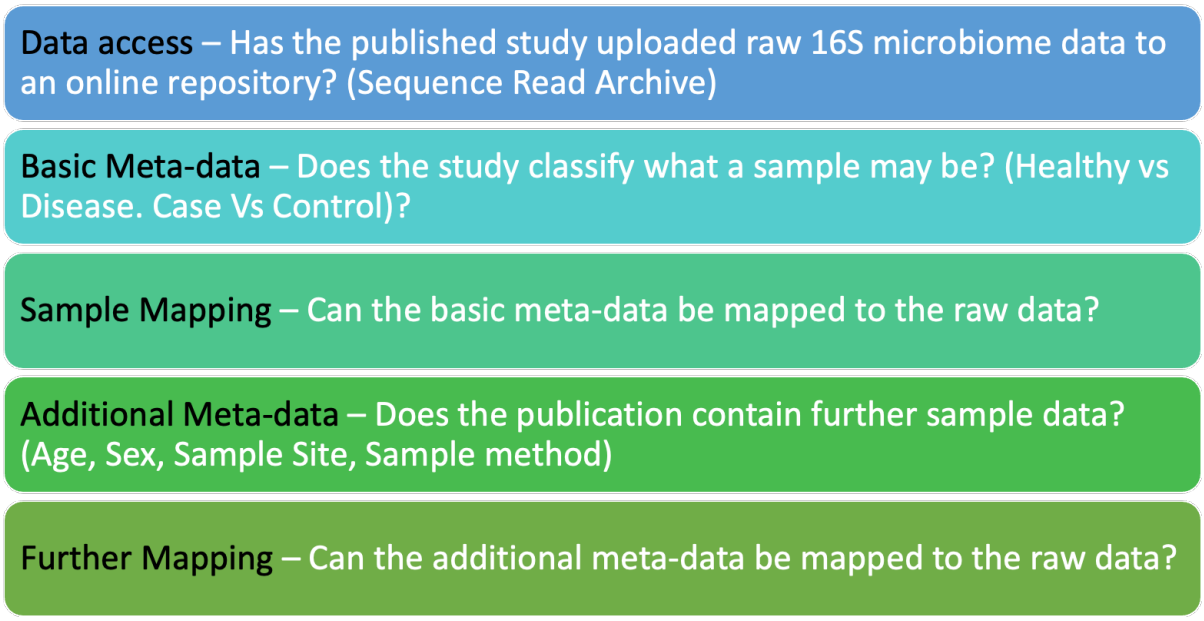


**Figure 2-2 - Identifying basic parameters for data access scoring.** Depiction of the 5 basic criteria assigned to curating accessible data from NGS sequencing studies. Data were scored from 1 to 5 based on which of the above parameters they were able to satisfy.

Firstly, all PubMed search results were exported to EndNote and upon exportation study titles and abstracts were screened for relevance and shortlisted. Studies were excluded that were not related to the oral microbiome 16s rRNA, had no data accession number, were not mappable to individual samples, had no additional metadata like age, sex, site and smoking status of the individuals under study. We also excluded studies with data "available upon reasonable request", *in-vitro* studies, transcriptomic studies, and data deposited in other repositories other than the National Centre for Biotechnology Information (NCBI) or European Nucleotide Archive (ENA) database.

Shortlisted studies were interrogated in the style of a scoping review, and relevant information related to shortlisted studies was recorded by MB and BS. This relevant information included study details which may influence the microbiome or downstream data analysis, such as sampling method and site, number of cases, controls, Decayed, Missing and Filled Teeth (DMFT) index, additional cohorts, DNA extraction method, next-generation sequencing platform, primer sequences and region of 16s rRNA. We also included the data accession number and Digital Object identifier (DOI), for further data retrieval. We then employed a two-step approach to review shortlisted studies whereby other laboratory-based clinicians (CLRV and SS) assessed study relevance and confirmed study detail collection. Shortlisted articles were then subjected to a scoring system, as depicted in Figure 2-2, where they could earn up to a maximum of 5 points. A study was awarded one point for each positive 'yes' to each of these parameters.

Studies were included in final analysis if they were scored as ≥3, as data access and mappability of samples to health or disease states were the minimum required criteria for further processing. The full list of studies is outlined in the following Table 2-1.

| Publication | Location | Study Design | Controls | N_Controls | Cases | N _Cases | Extraction Method | Forward Primer | Reverse Primer | Sequencer | Region | Data Accession | Reference |
|---|---|---|---|---|---|---|---|---|---|---|---|---|---|
| Jiang, 2019 | Chongqing, China | Cross-Sectional | Caries Free | 22 | Active Caries | 24 | EZNA Soil Kit | 338F (5'-ACTCCTACGGGAGGCAGCAG-3') | 806R (5'-GGACTACHVGGGTWTCTAAT-3') | MiSeq | 16S V3-V4 | PRJNA495719 | (Jiang et al., 2018) |
| Zhu, 2018 | Beijing, China | Cross-Sectional | Early Childhood Caries Free | 15 | Early Childhood Caries Recurrence | 13 | QIAamp DNA Mini Kit | 336F (5'-GTACTCCTACGGGAGGCAGCA-3') | 806R (5'-GTGGACTACHVGGGTWTCTAAT-3') | MiSeq | 16S V3-V4 | PRJNA493618 | (Zhu et al., 2018) |
| Kashimoglu, 2020 | Istanbul, Turkey | Cross-Sectional | Monozygotic twins | 49 | Dizygotic twins | 50 | Saliva DNA Isolation Kit | Bakt_341F (5'-CCTACGGGNGGCWGCAG-3') | Bakt_805R (5'-GACTACHVGGGTATCTAATCC-3') | MiSeq | 16S V3-V4 | PRJNA613586 | (Kasimoglu et al., 2020) |
| Xiao, 2016 | Shanghai, China | Cross-Sectional | Caries Free | 29 | Low-High Caries | 131 | TIANamp Bacteria DNA Kit | 8F (5'-AGAGTTTGATCCTGGCTCAG-3') | 533R (5'-TTACCGCGGCTGCTGGCAC-3') | 454 | 16S V1-V3 | PRJNA325084 | (Xiao et al., 2016) |
| Havsed, 2021 | Jönköping, Sweden | Cross-Sectional | Caries Free | 20 | Caries | 20 | MagNa Pure LC DNA Isolation kit II | 341F (5'-CCTACGGGNGGCWGCAG-3') | 805R (5'-GACTACHVGGGTATCTAATCC-3') | MiSeq | 16S V3-V4 | PRJNA681486 | (Havsed et al., 2021) |
| Cherkasov, 2018 | Orenburg, Russia | Cross-Sectional | Caries Free (Asthma) | 8 | Asthma with Caries | 10 | Tissue Lyser LT | S-D-Bact-0341-b-S-17 | S-D-Bact-0785-a-A-2 | MiSeq | 16S V3-V4 | PRJNA495738 | (Cherkasov et al., 2019) |
| Bong-Soo, 2017 | Chuncheon, South Korea | Longitudinal | Caries Free | 27 | Dental Caries (4 years) | 12 | Fast DNA SPIN extraction kit | ND | ND | 454 | 16S V1-V3 | PRJEB19674 | (Kim et al., 2018a) |
| Gomez, 2017 | California, USA | Cross-Sectional | Caries Free | 382 | Dental Caries | 247 | Qiagen PCR purification kit | 515F (5'-GTGCCAGCMGCCGCGGTAA-3') | 806R (5'-GGACTACHVGGGTWTCTAAT-3') | MiSeq | 16S V4 | PRJNA383868 | (Gomez and Nelson, 2017) |
| De Jesus, 2020 | Manitoba, Canada | Cross-Sectional | Caries Free | 40 | Severe early chilhood caries (SECC) | 50 | ND | ND | ND | MiSeq | 16S V4/ ITS1 | PRJNA555320 | (de Jesus et al., 2020) |
| Kalpana, 2020 | Tamil Nadu, India | Cross-Sectional | Caries Free | 15 | Severe/Early childhood caries | 40 | QIAamp DNA microbiome Kit | 341F (5'-CCTACGGGNBGCASCAG-3') | 805R (5'-GACTACNVGGGTATCTAATCC-3') | MiSeq | 16S V3-V4 | PRJNA454811 | (Kalpana et al., 2020) |
| deJesus, 2021 | Manitoba, Canada | Cross-Sectional | Caries Free | 40 | S-ECC | 40 | QIAamp DNA mini kit | 515F (5'-GTGCCAGCMGCCGCGGTAA-3') | 806R (5'-GGACTACHVGGGTWTCTAAT-3') | MiSeq | 16S V4 | PRJNA555320, PRJNA714139 | (de Jesus et al., 2021) |
| Simon-Soro, 2018 | Glasgow, Scotland | Longitudinal | Caries Free (Baseline-Follow Up) | 14 | Caries/Developed Caries (Baseline-Follow Up) | 19 | MasterPure DNA isolation kit | 8 F (5'-AGAGTTTGATCMTGGCTCAG-3') | 533 R (5'-GCCTTGCCAGCCCGCTCAGGC-3') | 454 | 16S V1-V3 | PRJNA421952 | (Simon-Soro et al., 2018) |
| Xu, 2018 | Beijing, China | Longitudinal | Caries Free | 19 | Active Caries | 10 | Wizard Genomic DNA Purification Kit | ND | ND | MiSeq | 16S V3-V4 | PRJNA480252 | (Xu et al., 2018) |
| Zheng, 2017 | Chengdu, China | Longitudinal | Caries Free pre/post arginine | 42 | Caries pre/post arginine | 42 | TIANamp Bacteria DNA Kit | 27F (5'-AGAGTTTGATCCTGGCTCAG-3') | 338R (5'-TGCTGCCTCCCGTAGGAGT-3') | MiSeq | 16S V1-V2 | PRJNA339212 | (Zheng et al., 2017) |
| He, 2017 | Sichuan, China | Cross-Sectional | Caries Free | 12 | Caries | 25 | QIAamp DNA Mini Kit | F515 (5'-GTGCCAGCMGCCGCGG-3') | 806R (5'-GGACTACHVGGGTWTCTAAT-3') | MiSeq | 16S V4 | PRJNA330533 | (He et al., 2018) |
| Onyango, 2020 | Ghent, Belgium | Interventional | Healthy | 11 | Post-treatment | 11 | ND | 341F (5'-CCTACGGGNBGCASCAG-3') | 785R (5'-GACTACHVGGGTATCTAATCC-3') | MiSeq | 16S V3-V4 | PRJNA601417 | (Onyango et al., 2020) |
| Premaraj, 2020 | Nebraska, USA | Cross-Sectional | NA | 0 | Caries (between Ethnic groups) | 96 | QIAamp DNA mini kit | 341F (5'-CCTACGGGNBGCASCAG-3') | 785R (5'-GACTACHVGGGTATCTAATCC-3') | MiSeq | 16S V3-V4 | PRJNA555622 | (Premaraj et al., 2020) |
| Ferrer, 2020 | Valencia, Spain | RCT | Placebo | 29 | Probiotic | 30 | MagNa Pure LC DNA Isolation kit | Universal | Universal | MiSeq | 16S V3-V4 | PRJNA629283 | (Ferrer et al., 2020) |
| Schulz-Weidner, 2021 | Giessen, Germany | Cross-Sectional | ECC | 20 | ECC | 20 | DNeasy PowerSoil Pro Kit protocol | F515 (5'-GTGCCAGCMGCCGCGG-3') | R806 (3'-TAATCTWTGGGVHCATCAG-5') | MiSeq | 16S V4 | PRJNA731066 | (Schulz-Weidner et al., 2021) |

**Table 2-1 - List of studies and study parameters relating to caries microbiome.**

List of 19 studies carried forward for data analysis inclusive of study location, DNA extraction protocol, primer sequences used, 16S region amplified and types of samples identified.

### *2.3.3 Data retrieval and processing*

Available data was downloaded from the ENA database before quality control protocols were carried out using a standardised pipeline in Qiime2 (Bolyen et al., 2019). Primers and barcodes were removed from reads before trimming poor quality reads to a minimum length of 100bp. Paired end reads were merged and then all reads were prefiltered using sortMeRNA against the SILVA-Bac-16S-id90 database (Kopylova et al., 2012). Filtered reads were assigned to operational taxonomic units (OTUs) by mapping to the human oral microbiome database (HOMD) and GreenGenes for downstream analysis using the Picrust databases at 97% confidence. Greengenes OTU tables were converted to a biom file before the PICRUSt normalise_by_copy_number.py and predict_metagenomes.py scripts were used to predict the functional abundancies of the microbiome for each study (Langille et al., 2013).

OTU clustering was performed closed-reference mode using Vsearch (https://github.com/qiime2/q2-vsearch) package within the Qiime2 (v 2019.10) analysis pipeline using the – strand both options. All representative sequences from the Qiime2 artifacts were combined before phylogenetic trees were constructed for all representative OTUs using the FastTree algorithm within Qiime2 (Price et al., 2010).

OTU tables were exported from Qiime2 artefacts to tabular tables before both OTU tables and study meta-data tables were combined and imported into R for manipulation and visualisation.

### *2.3.4 Microbiome diversity and compositional analyses*

We calculated sample-based metrics upon the common Alpha diversity metrics Chao, Simpson and Shannon within a given sample (Kim et al., 2017a). Alpha diversity metrics aim to apply an individual metric to each individual sample's microbiome.

Chao1 gives greater weighting to low abundance calls in estimating overall species richness whereas the Simpson index is more influenced by common and dominant species. The Shannon index increases with both richness and evenness of the community. We provide 3 indexes here to avoid bias introduced by using one index over another.

Analyses were performed on all studies collectively and on a per-study basis. The built-in estimate_richness function in the phyloseq package (v1.30.0) was used to calculate Shannon and Simpson diversity indices and Chao1 estimates (McMurdie and Holmes, 2013). Pairwise comparisons for two groups was performed by the Wilcoxon test to derive significance $p < 0.05$. For multiple groups, a Kruskal-Wallis test was performed followed by a post hoc Wilcoxon with a Bonferroni correction for multiple testing. All samples within the case control studies were normalised to the geometric mean of the caries health group, and significance was determined using a Welch's t-test. Additionally, the mean Log fold change was also calculated for each of the disease compared to health for visualisation. Next, Beta-diversity indices were employed to infer dissimilarity between samples in terms of direct distance (Euclidean), presence, absence and abundance (Bray) and phylogenetic distance (Unifrac). Matrixes were produced to estimate the diversity between each individual sample before being ordinated into the two dimensions which provided the greatest level of variation. Beta-diversity distances were also calculated in phyloseq using the distance functions. The Centred Log Ratio (CLR) Euclidean distance matrix was calculated using the make.CLR function within MicrobeR with replacement of 0 counts using the zCompositions function and then calculating the distance matrix in base R. The phylogenetic isometric log ratio transformation (PhiLR) from the phylogenetic

trees, created as described above, using the R package philr (Silverman et al., 2017). Distances are then calculated in base R using the dist function as described.

The function ape::PCoA was then used to ordinate the distance matrixes into a 2D plot (Paradis and Schliep, 2018). Ggplot2 was used for visualisation and combining of plots within R. Permutational multivariate analysis of variance was performed on the beta diversity distance matrix which was assessed for statistical significance using the ADONIS function within the vegan package (https://github.com/vegandevs/vegan) this was performed individually on all distance matrix with 999 replications.

### *2.3.5 Random forest classifiers*

Adapting methods developed by Chen et al in 2021., 4 high-impact case-controlled studies were selected as training datasets for random forest classifiers (Chen et al., 2022). This was determined based on highest sample cohort, highest number of citations and most clearly defined sample data. The test set was comprised of the remaining studies. An additional training set was produced by randomly splitting the data in 80:20 ratio to create a training and validation data set. Centre log ratio (CLR) normalised OTUs were used as predictor variables for healthy/disease cases. OTU tables were also summarised to Genus and Species levels using the taxonomy. CLR normalised features from the PICRUSt derived KEGG orthology (KO) feature abundances and PhiLR abundances were additionally used within the random forest classifier.

Random forest models were built using the randomforest package and receiver operator characteristic (ROC) curves were built based on random forest models using the pROC and ggROC packages (Breiman, 2001, Robin et al., 2011). Prediction and performance metrics were extracted using the predict and performance functions from

ROCR (Sing et al., 2005). The training set was derived from subsets of the case-controlled ‘caries vs health’ studies. Performance metrics were derived from each of the subsets of data in the remaining case-controlled studies or the caries only studies. The most important features were extracted from random forest models by ranking MeanDecreaseGini scores and plotted using ggplot2. 10-fold cross validation was used to determine the most optimal number of features from random forests built on CLR. Normalised OTUs from the PICRUSt derived database were then used to inform on the functionality of microbiome datasets and the most important features of this model were used to identify enriched metabolic pathways by matching to the KEGG database using the clusterProfiler package in R (Wu et al., 2021a). Random forest models based upon the random assignment 80:20 ratio for 80% training and 20% validation were built iteratively for each individual case-controlled study. The area under the curve was produced using the predict and performance functions for assessment of each study.

#### *2.3.6 Statistical analysis*

All statistical analyses and graph production were performed using the appropriate functions in R (4.1.2) unless stated otherwise. Statistical significance was determined when $P < 0.05$.

## 2.4 Results

### *2.4.1 Review of eligible studies*

First, our initial search on PubMed® produced 953 results, of which 880 were screened out based on the following exclusion criteria: review studies with no accessible sequencing data, studies not in English or not readily translatable, studies that did not specifically focus on 16S microbiome sequencing, and non-caries-based research. These were then assessed and scored based on data accessibility using the criteria questions outlined in Figure 2-2.

In brief, it was found that 37 studies had provided no accessible sequencing data, and as such were given a 0 grading for data access. 32 studies provided access to data through publicly accessible means but had provided no means to map the samples and disease or health conditions together and were scored as 1. 8 studies provided data access and identified cohort data in the published text, usually in the form of percentage of samples associated with health or disease, but again had no means to map samples to data and received a score of 2.

Six (6) studies provided access to sample data that was clearly associated via sample identifiers to patients with either caries or health, and were classified as data score 3, i.e. the minimum criterion from the meta-analysis. A further 7 studies provided mappable data with additional cohort data, such as age, sex and sample site, but could not match additional cohort meta-data to samples and were classed as data score 4. Finally, 17 publications provided all previous criteria mentioned, with the added capacity to match additional cohort meta-data to samples, receiving the highest data

score of 5. This resulted in 30 publications with data access above the minimum criteria.

Further scrutiny of these 30 publications was performed, where 11 of these were then excluded based on data quality (improperly uploaded or corrupted data files), low sample number (<5 samples sequenced), sequenced region (Not individual 16S rRNA regions), and *in-vitro* as opposed to *in-vivo* samples. For example, 5 were not case controlled and used a 'disease only' cohort. This resulted in 2016 total processable samples from 19 studies for final analyses, the details of which are outlined in Table 2-1. These studies were initially analysed with respect to basic factors associated with study design and sample processing. Figure 2-3**,** below, illustrates some variability in study characteristics, location, and methodologies across this cohort of 19 combined studies. When sorted by sample number, Australia was the most prominent location for caries led 16S microbiome analysis. Additionally, more than two thirds of the overall sample population were taken from children. Supragingival plaque and saliva were the two most favoured sampling sites. Illumina was the preferred sequencing platform with majority of samples being processed via Illumina MiSeq. The most prominent variability was observed in the sequenced region of the 16S gene, though the V1-V3 and V3-V4 regions were favoured. Moreover, the DNA extraction methods varied significantly from study to study, with chloroform extraction being the most favoured methodology.

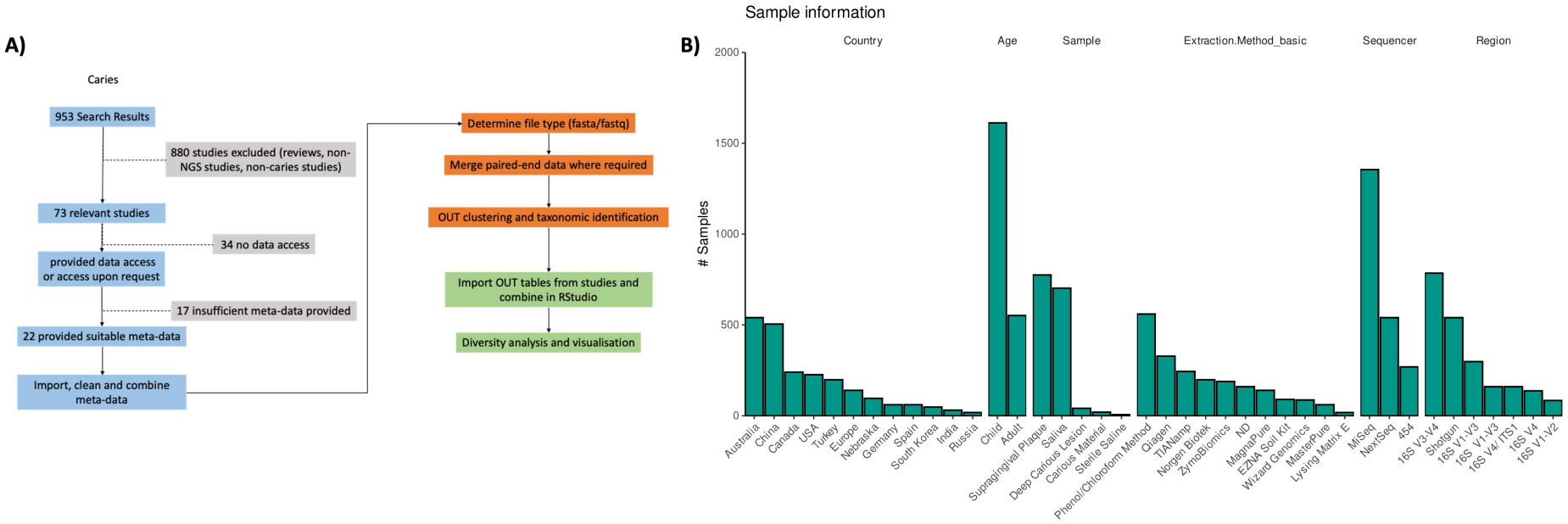


**Figure 2-3 - Study curation, meta-data processing and study characteristics**. A total of 953 studies were assessed for inclusion, of which 19 suitable studies provided suitable data for meta-analyses (a). Breakdown of samples represented as a histogram of total samples for Country, Age, Sample Source, Extraction Method, Platform and Region sequenced (b). Sample data provides an indication of overlaps in interest across studies. Childhood caries was more frequently sampled than adult. Supragingival plaque and saliva are the most common sample types. Chloroform based extraction methodologies represent the largest proportion of extracted DNA. Illumina Miseq was the most popular platform by sample and the V3-V4 site of 16SrRNA was the most prevalently sequenced region.

### *2.4.2 Meta-analytical diversity analysis*

Initial examination of the full study cohort was designed to consider differences in sample diversity both intra- and inter-study through examination of alpha and beta diversity matrices, as shown below in Figure 2-4. Sample data were processed and removed if less than 1000 total passed reads before plotting to show the average reads per sample per study. Alpha diversity analysis was conducted using the observed, Chao1, Shannon and Simpson diversity indexes on the combined sample set as shown in Figure 2-4a. Data were plotted and analysed according to whether the sample was classified as being derived from a caries or healthy patient sample. Median values across diversity indices were shown to be significantly higher in average alpha diversity across all measures of diversity, abundance and richness for caries when compared to health ($p < 0.001$).

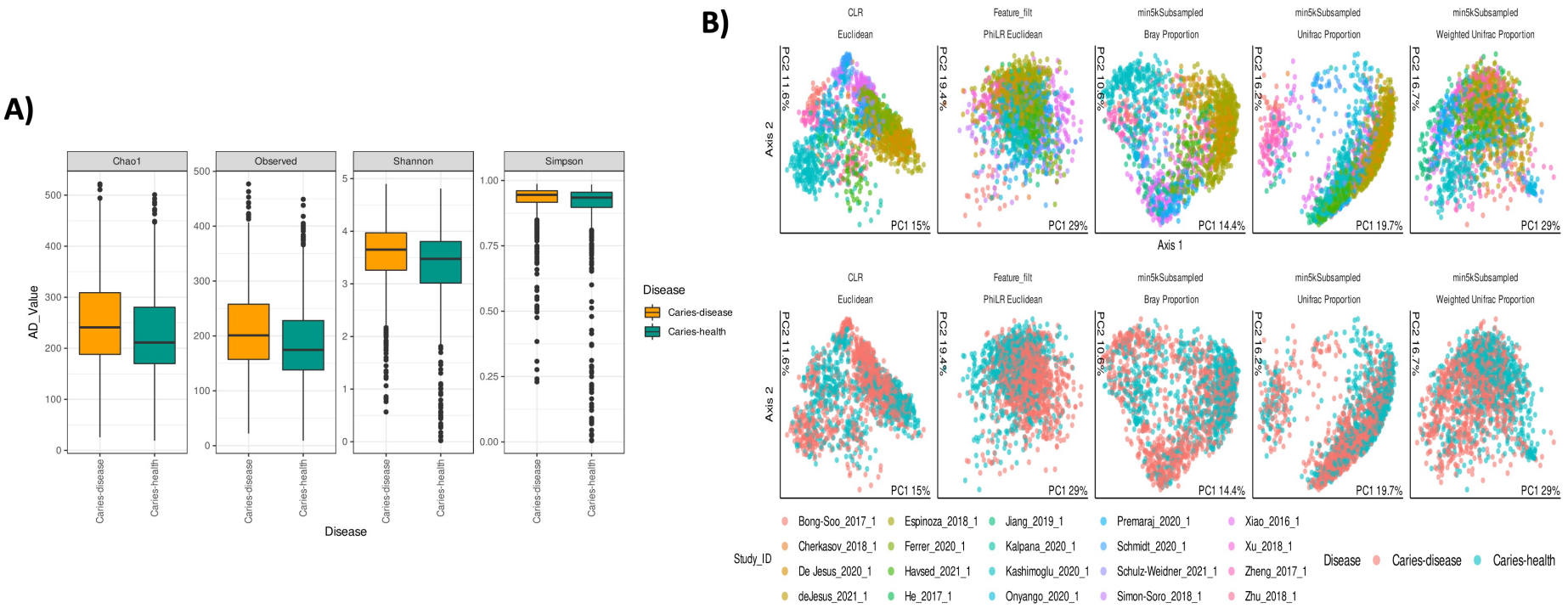


**Figure 2-4 - Alpha and beta diversity of 19 key caries microbiome sequencing studies.** Diversity within samples, **a**), displayed statistically significant differences across all diversity metrics connected to abundance (chao1), observed diversity, richness and distribution (Shannon) and proportional biodiversity (*P < 0.0001*). Diversity between samples, **b**), displayed visually distinct and statistically significant clustering of samples based on study ID, sample type (health/disease) in distance variables.

We next utilized visualization of beta diversity to assess the differences in community composition based upon our different parameters through principal coordinates analysis of multiple distance metrics as in Figure 2-4b, above.

Data were separated through colour demarcation where colours were assigned to caries (pink) and health samples (blue) in the top panel, and individual studies in the bottom panel. As noted by Bisanz et al (2019), due to matrix sparcity, phylogeny aware matrix was used, and visual clustering was observed (19). Specifically, Unifrac, Bray–Curtis and Euclidean, based on CLR normalized data, diversity matrices observed clear clustering of samples from the same study when analysing study-to-study diversity.

### *2.4.3 Diversity analysis of Adult Vs. Childhood caries*

Next, we separated the sample data to assess potential differences between by childhood versus adult caries, as depicted below in Figure 2-5. This was motivated by the volume of samples identified as taken from children in the cohort data being approximately one third of the total sample population.

The Chao1 and Observed diversity indexes show that there was no significant difference between disease and health in adults. However, Shannon diversity index revealed significant differences ($p < 0.001$) between caries and health in adults and children. While the matrices were successful in determining significance between disease and health, there were less significant differences between adult and childhood organism diversity in the Chao1 ($p < 0.05$) and Shannon ($p < 0.01$).

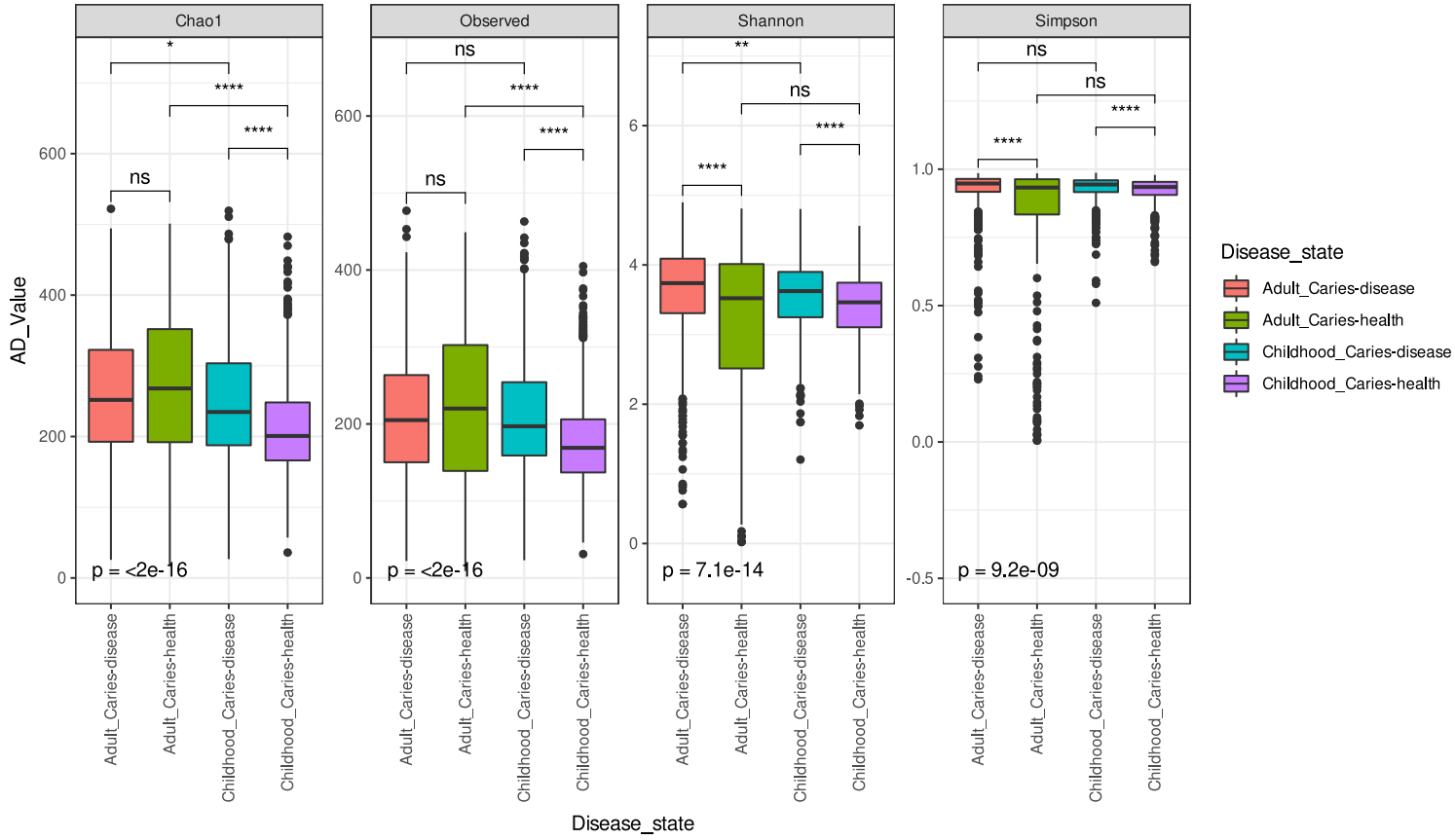


**Figure 2-5 - Alpha diversity matrices comparing adult and childhood caries.** Chao1, Observed, Shannon and Simpson diversity indexes are shown for each comparison. Lower median values for childhood samples in Chao1, Observed and Shannon indexes reveal lower microbial diversity in healthy childhood samples when compared with all other samples.

Similar observations were also noted in Figure 2-6 when analysing sequencing region chosen, where clearly defined clustering was observed by sequenced region across all diversity metrics. This significant difference was also observable when comparing sample types, or health versus disease, across studies. Statistical Significance was observed in the ADONIS statistical metrics across all diversity matrices ($p < 0.001$) as described in Table 2-2.

| | Metric | | | | | | | | | |
|---|---|---|---|---|---|---|---|---|---|---|
| | PhiLR Euclidean | | Unifrac | | Weighted Unifrac | | Euclidean-CLR | | Bray-Curtis | |
| term | R2 | p.value | R2 | p.value | R2 | p.value | R2 | p.value | R2 | p.value |
| Study_age | 0.101938388 | 0.001 | 0.074771487 | 0.001 | 0.063447193 | 0.001 | 0.051072196 | 0.001 | 0.061364569 | 0.001 |
| Disease | 0.017490096 | 0.001 | 0.008774131 | 0.001 | 0.014906838 | 0.001 | 0.007927423 | 0.001 | 0.009398962 | 0.001 |
| Sample_type | 0.193120375 | 0.001 | 0.222602532 | 0.001 | 0.215635827 | 0.001 | 0.246765898 | 0.001 | 0.206706727 | 0.001 |
| Region | 0.064454185 | 0.001 | 0.068419257 | 0.001 | 0.081760249 | 0.001 | 0.084076437 | 0.001 | 0.065316285 | 0.001 |
| Study_ID | 0.086367789 | 0.001 | 0.041523423 | 0.001 | 0.069006055 | 0.001 | 0.072047183 | 0.001 | 0.063841874 | 0.001 |
| Residual | 0.536629167 | | 0.58390917 | | 0.555243838 | | 0.538110864 | | 0.593371582 | |

**Table 2-2 - ADONIS values of diversity across sample cohort.** Statistical analysis reveals significance ($P < 0.001$) across all diversity matrices**.**

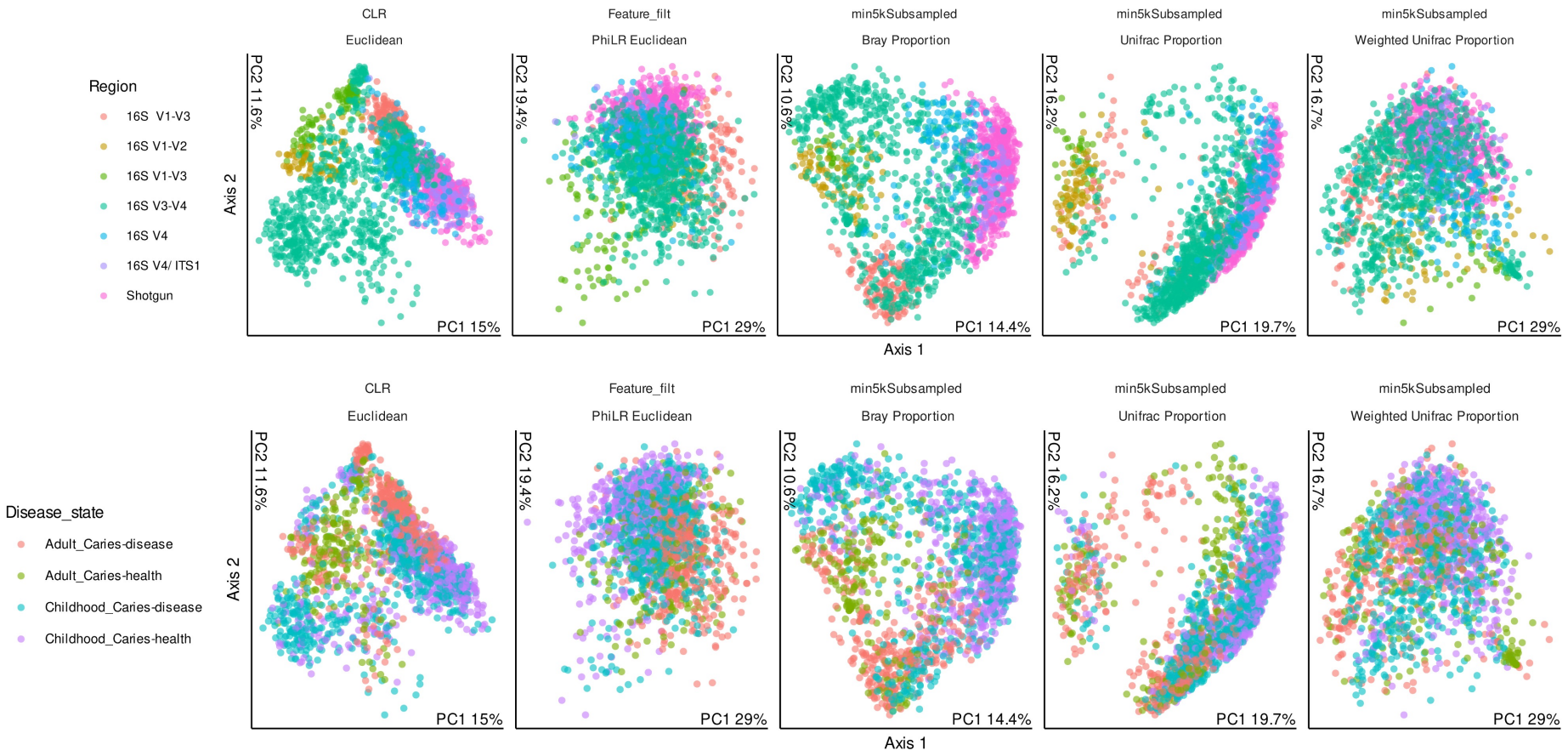


**Figure 2-6 - Principal coordinate analysis of caries oral samples depicting beta diversity of microbial population.** (Top) Amplified 16S sequence region and (Bottom) Adult and childhood health and disease. Overall, clustering of samples based on sequence region is most prominently identifiable when observed using Euclidian, Bray-Curtis and Unifrac similarity metrics. When comparing health and disease, sample clustering is only marginally distinguishable using Euclidian metrics.

### *2.4.4 Prediction of caries status based on sequencing data.*

Following this, we aimed to evaluate the predictability of caries disease state using Receiver operating characteristic curves (ROC) derived from random forest classifiers across Genus, Kegg Orthology (KO) assignment, OTUs, Phylogenetic Isometric Log-Ratio Transform (PhILR) and Species. We initially adapted a training set from a subset of 4 high-impact studies out of the 20 case-controlled sample set. We demonstrated that the ‘disease only’ study test set was the only one found to be predictable in the KO group, with an approximate Area Under the Curve (AUC) of 0.75. We observed marginal improvement of the predictability of health and disease in the complete test data set when applying a 80/20 train-test split.

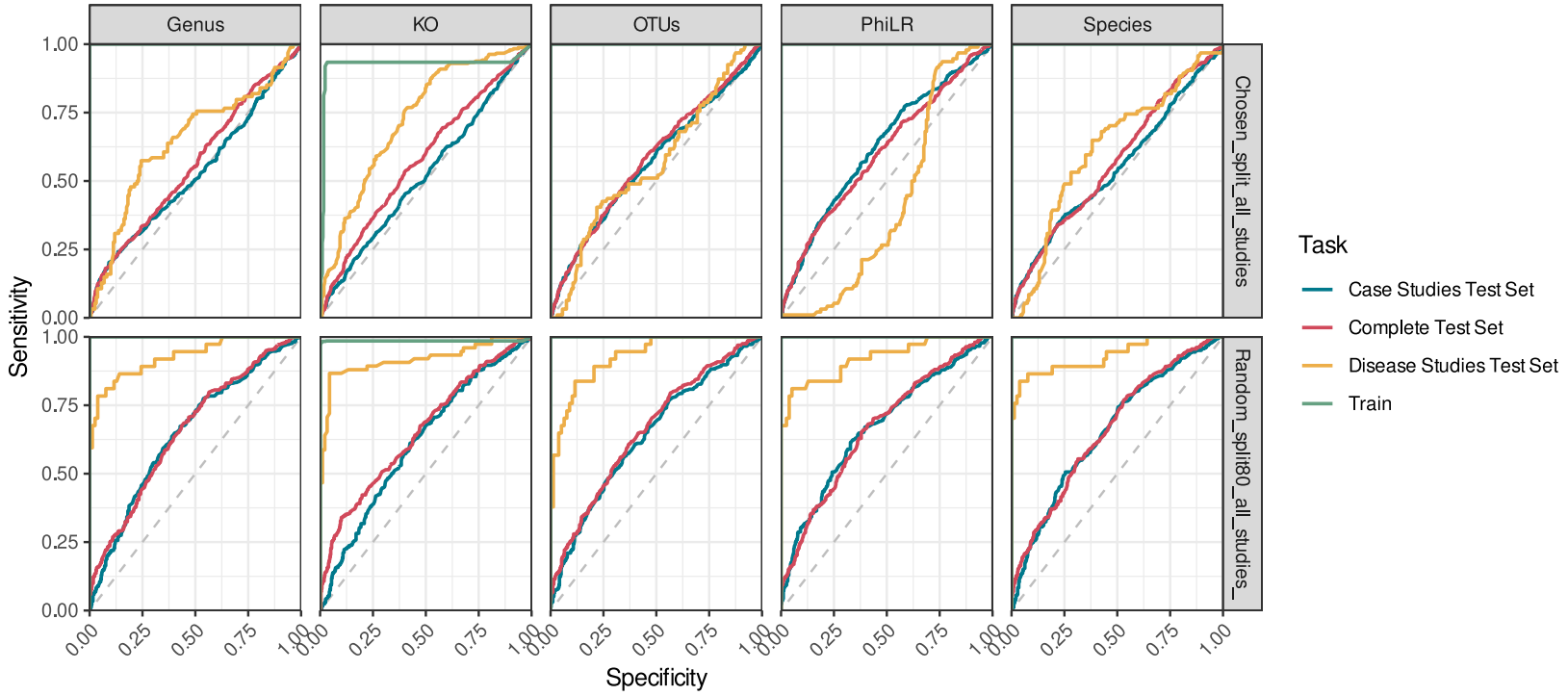


**Figure 2-7 - Receiver operator curves (ROC) from random forest based upon feature tables summarised to OTU, Genus, Species, PhilR, and Kegg Orthology (KO).** Sample differentiation determined by area over curve compared for each functional group, where a value closer to 1.00 represents a clear ability to predict caries status. Data was trained using 4 case-controlled studies compared to all remaining studies (top) and an 80/20 split of all available sample data to training dataset (bottom). Chosen split training data provided no clear trend in sensitivity or specificity across characteristics. Random split data provided a clearer identification of disease specific studies but not in case controlled or complete data test studies.

### *2.4.5 Observing trends in metabolic activity across taxonomic profiles.*

Next, we observed biological pathways associated with cohort microbiome data assessment of KO, as shown in Figure 2-8, below. In this we found the highest number of distinct pathways that were associated with caries to be phosphonate and phosphinate metabolism and glyoxylate and dicarboxylate metabolism (p.adj = 0.04), both key processes in fuelling carbohydrate metabolism (Moye et al., 2014, He et al., 2017). Conversely, we found carbon metabolism and cofactor biosynthesis to be less significantly associated with caries across the cohort of studies (p.adj = 0.09), both of which are essential metabolic pathways associated with cell synthesis (Ducker and Rabinowitz, 2017). The most abundant feature observed was that of the two-component regulatory system, which is associated with a response to environmental factors, as well as an upregulation in microbiological virulence factors (Tiwari et al., 2017, Jacob-Dubuisson et al., 2018).

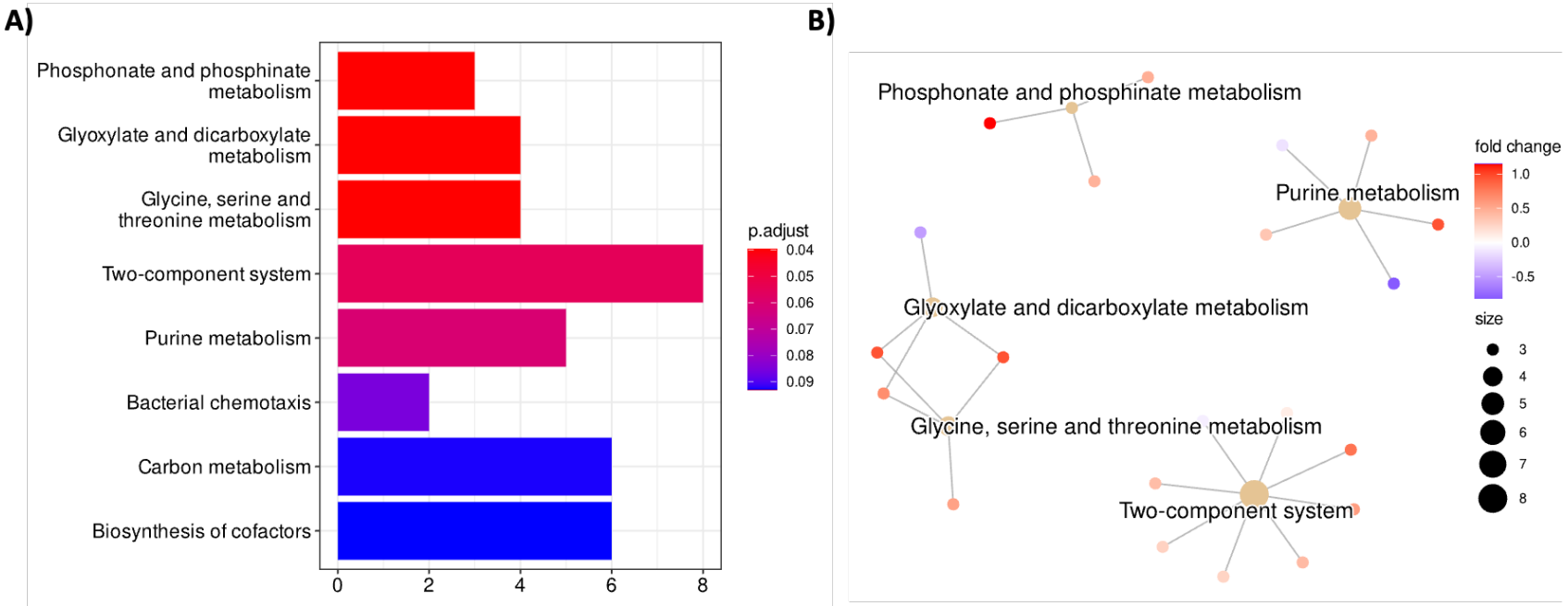


**Figure 2-8 - Metabolic activity outlined using Kegg Orthology and taxonomic predictive values.** 140 features chosen by cross validation of the the random forest training set. KEGG ontology over representation analysis was performed within clusterprofiler. The most overenriched pathways are shown. Number of kegg orthology features derived from picrust and the coloured by their adjusted p-value (**A**). Pathways are also shown in relation to one another with the feature colourised to indicated whether more represented in disease (red) or more represented in health (blue) (**B**).

### *2.4.6 Trends in microbial influence across disease and health.*

Next, differential weighting of microbial taxonomy was examined to predict organisms which would be of relevance in both health and disease based on study cohort data. When assessing differential microbial distribution across all studies as in Figure 2-9, a mean decrease in accuracy was most obvious in *Capnocytophagia* spp HMT-338, *Lactobacillus panis, Treponema* spp. HMT-230, *Bifidobacterium longum, Delftia acidovorans* and *Staphylococcus schlieferi* inferring that these organisms are important when predicting between or “health” and disease groups. Conversely, *Selenomonas* spp HMT-146., *Agregatibacter actinomycetemcomitans*, *Actinomyces* spp HMT-896 and *Treponema* spp HMT-257 observed a higher $\log_2$ fold change in prediction of the carious microbiome

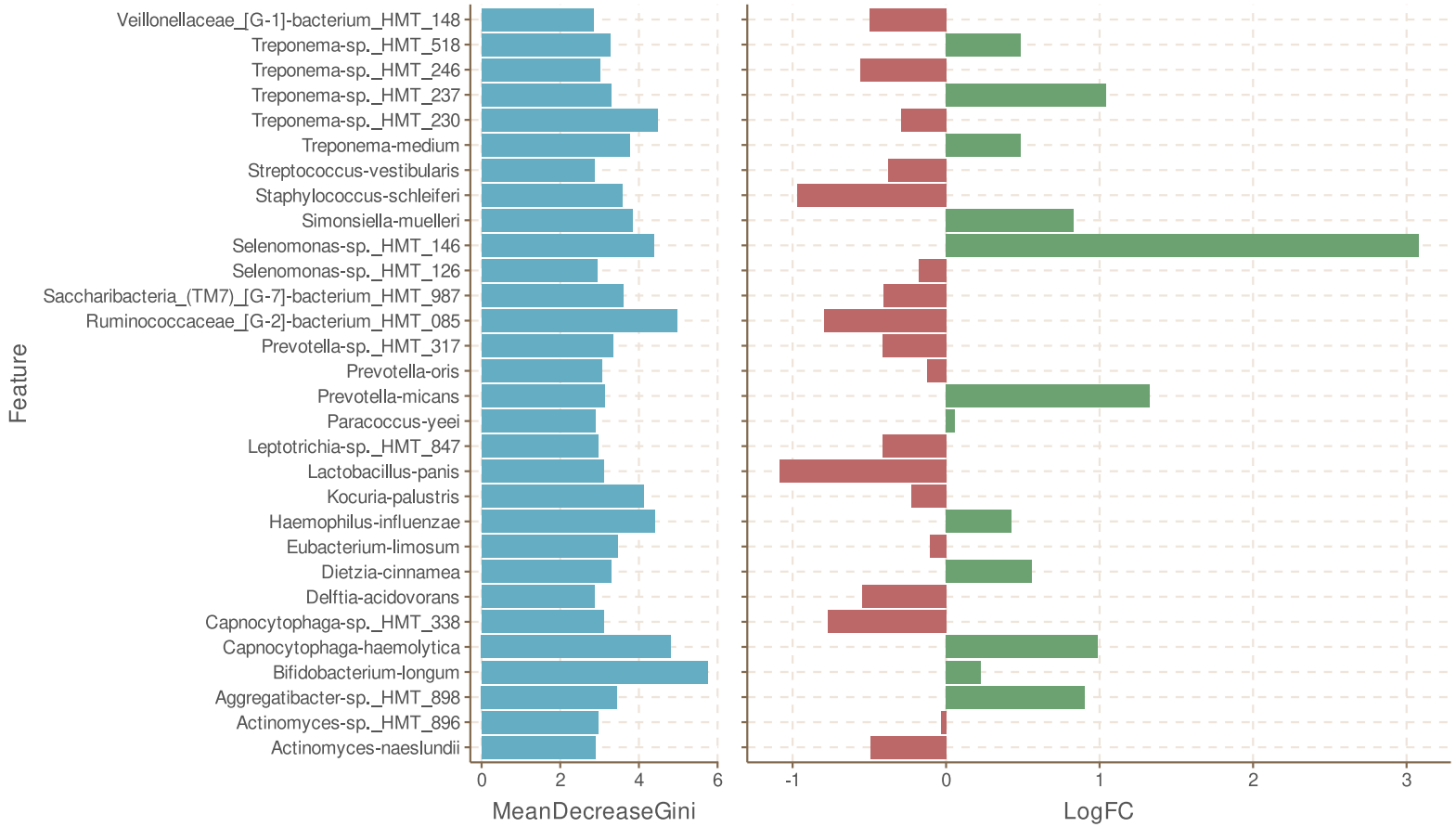


**Figure 2-9 - Differential distribution of microbes when comparing caries and health across study cohort.** Bacterial species selected by mean decrease in accuracy of the Gini coefficient in the random forest classifier for determining differences between the two groups. The corresponding differential abundance of each of the features is represented by its log2 fold change between Caries and Health. Organisms denoted in green are more important in prediction of carious microbiome while those in red are more predictive of “healthy” microbiome**.**

### *2.4.7 Comparing impacts of individual studies across diversity matrices*

Finally, we wished to examine the overall “predictive” ability of individual studies within the cohort when compared to the collated data. Finally, as depicted in Figure 2-10 we calculated area under the curve using random forest classifiers for 15 individual studies to identify their predictive capacity for determining caries microbiome. 3 studies were removed from the initial cohort as they did not contain comparisons between health and disease, either being health only or disease only. Among these classifiers, studies performed by Bong-Soo et al (2017), Zhu et al (2018), and Jiang et al (2019) (Kim et al., 2018a, Zhu et al., 2018, Jiang et al., 2018), were found to perform the best as differentiators between health and disease, with mean AUC scores over 0.75 Figure 2-10a. No correlation was observed between cohorts to determine which diversity metric was the most accurate predictor of disease. Additionally, we calculated alpha diversity indices denoted by $Log_2$ fold change between disease and health across these studies Figure 2-10b. A significant increase in Chao1 richness was observed in 3 of the 15 studies, while observed abundance was also increased significantly ($P < 0.05$) in the same 3 studies, as well as pooled studies. Overall, there was little significance to be observed in alpha diversity metrics across the sample study groups.

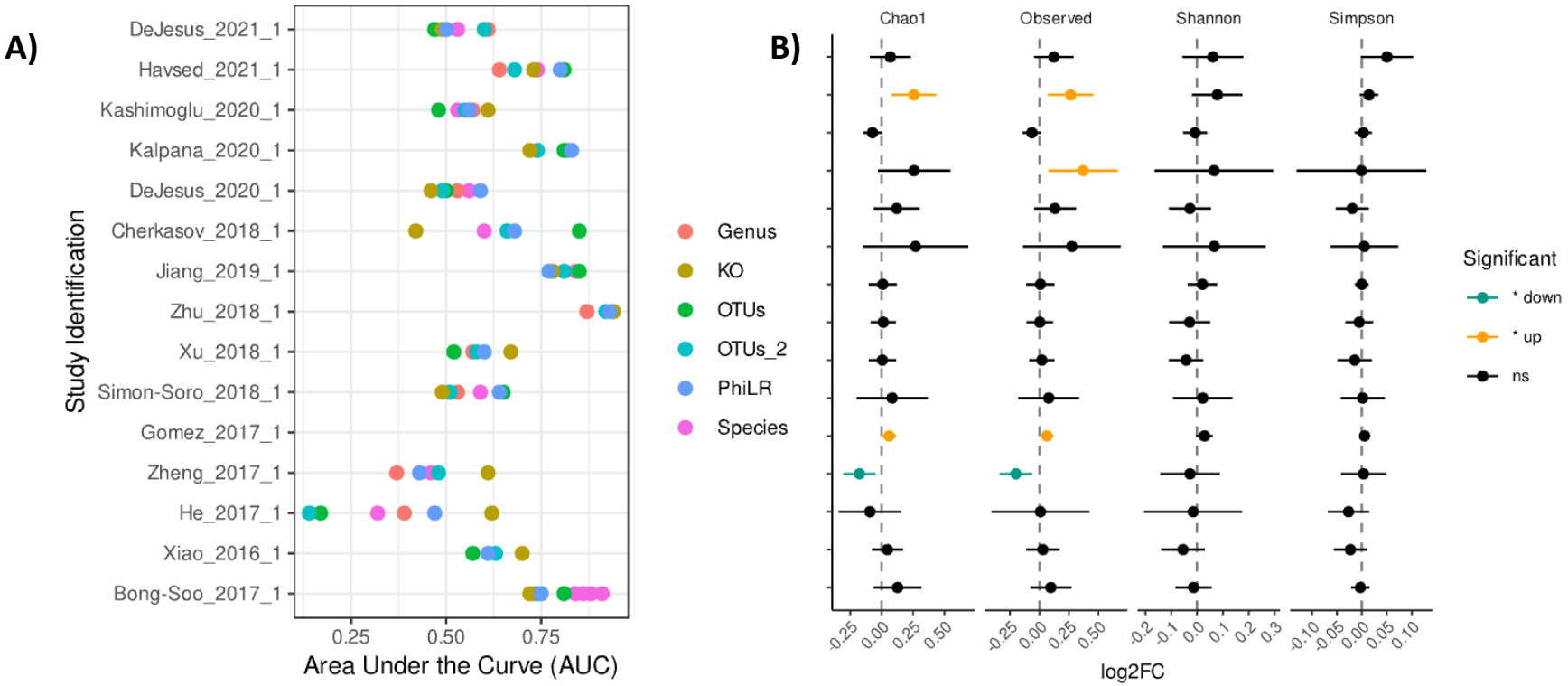


**Figure 2-10 - Comparison of microbiome diversity across case-controlled studies. A**) Area Under the Curve was calculated for the performance of the random forest classifier in each of the case-controlled studies between the Caries and Health groups. Random forest classification was performed by categorization on feature tables at OTU, Alternate mapped OTUs (OTUs_2), Genus and species level. Additionally, it was performed on Kegg Orthology (KO) derived from picrust and phylogentic transformed data (PhILR). **B**) For each study, the diversity indexes Chao1, Shannon and Simpson were calculated and are represented as a Log2 fold change between disease and health. Welch's t-test was performed, and points were coloured when the significance = $p < 0.05$.

## 2.5 Discussion

The microbiome has been closely linked to human health and disease in many contexts and continues to gain ground in terms of accessibility through technological breakthroughs, economic viability, and higher throughput sample processing (Shreiner et al., 2015, Zheng et al., 2020, Young, 2017). In the oral cavity, the concept of ecological changes to the environment has been examined in detail as a fundamental starting point for hypotheses surrounding disease development (Nyvad and Takahashi, 2020, Rosier et al., 2014, Hajishengallis et al., 2012). Indeed, as the microbiome has been explored in the context of oral healthcare, many positive implications have been found to support defined taxonomic differences in health and disease in periodontitis (Guerra et al., 2018, Chen et al., 2018). However, it is largely understood that development of the disease microbiome in periodontitis remains ecologically distinct from caries due to key differences in subgingival sample sites and mounting immunological pressure from the host response (Shi et al., 2018a, Hong et al., 2015).

In this study we sought to take a broader contextual view of caries and examine multiple studies related to caries microbiome research to determine what, if any, key microbiological markers could be used to provide discern whether there was distinct cariogenic microbiome profile. We hypothesised that individual studies lack power to accurately describe whether a specific microbiome profile is associated with caries, and through amalgamation of publicly available study data. To begin with, we examined the literature in a wider scale, using study selection and data extraction techniques derived from systematic reviews and meta-analytic microbiome research, comparable to those studies carried out by Guerra et al (2018) and Romano et al

(2021) (Romano et al., 2021, Guerra et al., 2018). This approach ensured a stringent and non-biased collection of study data that could be used to inform our analytics of the landscape of caries sequencing research. This initial examination of the literature, as summarised in Figure 2-3b, outlined a lack of uniformity in study methods and drew to our attention to the wide differentiation between many different, and potentially severely impactful, metrics across the available datasets. Indeed, work carried out by Scherz et al (2021) has highlighted the need for quality control in microbiome driven research, and a call for uniformity across methodologies to ensure the collectively available pool of knowledge surrounding microbiome research, not only for oral health, is as accurate, reproducible and representative as possible (Scherz et al., 2022). In addition to this, of the initial 73 studies we determined to meet the minimum criteria for data collection, worryingly only 30% of these were found to have sufficient access to data that would permit meta-analysis. While there is a trend towards better inclusion rates for sample data, as peer-review requirements for data upload have improved over the last decade, there is still an obvious gap in the standard of uploaded data in terms of its completion and consistency, as highlighted by Langille et al (2018) (Langille et al., 2018). Indeed, the implementation of protocols such as “Strengthening The Organization and Reporting of Microbiome Studies” (STORMS) further emphasise our call for consistent and standardised reporting of microbiome data in oral research (Mirzayi et al., 2021). Indeed, little is done to address the potentially multi-factorial impact of circumstances surrounding environment and healthcare as would be covered by Social Determinants of Health (SDH) (Tellez et al., 2014).

Like landmark meta-analysis of microbiome data that have been performed on the gut microbiome, the data utilised was accessed through the PubMed® database(Duvallet et al., 2017).

It should be stated, however, that as we have limited published studies to those only obtainable via PubMed®, this leaves a wide array of published material available via other archives to be interrogated. We also acknowledge that studies excluded from pre-2012 may have provided more data but we do not believe would have inferred any different outcome in terms of standardised methodologies.

Despite these barriers, we were however able to access and process data from 19 studies. In alpha diversity metrics across these combined studies, we observed significant differences in diversity, richness and abundance across health and caries. This is a significant and novel finding because at an individual study level previous data sets from within some of the cohorts were unable to report any significant differences in their populations (Chen et al., 2015, Shi et al., 2018b, Jiang et al., 2018, Hurley et al., 2019, Baraniya et al., 2020). This would immediately imply the value in collaborative combination of study cohorts in predicting disease outcomes, while also indicating the benefit of larger cohort sizes within individual studies as a potential compensatory mechanism. Moreover, while some studies have indicated that age can be an important factor in caries status (Foxman et al., 2016, Burcham et al., 2020), and while we found some significant differentiation in alpha diversity between childhood and adult caries and health in the cohort metadata, the comparisons of interest between health and disease in each sub-group also showed significant differences. We also aimed to examine other confounding factors that could explain some negative findings to individual studies. We therefore assessed the impact that

the sequencing region played amongst the combined study cohort. As stated previously, it has been well defined in the literature that the selected 16S rRNA region amplicon can have a profound impact on the amplification of select taxa within the sample (Clooney et al., 2016, Chen et al., 2019). Indeed, our own findings indicated clear clustering amongst amplicon region, while showing minimal definable clustering between health and disease across beta diversity matrices.

We next applied area under the receiver operator curve (ROC) analysis based on random forest feature tables to investigate the ability to predict caries. This was accurate across each feature parameters when disease specific studies were separated but was unable to reliably predict caries status on the full combined cohort. This is reflective of results found by Zhang et al (2020), where prediction of caries disease was not achievable from tested genera (Zhang et al., 2020). Notably, this conflicts with studies conducted by Teng et al (2015), Zhu et al (2018) and Wu et al (2021) (Teng et al., 2015, Zhu et al., 2018, Wu et al., 2021b), where they have reported reliable prediction of caries onset through microbiome analysis. However, it should be stated that multifactorial differences are visible in the ability to readily predict disease outcome. For instance, It has been reported that onset of caries in a longitudinal setting is independent of genetic factors, while being impacted by acquired behaviours, and that predictability of disease is compounded by these factors as well as other microbial elements, such as the prevalence of *Candida albicans* (Freire et al., 2020, Lif Holgerson et al., 2020, Wu et al., 2021b). This is a glaring omission in all of these studies, and the inclusion of mycobiome analysis may be a helpful tool to support our understanding of caries-related plaque. Indeed, while our initial analytic intent was to encompass the mycobiome and fungal related research, we found only 1 fungal

mycobiome study that we were able to shortlist from available publications to carry forward for robust analysis. Interestingly, our analysis of KO elements provides valuable insight into the potential mapping of metabolic profile to disease prediction given the observed trend from common baseline metabolic pathways to those more abundant in virulence and sugar metabolism which are key factors in degradation of caries outlook. Taken together, the use of sophisticated bioinformatic tools from profiled microbiomes and mycobiomes will enhance our ability to predict and manage oral disease with a greater level of confidence. Indeed, we identified *Selenomonas* spp HMT-146., *Aggregatibacter actinomycetemcomitans*, *Actinomyces* spp HMT-896 and *Treponema* spp HMT-257 as prevalent within the cohort data as markers of caries. These organisms have been routinely isolated in previous studies investigating caries microbiome, while also being linked to cariogenesis and abundance in high sucrose environments (Gross et al., 2010, Lamont et al., 2018, Chen et al., 2001). This, again, emphasises the essential need to assess environmental factors in determination of caries outcome alongside microbiome driven research to predict a definitive outcome. Additionally, the recurrence of *Treponema* species as potential differentiators for both health and caries continue to drive the emphasis that being able to reliably speciate within microbiome analysis is essential in disease profiling (Allaband et al., 2019). Finally, the lack of representation of *Streptococcus*, particularly *Streptococcus mutans*, as an impactful predictor of caries does not mesh with the conventional understanding of the disease profile and perhaps encourages the need to move away from convention and pre-disposed bias in the light of new methodologies and data.

Finally, we analysed the study cohort data on an individual level, using AUC scores to determine predictability of caries on a case-by-case basis. These individual studies

were then investigated for correlating factors in study design which may have provided insight into the “best-practice” for achieving a microbiota specific diagnosis. We were unable, however, to determine any obvious overlapping factors in study design which could be attributed to this but may be resultant from factors that were not readily shared in the study publication. Surprisingly, AUC scores were not heavily impacted by sample site, as sample type varied across studies. The inconsistencies that are visible from these analyses also have wider reaching implications in the reliability of producing pre-clinical biofilm models that can accurately provide a basis for experimentation on caries *in-vitro,* such as those previously published by our own group (Zhou et al., 2018, O'Donnell et al., 2015a). Indeed, the future direction of travel for the development and testing of new oral hygiene therapeutics may be in the use of undefined biofilm consortia that can be easily analysed using cheaper and more reliable sequencing technologies.

## 2.6 Concluding remarks

As the field of microbiome research continues to expand at a rapid pace, and the volume of microbiome data that is generated increased, then we should be mindful of a potential trend towards continuing to develop non-standardised methodologies or insufficiently differentiated microbiome analyses which, as previously indicated by Holman et al (2015), may provide room for bias (Holman et al., 2015). This is of relevance when considering the sequencing region selected for analysis. In addition, we re-iterate the need for larger volumes of samples being sequenced to increase the relevance of individual studies being generated as a reliable metric for microbiome characterisation. Indeed, through advancement of available sequencing technologies and techniques which can analyse the entire 16S gene in a cost and time-effective

manner, we believe that a shift towards broad standardisation of methods is attainable in the near future (Jeong et al., 2021, Matsuo et al., 2021)

# 3 *C. albicans* phenotype affects key caries outputs *in-vitro* and *ex-vivo.*

## 3.1 Introduction

Dental caries is one of the most prevalent chronic diseases in humans, which is influenced by both the biofilm structure and microbiome composition (Casamassimo et al., 2009, Struzycka, 2014) While the role of bacteria in such conditions is well recognised (e.g. *S. mutans* and *Lactobacillus* spp.), the role of *Candida* spp. is largely unknown, unexplored or disregarded due to the bias towards bacterial biofilm communities. Indeed, the previous chapter has shown that these data are rarely available in sequencing datasets for consideration when looking for critical microbial drivers of caries.

There is growing evidence that *Candida* have a significant influence on oral microbiome composition and pathogenicity. High levels of *Candida* species have been reported in children with caries (Raja et al., 2010a), though, there is limited evidence for its direct association with dental caries (Sridhar et al., 2020). Indeed, it was recently shown that *C. albicans* was not more abundant in children with caries, although those children showed less fungal abundance and diversity compared with caries free children (Fechney et al., 2019b). There is also evidence that caries is not limited to children, with adult caries also linked to *Candida* spp. Furthermore, there is also a growing body of evidence that *C. albicans* presence is sufficient to catalyse bacteria to promote caries, suggesting interkingdom interactions are critically important (Caroline de Abreu Brandi et al., 2016). These factors may explain why so little is known, or little emphasis is given, to *Candida* with respect to caries.

Typically commensal in nature, *C. albicans* has also been well established that the development of pathogenicity is driven by environmental factors which lead to its

overabundance or phenotypic switching to a more pathogenic hyphal morphology (Slutsky et al., 1985). While this has been found to aid in adhesion to oral surfaces, both biological and inert, it also provides a substrate and environmental niche for other micro-organisms. O'Donnell and colleagues (2017) previously reported that there is significant heterogeneity in *C. albicans* isolated from saliva, and dental and denture plaque from the oral cavity of denture patients (O'Donnell et al., 2017). These same data also suggest that *Candida* influences the oral microbiome in patients that are partially dentate. *Candida* heterogeneity is a phenomenon that the Ramage laboratory have focused on, showing that metabolic processes and responses to environmental stressors are different depending on the biofilm phenotype of the *C. albicans* isolate (O'Donnell et al., 2017, Sherry et al., 2014). These low and high biofilm forming phenotypes are distinct, with biofilm formation being inducible under certain circumstances.

## 3.2 Hypothesis and aims

In this study, it was hypothesised that alteration of *Candida* phenotype directly influences the microbial and cariogenic profile of a multi-species biofilm. *C. albicans* isolates with high and low biofilm phenotype were selected for co-aggregation assessment with other organisms of a previously published "caries" biofilm model and profiled based on biomass, metabolism, drug response and response to environmental stimuli such as sucrose. Multi-species biofilm models were grown on bovine enamel and assessed for shifting microbial profile, acidogenesis and alteration of substrate when exposed to environmental stimuli.

## 3.3 Methodology

### *3.3.1 Microbial culture, maintenance and standardisation*

In this study, 72 clinical isolates of *C. albicans*, collected as part of previous studies by O'Donnell et al., in 2017, were utilised (O'Donnell et al., 2017). Additionally, a type-strain of *C. albicans*, SC5314, and a biofilm deficient strain SSY-50B (SSY) were utilised as control organisms (Saville et al., 2008). Bacteria from a previously established complex biofilm model, alongside *Staphylococcus schleiferi*, identified as an organism of interest in the meta-analysis (Figure 2-92.4.6 Trends in microbial influence across disease and health.), were utilised throughout the study (Brown et al., 2023). Additionally, Table 3-1, below, outlined detailed culture criteria for each organism grown during this study.

Cultures used were recovered from Microbank™ beads (Pro-Lab Diagnostics, Wirral, UK) which had been stored at -80°C until required. All cultures were recovered on solid media, identified in the list below, and with relevant culture and incubation conditions (Table 3-1):

- Sabouraud's Dextrose Agar (SAB; ThermoFisher®, Renfrew, UK)
- Columbia Agar supplemented with 5% Defibrinated Sheep Blood (CBA; E&O Laboratories, Bonnybridge, UK)
- Fastidious Anaerobic Agar (FAA; ThermoFisher®, Renfrew, UK)
- DeMan-Rogosa-Sharpe Agar (MRS; ThermoFisher®, Renfrew, UK)

Following growth, cultures were maintained as required at 4°C. To standardise organisms in preparation for experimental conditions, cultures were propagated

overnight in the relevant liquid media outlined in Table 3-1, and as identified in the list below:

- Yeast Peptone Dextrose broth (YPD; Merck LTD, Livingston, UK)
- Tryptone Soya Broth (TSB; ThermoFisher®, Renfrew, UK)
- Schaedler Anaerobe broth (SCH; ThermoFisher®, Renfrew, UK)
- Brain-Heart Infusion broth (BHI; ThermoFisher®, Renfrew, UK)
- DeMan-Rogosa-Sharpe broth (MRS; ThermoFisher, Renfrew, UK)

To aid propagation, microbial cultures were shaken while propagating overnight at a speed of 200RPM. Before standardising to a known concentration, overnight cultures were pelleted, via centrifugation at a speed of 3,000 x g, and washed twice via resuspension in phosphate buffered saline (PBS; ThermoFisher, Renfrew, UK). *Candida* cultures were counted via Neubauer Haemocytometer (Scientific Lab Supplies, Nottingham, UK) while bacterial cultures were adjusted, via dilution, to a known optical density (OD) which corresponded to $1x10^8$ cells/mL, outlined in Table 3-1, using a Biochrom LTD benchtop colorimeter (SciQuip, Rotherham, UK).

| Microorganisms | Strain | Solid medium | Liquid medium | Growth conditions | Abs. for $1 \times 10^8$ cells/mL (OD) |
|---|---|---|---|---|---|
| *Candida albicans* | SC5314 | SAB | YPD | 30°C | Cell Count |
| *Candida albicans* | SSY-50B | SAB | YPD | 30°C | Cell Count |
| *Streptococcus mutans* | ATCC 25175 | CBA | TSB | 37 °C, 5% CO2 | 0.5 (550 nm) |
| *Fusobacterium nucleatum* | ATCC 10596 | FAA | SCH | 37 °C, AnO2 | 0.2 (550 nm) |
| *Actinomyces naeslundii* | ATCC 19039 | FAA | BHI | 37 °C, AnO2 | 0.2 (550 nm) |
| *Veillonella dispar* | ATCC 27335 | FAA | BHI | 37 °C, AnO2 | 0.5 (550 nm) |
| *Lactobacillus casei* | DSM 20011 | MRS | MRS | 37 °C | 0.6 (550 nm) |
| *Staphylococcus schleiferi* | DSM 4807 | CBA | TSB | 37 °C | 0.5 (550 nm) |

**Table 3-1 – List of organisms, growth conditions, and standardisation data associated with study design.** All organisms utilised throughout this chapter have been included alongside strain identifier number based on their associated collection library of the American Type Culture Collection (ATCC) or the Leibniz-Institut Deutsche Sammlung von Mikroorganismen und Zellkulturen GmbH (DSMZ). Also included are the culture mediums for reconstitution and liquid culture as well as optimal growth conditions and culture standardisation details. Table adapted from Brown et al., 2023.

### *3.3.2 Complex media preparation*

Beyond media requirements for maintenance and overnight growth (Table 3-1), all other experimental processes were performed using a complex media combining Roswell Park Memorial Media-1640 (RPMI; Merck, Livingston, UK) in a 1:1 ratio with Todd Hewitt broth (THB; Merck, Livingston, UK), supplemented with 4mg of haemin (ThermoFisher, Renfrew, UK) and 80μL of 10μM menadione (Merck, Livingston, UK) as adapted from methodologies outlined by Abusrewil et al., in 2020, and Montelongo-Jauregui et al., in 2016 (Montelongo-Jauregui et al., 2016, Abusrewil et al., 2020). The resulting solution would be referred to as RPMI:THB throughout the study.

### *3.3.3 Isolate screening for pH, metabolic activity, and biomass*

Prior to standardisation, overnight cultures of *C. albicans* were assessed via OD at a wavelength of 600nm as an indication of overnight growth. Isolates were then standardised as indicated above (3.3.1) before being diluted to a concentration of $1x10^6$ cells/mL in RPMI:THB media. 200μL of this inocula were transferred to all relevant wells of a Corning™ Costar™ 96-well, flat bottom, microtiter plates and incubated at 37°C, with 5% $CO_2$ for 24-hours (ThermoFisher, Renfrew, UK) for downstream assessment in the following ways:

#### *3.3.3.1 pH*

After overnight incubation, 200μL of supernatant from *Candida* cultures was transferred to a fresh 96-well, round bottom, plate, and assessed for changes in pH via a Mettler-Toledo™ FiveEasy™ pH meter with attached Micro pH electrode (Mettler-Toledo, Leicester, UK). This probe was calibrated via pH 4 and pH 7 buffer solutions (Merck, Livingston, UK), and washed and dried between samples. Sample assessment was carried out in triplicate with an average taken for each isolate.

#### *3.3.3.2 XTT metabolic assay*

Prior to assay, biofilms were washed twice with 200μL of sterile PBS. A solution of XTT, (2,3-bis(2-methoxy-4-nitro-5-sulfo-phenyl)-2H-tetrazolium-5-carboxanilide) tetrazolium salt, supplemented with 1μM menadione was prepared prior to washing and kept covered to prevent photodegradation. 100μL of XTT solution was added to all relevant wells of the biofilm plate before incubation, in the dark, for 1hr at 37°C, 5% $CO_2$ before being transferred to a fresh 96-well microtiter plate to be quantified by absorbance at 492nm using a FLUOstar Omega Microplate reader (FLUOstar™, BMG Labtech, UK). (Ramage et al., 2001b).

#### *3.3.3.3 Crystal Violet biomass assay*

Upon recording of metabolic activity, biofilm plates were aspirated of liquid and washed once more with PBS to remove residual XTT before being incubated for 24-hours at room temperature to allow biofilms to dry. A solution of 0.05% Crystal Violet (CV) was prepared via dilution of a 1% stock solution (Merck, Livingston, UK) in water. 100μL of CV solution was then transferred to each relevant well of the biofilm plates and incubated for 20 minutes with mild agitation on a PMR-30 platform rocker (Grant Instruments, Cambridge, UK). Excess CV was aspirated and washed gently with PBS before destaining with 100μL of 100% ethanol (EtOH) where released dye was mixed via pipette 8 times to ensure dispersal before transfer to a fresh 96-well plate for quantification at 570nm using a FLUOstar Omega Microplate reader. (O'Toole, 2011).

### *3.3.4 Quantification of RPMI:THB media effects on growth*

Isolate screening identified 7 strains of *C. albicans* (GSK22, 79, 107, 115, 117,121 and 122) to be carried forward for subsequent analysis alongside type-strain SC5314 using the following methods:

#### *3.3.4.1 Growth kinetics*

Organism growth curves were established via dilution to $2x10^4$ cells/mL in RPMI:THB media for clinical isolates and SC5314, with SC5314 also grown in standard RPMI media as a comparator. Cultures were transferred to 96-well, round-bottom microtiter plates and incubated at 30°C using a FLUOstar Omega Plate reader, over a period of 24-hours, with absorbance readings at 570nm every 15 minutes. Plates were agitated via orbital shaking prior to reading.

#### *3.3.4.2 Effect of dilution on growth and viability*

Isolates GSK22 and 107, were carried forward as exemplary of low and high biofilm formation for subsequent analyses. In addition, SC5314 and SSY-50B were utilised as control organisms to examine how altered nutritional availability might impact biofilm development. To examine this, a dilution series of 100-0% RPMI in supplemented THB was created in 10mL volumes in universal tubes (ThermoFisher, Renfrew, UK). *C. albicans* cultures were then propagated and standardised as in section 3.3.1, before being resuspended and diluted across a gradient from $1x10^6$ cells/mL. to $1x10^3$ cells/mL in 10mL volumes. Isolates were then pelleted via centrifugation for 5 minutes at 3000 x g before being resuspended in the diluted volumes of 100%-0% RPMI in THB. These were then transferred to a 96-well, flat-bottom microtiter plate for growth at 37°C, 5% $CO_2$ for 24-hours before being assessed via biomass and viability assays as outlined in section 3.3.3.

#### *3.3.4.3 Effect of dilution on SC5314 growth kinetics*

*C. albicans* SC5314 was grown and standardised, in the manner described in section 3.3.1, to concentrations of $1x10^6$ cells/mL and $1x10^4$ cells/mL, before being pelleted via centrifugation and resuspended in RPMI:THB which had been diluted in the same gradient as described in the previous section. These inocula were then transferred to

96-well, round-bottom plates and assessed for growth kinetics at 30°C using a FLUOstar Omega plate reader at a wavelength of 570nm over a period of 40-hours with readings taken every hour. Plates were agitated via orbital shaking prior to reading.

### *3.3.5 Quantification of sucrose and starch effects on media*

Isolates were processed and analysed as outlined in section 3.3.4.2 but using RPMI:THB media supplemented with 2.5% starch diluted across a gradient to 0.0045% and 10% sucrose diluted to 0.02%.

### *3.3.6 Quantification of sucrose effects on biofilm pH*

Fungal isolates were standardised to concentrations of $1x10^6$ cells/mL in RPMI:THB and serially diluted to $1x10^3$ cells/mL before being transferred to flat-bottom, 96-well microtiter plates to allow for biofilm development as mentioned previously in section 3.3.3.

All bacterial organisms, as outlined in Table 3-1, were standardised to concentrations of $1x10^7$ cells/mL in RPMI:THB and serially diluted to $1x10^4$ cells/mL and also transferred to flat-bottom microtiter plates for biofilm development over 24-hours in the optimal growth conditions outlined in Table 1.

In separate 96-well plates, a doubling dilution gradient of 10%-0.02% sucrose in RPMI:THB was prepared. After incubation of fungal and bacterial plates, organism growth media was aspirated, discarded and replaced with the diluted RPMI:THB media and re-incubated at optimal growth conditions for a further 24-hours. Following this, sample supernatants were aspirated and transferred to fresh 96-well microtiter plates and assessed for pH changes as outlined in section 3.3.3.1

### *3.3.7 Compositional analysis of caries biofilm model via qPCR*

For compositional analysis of multispecies biofilms, organisms were grown using the culture and standardisation methods outlined in 3.3.1. This would be done in a time-dependent manner to include organisms at relevant stages of biofilm development. Firstly, after standardisation, cultures of *C. albicans* SC5314, GSK22, or GSK107, alongside a culture of *S. mutans,* were diluted, in the same 10mL universal, to $1x10^7$ cells/mL in RPMI:THB media. 1mL of this consortium was then transferred to relevant wells of a Corning™ Costar™ 6-well microtiter plate (ThermoFisher, Renfrew, UK) and incubated for 24-hours at 37°C, 5% $CO_2$. After 24-hours development, cultures of *L. casei*, *F. nucleatum*, *A. naeslundii,* and *V. dispar* would be combined in the same fashion. Prior to their addition to the biofilm, the supernatant of culture media from the previous 24-hours growth was removed and discarded and, again, 1mL of bacterial consortia was added to the plate before incubation at 37°C, 5% $CO_2$ for a further 24-hours. Biofilms were then matured for 4-days, with media removal and replenishment every 24-hours before downstream analysis.

#### *3.3.7.1 Development of caries biofilms*

Once matured, culture media was removed and discarded and biofilms were gently washed, twice, with PBS, with great care taken not to disrupt the biomass. After this second washing, the remaining PBS would be left in the well and the biomass was scraped from the bottom of each well using a Corning® Falcon® Cell Scraper, with a fresh scraper employed for each experimental parameter, until all visible biomass had been resuspended in 1mL of PBS. This cell suspension was transferred to sterile 1.5mL Invitrogen™ DNase- and RNase-free microfuge tubes. All experimental parameters were carried out in triplicate.

#### *3.3.7.2 PMAxx™ treatment of caries biofilms*

Following suspension, DNA from lysed cells was removed from samples before extraction by adding 2.5μL of 20mM PMAxx™ (Biotium Inc, CA, USA), a photoreactive, intercalating dye, which renders DNA insoluble via exposure to UV light (Lv et al., 2020). Samples were then incubated at room temperature, in the dark, for 10-minutes on rocking platform before being transferred to a PMA-Lite™ LED Photolysis device (Biotium Inc, CA, USA) for 15-minutes at a UV wavelength of 465-475nm. Samples were then carried forward for DNA extraction from this point.

#### *3.3.7.3 DNA extraction of caries biofilms*

DNA extraction was carried out using a Masterpure™ Yeast DNA purification kit (LGC Biosearch Technologies, Berlin, DE). To begin with, PMAxx™ treated samples were centrifuged at 13000RPM using a ThermoScientific™ Fresco™ 21 Microcentrifuge (ThermoFisher, Renfrew, UK), set to 4°C, for 5 minutes to pellet samples before removal of supernatant and re-suspension in 300μL Yeast Cell Lysis Solution via pipette mixing. Samples were then transferred to a Grant Academy Unstirred Water Bath (SLS, Nottingham, UK) and incubated for 15 minutes at 65°C before briefly being placed on ice for 5 minutes. 150μL of Milk Protein Concentrate (MPC) precipitation reagent was then added to samples and vortexed for 10 seconds before centrifugation at 13000RPM to remove cellular debris. Sample supernatants were transferred to fresh microcentrifuge tubes containing 500μL of ice-cold Isopropanol and mixed via inversion. Samples were, again, centrifuged at 13000RPM to pellet DNA before removing the sample supernatant and washing the DNA pellet twice with 70% ice-cold ethanol. Excess ethanol was removed and discarded, and samples were left to evaporate for 1-minute before re-suspension of the DNA pellet in 35μL elution buffer

(TE). Samples for short-term or direct use were stored at 4°C or -20°C for long term storage and preparation for quantitative polymerase chain reaction (qPCR).

#### *3.3.7.4 Quantification of DNA via Qubit™ Fluorometer*

Sample DNA was quantified using a Qubit™ dsDNA Broad Range (BR) Assay kit. In brief, a working solution of Qubit™ solution was prepared by bulk diluting Qubit™ dsDNA BR Reagent in Qubit™ dsDNA BR Buffer at a ratio of 1:200 for as many samples as required.

To create a standard calibration curve for DNA quantification, 10μL of Qubit™ dsDNA BR Standard #1 (0ng/μL DNA concentration) was added to 190μL of working solution in a Qubit™ 0.5mL thin-walled assay tube. This was repeated for Qubit™ dsDNA BR Standard #2 (100ng/μL DNA concentration). Standards were then vortexed for 20 seconds and incubated, in the dark, for 2 minutes, before reading standards fluorometrically via the Invitrogen™ Qubit™ 4 Fluorometer.

To quantify sample DNA, Qubit™ 0.5mL thin-walled assay tubes were labelled on the lid with sample identifiers, and pre-prepared with 198μL of working solution before addition of 2μL of sample DNA. Samples were, again, vortexed and incubated before reading.

#### *3.3.7.5 PCR analysis of caries biofilm composition*

To determine the composition of organisms within the biofilm models, Colony forming equivalent (CFE) counts were generated via amplification of extracted DNA using organism specific primer sequences identified in Table 3-2, below. To begin with, a master mix of PCR reagents was prepared containing 10μL of qPCRBIO SyGreen® mix Lo-ROX (PCR Biosystems, Oxford, UK), 7μL of UltraPure™ DNase/RNase-Free Distilled Water (ThermoFisher, Renfrew, UK), and 1μL each of forward and reverse primers as identified in the table below, with a different master mix made up for each

organism. This 19μL master mix was applied to all relevant wells of an Applied Biosystems™ MicroAmp™ Fast Optical 96-Well Reaction Plate (ThermoFisher, Renfrew, UK) before addition of 1μL of sample DNA with the plate then sealed using flat PCR cap strips (ThermoFisher, Renfrew, UK). The contents of each well were gently flicked to mix the contents before being spun briefly in a microcentrifuge with a 96-well plate adapter before being placed in an Applied Biosystems StepOne™ Real-Time PCR system (ThermoFisher, Renfrew, UK). The plate was then run using the following thermal profile: Holding stage of 50°C for 2 minutes, followed by a denaturation stage of 95°C for 10 minutes and 40 cycles of 95°C for 3 seconds followed by 55°C for 30 seconds. Samples were run in duplicate and with negative controls containing only the PCR master mix and nuclease-free water. Organism CFEs were determined via PCR of known concentrations of DNA extracted from $1x10^8$ cells/mL and diluted to $1x10^3$ cells/mL, for bacteria, or $1x10^7$ cells/mL to $1x10^3$ cells/mL of *Candida* with the resulting standard curves being used to plot the relative CFEs of the sample DNA. CFEs were extrapolated from threshold cycles (CT) using the 2-ΔCt method, and quantified using the 2-ΔΔCt method, as outlined by Rao et al in 2013 (Rao et al., 2013).

| Target | Sequence (5'-3') | Reference |
|---|---|---|
| *C. albicans* | F – GGGTTTGCTTGAAAGACGGTA<br>R - TTGAAGATATACGTGGTGGACGTTA | (Sherry et al., 2016) |
| *S. mutans* | F – GATACATAGCCGACCTGAG<br>R - CCATTGCCGAAGATTCC | (Sherry et al., 2013) |
| *L. casei* | F – TGCACTGAGATTCGACTTAA<br>R - CCCACTGCTGCCTCCCGTAGGAGT | (Desai et al., 2006) |
| *F. nucleatum* | F – GGATTTATTGGGCGTAAAGC<br>R - GGCATTCCTACAAAATATCTACGAA | (Sherry et al., 2013) |
| *A. naeslundii* | F – GGCTGCGATACCGTGAGG<br>R - TCTGCGATTACTAGCGACTCC | (Periasamy et al., 2009) |
| *V. dispar* | F – CCGTGATGGGATGGAAACTGC<br>R - CCTTCGCCACTGGTGTTCTTC | (Periasamy and Kolenbrander, 2009) |

**Table 3-2 - Table of primer sequences used for compositional analysis of caries biofilms.** (Sherry et al., 2016), (Sherry et al., 2013), (Desai et al., 2006), (Periasamy et al., 2009)

### *3.3.8 Study design of ex-vivo biofilms and interventions*

To elucidate the effects of a complex, saliva based *ex-vivo* biofilm model and how it developed in the context of a caries relevant substrate and oral hygiene regimen, the following study design was employed, as outlined in the following sub-sections and as visualised in Figure 3-1**.** In brief, the study was designed to encompass the use of donor saliva as a starting inoculum for the growth of undefined biofilm models and to track their development over a minimum of 3-days. In addition, the biofilms would be grown with, and without, $1x10^6$ cells/mL of *C. albicans* strains SC5314, GSK22, and GSK107 alongside the starting inoculum. Once determined to be mature, the biofilms would be challenged with a 1:1 toothpaste slurry (**Tx**) containing stannous fluoride as an active agent (Proprietary; Haleon LTD, Surrey, UK) and following a toothbrushing regimen, to imitate an oral hygiene method, as observed by studies such as those by Ramage et al., in 2019 (Ramage et al., 2019). To observe subsequent re-colonisation of surfaces, samples would be allowed to regrow for 24-hours (**Re**). These experiments would be carried out with and without the presence of 1% sucrose, as outlined previously, while being grown on $3cm^2$ bovine enamel disks (Intertek, Aberdeen, UK).

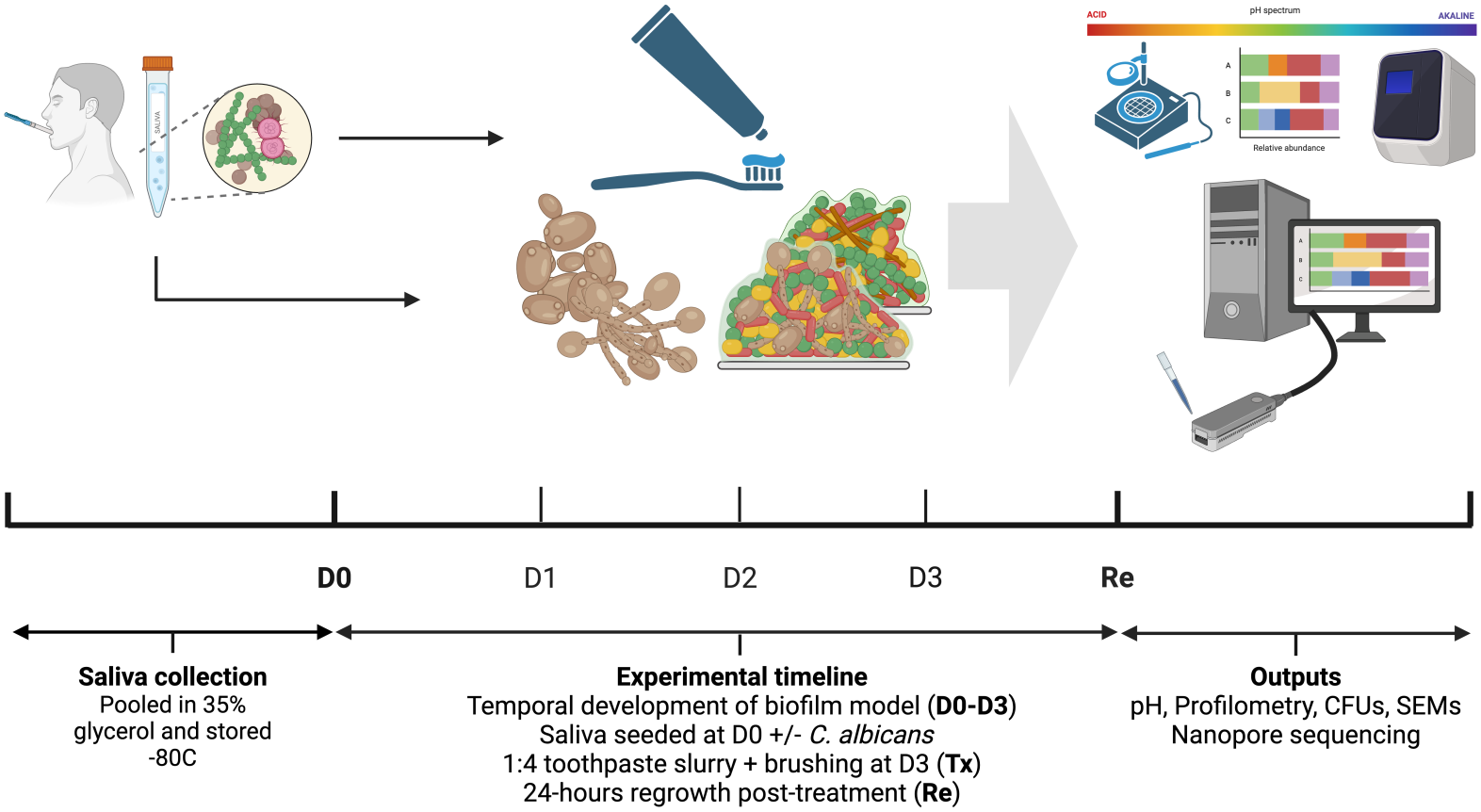


**Figure 3-1 - Experimental study design of planned intervention of *ex-vivo* biofilms through dental hygiene regimen.** Study initiation involved acquisition of saliva samples from ”healthy” donors to be pooled and retained for use as starting inocula. Experimental timeline outlines development of *ex-vivo* biofilm models over a 3-day timepoint with subsequent interventions (**Tx**) and regrowth (**Re**). Analysis outputs were established including 3D-profilometry, pH, and 16S rRNA sequencing. Created with BioRender®.

#### *3.3.8.1 Sample collection and criteria.*

Nineteen (19) Volunteers present in the Glasgow Dental Hospital & School's Department of Oral Medicine were invited to take part in the study. This recruitment was carried out as an addendum to pre-existing University of Glasgow and NHS-approved ethics for study "Host-microbiota interactions in Oral Health and Disease", project number 200160159.

Inclusion criteria included:

- Volunteers having no known disease of oral dysbiosis.

Exclusion criteria included:

- Antibiotic therapy either current or within a 6-month period

Unstimulated saliva samples were obtained using the passive drool method (Fernandes et al., 2013). In brief, 50mL RNAse and DNAse free polypropylene centrifuge tubes (ThermoFisher, Renfrew, UK) were pre-emptively sterilised using UV-light exposure at a wavelength of 365-nm for 15 minutes before being demarcated to indicate the desired volume of saliva for sampling (5mL). If after 5 minutes 5mL of saliva was not collected, the participant would be asked to stop, and the volume of saliva recorded. Once collected, the samples would be briefly centrifuged at 2,600g for 10 minutes to separate cellular debris. The resulting supernatants from all volunteers would then be retained for no longer than 45-minutes before being pooled together with an additional 35% glycerol to provide added stability for microbial samples. The pooled sample would then be aliquoted into 1mL volumes in 1.5mL microcentrifuge tubes and stored at -80°C to be used as a starter culture for biofilm analysis.

#### *3.3.8.2 ex-vivo Biofilm model growth and development*

Upon receipt, to attempt decontamination, bovine enamel disks were swabbed with 70% ethanol and allowed to evaporate in a fume hood for 1 hour before being placed into 24-well microtiter plates. Once dry, disks were transferred to a laminar flow cabinet and sterilised under UV light for 15 minutes prior to inoculation. Pooled saliva was then inoculated into RPMI:THB media, with or without $1x10^6$ cells/mL of *C. albicans*, at a ratio of 1:10 and transferred to all relevant wells of the microtiter plate.

#### *3.3.8.3 Biofilm maturity determined through colony forming units*

To examine the minimum development requirements for biofilm maturity, *ex-vivo* biofilms were grown as outlined for 3-6 days under aerobic and anaerobic conditions, based on the development of the original Zurich biofilm model (Guggenheim et al., 2004). Enamel disks were removed at each timepoint and transferred to 5ml Bijoux containing 1mL PBS for sonication at 35kHz for 10 mins to remove biomass before being serially diluted and counted using the method outlined by Miles and Misra, on CBA, FAA, and SAB agar, in aerobic and anaerobic conditions (Hedges et al., 1978). In brief, samples were serially diluted 1:10 in PBS across a 96-well microtiter plate. These dilutions would then be transferred in 10μL increments, in triplicate, onto the relevant agar media which had previously been split into sections for dilutions ranging from $10^{-1}$ to $10^{-6}$. The plates were then incubated for 24- to 48-hours aerobically or anaerobically, until colonies were visible for enumeration, at 37°C.

#### *3.3.8.4 Scanning Electron Micrography*

To visualise developing biofilms on enamel surfaces, Scanning Electron Micrography was employed. In brief, biofilm models on enamel were grown in 24-well microtiter plates as outlined in 3.3.8.2 before being washed twice with PBS and incubated in 1mL fixing solution of 2% glutaraldehyde, 2% para-formaldehyde, 0.15% w/v alcian

blue and 0.15M sodium cacodylate, pH 7.4 for 24 hours. This solution was removed, and samples were washed 3 times with 1mL of 0.15M sodium cacodylate buffer to remove excess glutaraldehyde before being transferred to a fume hood and incubated for 1 hour with a 1:1 solution of Osmium Tetroxide and 0.15M sodium cacodylate. Samples were then rinsed in dd$H_2O$ for 3 sets of 10-minute washes before staining with 0.5% uranyl acetate. Samples were then dehydrated via a gradient of alcohol, from 30-90% ethanol, before 4 sets of 10-minute rinses with absolute ethanol. Finally, samples underwent critical point drying with Hexamethyldisilizane (HMDS) in a desiccator, for 24-hours before being mounted on stainless steel imaging stubs and vacuum sputter-coated with gold/palladium coating (Quorom Technologies, Lewes, UK). Images were then obtained using a JEOL JSM-6400 scanning electron microscope (JEOL Ltd, Hertfordshire, UK).

#### *3.3.8.5 Profilometry readings of enamel substrates*

After development of biofilm models on enamel surfaces, as outlined in 3.3.8.2, biofilms were removed via sonication and swabbed with 70% ethanol before being left to dry overnight. Enamel disks were sent to Intertek LTD for analysis via 3D optical profilometry, surface microhardness and surface roughness measurement. Analyses generated by Intertek LTD.

### *3.3.9 Statistical analysis and data presentation*

Statistical analyses were generated using GraphPad® Prism® (Version 10.1.2; GraphPad Software Inc., La Jolla, CA). Comparison of means across biomass, viability and pH were determined via One-way Analysis of Variables (ANOVA) Tukey's post-test was applied to the *P* value for multiple comparisons of the data. Statistical significance was achieved if $P < 0.05$.

Tables were created via Microsoft® Excel® for Microsoft 365 (Mac), Microsoft Corporation®, Version 16.92.0. Table and image editing were achieved using Microsoft® PowerPoint® for Microsoft 365 (Mac), Microsoft Corporation®, Version 16.89.1.

## 3.4 Results

### *3.4.1 Isolate screening and phenotyping*

Isolates were firstly assessed for key characteristics which were determined through conventional biomass and metabolic activity assays, as well as the alteration of media pH through analysis of spent supernatants. As shown in Table 3-3, 72 salivary isolates of *Candida albicans* were assessed in this way. There was determined to be a wide spread of phenotypic variation across salivary isolates when assessing various, standardised, methodological techniques for assessing fungal isolates.

While these data are outlined in their entirety in Table 3-3, this has been summarised in Table 3-4 for visual simplicity. As also visualised in Figure 3-2**,** of isolates tested, the majority (50-52%) were determined to fall into the intermediate range of biofilm formers, metabolic activity and with overall influence on supernatant pH (**I-pH**) when compared to a type-strain positive control of *C. albicans* SC5314. Developmentally, in overnight cultures, there was determined to be a majority (57%) of strains with an intermediate rate of growth (**IRG**), again determined by comparison with *C. albicans* SC5314. By assessing the isolates in this way, we were readily able to identify key strains of interest regarding their capacity for biofilm production, as high or low biofilm formers, for downstream applications.

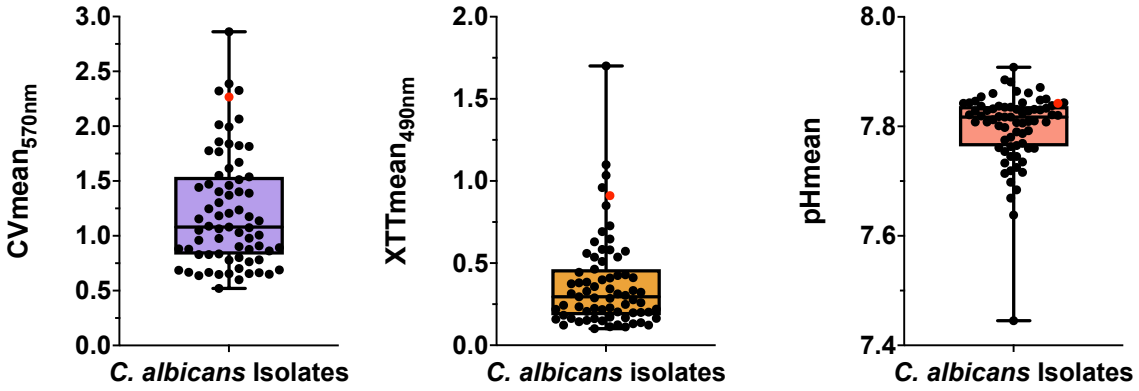


**Figure 3-2- Mean biomass, metabolic activity, and pH of 72 *C. albicans* isolates.** Mean values derived from crystal violet (A), XTT reduction (B) and pH reading (C) of *Candida albicans* isolates obtained from saliva. Isolate parameters are determined by positioning upon the demarcated boxplot where samples fall within or without interquartile ranges to determine key phenotypical characteristics.

| Isolate No. | 1 | 2 | 4 | 6 | 10 | 11 | 12 | 13 | 16 | 19 | 21 | 22 | 23 | 25 | 26 | 27 | 29 | 31 |
|---|---|---|---|---|---|---|---|---|---|---|---|---|---|---|---|---|---|---|
| Overnight OD | 2.4 | 2.5 | 2.5 | 2.6 | 1.5 | 2.5 | 1.4 | 2.3 | 2 | 2.5 | 2 | 2.3 | 2.2 | 2.4 | 2.3 | 2.3 | 1.5 | 1.6 |
| pH | 7.669 | 7.684 | 7.821 | 7.819 | 7.445 | 7.792 | 7.843 | 7.85 | 7.638 | 7.798 | 7.745 | 7.765 | 7.725 | 7.761 | 7.828 | 7.714 | 7.719 | 7.754 |
| CV mean | 1.37 | 0.7628 | 1.247 | 1.05 | 2.326 | 1.401 | 1.302 | 0.7013 | 0.9779 | 0.637 | 0.6542 | 0.5991 | 0.8288 | 1.551 | 0.8915 | 0.9594 | 0.6858 | 1.402 |
| XTT mean | 0.4444 | 0.3035 | 0.5365 | 0.1433 | 1.7 | 0.6467 | 0.3126 | 0.1226 | 0.3329 | 0.1007 | 0.1671 | 0.1114 | 0.1976 | 0.3437 | 0.1228 | 0.3803 | 0.2063 | 0.2173 |
| Biofilm Type | IBF | LBF | IBF | IBF | HBF | IBF | IBF | LBF | IBF | LBF | LBF | LBF | IBF | HBF | IBF | IBF | LBF | IBF |
| Metabolism | IMR | IMR | HMR | LMR | HMR | HMR | IMR | LMR | IMR | LMR | LMR | LMR | IMR | IMR | LMR | IMR | IMR | IMR |
| pH profile | Lo-pH | Lo-pH | I-pH | I-pH | Lo-pH | I-pH | Hi-pH | Hi-pH | Lo-pH | I-pH | Lo-pH | I-pH | Lo-pH | Lo-pH | I-pH | Lo-pH | Lo-pH | Lo-pH |
| Overnight Growth | HRG | HRG | HRG | HRG | LRG | HRG | LRG | HRG | IRG | HRG | IRG | HRG | IRG | HRG | HRG | HRG | LRG | LRG |

| Isolate No. | 37 | 44 | 45 | 46 | 47 | 48 | 49 | 53 | 54 | 55 | 56 | 57 | 60 | 61 | 65 | 66 | 67 | 69 |
|---|---|---|---|---|---|---|---|---|---|---|---|---|---|---|---|---|---|---|
| Overnight OD | 1.8 | 2.1 | 2 | 1.6 | 2 | 2.1 | 1.9 | 1.9 | 1.9 | 1.7 | 2 | 2 | 2 | 2 | 2.3 | 1.3 | 2.7 | 1.7 |
| pH | 7.848 | 7.908 | 7.871 | 7.86 | 7.832 | 7.817 | 7.808 | 7.808 | 7.809 | 7.838 | 7.76 | 7.76 | 7.801 | 7.829 | 7.775 | 7.78 | 7.843 | 7.817 |
| CV mean | 1.389 | 1.815 | 1.08 | 1.137 | 0.7782 | 0.8346 | 1.993 | 0.9764 | 1.205 | 1.442 | 0.5202 | 0.8777 | 0.6637 | 0.6557 | 1.776 | 0.9011 | 0.9079 | 1.471 |
| XTT mean | 0.2488 | 1.099 | 0.3139 | 0.2014 | 0.2027 | 0.2243 | 0.6919 | 0.1998 | 0.5369 | 0.5593 | 0.5835 | 0.4098 | 0.3226 | 0.2342 | 0.4244 | 0.1128 | 0.1616 | 0.2436 |
| Biofilm Type | IBF | HBF | IBF | IBF | LBF | IBF | HBF | IBF | IBF | IBF | LBF | LBF | LBF | LBF | HBF | IBF | IBF | IBF |
| Metabolism | IMR | HMR | IMR | IMR | IMR | IMR | HMR | IMR | HMR | HMR | HMR | IMR | IMR | IMR | IMR | LMR | LMR | IMR |
| pH profile | Hi-pH | Hi-pH | Hi-pH | Hi-pH | I-pH | I-pH | I-pH | I-pH | I-pH | Hi-pH | Lo-pH | Lo-pH | I-pH | I-pH | I-pH | I-pH | Hi-pH | I-pH |
| Overnight Growth | IRG | IRG | IRG | LRG | IRG | IRG | IRG | IRG | IRG | IRG | IRG | IRG | IRG | IRG | HRG | LRG | HRG | IRG |

| Isolate No. | 70 | 72 | 78 | 79 | 80 | 81 | 82 | 86 | 88 | 89 | 90 | 91 | 92 | 93 | 95 | 98 | 100 | 104 |
|---|---|---|---|---|---|---|---|---|---|---|---|---|---|---|---|---|---|---|
| Overnight OD | 2.3 | 2.4 | 2 | 2 | 2 | 2 | 2 | 2 | 2 | 2 | 2 | 2 | 1.9 | 2.2 | 1.6 | 2 | 1.7 | 1.9 |
| pH | 7.716 | 7.745 | 7.835 | 7.769 | 7.821 | 7.837 | 7.837 | 7.83 | 7.806 | 7.808 | 7.864 | 7.861 | 7.812 | 7.854 | 7.843 | 7.835 | 7.831 | 7.846 |
| CV mean | 0.7808 | 0.8808 | 0.6889 | 0.6473 | 1.074 | 0.8621 | 1.175 | 0.6663 | 1.538 | 1.46 | 1.839 | 1.088 | 2.013 | 1.767 | 1.006 | 1.615 | 1.823 | 1.857 |
| XTT mean | 0.2862 | 0.2953 | 0.2188 | 0.3744 | 0.3843 | 0.4117 | 0.3283 | 0.2277 | 0.3986 | 0.5099 | 0.7272 | 0.2766 | 0.4293 | 0.3572 | 0.2884 | 0.8502 | 0.63 | 0.5804 |
| Biofilm Type | LBF | IBF | LBF | LBF | IBF | IBF | IBF | LBF | IBF | IBF | HBF | IBF | HBF | HBF | IBF | HBF | HBF | HBF |
| Metabolism | IMR | IMR | IMR | IMR | IMR | IMR | IMR | IMR | IMR | HMR | HMR | IMR | IMR | IMR | IMR | HMR | HMR | HMR |
| pH profile | Lo-pH | Lo-pH | I-pH | I-pH | I-pH | I-pH | I-pH | I-pH | I-pH | I-pH | Hi-pH | Hi-pH | I-pH | Hi-pH | Hi-pH | I-pH | I-pH | Hi-pH |
| Overnight Growth | HRG | HRG | IRG | IRG | IRG | IRG | IRG | IRG | IRG | IRG | IRG | IRG | IRG | IRG | LRG | IRG | IRG | IRG |

| Isolate No. | 105 | 106 | 107 | 109 | 113 | 114 | 115 | 117 | 120 | 121 | 122 | 123 | 126 | 128 | 129 | 131 | SC5 | Media |
|---|---|---|---|---|---|---|---|---|---|---|---|---|---|---|---|---|---|---|
| Overnight OD | 1.8 | 1.9 | 1.8 | 1.8 | 2.2 | 1.3 | 2 | 1.1 | 2.2 | 1.3 | 1.5 | 1.1 | 1.3 | 1.1 | 1.2 | 1.9 | 2 | 0 |
| pH | 7.824 | 7.828 | 7.885 | 7.881 | 7.733 | 7.818 | 7.763 | 7.807 | 7.81 | 7.82 | 7.79 | 7.833 | 7.787 | 7.698 | 7.735 | 7.842 | 7.842 | 7.831 |
| CV mean | 1.03 | 1.154 | 2.861 | 1.512 | 0.8764 | 0.8014 | 0.6498 | 2.321 | 0.6668 | 2.065 | 2.387 | 1.064 | 1.183 | 0.8291 | 1.236 | 1.67 | 2.266 | 0 |
| XTT mean | 0.2593 | 0.1516 | 1.034 | 0.1487 | 0.5722 | 0.1631 | 0.1378 | 0.1708 | 0.1246 | 0.4633 | 0.9598 | 0.1587 | 0.2199 | 0.1312 | 0.1824 | 0.1636 | 0.9108 | 0 |
| Biofilm Type | IBF | IBF | HBF | IBF | IBF | LBF | LBF | HBF | LBF | HBF | HBF | IBF | IBF | IBF | IBF | HBF | HBF | LBF |
| Metabolism | IMR | LMR | HMR | LMR | HMR | LMR | LMR | LMR | LMR | IMR | HMR | LMR | IMR | LMR | IMR | LMR | HMR | LMR |
| pH profile | I-pH | I-pH | Hi-pH | Hi-pH | Lo-pH | I-pH | Lo-pH | I-pH | I-pH | I-pH | I-pH | I-pH | I-pH | Lo-pH | Lo-pH | Hi-pH | Hi-pH | I-pH |
| Overnight Growth | IRG | IRG | IRG | IRG | IRG | LRG | IRG | LRG | IRG | LRG | LRG | LRG | LRG | LRG | LRG | IRG | IRG | LRG |

**Table 3-3 - Analysis of screening parameters of *C. albicans* saliva isolates.** Complete assessment of 72 *C. albicans* isolates across a range of means and methods. Average data for overnight growth, pH, Crystal violet biomass (CV) and metabolism (XTT) presented to highlight distribution of organisms in the context of biofilm capacity. Samples were identified via CV biomass assay as being High, Low, or Intermediate Biofilm Formers (HBF, LBF, IBF), via XTT assay for metabolic rate (HMR, LMR, IMR), supernatant pH (Hi-pH, Lo-pH, I-pH), and rate of overnight growth (HRG, LRG, IRG). Samples were categorised based on distribution across interquartile ranges with “High” samples falling in the 3$^{rd}$ quartile and “Low” samples falling in the 1$^{st}$ quartile across the sample range. Averages of isolate parameters determined across n=3 technical replicates on 3 separate occasions

| | % Distribution of Strains | | | | | | |
|---|---|---|---|---|---|---|---|
| **% HBF** | 23.94 | **% HMR** | 23.94 | **% Hi-pH** | 23.94 | **% HRG** | 21.13 |
| **% LBF** | 23.94 | **% LMR** | 23.94 | **% Lo-pH** | 25.35 | **% LRG** | 21.13 |
| **% IBF** | 52.11 | **% IMR** | 52.11 | **% I-pH** | 50.70 | **% IRG** | 57.75 |

**Table 3-4 - Percentage distribution of *C. albicans* strains across experimental parameters.** Organisms were categorised, via assessment through biofilm biomass, metabolic assay, pH, and overnight turbidity, as follows: High, Low and Intermediate Biofilm formers (HBF, LBF, IBF), metabolic rates (HMR, LMR, IMR), pH profile (Hi-pH, Lo-pH, I-pH), and overnight rate of growth (HRG, LRG, IRG).

To better elucidate potential correlations between phenotypic characteristics across isolates, these data were further analysed for linear regression patterns across parameters, as shown in Figure 3-3. Generally, a weak correlation of $R^2 = 0.44$ was observed when comparing isolates biomass with their metabolic activity. When comparing pH and biomass, as well as pH and metabolic activity, $R^2$ values of 0.01 and 0.04 were observed, respectively, indicating no correlation between these parameters across isolates. This is indicative that those strains of organisms capable of producing more biomass, either via hyphal growth or production of EPS and associated metrics, may, more often than not, be more metabolically active than an isolate which produces less biomass. It is also clear that pH in the surrounding media is not greatly influenced by metabolic activity or the capacity for increasing biofilm production in *C. albicans*. Indeed, there is no significant difference observed between the pH of the media only control and that of the supernatant pH across all isolates, indicating that any impetus for modulation of environmental pH must be influenced by further internal or external factors.

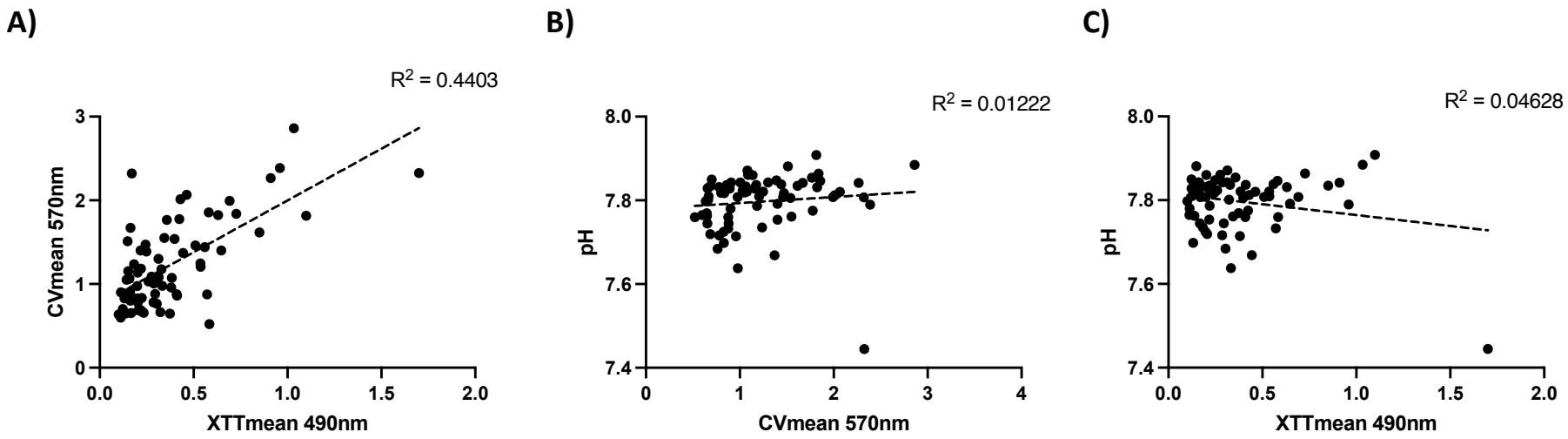


**Figure 3-3 - Linear regression curves examining relationship between Biomass, metabolism and pH.** Lines of best fit between data points provide $R^2$ values of 0.4403 for CV/XTT (A), 0.01222 for pH/CV (B) and 0.04628 for pH/XTT (C). These data predict no relationship between pH and biomass/metabolism for these isolates and an approximately 66% variation when comparing biomass and metabolic activity for individual isolates.

From these isolates, 7 (4 HBF and 3 LBF) were carried forward for further comparisons to a type strain of *C. albicans* (SC5314). As can be observed in Figure 3-4, while biomass for HBF isolates was observed to increase between 100-120% in comparison to SC5314, this was not always reflected in the metabolic activity of a given strain, reflective of the weak correlation observed in Figure 3-3.

Of the HBF isolates, strain 107 was observed to have the greatest increase in biomass in comparison to SC5314 at an increase of 126% ($P < 0.0001$), but no significant difference when comparing metabolic activity. This increase in biomass also reflected in the average delta pH, showing a reduction in supernatant pH of -0.05ΔpH based on the pH of the starting media, compared to -0.01ΔpH of SC5314 ($P < 0.0001$). It is also worth mentioning that HBF strain 122 was observed to have increased pH compared to the starting culture media ($P < 0.01$).

Conversely, all LBF isolates were observed to be approximately 75-80% lower in biomass when compared to SC5314 ($P < 0.0001$) and between 59-88% less metabolically active ($P < 0.0001$). This comparison between biomass and supernatant pH was compounded when observing shifts in delta pH across the LBF isolates where all were observed to be statistically significant in reducing their supernatant pH when compared to the starting media ($P < 0.0001$).

These respective increases in culture pH for HBF strains, and decreases for LBF strains, reinforce our hypothesis of a potential deleterious effect in the context of acidification of tooth enamel when lower biofilm forming strains of *C. albicans* are present in a clinical setting and that the capability of higher biomass strains of *C. albicans* provide a clinically relevant buffering of pH in their direct microenvironment.

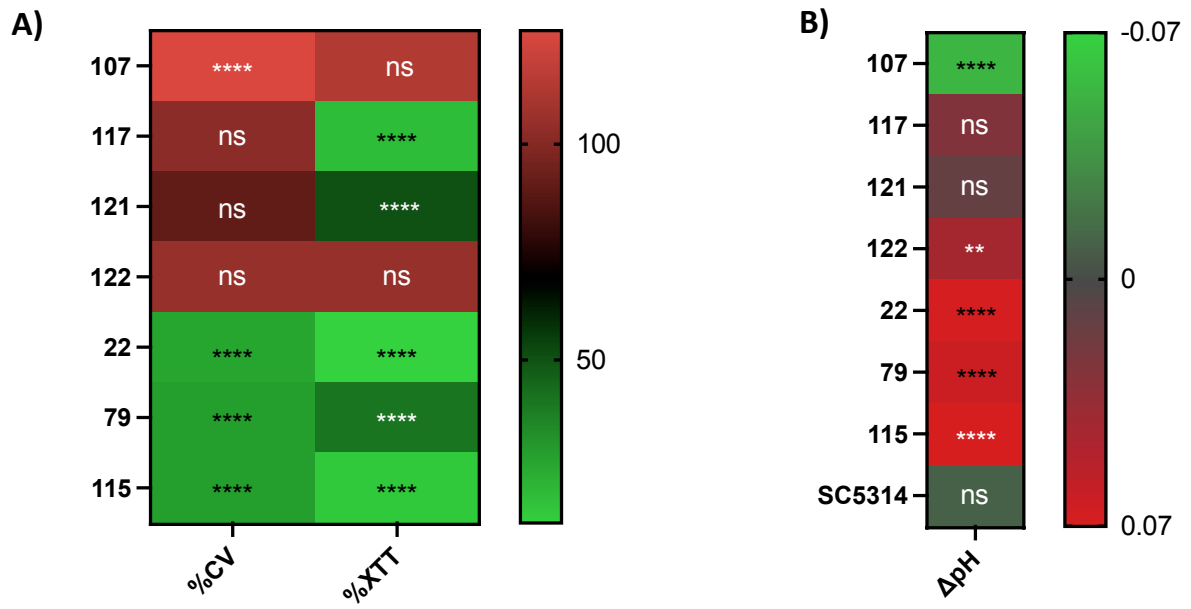


**Figure 3-4 - Comparison of phenotype characteristics between clinical and type strains of *C. albicans*.** 7 samples were selected for comparison of biomass and metabolic activity to that of *C. albicans* SC5314. In (A), comparisons were drawn between mean biomass and metabolic activity of selected strains. In HBF strains, biomass ranges from 100% to 120% of SC5314 with a statistically significant increase in biomass observed for strain 107 ($P < 0.0001$). In LBF strains, reductions in biomass were observed to range from 25-30% and were statistically significant across all LBF strains ($P < 0.0001$). Metabolic activity for HBF strains ranged between 18-115% when compared with SC5314, with a statistically significant reduction in activity was observed in strains 117 and 121 ($P < 0.0001$). LBF strains ranged between 12-41% metabolic activity and were also considered statistically significant reductions ($P < 0.0001$). In (B), mean pH of media after growth was compared to initial pH of media for all strains and was represented as ΔpH. Strain 107 was observed to have a significantly higher ($P < 0.0001$) pH after growth, while all LBF strains were shown to have a pH significantly lower than the initial media ($P < 0.0001$). HBF strain 122 was also shown to have a significant reduction in pH ($P < 0.01$).

To further characterise the activity of these organisms, assessment of growth rates were carried out over a 24-hour period, as shown in

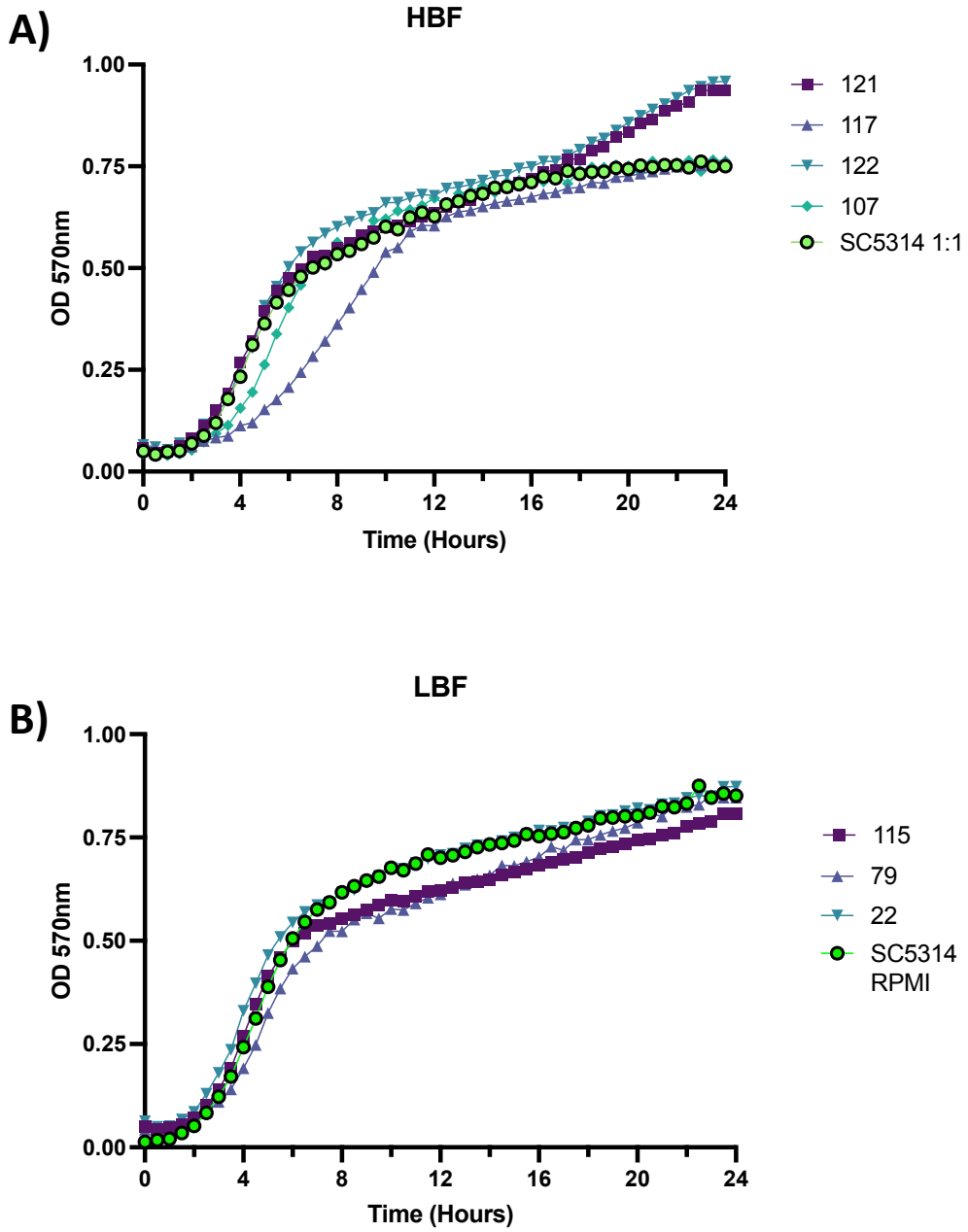


Figure 3-5. Of the HBF isolates, strain 117 was observed to have the longest exponential growth phase of approximately 10hrs, a much slower developmental time than observed in strains 121, 122 and 107, each approximating 4-6hrs of growth before reaching a latent phase of growth. This may be reflective of previous data in Figure 3-4, where strain 117 was observed to have a significantly lower metabolic

activity than type strain SC5314 and could be indicative of metabolic processes associated with growth being downregulated in favour of pathways associated with biofilm formation.

In the case of LBF isolates, all organisms were observed to reach a stationary phase of growth within a similar timeframe of approximately 6-8 hours after inoculation with no clear deviation between strains. Additionally, HBF strains 121 and 122 maintained growth beyond the end-point of the experiment. This would be reflective of a shift in growth requirements as organisms deplete the resources available to them in the media, resulting in a burst of growth. As there was no significance associated with their biomass compared to the control organism, as in Figure 3-4, this may again be indicative of the shift in metabolic processes associated with biofilm formation being prioritised differently across yeast strains. Indeed, this is further compounded in the LBF samples, where although the organisms exit their exponential phase of growth, there is no clear decline in growth across any of the LBF strains.

When considering the control strain, SC5314, we observe a similar trend when comparing the different growth rates associated with different media types. We observed the growth of this organism using a complex media used to sustain polymicrobial communities (1:1 media) and a high glucose RPMI media. When sustained only on RPMI media, SC5314 was observed to maintain a similar growth profile to that of the LBF strains of *C. albicans*, i.e. sustained growth even beyond the stationary phase. When sustained using the equal parts RPMI and THB media, we observed this organism to follow the profile of other HBF strains, 117 and 107.

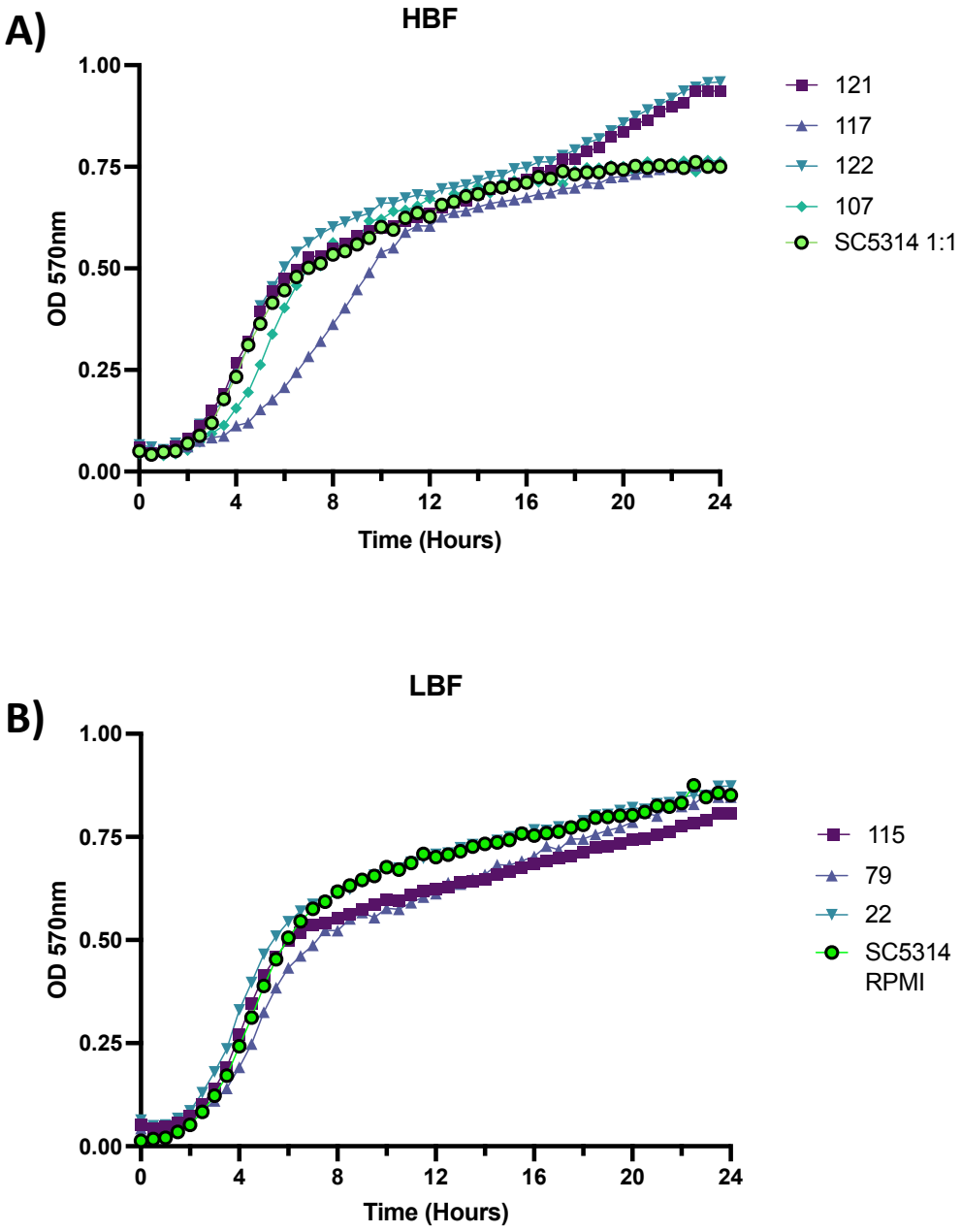


**Figure 3-5 – Growth kinetics of HBF and LBF phenotype *C. albicans*.** Organism growth rates determined over 24 hours with spectrophotometric readings taken at 30-minute intervals at a wavelength of 570nm. **A)** Exponential phase growth shifts slightly to the right for isolates 117 and 107 while isolates 121 and 117 display a delayed stationary phase. **B)** LBF isolate growth consistent with SC5314 control. No obvious difference in growth kinetics between media in both SC5314 controls.

### *3.4.2 Assessing starting concentration and environmental factors*

In conjunction with assessing biofilm phenotype using "conventional" model development techniques, it was also considered valuable to assess the capacity for clinical isolates to form biofilms at much lower, clinically-relevant, starting concentrations. In addition to this, as altering the nutritional availability in growth media can affect metabolic activity, it was also needful to assess the effect of varying concentrations of growth media. To achieve this, HBF isolate 107 and LBF isolate 22 were carried forward from previous screening, as well as type strain SC5314.

As SC5314 provided a control organism representative of strong biofilm growth, we next opted to examine a genetically modified strain of *C. albicans* SSY50-B. Strain SSY50-B was designed to incorporate *tetO* promoter sequences, regulatory sequences which control expression of genes associated with tetracycline resistance, upstream of the Negative Regulator of Glucose-controlled genes 1 (*NRG1*) gene sequence, a sequence closely associated with yeast-to-hyphal morphological switching. In this way, through modulation of expression of the protein Nrg1, hyphal morphology can be supressed, and the yeast phenotype of *C. albicans* can be maintained or manipulated via the presence of tetracycline or its derivatives such as doxycycline. This allowed us to use SSY50-B as a control organism for low biofilm production.

To exemplify the activity of these organisms under clinically relevant concentrations, and comparing to standardised laboratory methods, Figure 3-6, below, outlines changes in biomass for organisms SC5314, 22, 107 and SSY50B under a gradient shift in concentration of RPMI:THB, the preferred media for multi-species model growth.

From this it was determined that increasing seeding concentration has a visible effect on the density of biomass across 107, 22 and SC5314 with no observed impact on biofilm deficient SSY50B. Moreover, isolates were shown to increase in biomass when grown in 100% RPMI with biomass reducing as concentration of THB is increased until approximately 55% RPMI. The sharp spike in biomass as the availability of RPMI diminishes and THB increases may be evidence of a switch in substrate utilisation for growth and alteration of metabolic pathways.

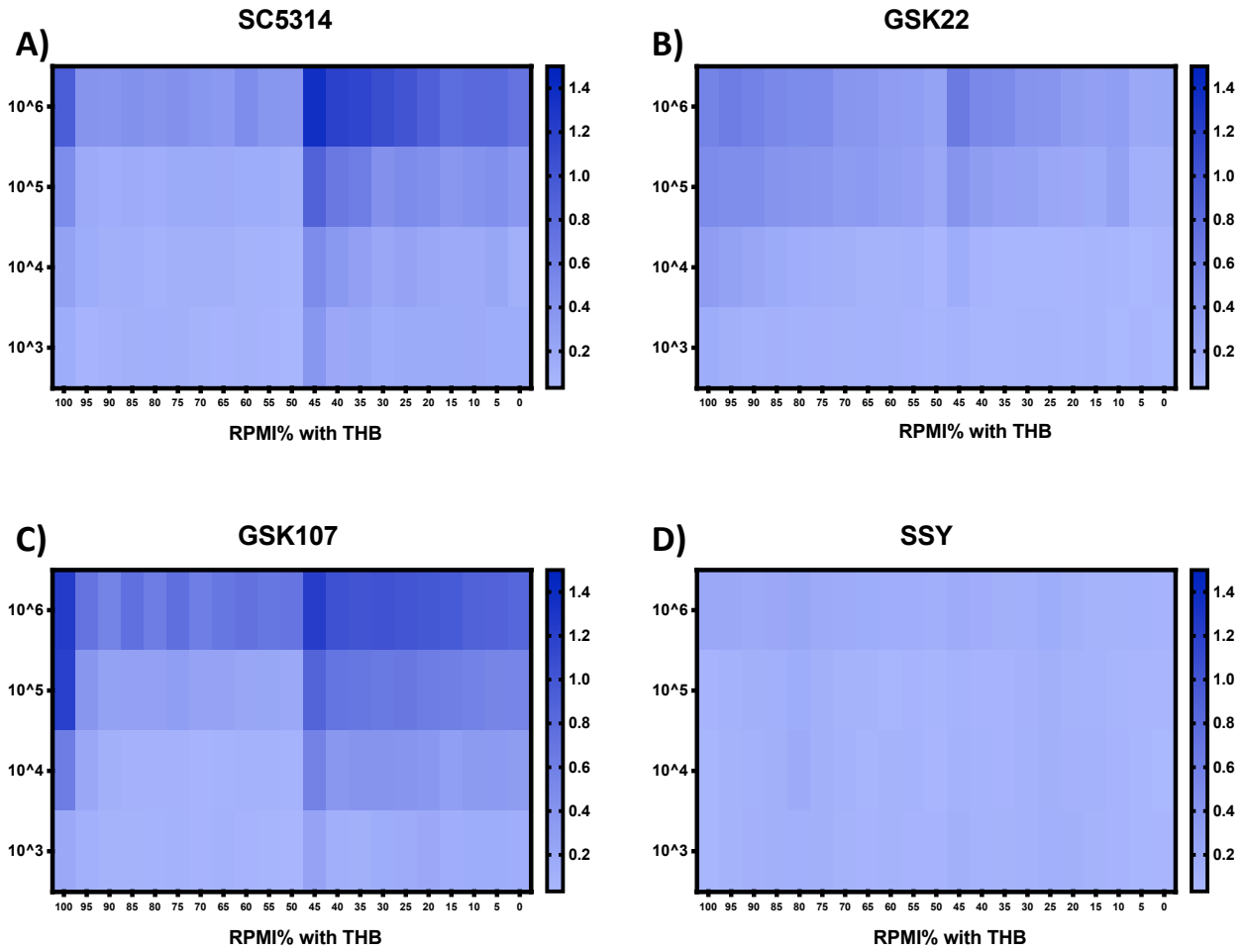


**Figure 3-6 - Evaluation of %RPMI on biofilm phenotype.** Heatmap visualization of Crystal Violet biomass assay of *C. albicans* SC5314, GSK107, GSK22 and SSY-50B. Biomass is shown to increase in parallel with starting concentration as well as concentration of available RPMI/THB**.**

To further elucidate this, we moved on to assess the metabolic activity of these same organisms under these conditions. As below, Figure 3-7 highlighted the overall lack of impact generated by altering the starting concentration of *C. albicans* isolates and the largely unintrusive impact of altering media conditions across the gradient.

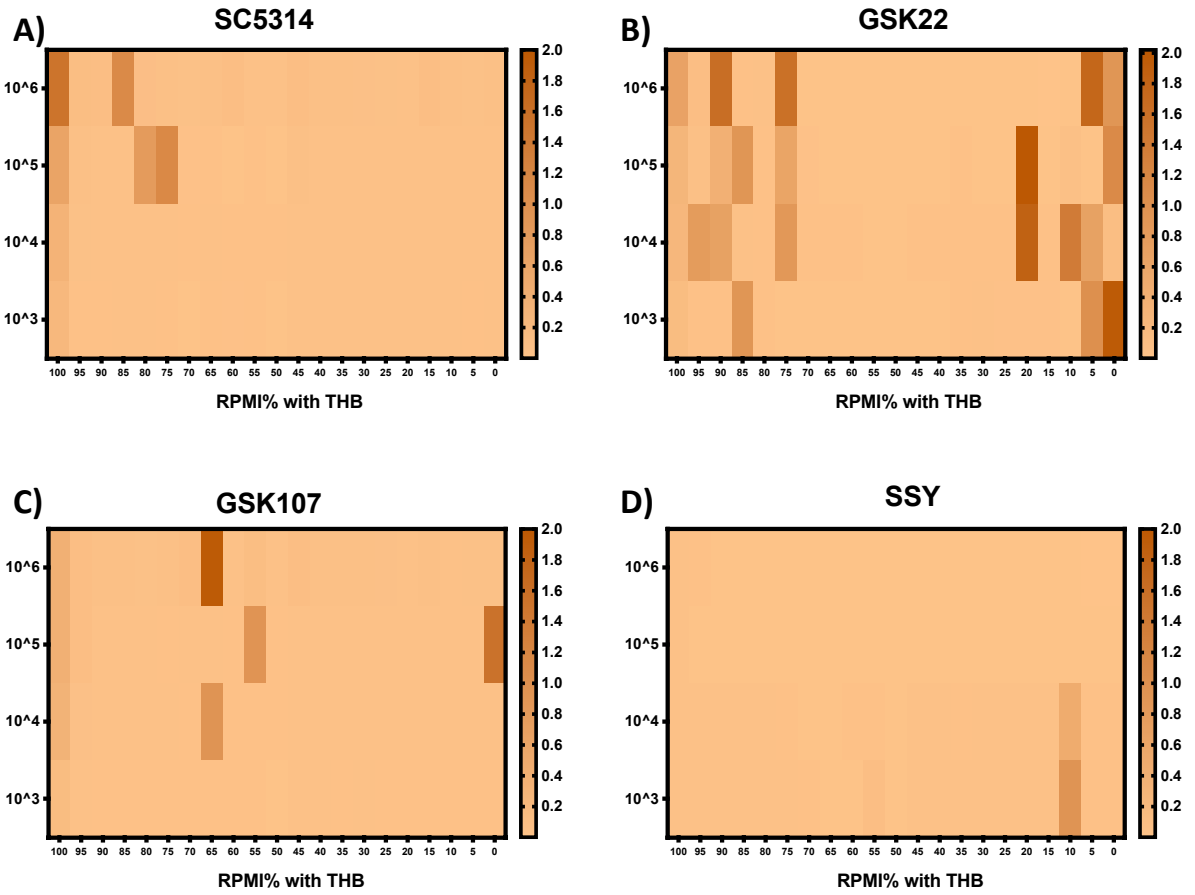


**Figure 3-7 - Evaluation of %RPMI on metabolic activity.** Heatmap visualization of XTT viability assay of *C. albicans* SC5314, GSK107, GSK22 and SSY-50B. Metabolic activity is shown to be, largely, independent of starting concentration and ratio of RPMI/THB.

To further exemplify the shifting growth conditions when altering environmental availability of nutrients, growth curves of SC5314 under different concentration gradients were performed over 48 hours. Observation of SC5314 curves over 48 hours under the same conditions, as shown in Figure 3-8, highlighted this shift in growth at concentrations ranging from 0-55% RPMI which is reflective of the changes observed in biomass data.

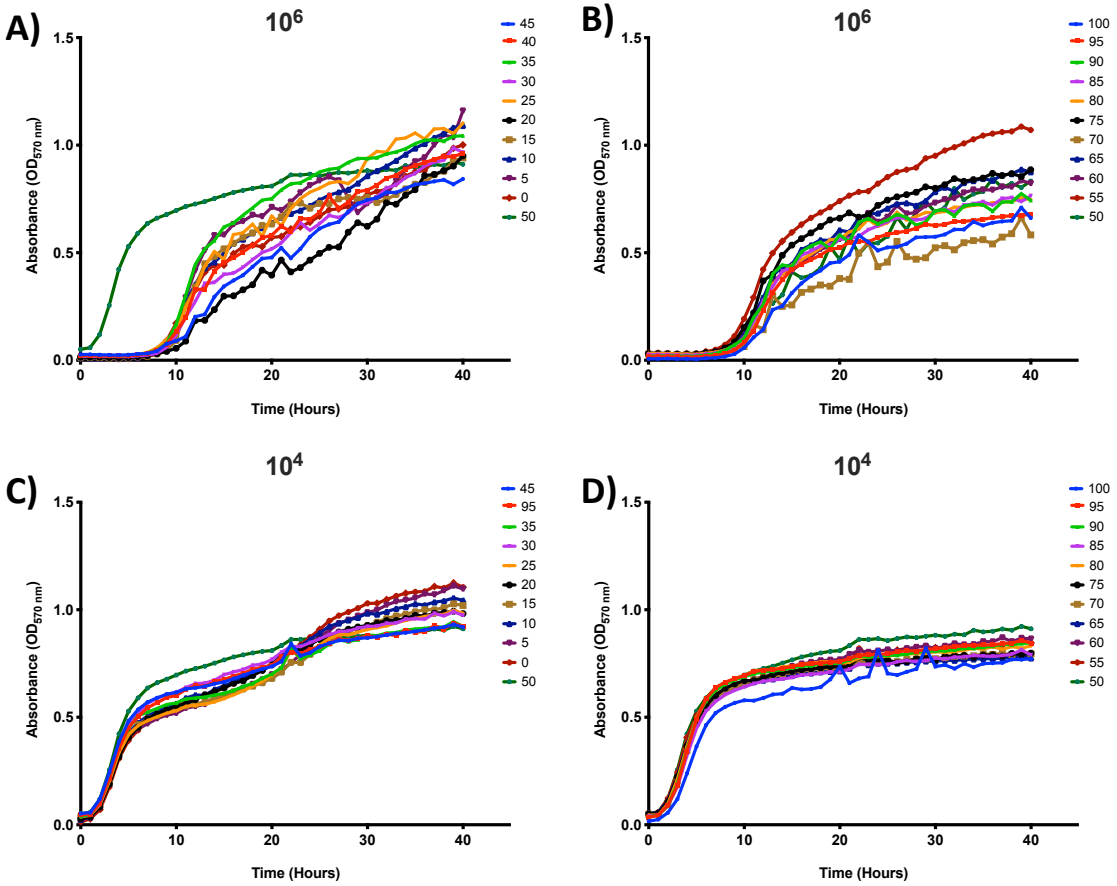


**Figure 3-8 - Evaluation of starting concentration and %RPMI/THB on growth rate.** Growth curve of *C. albicans* SC5314 across different starting concentrations and containing alternating ratios of growth media. **A)** SC5314 seeded at a concentration of $1x10^6$cells/mL and ranging from a concentration of 0-50% RPMI. The greatest impact of growth can be observed in samples containing 50% RPMI. **B)** SC5314 seeded at a concentration of $1x10^6$cells/mL and ranging between 50-100% RPMI. Exponential growth becomes marginally delayed as concentration of RPMI increases. **C)** Starting concentration of $10^4$ cells/mL, 0-50% RPMI, shifts exponential growth phase to the left, and entering stationary phase more consistently than higher seeding concentrations. **D)** Starting concentration of $10^4$ cells/mL, 50-100% RPMI, organisms achieve and maintain a steady stationary phase of growth after approximately 10hrs.

### *3.4.3 Influence of dietary carbohydrates on microbial phenotype*

In addition to assessing the intended growth media for multispecies experimentation, in the context of dental caries it was also essential to assess what impact dietary carbohydrate dosing may have had on organisms associated with the oral microbiome. As shown in Figure 3-9 and Figure 3-10, below, we observed largely independent fluctuations in biomass across a gradient of 2.5-0.0045% Starch and 10-0.02% Sucrose. However, when observing changes in metabolic activity, a slight increase in overall metabolic activity was observable at higher concentrations of starch and sucrose across isolates which reduced incrementally across the gradient.

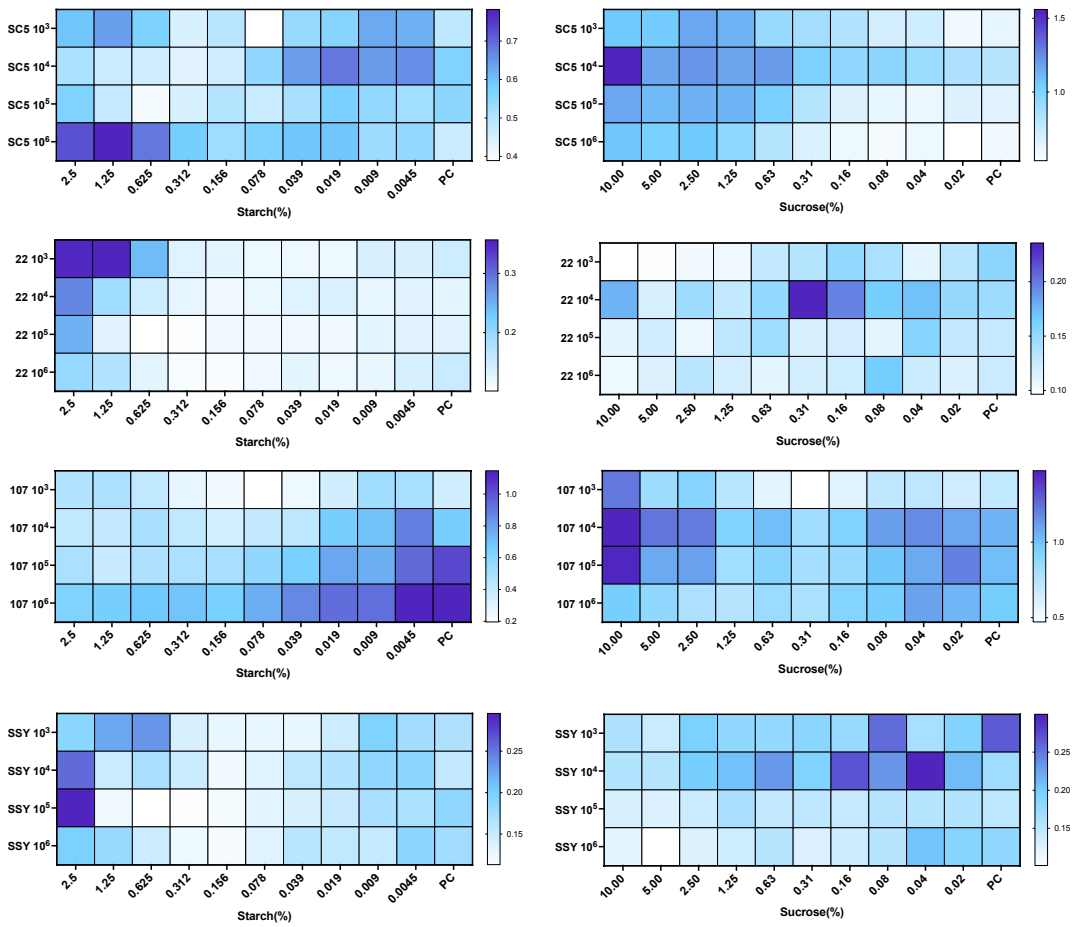


**Figure 3-9 - Evaluation of starting concentration, sucrose and starch on biomass of *C. albicans*.** Heatmap visualization of Crystal Violet biomass assay of *C. albicans* isolates across a concentration gradient of Sucrose and Starch. Indicating that biomass development is independent of carbohydrate concentration.

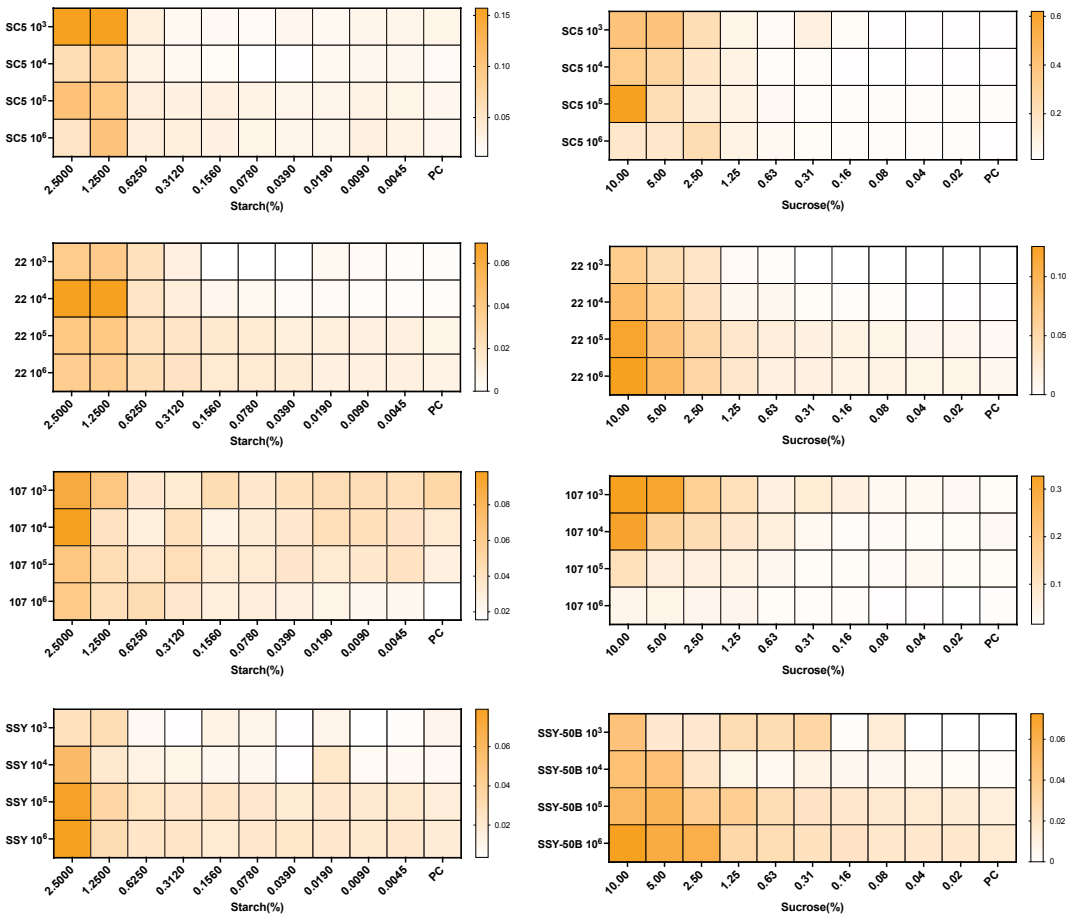


**Figure 3-10 - Evaluation of starting concentration, sucrose and starch on metabolic activity of *C. albicans*.** Heatmap visualization of XTT metabolic assay of *C. albicans* isolates across a concentration gradient of Sucrose and Starch. Metabolic activity may be influenced by carbohydrate availability across the gradient of concentrations.

We then selected to observe any changes in pH provoked by the inclusion of dietary carbohydrates in media with *C. albicans* isolates. As per Figure 3-11, below, there was no major shift in pH for media supernatants from *C. albicans* isolates across a range of concentrations and across sucrose/starch gradient. Small changes in pH could be observed in higher concentrations of sucrose (1.25-10%) which were not observed in the media control, indicating environmental pH can be influenced by very high concentrations of sucrose in the presence of *C. albicans*. This same pattern was not observed in the samples containing starch.

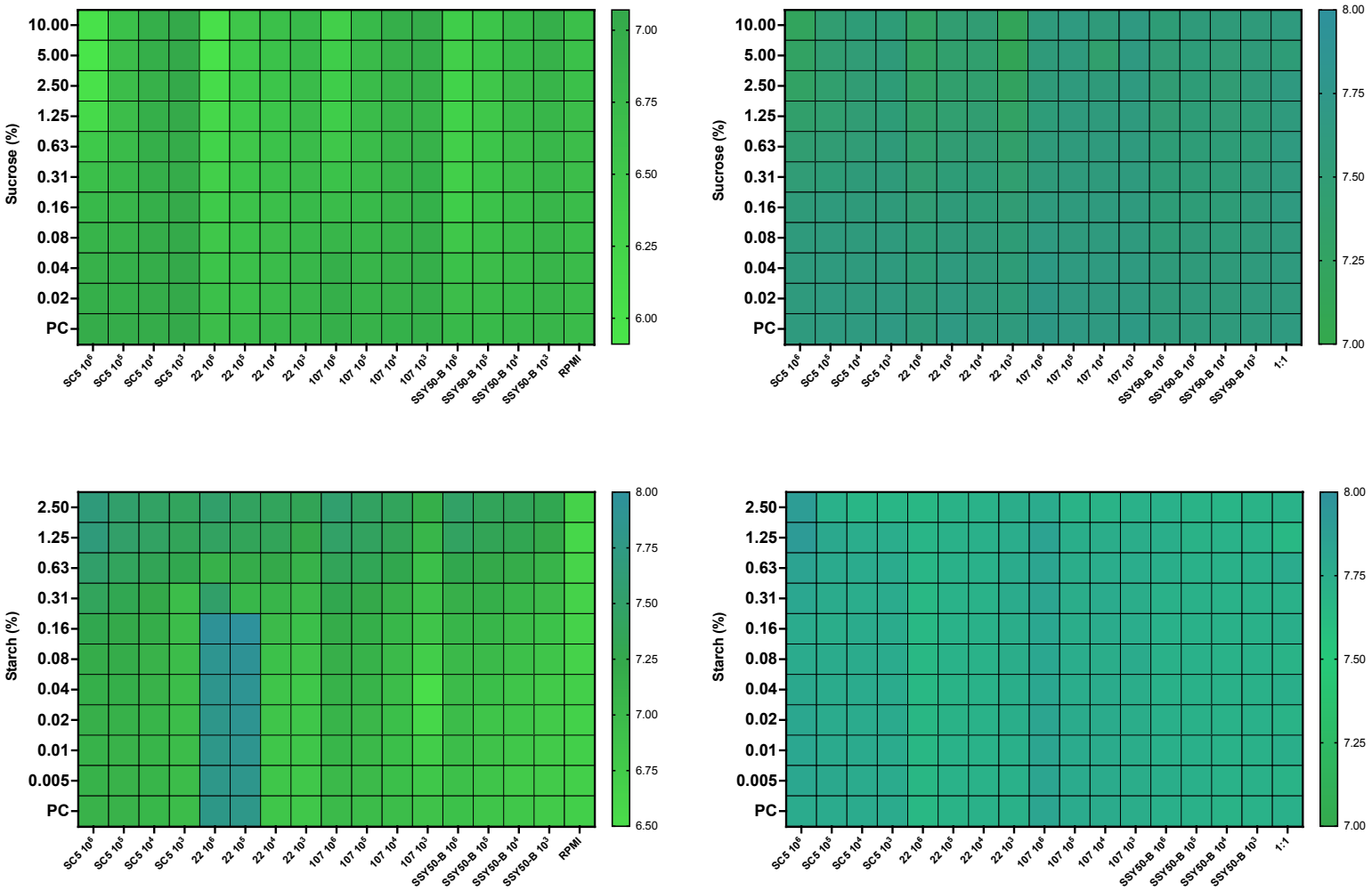


**Figure 3-11 - Evaluation of starting concentration, media, sucrose, and starch on *C. albicans*.** Heatmap visualization of pH of *C. albicans* isolates across a concentration gradient of Sucrose and Starch in RPMI (left) and RPMI:THB (right). pH remains uniform across variable seeding concentrations of Candida and across sucrose/starch concentration.

Following on from this, it was essential to observe similar influences of starting concentration, media type and dietary carbohydrate on organisms known to be major influential factors in oral caries, as evidenced by previous work (Brown et al., 2019, Butcher et al., 2022). Due to confounding factors of starch solubility, it was deemed necessary from this point to focus singularly on the influence of sucrose concentration on the microenvironment. Figure 3-12, below, highlights the stark difference in influence of caries relevant bacteria in the context of environmental pH in a manner that is, at times, not just dependent on carbohydrate concentration but also starting concentration of bacteria. For example, *Actinomyces naeslundii* was observed to reduce media pH from approx. 7.6 to a pH of 5.4 at a concentration of $1x10^7$ cells/mL but did not obviously alter pH at a concentration of $1x10^4$ cells/mL. However, at $1x10^7$ cells/mL, in the presence of 1.25% sucrose, *A. naeslundii* was observed to reduce the environmental further, to pH4.18. Similar observations were made with *Lactobacillus casei* albeit not as pronounced as *A. naeslundii* at lower starting concentrations of bacteria. *Staphylococcus schleiferi,* identified as a health-associated organism in previous work, did not display major changes in environmental pH regardless of starting concentration or carbohydrate availability. The inverse was true of known cariogenic organism *Streptococcus mutans,* displaying a major reduction in pH from the media standard at all concentrations. Finally, *Veillonella dispar* was observed to reduce environmental pH at all starting concentrations but in a dose-dependent manner, with pH at its lowest of 4.58 in 10% sucrose. Given that it was observed that these organism-dependent changes in micro-environmental pH between bacteria and fungi in mono-species environments, then it was essential to determine how these environmental differences would be affected in a poly-microbial, inter-kingdom setting

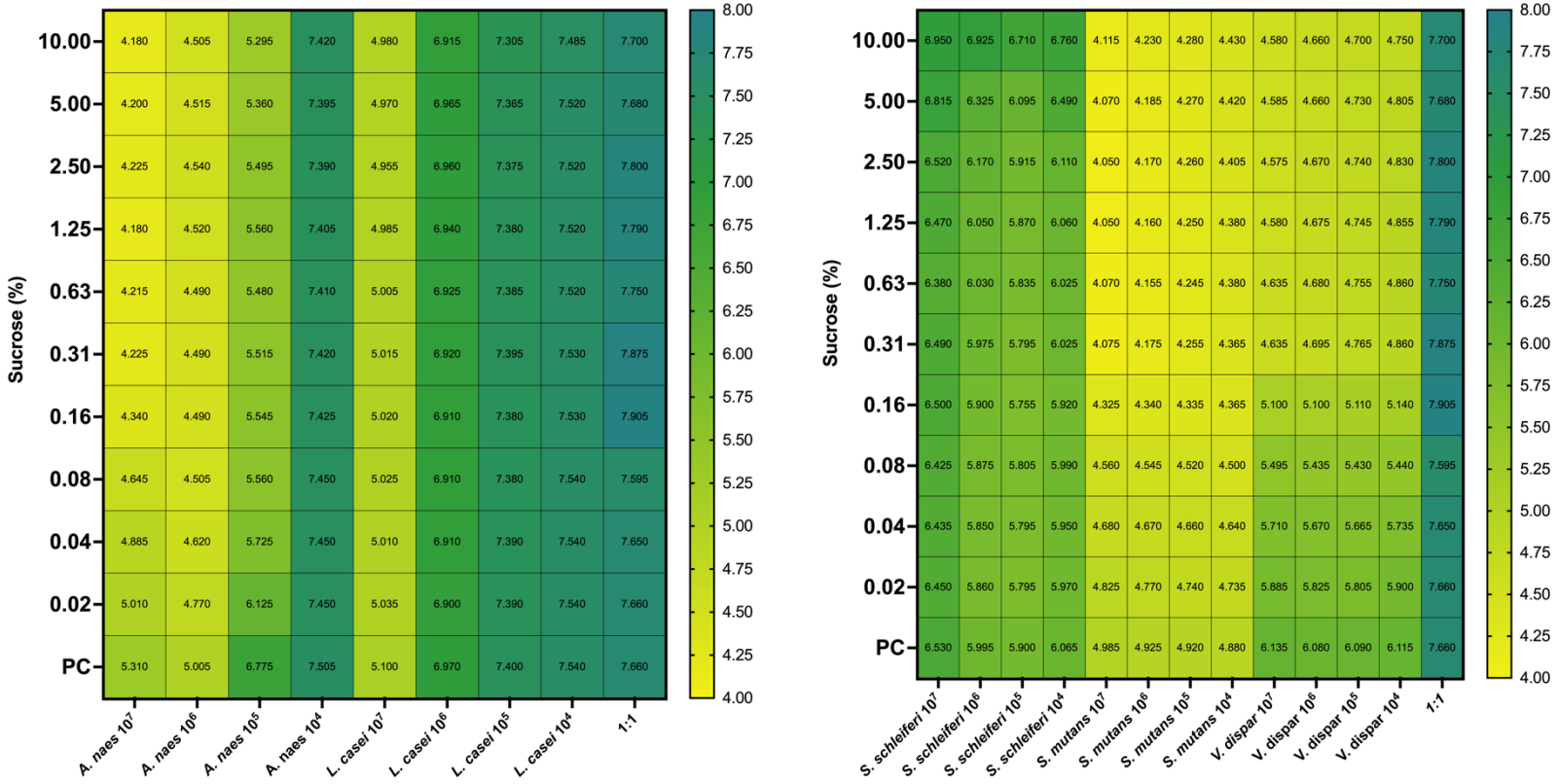


**Figure 3-12 - Evaluation of starting concentration and sucrose on caries bacteria.** Heatmap visualization of pH of caries bacteria isolates across a concentration gradient of Sucrose. pH is shown to be affected by starting concentrations across all organisms. pH is shown to increase in a dose dependent manner for *V. dispar.*

### *3.4.4 Influence of C. albicans phenotype on fixed models*

Having observed the impact of these organisms on micro-environmental pH, it was essential to observe how they come together in a multi-species biofilm model to infer the potential cariogenic impact which may be generated by shifting phenotypes of *C. albicans* and the implications of a relevant oral intervention.

A previously established biofilm model (Millhouse et al., 2014), which was developed to observe changes in micro-environment using pathologically relevant organisms, was leveraged to observe compositional changes in biofilm dynamics alongside these pre-screened isolates of *C. albicans*. As outlined below, in Figure 3-13, organism distribution shifts noticeably in the favour of cariogenic bacteria *Streptococcus mutans* when combined in a polymicrobial biofilm with Low-biofilm phenotype *C. albicans* 22, increasing from 14.22% in type strain SC5314 model to 36.72%. Biofilms containing high biofilm forming isolate 107 observed an increase in *S. mutans* of only 2% in comparison. These results are indicative that a biofilm model containing a low biofilm forming phenotype of *C. albicans* could produce results more representative of a cariogenic environment.

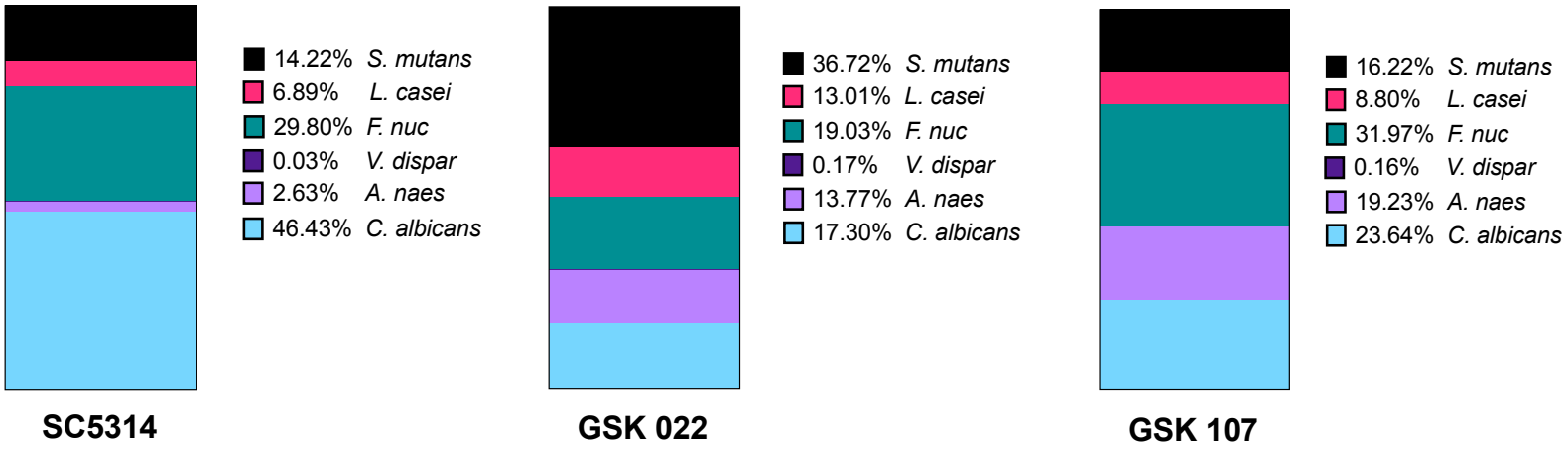


**Figure 3-13 - Compositional analysis of caries model across biofilm phenotypes.** Bacterial composition charted across, from left to right, type-strain *C. albicans* SC5314, low-biofilm forming isolate (22) and High-biofilm forming isolate (107) phenotypes of *Candida albicans*. Organism distribution is seen to change across all phenotypes of *C. albicans*.

To further test this, environmental pH was examined across multiple days and with treatment intervention. This was visualised via heatmap in Figure 3-14, below, where the cariogenic biofilm models containing SC5314 and HBF 107 were observed to have an average pH of approximately 7 after 2 days of growth when provided with 1% sucrose in the media.

Inversely, the biofilms grown with LBF isolate 22 were seen to drop to a pH level lower than 5 after the same incubation period. Bacteria-only models were shown to drop further than those containing *C. albicans*, reaching pH levels lower than 4.5. This directly evidences the impact of *C. albicans* phenotype on the environmental pH. When presented with a treatment of toothpaste slurry, pH was observed to increase again to range between 7.5-8 for all models but was shown to drop to approximately 6 after 24 hours of regrowth.

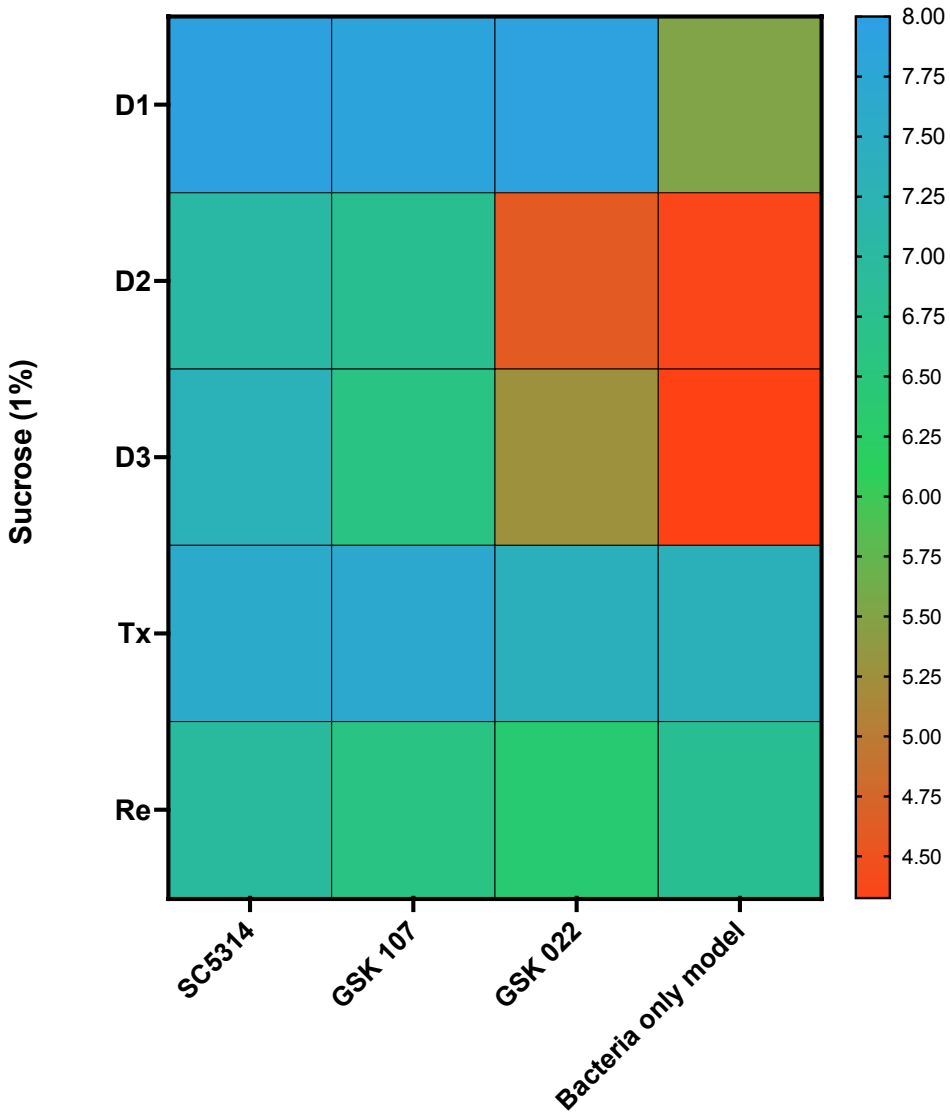


**Figure 3-14 - Influence of *C. albicans* phenotype on supernatant pH of caries biofilm model.** Heatmap visualization of pH of caries model with Sucrose (1%). pH is shown to be affected by initial seeding of substrate with *C. albicans* in comparison to "Bacterial only" development of caries biofilm model. Treatment on Day 4 with toothpaste slurry (Tx) and allowed to regrow for 24 hours post treatment (Re).

Having established the impact on the micro-environmental pH driven by shifting phenotypes of *C. albicans* in a fixed model, it was essential to determine that impact in a model derived from whole saliva as opposed to a strictly defined and targeted cariogenic model.

### *3.4.5 Establishing parameters for ex-vivo models*

To establish optimal growth conditions for these *ex-vivo* models, standard enumeration of organisms at different timepoints and conditions was conducted. As can be seen below in Figure 3-15, represented organisms had reached a standard level of growth within 3-days (72hrs) of growth across all conditions. This approximated $6x10^7$CFE/mL relative aerobic organisms, as determined through enumeration on Columbia Blood Agar (CBA) and incubation at 37°C. Enumeration of anaerobic organisms, incubated anaerobically, on Fastidious Anaerobic Agar (FAA), at 37°C, produced a count of $3x10^8$CFU/mL. Fungal organisms, grown on Sabouraud's Dextrose Agar (SAB) at 37°C, reached a value of $2x10^8$CFU/mL. By comparison, on the final day of testing, aerobes were found to a count of $3x10^8$CFU/mL, anaerobes to a count of $1x10^8$CFU/mL, and fungi to a count of $2x10^8$CFU/mL. No major differences in growth, therefore, could be established when including prolonged incubation.

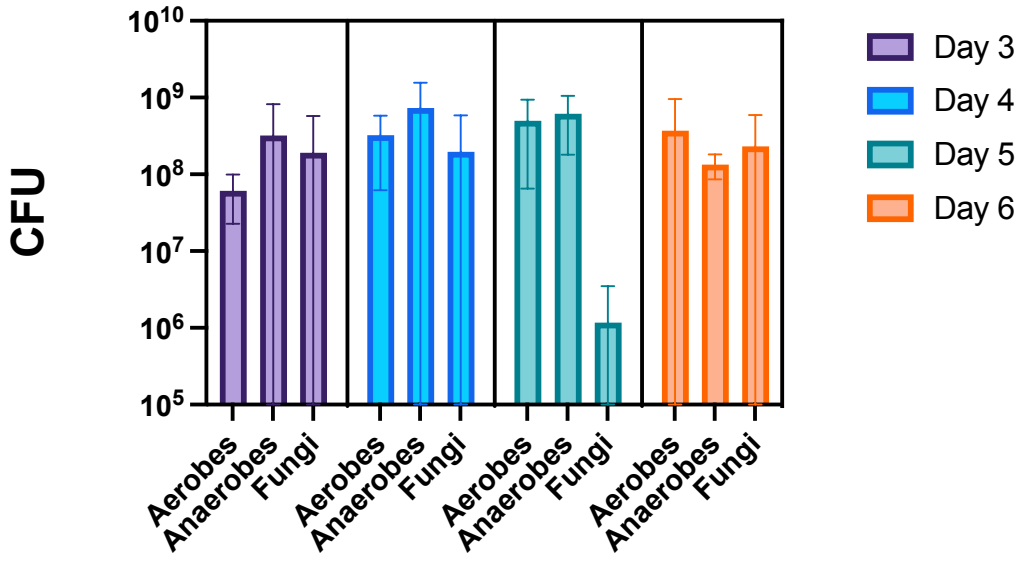


**Figure 3-15 - Determination of optimal maturation time for ex-vivo biofilm models.** Standard enumeration of organisms in saliva-derived biofilms, using CFU/mL as a representation of types of organisms present at varying timepoints of *ex-vivo* biofilm model development. Samples were incubated under aerobic, anaerobic conditions, as well as using culture media suitable for fungal growth.

Having established this baseline enumeration of organisms present, it was clear that a minimum incubation term of 3-days would be required to establish equivalent distribution of organisms within the biofilms for "fairer" representation within the model. Knowing this, it was essential to establish the impact the maturity of these biofilms may have on the enamel substrate, based on the parameters we have seen for environmental pH in Figure 3-14.

### *3.4.6 Examining the impact of ex-vivo models on enamel surfaces.*

Having established potential parameters for the growth of *ex-vivo* biofilm models, it was essential to examine how these models may develop in the context of being grown on enamel surfaces and to assess their effects on different parameters related to enamel integrity such as surface roughness, microhardness, electron micrography and optical profilometry.

As depicted below, in Figure 3-16, *ex-vivo* saliva-derived biofilms were again grown for a period of 3-5 days (72-120hrs) to establish the impact of microbial growth on the surface of the enamel with, and without, 1% sucrose. It was determined that, overall, no major impact was obvious in those samples grown for 3, 4, or 5 days when compared to a control disk in terms of surface roughness (Sa). However, once 1% sucrose was introduced to the system, an obvious shift in surface roughness was observed, in a biofilm-maturity dependant manner, across each timepoint. This resulted in a shift from the control surface of 1.8Sa after 3 days, 3.3Sa after 4 days, and 4Sa after 5 days. This emphasises the deleterious effects of continued acidification exemplified in our *in-vitro* biofilm models and mimics neglect in oral hygiene resulting in cariogenic biofilm build-up over time.

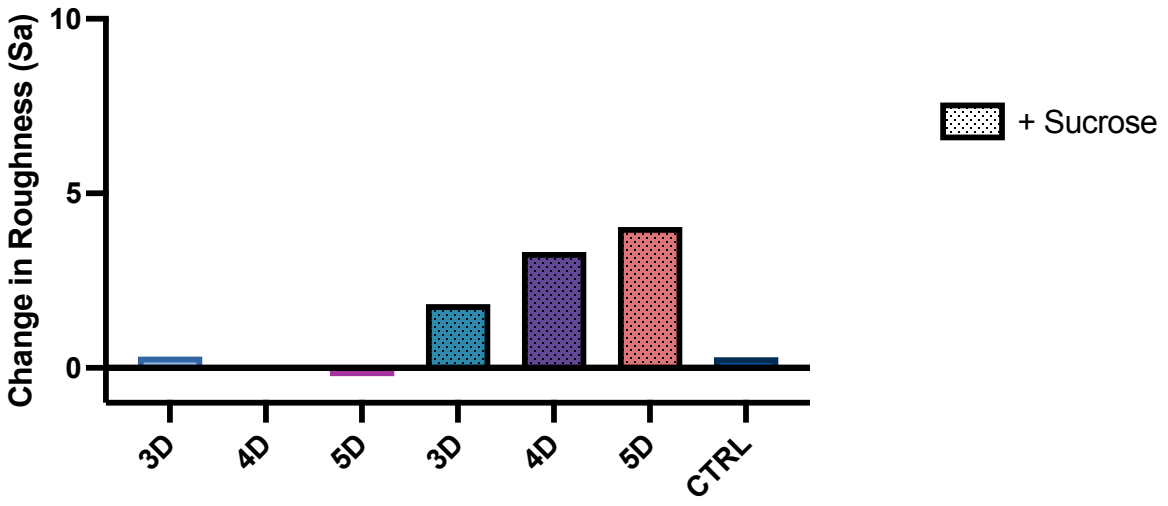


**Figure 3-16 - Changes in bovine enamel surface roughness at biofilm developmental timepoints.** *ex-vivo* biofilms grown in 1:1 RPMI:THB media with and without 1% sucrose. Biofilms grown without environmental sucrose did not shift significantly in overall surface roughness (Sa). Biofilms with 1% sucrose steadily increased in surface roughness across the 5-day timepoints.

In addition to assessing changes in surface roughness driven by biofilm development, surfaces were next examined in the context of changes to surface microhardness (HK) when compared with a baseline reading from each disk. As in Figure 3-17, below, samples without environmental sucrose (1%) were seen to reduce in hardness across 5-day timepoints. By 3 days, surface microhardness had reduced by -28.2HK when compared with the sample surface baseline reading. After 4-days, the surface hardness had reduced by -116.8HK. Interestingly, this reduction was seen to invert somewhat after 5-days of growth, reducing by -46.4 compared to baseline.

In samples containing 1% sucrose, differences were far more readily apparent, having dropped to -237HK when compared with baseline by 3-days of biofilm growth. By day 4, these samples had reduced by -315.8HK. Again, the same inversion in hardness was seen by day 5 where the reduction was -270.2HK. For comparison, a negative control disk which had neither biofilm growth nor exposure to growth media, had reduced by -12HK compared to its baseline readout. This would indicate that, while biofilm growth has some, time-dependant, impact on surface microhardness, this is more in-line with fluctuations in hardness evidenced by the untouched enamel surfaces than that of the changes induced by biofilms given 1% sucrose.

Given that we have seen that surface roughness and microhardness are both substantially affected by the presence of environmental sucrose, we can establish that these *ex-vivo* biofilms were developmentally consistent with cariogenicity.

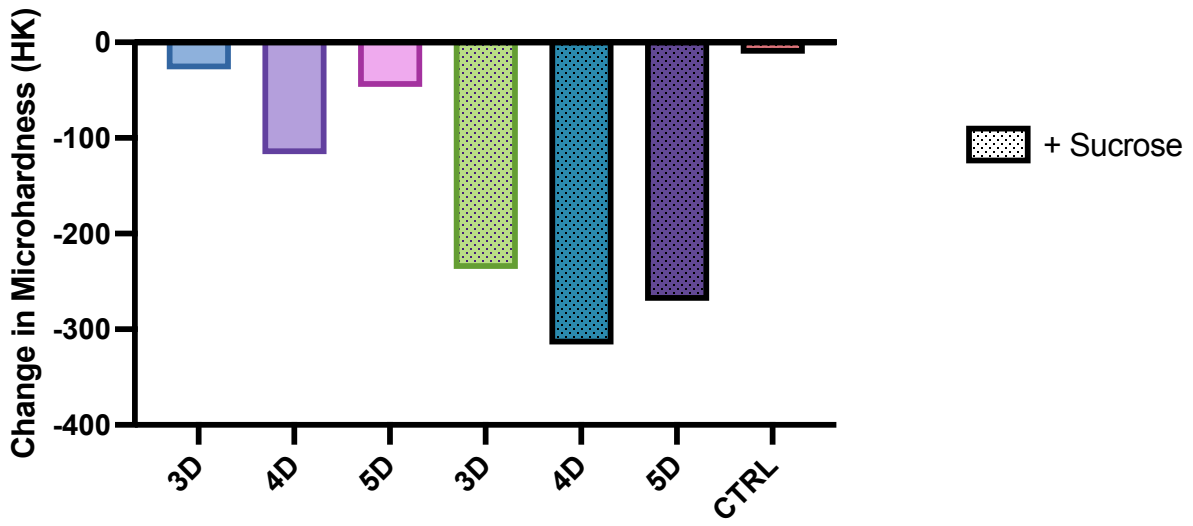


**Figure 3-17 - Changes in surface microhardness in development of ex-vivo biofilms.** *ex-vivo* biofilms grown *ex-vivo* biofilms grown in 1:1 RPMI:THB media with and without 1% sucrose. Biofilms grown without sucrose exhibit a reduction in surface microhardness when compared to a clean control disk. Samples containing 1% sucrose exhibit substantial reduction in biomass by comparison.

As these conditions matched our hypothesised expectations of the dietary influence of shifting phenotype, it was important to attempt to visualise this shift in organism structure through influence of 1% sucrose. To attempt this, Scanning Electron Micrography was employed as a tool to visualise the enamel surface and the phenotypic differences that we believed to be taking place on the surface of the enamel and driving this cariogenic development of the *ex-vivo* biofilm.

The changing landscape of the biofilm, as exemplified below in Figure 3-18, exhibited changes in bacterial morphology when samples were free from sucrose, being overall more coccoid in morphology, which would track with our expectations that *Streptococcus* species would be a key organism in the maintenance of a “standard” oral biofilm model. This is further emphasised by the ubiquitous nature of *Streptococcus* species in *in-vitro* defined models for biofilm research, such as those we have already examined in our defined compositional analysis in Figure 3-13. Inversely, when visualising the samples given 1% sucrose in the culture media, we see a complete shift in visible organism morphology, taking on an overall more bacillus, rod-shaped, morphology which would potentially be consistent with organisms which favour lactic acid production such as *Lactobacilli*. As these images are qualitative in nature, we cannot draw firm conclusions about the organisms present. However, given the examples of biofilm composition and analysis related to surface dynamics and profilometry, it would be fair to hypothesise the presence of these key organisms under each condition. This could be confirmed through potential routine culture methods using specific growth media but would also be elucidated by sequencing of saliva samples as outlined in the following section.

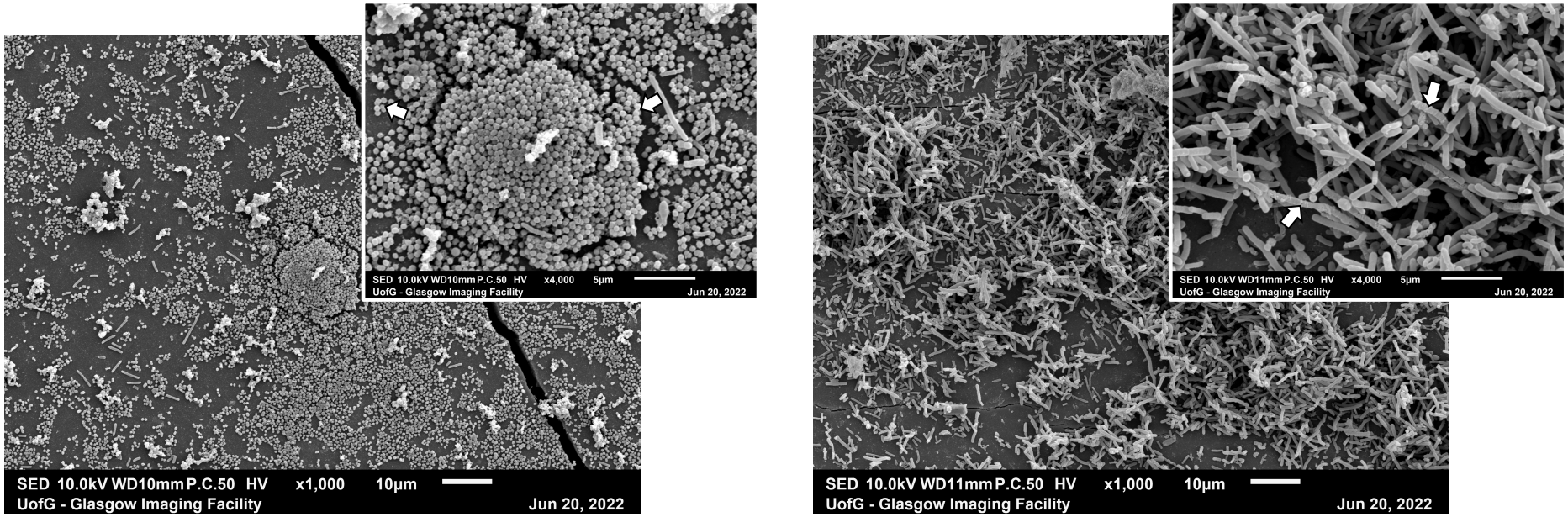


**Figure 3-18 - Sucrose dosing of ex-vivo biofilms reveal shift in organism phenotype across samples.** Scanning electron micrographs (SEM) of *ex-vivo* biofilms with (LEFT) and without (RIGHT) 1% sucrose. Images represent a shift in organism morphology between experimental parameters. White arrows have been used to clarify key morphological differences between organisms present. Main image: x1000 magnification; Inset: X4000 magnification. Images generated by M. Butcher courtesy of Glasgow Imaging Facility.

Having visualised the phenotypic, morphological changes of the biofilms present on the material surface and having established the impact on surface roughness and microhardness, it was important to visualise the surfaces for changes in profilometry as a biomarker for pathological changes.

As shown below in Figure 3-19, control enamel, having no biofilm growth, was observed to retain a uniformity in surface depth and roughness consistent with previous results, visualised by the uniform colouration of the heat-map profilometry. When examining those samples with biofilm growth but no sucrose, this uniformity in surface profile had begun to lose definition, becoming warped toward one side of the disk. Despite this, the overall profile still closely resembled that of the control disk, indicating less impact on the enamel which also was reflective of previous data generated in this report. However, those samples which were exposed to 1% environmental sucrose were observed to dramatically alter in structure, revealing a large cavity within the centre of the enamel disk and an overall loss of structure unrecognisable to that of the control disks. Again, this could be representative of those alterations to surface hardness and roughness that we had previously exhibited in biofilms grown with access to sucrose as shown in Figure 3-16 and Figure 3-17. Much like the electron micrographs depicted in Figure 3-18, these images paint a greater picture of the deleterious effect of these biofilm models when induced toward a cariogenic profile.

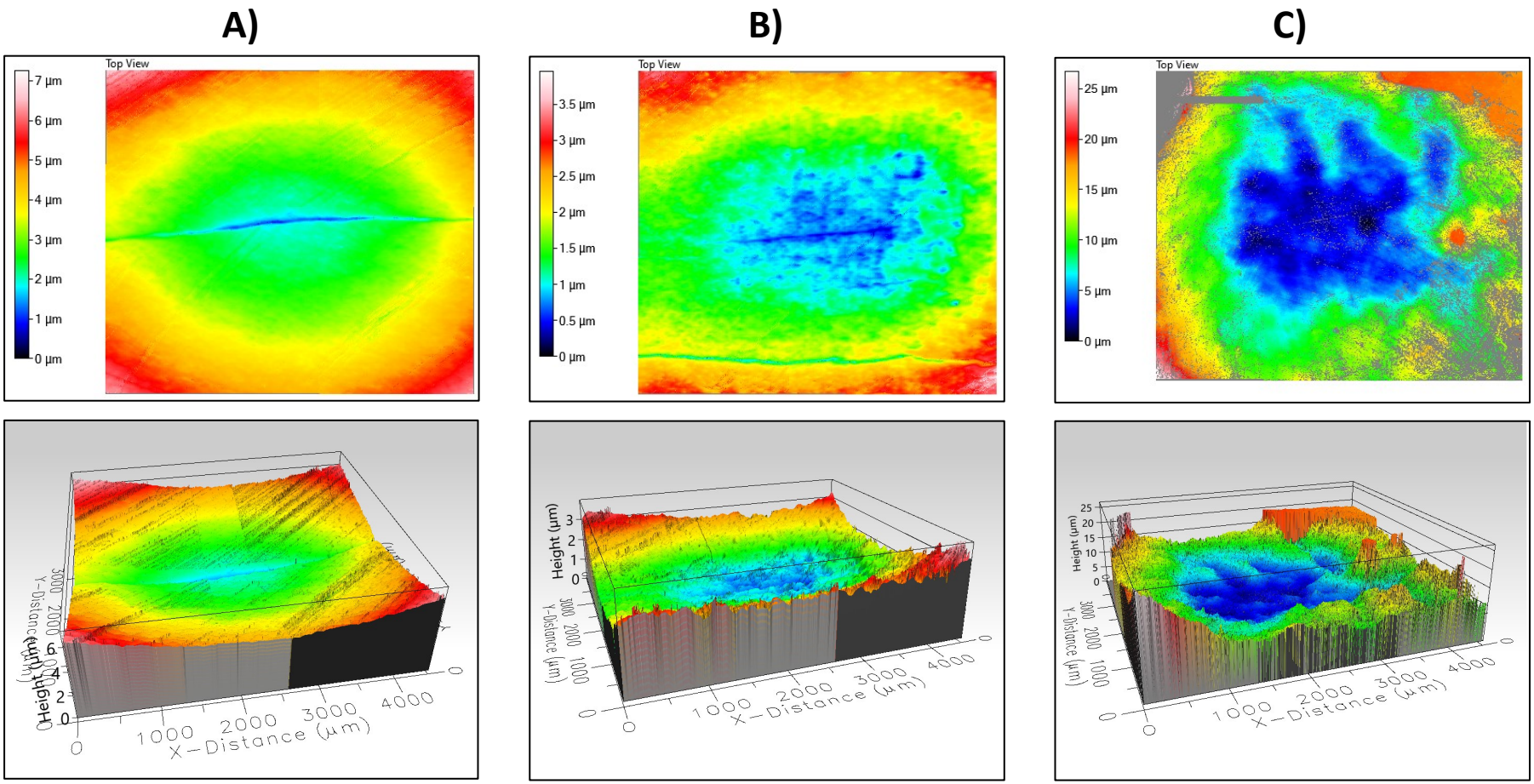


**Figure 3-19 - Mapping of enamel surface reveals cavity formation through influence of sucrose on ex-vivo models.** Images depict surface characterization through 3D optical profilometry, visualized as heatmap images of enamel surface. A) enamel surface control, B) enamel surface with *ex-vivo* biofilm without sucrose, C) enamel surface with *ex-vivo* biofilm growth with 1% sucrose. Surface changes are most visually evident in the samples containing sucrose, where depth of sample is much lower and less uniform in comparison to control enamel. Images generated by Intertek®.

### *3.4.7 The inclusion of C. albicans influences enamel outcomes*

Having established the parameters required for assessment of enamel in the context of *ex-vivo* biofilms, it was important to continue examination of how these outcomes may be influenced by the presence of key fungal organism *C. albicans* and how that influence may be affected by strain dependant differences in phenotype. To that end, samples were next assessed in the same format as in section 3.4.6, but with the inclusion of *C. albicans* SC5314, 22, and 107. Additionally, to exemplify how these outputs may be influenced by oral hygiene regimen and the subsequent regrowth of biofilms, as previously outlined in Figure 3-14.

To begin with, enamel was assessed for changes in surface roughness in comparison to enamel baseline established before experimentation. As shown in Figure 3-20, once *C. albicans* has been introduced to *ex-vivo* models, the influence of dietary sucrose is diminished in terms of changing surface roughness when compared to a media only control enamel. Indeed, no statistically significant difference was observed across experiment parameters of strain type and intervention. This would imply that changes in surface roughness from a baseline reading can happen independently of microbial growth, and that *C. albicans* may limit these large fluctuations observed in previous outputs, such as those seen in Figure 3-16. Indeed, in this example, no sample was observed to exceed a change in roughness value of 1Sa, which is in stark contrast to the values presented in the previous experiment. As previously, it was essential to examine this further to examine if this uniformity of parameters was exhibited in the enamel microhardness.

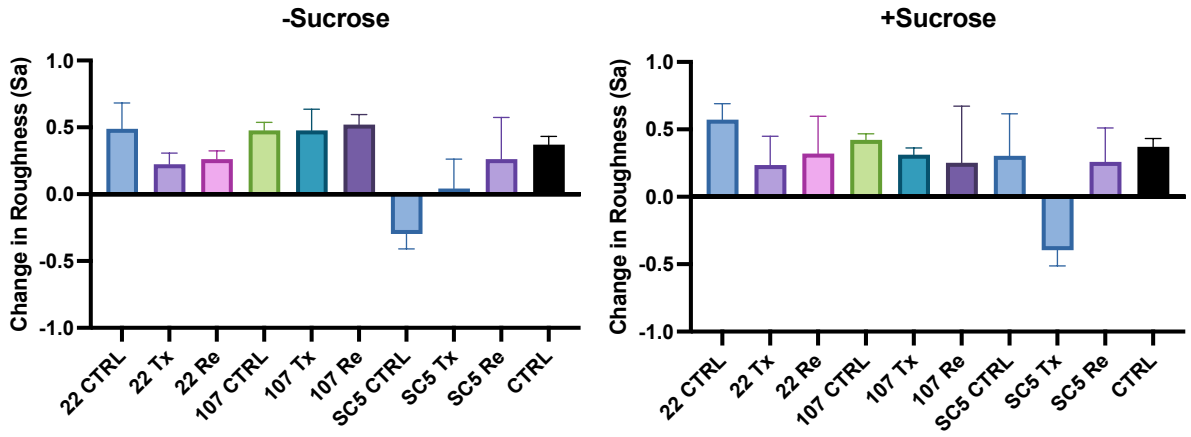


**Figure 3-20 - Changes in surface roughness in presence of *C. albicans*.** *ex-vivo* biofilms grown in 1:1 RPMI:THB media with (RIGHT) and without (LEFT) 1% sucrose. No significant differences were observed in sample roughness (Sa) across isolates of *C. albicans* and inclusive of treatment regimen (Tx) and biofilm regrowth (Re) when compared to media only control enamel grown for 24 hours (CTRL). All biofilms except SC5 CTRL without sucrose and SC5 Tx with sucrose resulted in surface roughness greater than baseline.

Bovine enamel was assessed for surface microhardness, as shown in Figure 3-21, below. In those samples without sucrose, the impact of LBF isolate 22 on the surface microhardness was visible, being approximately 50HK lower than control enamel in both the control and regrowth models. This was not visually evident in the other isolates of *Candida*. However, a stark difference was observed in those biofilms dosed with 1% sucrose where surface microhardness was seen to be reduced by values, at times, as low as -235HK in comparison to the enamel control. This reduction was observed to be independent of the influence of *C. albicans* phenotype. In essence, we can establish from this process that surface microhardness was seen to moderately improve post-treatment in regrowth samples. Additionally, we can conclude that the influence of sucrose on the biofilm model has the capacity to override any nuanced output that may be determinable by the influence of *C. albicans*.

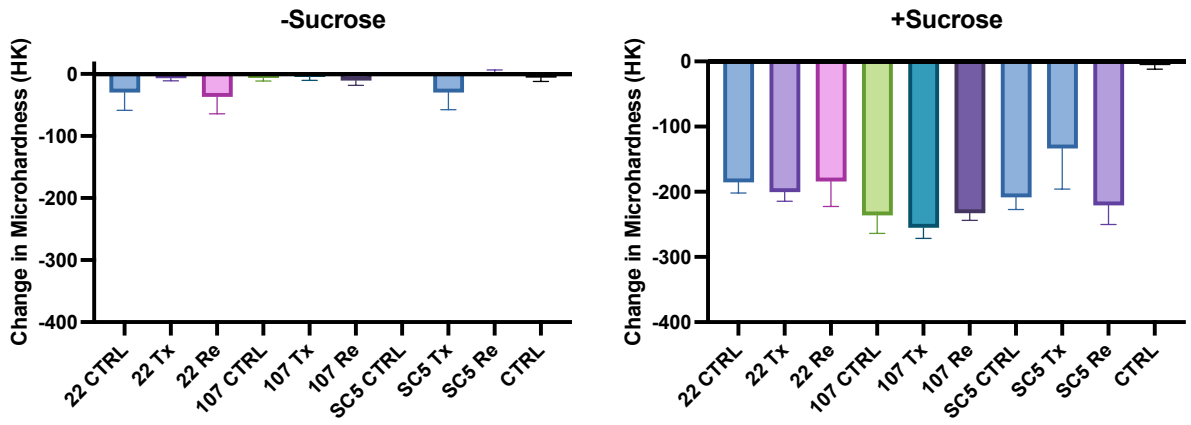


**Figure 3-21 – Surface microhardness (HK) in the presence of *C. albicans* and 1% Sucrose.** Surface microhardness is in stark contrast when saliva-derived biofilms are provided with sucrose. Impact of *C. albicans* phenotype is diminished in the presence of sucrose post 24 hours growth.

Having observed this influence of *C. albicans* strain and environmental sucrose on the integrity of enamel, in the context of roughness and micro-hardness, we sought to once again assess the surface profile in a qualitative fashion, as exemplified previously in Figure 3-19. In addition to this, we wished to observe how the enamel may be affected by the introduction of a therapeutic regimen like toothbrushing. This would allow us to visualise the effect of *C. albicans* strain type along with the potentially restorative effects of stannous fluoride treatment to the enamel surface in the same context to that shown in Figure 3-14. Depicted below in Figure 3-22, surface characterisation depicts **CTRL** biofilms as having a clear erosive effect on the enamel surface denoted by the areas of light-dark blue clearing in the central section of the disk.

Overall, the differences between the two strains of *C. albicans* were not immediately apparent at this stage, albeit there appeared to be slightly less uniformity to the surface of samples containing LBF strain **GSK022**. Surfaces treated with stannous fluoride and brushing, shown in (**Tx**) continued to show a reduction in surface enamel potentially exacerbated by the addition of brushing. Minor observable differences were

seen in those samples containing **GSK107** where the numerous peaks visible on the sample could be indicative of an increase in surface roughness as depicted in Figure 3-20, a potential outcome that is also reflected in the apparent smoothness of the surface in **GSK022**(**Tx**) when observing the samples surface roughness data.

However, when observing those samples which were allowed to regrow for 24hrs in (**Re**) there is a stark difference between the two strains in terms of height distribution and uniformity, with the **GSK107** samples appearing similar to those depicted in the original unaltered control enamel in Figure 3-19, albeit with an increased surface roughness. When compared with **GSK022**, this could be indicative of worsened outcomes for the enamel surface and a greater profile of erosion by comparison. Most importantly, these enamel outcomes do not appear to mirror the level of damage imposed by introducing sucrose into the system when comparing, again, to enamel in Figure 3-19.

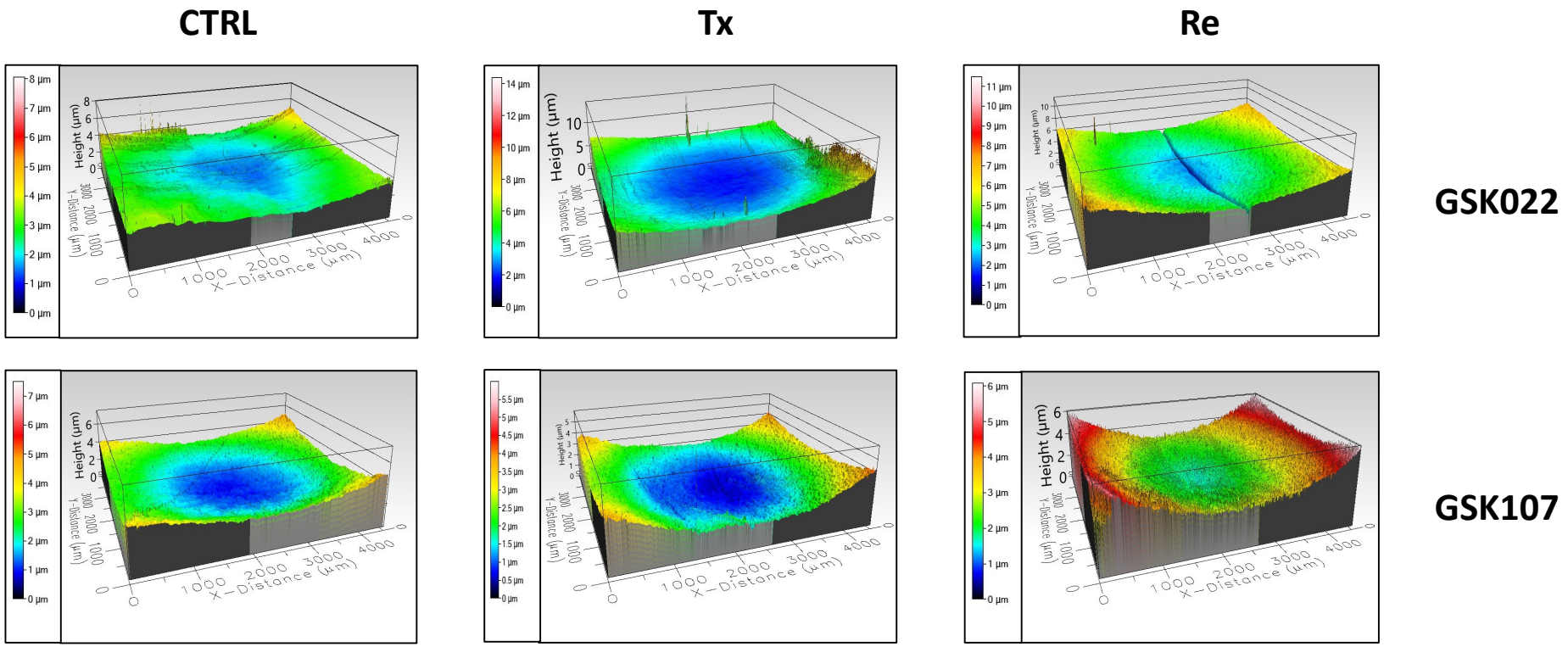


**Figure 3-22 – *C. albicans* phenotype differences may influence treatment outcomes.** Images depict surface characterisation through 3D optical profilometry. Surface profiles reflect *ex-vivo* biofilms grown with the inclusion of Candida strains GSK022 (TOP) and GSK107 (BOTTOM) and without 1% additional sucrose. These are further categorised into enamel used as a substrate for unhindered control biofilms (CTRL), biofilms immediately after treatment with 1:4 Stannous fluoride slurry and a standardised brushing method outlined in section 3.3.8 (Tx) and biofilms allowed to regrow for 24hrs post-treatment (Re). Colour mapping of surfaces depicts depth changes in substrate from (Red/White) at the highest point to (Blue/Black) at the lowest. Images generated by Intertek®.

Having observed these differences in the enamel without the presence of sucrose, it was essential to observe how the depicted changes in surface roughness and microhardness could be influenced by this environmental factor. This was achieved by growing biofilm samples in the same way described previously but introducing 1% sucrose to the growth media.

Shown below, in Figure 3-23, the difference between strains in terms of biofilm control samples (**CTRL**) is immediately apparent, with a large range in height from the lowest point to the highest point in **GSK022** samples and a sample more reflective of the unaltered control enamel from Figure 3-19 in those samples exposed to **GSK107** indicating the HBF strain having a more protective effect on the enamel surface, if left untreated, when there is a high concentration of polysaccharide present. After treatment (**Tx**) the enamel surface appears to regain a semblance of uniformity, regardless of *Candida* strain, which is again reflective of the surface roughness data depicted in Figure 3-20, which observed a lower shift in surface roughness post-treatment. It should be noted, however, that despite the experiment being carried out in triplicate to ensure viable replicates of treatment values, the image depicting the sample containing **GSK022** is poor and appears to have been affected by the post-processing of enamel disks when returned to the manufacturer for analysis. This is, again, the case for those samples which were allowed to regrow for 24hrs (**Re**) which again obscure the visual output present on the enamel surface. However, the samples containing **GSK107** appeared to produce comparable results to those of the enamel exposed to biofilm growth and 1% sucrose depicted in Figure 3-19, where integrity of the enamel surface appears to be considerably altered by the regrowth of microbial populations after treatment. This, again, is reflective of those images of biofilm

depicted previously in SEM images from Figure 3-18, and may be reflective of a potentially more deleterious biofilm being allowed to regrow after treatment. This would be further compounded by the analysis of pH present from Figure 3-14, where samples were observed to drop in pH rapidly post-treatment.

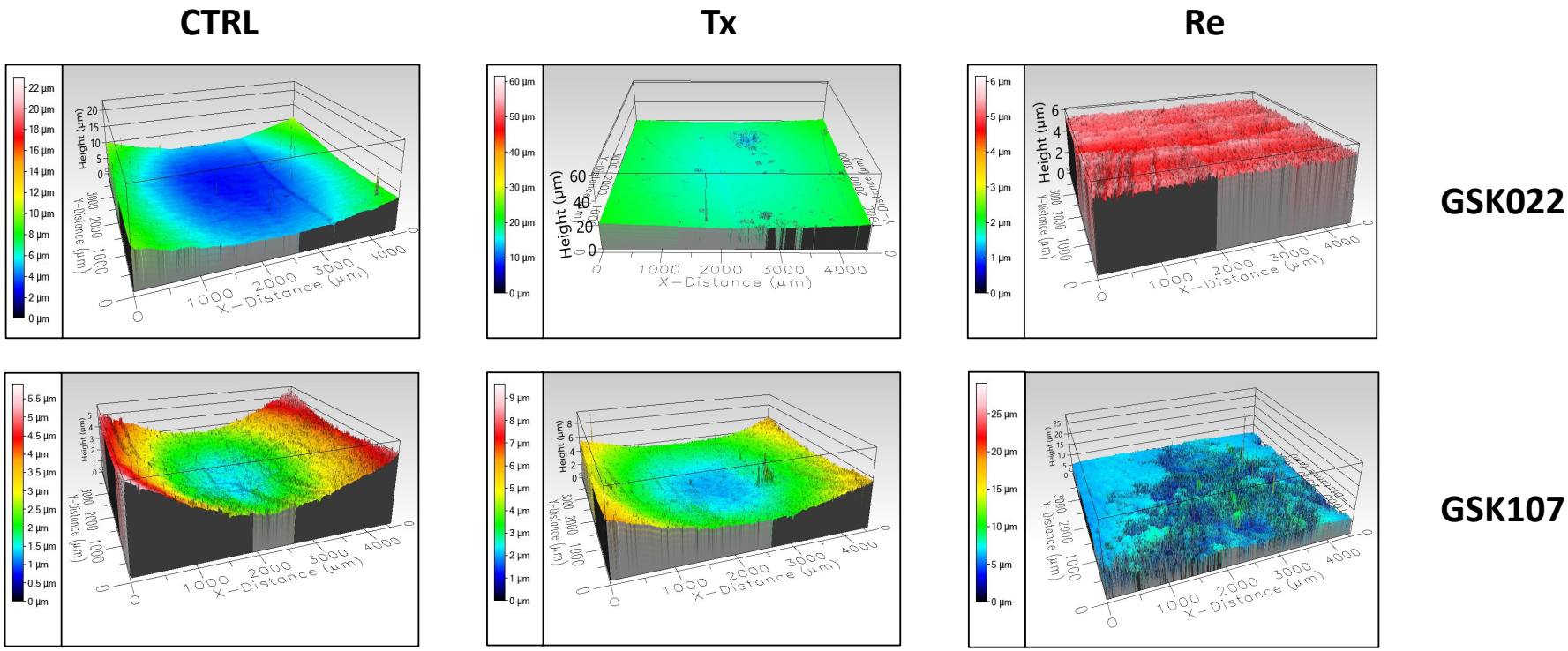


**Figure 3-23 - Additional sucrose exacerbates enamel outcomes post-treatment.** Images depict surface characterization through 3D optical profilometry. Surface profiles reflect *ex-vivo* biofilms grown with the inclusion of *Candida* strains GSK022 (TOP) and GSK107 (BOTTOM) and with 1% additional sucrose. These are further categorised into enamel used as a substrate for unhindered control biofilms (CTRL), biofilms immediately after treatment with 1:4 Stannous fluoride slurry and brushing (Tx) and biofilms allowed to regrow for 24hrs post-treatment (Re). Colour mapping of surfaces depicts depth changes in substrate from (Red/White) at the highest point to (Blue/Black) at the lowest. Images generated by Intertek®.

Having observed fundamental differences in the condition of the enamel in terms or surface roughness, microhardness, and 3D profilometry, and having observed the morphological changes in organisms present through SEM imaging (Figure 3-18), particularly through the inclusion of 1% Sucrose, it was important to observe how these conditions influence the morphology of organisms under each of our defined growth parameters.

As shown in Figure 3-24, below, distinct morphological differences are depicted across all experimental parameters. Most notably, control samples (**CTRL**) containing type strain **SC5314** displayed large coverage of the enamel with a variety of cell morphologies present in the sample. This, however, was not the case for samples containing **GSK022** and **GSK107**, with a notable lack of fungal filamentation present in the **GSK022** samples, reflective of the yeast morphology and low biomass phenotype that was established earlier. Moreover, there was more enamel surface visible on the sample, which could be indicative of an increased exposure to environmental factors which would enhance cariogenic activity on the enamel.
Interestingly, while those samples containing **GSK107** displayed the filamentous phenotype we have associated with biofilm formation, the overall biomass visible on the **CTRL** enamel surface was relatively poor by comparison to the type-strain **SC5314**. This could indicate that, despite this strain forming a significantly larger biofilm *in-vitro*, the nuance of being included in a complex community in an *ex-vivo* saliva model may have bearing on the development of this organism.

It was also clear from the images presented for the treatment (**Tx**) that regardless of *Candida* phenotype, samples exposed to stannous fluoride and brushing had severely

diminished biomass visible on the sample surface, indicating a successful treatment regimen in the context of oral healthcare. Despite this, some leftover biomass and visible cells are present on the enamel surface and provided a clear indicator of the survival of organisms necessary to sustain the rapid regrowth of biofilms exemplified in the regrowth samples (**Re**). Interestingly, more biomass was observable on those samples containing high biofilm phenotype **SC5314** and **GSK107** than in that of the LBF **GSK022**. This may indicate that the enhanced capability for adhesion provided by these strains filamentous phenotype switching could provide structure and support for surrounding organisms which would otherwise have been lost during treatment and allowing rapid regrowth of biofilm post-treatment.

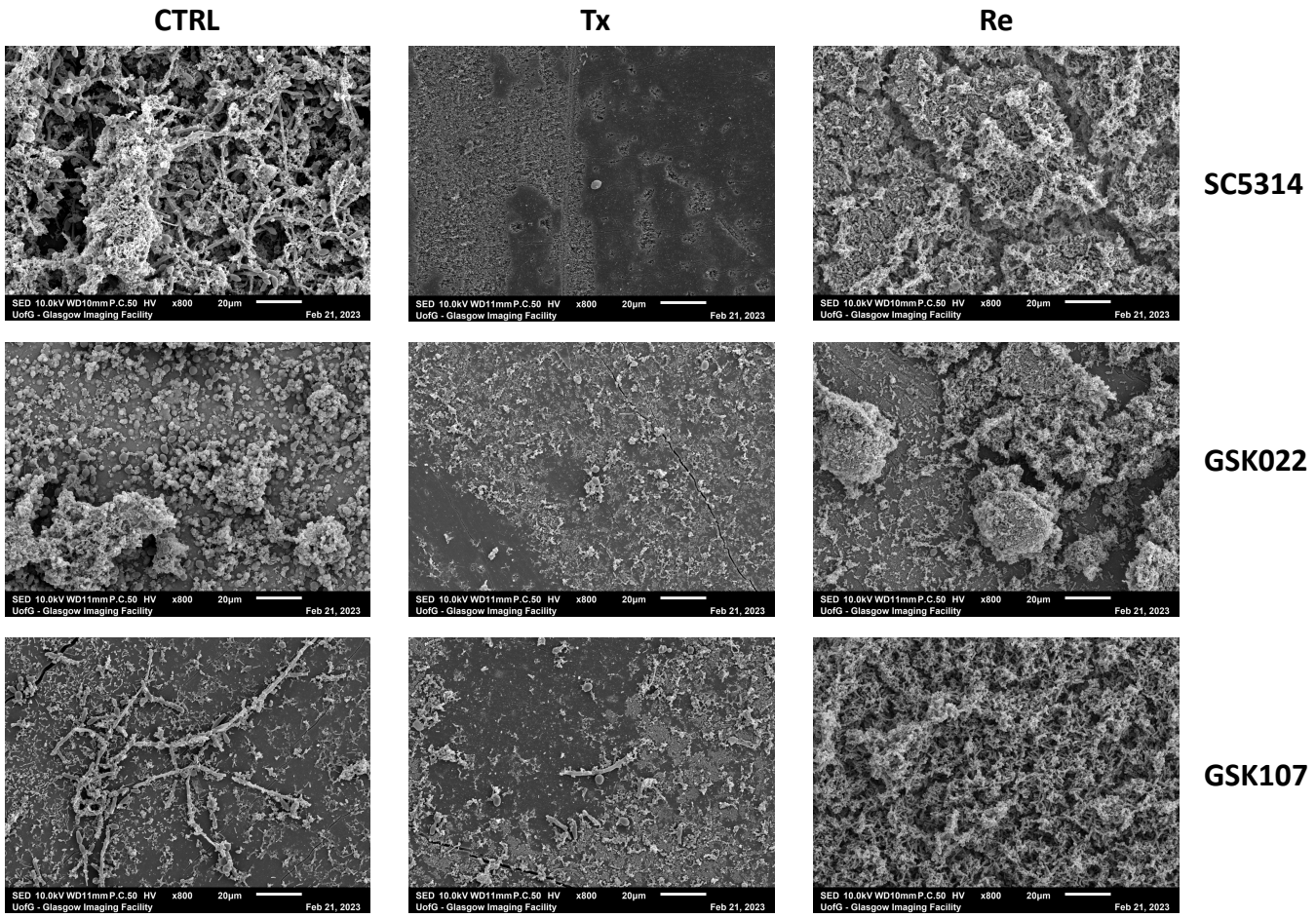


**Figure 3-24 – Electron micrography reveals morphological differences in ex-vivo models across *C. albicans* phenotypes.** Scanning Electron Micrograph (SEM) images of *ex-vivo* biofilms grown with inclusion of *C. albicans* SC5314, horizontally (TOP), GSK022 (MIDDLE), GSK107 (BOTTOM) grown with 1% sucrose. Biofilms imaged were grown on bovine enamel and represent unhindered control growth, vertically (LEFT), treated with 1:4 Stannous fluoride (CENTRE), and regrown for 24hrs post treatment (RIGHT). 800x magnification. Images generated by M. Butcher courtesy of facilities at the Glasgow Imaging Facility.

## 3.5 Discussion

### *3.5.1 Overview*

Having identified, in the previous chapter, a consistent gap in the literature relevant to the activity of fungal organisms in the context of the oral microbiome, it was essential to investigate the nuance of why these organisms are under-represented in the context of microbiome research.

Indeed, it has been identified by reviews of microbiome research, such as those produced by Zhang et al., in 2021, that fungal microbiome research, as of 2021, made up less than 3% of relevant microbiome literature (Zhang et al., 2021). Wojciechowska et al., for example, in 2024, announced a call for the scientific community to stop neglecting the established relevance of fungi in the micro-environment (Wojciechowska et al., 2024). This sentiment has been repeated in many reviews of the literature, particularly with reference to well-defined research conducted into the gut microbiome (Jaswal et al., 2023, Enaud et al., 2018, Zhang et al., 2022a, Guzzo et al., 2022).

In the oral cavity, studies into the complexity of the oral microbiome, such as those conducted by Peters et al., in 2017, also highlight the lack of community interest in fungal influence of the microbiome in oral conditions such as periodontitis (Peters et al., 2017). Again, this sentiment of neglect has been parallelled by other comparative studies and reviews in the field of oral microbiome research (Ghannoum et al., 2010b, Defta et al., 2024).

### *3.5.2 Hurdles to fungal inclusion in microbiome sequencing.*

Having established the relative lack of emphasis in the literature, it was important to consider what issues may be present to prevent the inclusion of fungi in the scope of microbiome research. This perceived bias in the literature, however, may not be resultant from a lack of interest in the field but from a potentially inherent difficulty in applying the same, now well-established, sequencing protocols for bacterial genome and 16S rRNA sequencing to fungal organisms.

For example, fungal genome complexity, as inferred by Thacker in 2003, poses a unique challenge in the context of sequencing (Thacker, 2003). This is compounded further by the relative lack of complete genetic reference databases available for accurate phylogenetic determination of fungal organisms (Ohta et al., 2023, Banos et al., 2018, Nilsson et al., 2009). Indeed, this issue of inclusivity and accuracy in reference databases was called to attention in 2013 by Kõljalg et al., in a call to standardise protocols for the accurate uploading of fungal ITS sequencing data (Koljalg et al., 2013).

Despite these challenges with direct fungal sequencing, it is well established in the literature that fungal organisms have a significant impact on the surrounding micro-environment which has a lasting influence on other microbial communities (Bahram and Netherway, 2021, Denham et al., 2019, Diaz et al., 2014). Complex microbiome studies, such as that conducted by Harrison et al., in 2021, show clear consequences for host animals in the context of adjusting bacterial populations through the inclusion of fungal organisms (Harrison et al., 2021). Despite this, however, these complex relationships and their role in the oral cavity remain under-examined. Research, such as that conducted by Robinson et al., in 2020, examined the importance of cross-

domain associations between fungal and bacterial organisms in the oral microbiome, in the context of therapeutic outputs for leukaemia patients, but this remains an under-explored aspect of oral microbiome research (Robinson et al., 2020).

Understanding these nuanced issues in microbiome research in the context of fungi was crucial to the intention of this study. *Candida albicans* has often been exemplified as a keystone organism, not only in the context of oral caries but also as a critical component in complex polymicrobial communities, such as those established by Guggenheim et al., in 2004, for *in-vitro* research (Guggenheim et al., 2004, Xiao et al., 2018, Du et al., 2021a). Despite inconsistencies in results associated with *C. albicans* impact on surface roughness, its capacity for altering bacterial composition as well as adjusting the microhardness of enamel samples would indicate that there is an effect on cariogenic communities. As such, it was essential to investigate further interactions with *C. albicans* in the context of the oral microbiome.

### *3.5.3 C. albicans biofilm related strain dependencies*

To begin establishing the impact of *C. albicans* in caries outcomes, it was essential to observe how relevant clinical isolates could impact their environment in comparison to an established type-strain organism. Indeed, we established a wide range of effects in terms of organism growth rates, biomass production and metabolic activity (Figure 3-2), across the included isolates, which could infer wide-ranging effects on pathogenicity *in-vivo*, particularly in the dual contexts of cariogenic outputs derived from environmental pH and in biofilm/metabolic activity and potential resistance to antimicrobial treatment. Indeed, *C. albicans* strain heterogeneity has been well established in the context of human health, where work such as that conducted in

2014 by Sherry et al., identified fluctuations in biofilm biomass and cell morphology across a range of clinical bloodstream isolates (Sherry et al., 2014). Moreover, Sánchez-Vargas et al., in 2013 observed a multitude of *Candida* isolates from oral mucosa, including *C. albicans*, and were able to observe significant variation in the capacity to produce biomass and relative metabolic activity across these isolates while also highlighting the importance of considering strain variance in biofilm related work (Sánchez-Vargas et al., 2013).

Perhaps most importantly, in the context of caries outcomes, we were able to observe statistically significant increases and reductions in environmental pH in specific isolates of *C. albicans*, namely GSK107 and GSK22 (Figure 3-4). While *C. albicans* has often been closely, negatively associated with caries outcomes, we began to hypothesise from these outputs, as well as the established literature considering it part of the commensal oral microbiota, that this relationship may be more nuanced through strain to strain phenotypes and environmental factors than commonly perceived (Du et al., 2021b, Eidt et al., 2020, Lu et al., 2023, Jin et al., 2024).

It should be noted, however, that many of these associations consider *Candida* as existing as part of the paradigm of acidogenesis which is predominantly contributed to by organisms such as *Streptococcus mutans*, as exemplified by Garcia et al., in 2021 (Garcia et al., 2021).

Moreover, studies which focus specifically on *Candida* species, such as an investigation into the effect of *Candida* in saliva biofilms on tooth enamel by Caroline de Abreu Brandi et al., in 2016, observed that isolates taken from children with ECC were shown to produce more cariogenic outcomes on the enamel (Caroline de Abreu Brandi et al., 2016). It should be noted, however, that these studies observed a small

sample size of isolates already associated with a cariogenic environment and that they were provided with in excess of 1% sucrose as part of their environmental substrate, which may also have produced profound downstream effects similar to those we were able to see at high sucrose concentrations during screening (Figure 3-11). Similar work conducted by Kim et al., in 2017, highlights the poor capacity for *C. albicans* to metabolise sucrose in lower environmental concentrations without additional metabolic assistance from *S. mutans* (Kim et al., 2017b). This was also reflective of our own data where minimal differences were observed in pH and biomass formation when concentrations of sucrose were diluted. Additionally, we observed a clear adjustment to biomass in samples which contained 50% RPMI and 50% THB media, indicating a sharp metabolic switch and a likely dependency on the abundance of glucose in RPMI media to maintain biomass production. This data is key in understanding further, not only the strain dependent nuances of oral isolates of *C. albicans,* but the influence provided by even minimal adjustments to growth media (Weerasekera et al., 2016, Alshanta et al., 2022, Serrano-Fujarte et al., 2015, Hosida et al., 2018).

### *3.5.4 Summary*

Through these data, we were able to infer that *C. albicans*, while clearly having a profound impact on its extracellular environment, is not a clear, singular, driving force for caries under all parameters. Indeed, a study by Willems et al., in 2016, also inferred that the relationship between *C. albicans* and other organisms of the oral microbiome may be more important in elucidating its role in oral caries (Willems et al., 2016). As such, it was essential for us to investigate the effect specific strains of *C. albicans* would have in a fixed, multi-species consortia of organisms which were reflective of

organisms commonly associated with caries *in-vivo*. However, the depth of understanding of the role of *C. albicans* in a fixed model setting is limited and leaves a clear opportunity for the investigation of an undefined consortia in the context of *C. albicans* and oral caries.

### *3.5.5 Key Findings*

In the interest of clarity and readability, the following points summarise the key findings and outputs from this results chapter.

- *C. albicans* strain dependency was integral in understanding its ability to form a biofilm and affect its surrounding microenvironment. This has downstream implications for LBF strains of *C. albicans* increasing the risk of caries.
- *C. albicans* influenced the distribution of organisms in a defined caries biofilm model which was, in turn, influenced by biofilm phenotype. This had clear implications on, not only, the cariogenicity of biofilm models but in their response to conventional treatments and subsequent regrowth.
- While there was definable effect generated by *C. albicans* in the presence of undefined saliva models and dental enamel, the nuance of this was ultimately superseded by the influence of environmental factors.

# 4 Limitations of an *ex-vivo* biofilm model for microbiome sequencing

## 4.1 Introduction

The oral microbiome refers to the diverse community of microorganisms residing in the oral cavity, including bacteria, fungi, viruses, and other microbes. This ecosystem is highly diverse, with hundreds of species coexisting in different parts of the mouth such as the teeth, gums, tongue, cheeks, and saliva (Deo and Deshmukh, 2019). The oral microbiome is primarily composed of bacteria, with over 700 species identified so far, belonging to phyla like Firmicutes, Bacteroidetes, Proteobacteria, Actinobacteria, and Fusobacteria (Kilian et al., 2016).

Different areas within the oral cavity provide specific habitats for microbial colonization, forming complex ecosystems. These microorganisms are not static and can change over time due to various factors including diet, oral hygiene, age, and disease. While the oral microbiome plays essential roles in maintaining oral health, dysbiosis or imbalances in its composition have been associated with oral diseases such as dental caries and periodontal disease, as well as systemic conditions like diabetes and cardiovascular diseases (Guerra et al., 2018, Radaic and Kapila, 2021).

Research on the oral microbiome, often conducted through techniques like 16S rRNA sequencing and metagenomics, sheds light on its composition, function, and its influence on both oral and systemic health (Zhu et al., 2018, Zaura et al., 2017). Understanding these interactions could lead to innovative approaches for preventing and treating oral and systemic diseases.

This study aimed to develop a robust, consistent, and reproducible pipeline for the development and analysis of biofilm models using unknown samples as a starter culture in an *ex-vivo* manner. By leveraging novel sequencing technologies through the Nanopore® platform, we aimed to assess several methods of DNA extraction on

the reliable reproduction of a bacterial mock community. Additionally, we aimed to quantify the use of saliva as a starter culture for biofilm models with and without the presence of *Candida albicans* with the understanding that the microbial distribution of a given sample could be altered by the presence of fungi at a given concentration. Lastly, we aimed to gain an understanding of the dynamic relationship between commonly administered antifungal drugs in the context of their impact on the oral microbiome in a time-dependent manner.

## 4.2 Hypothesis and Aims

In this study, it was hypothesised that factors relating to the growth and control of *C. albicans* would have a profound effect on the surrounding microbial composition of an *ex-vivo* saliva model and reveal potential markers of dysbiosis amongst the observed organisms. The study aimed to outline and validate a method for Nanopore® sequencing of 16S rRNA through phylogenetic analysis of microbial mock communities using different DNA extraction methods to observe variance across kits. Further, the study sought to examine the influence of *C. albicans* and sucrose of the microbial distribution of *ex-vivo* biofilm models grown on bovine enamel and their response to an oral hygiene treatment regimen and their subsequent regrowth. Finally, the study sought to observe the off-target effects of antifungal agents, Amphotericin B and Fluconazole, on these *ex-vivo* biofilm models alongside their influence on *C. albicans* of different biofilm forming phenotypes.

## 4.3 Methodology

### *4.3.1 Study Design – Mock community validation of Nanopore® pipeline.*

Firstly, by means of testing the validity of the Nanopore® sequencing pipeline, two template bacterial mock communities were selected to test the output, concentration and purity of bacterial DNA extracted using several different extraction protocols. Extraction was carried out using a Zymbiomics® Microbial community standard (Cambridge Bioscience, Cambridge, UK) containing a known distribution of the following organisms: *Listeria monocytogenes* (12%), *Pseudomonas aeruginosa* (12%), *Bacillus subtilis* (12%), *Escherichia coli* (12%), *Salmonella enterica* (12%), *Lactobacillus fermentum* (12%), *Enterococcus faecalis* (12%), *Staphylococcus aureus* (12%), *Saccharomyces cerevisiae* (2%), and *Cryptococcus neoformans* (2%). In addition, a Zymbiomics® Microbial community standard 2 (Log Distribution) was used, containing the following distribution of organisms: *L. monocytogenes* (89.1%), *P. aeruginosa* (8.9%), *Sac. cerevisiae* (0.89%), *B. subtilis* (0.89%), *E. coli* (0.089%), *Sal. enterica* (0.089%), *Lac. fermentum* (0.0089%), *Ent. faecalis* (0.00089%), *C. neoformans* (0.00089%), *S. aureus* (0.000089%).

### *4.3.2 DNA Extraction protocols for sample sequencing*

Herein is a comprehensive list of methodologies for the processing of samples for DNA extraction according to Manufacturer's guidelines unless otherwise stated. This is inclusive of the following DNA extraction kits:

#### *4.3.2.1 Masterpure® Yeast DNA Purification Kit*

Details of this extraction methodology are contained, in their entirety, within section 3.3.7.3 of the previous chapter.

#### *4.3.2.2 Masterpure® Complete DNA and RNA Purification Kit*

The Masterpure® Complete DNA and RNA Purification Kit (MP [LGC Genomics, Bellshill, UK]) was used to extract DNA from the microbial mock communities outlined previously. To begin with, a preparation of 150μL of 2x T and C Lysis solution and 1μL of proteinase K. was made up in 1.5mL RNase and DNase free tubes. 75μL of microbial mock communities (Even and Log) were transferred to the lysis solutions and incubated in a water bath at 65°C for 15 minutes with samples being vortexed every 5 minutes. Samples were then placed on ice for 5 minutes. Following this point, the protocol follows the same exact steps outlined for the Masterpure® Yeast kit in 3.3.7.3.

#### *4.3.2.3 Qiagen® DNEasy® Blood & Tissue Kit*

The Qiagen DNEasy® Blood & Tissue Kit (QIA [Fisher Scientific, Renfrew, UK]) was used following the recommended protocol for purification of total DNA from animal blood or cells (Spin-column protocol). To start, 75μL of microbial community samples were added to 200μL of AL buffer in a 1.5mL RNase and DNase free tube, mixed via vortexing, and incubated in a water bath for 10 minutes at 56°C. In addition, to elucidate the impact of mechanical homogenisation on the resulting microbial distribution of the mock community, this protocol was split into two arms, one with the standard protocol provided by the manufacturer and one with an additional step of mechanical bead beating after this initial incubation (QIA-BB). Samples undergoing bead beating were transferred from the water bath to Fisherbrand™ pre-filled bead mill tubes (ThermoFisher, Renfrew, UK) containing 1.4mm ceramic beads before being placed in a Fisherbrand™ bead mill 24 homogeniser (ThermoFisher, Renfrew, UK) for 3 cycles of 30 seconds with interim rest periods of 1 minute between cycles. Samples were briefly spun down in a microcentrifuge to reduce foaming from the buffer before

being transferred to fresh sterile microcentrifuge tubes and re-commencing with the protocol as directed. In brief and following incubation for the initial protocol or bead beating for the BB protocol, 200μL of ice-cold 100% ethanol was added and thoroughly mixed by vortexing before being transferred to DNeasy mini spin columns, within a 2mL collection tube, and spun in a microcentrifuge at 8000RPM for 1 minute. The eluent from the spin-column, along with the collection tube, were discarded and 500μL of AW1 buffer was added to the spin column before being placed in a fresh collection tube and returned to the microcentrifuge for a further 1 minute at 8000RPM. Again, the eluent and collection tube were discarded and 500μL of AW2 buffer was added to the spin column before being moved to a new collection tube and returned to the centrifuge for 3 minutes at 13000RPM. The DNeasy spin column was then transferred to a sterile 1.5mL DNase and RNase free tube, with the lid cut off, for the final elution step. 50μL of AE buffer was added to the spin column before being centrifuged for 1 minute at 8000RPM. This step was then repeated to achieve a final volume of 100μL eluted DNA before being stored at -20°C until required.

#### *4.3.2.4 QIAamp® DNA Microbiome Kit*

The QIAamp® DNA Microbiome Kit (QMB [Fisher Scientific, Renfrew, UK]) protocol was carried out according to manufacturer's instructions. In brief, 75μL of sample was transferred to a sterile 1.5mL DNase and RNase free tube containing 500μL of AHL buffer and incubated at room temperature for 30 minutes with end-over-end rotation in a Stuart Scientific SB1 rotator mixer (SLS, Nottingham, UK). Samples were then centrifuged at 13,000RPM to form a pellet before removal and discarding of sample supernatant. The pellet was then resuspended in 190μL of RDD buffer containing 2.5μL benzonase and incubated at 37°C in a water bath for 30 minutes. Following this, 20μL of proteinase K was added to the samples before a further 30-minute incubation

at 56°C. Samples were centrifuged, briefly, to remove residue from the cap of the tube, before adding 200μL of ATL buffer and pipette mixing to ensure sample homogenisation. Once mixed, the samples were transferred to pathogen lysis tubes containing microtube foam inserts before being vortexed for 10 minutes. Samples were centrifuged at 10,000RPM, briefly, to reduce foaming, before being transferred to fresh sterile microcentrifuge tubes containing 40μL of proteinase K before being vortexed to mix and incubated for 30 minutes at 56°C. Following this, 200μL of APL2 buffer was added to the samples and mixed via pulse vortexing for 30 seconds and incubated further, at 70°C for 10 minutes. After incubation, 200μL of ice-cold 100% ethanol was added to the samples before thorough vortex mixing. Once mixed, 700μL of each sample was transferred to QIAamp UCP Mini Columns and centrifuged at 8000RPM for 1 minute. Following this, the protocol method follows the same outline as the Qiagen® DNEasy Blood & Tissue Kit outlined in the previous section (4.3.2.3). Eluted DNA was stored at -20°C until required.

#### *4.3.2.5 Purelink™ Microbiome DNA Purification Kit*

The Purelink™ Microbiome DNA Purification Kit (PLI [Fisher Scientific, Renfrew, UK]) protocol was carried out as instructed by the manufacturer. In brief, the 75μL of microbial mock communities were transferred to sterile 1.5mL DNase and RNase free tubes before mixing the sample, via pipetting, with 800μL S1 – Lysis buffer before transferring to a bead beating tube and adding 100μL of S2 – Lysis Enhancer. Samples were incubated in a water bath at 65°C for 10 minutes before being homogenised via bead mill as outlined in section 4.3.2.3 and briefly centrifuged to reduce foaming. Samples were then transferred to fresh 1.5mL microcentrifuge tubes containing 900μL of S4 – Binding buffer and briefly mixed via vortexing before transferring 700μL of the

sample mixture to a spin column and collection tube and centrifuging for 1 minute at 13000RPM. Following this, the eluent and collection tube were discarded and 500μL of S5 – Wash buffer was added to the spin column before further centrifugation at 13000RPM for 1 minute. Following discard of this eluent, the column was centrifuged again for 30 seconds at 13000RPM to dry the column of excess ethanol. Following this, the sample was eluted, twice, in 50μL volumes of S6 elution buffer via centrifuging for 1 minute at 13000RPM into a fresh 1.5mL microfuge tube with the eluted DNA stored at -20°C until required.

### *4.3.3 Nanopore processing for 16S sequencing*

Before preparing samples for sequencing, DNA yields were quantified via Qubit™ fluorometer, as outlined in section 3.3.7.4, before being standardised to a concentration of 1ng/μL in Tris-EDTA buffer (Merck, Livingston, UK). Following this, samples would undergo PCR amplification using the PCR primer sequences identified in Table 4-1, below, to determine primer validity. For all follow-up experiments, the previously published “Bact” sequence would be used (Johnson et al., 2019).

| Primer | Sequence | Amplification |
|---|---|---|
| **Bact Forward** | 5′-GCG CGG CCA GTA TGG ATA TA-3′ | 57F |
| **Bact Reverse** | 5′-GAC TCA ACC CAA CGA GCT CC-3′ | 1530R |
| **Kat Forward** | 5′-AGA GTT TGA TYM TGG CTC AG-3′ | 27F |
| **Kat Reverse** | 5′-TAC CTT GTT AYG ACT T-3′ | 1492R |
| **Ont Forward** | 5'-AGA GTT TGA TCM TGG CTC AG-3' | 27F |
| **Ont Reverse** | 5'-TAC GGT TAC CTT GTT ACG ACT T–3' | 1492R |

**Table 4-1 - List of primers used for mock community amplification for 16S sequencing. "**Bact" - (Johnson et al., 2019), "Kat" – Proprietary, "Ont" - (Matsuo et al., 2021).

#### *4.3.3.1 PCR amplification of sample DNA for 16S sequencing*

Once sample DNA had been standardised to 1ng/μL, it was prepared for amplification using a PCR mastermix of LongAmp® *Taq* 2X Master Mix (New England Biolabs, Hitchin, UK). In FisherBrand™ thin-walled 0.2mL PCR tubes (ThermoFisher, Renfrew, UK), 12.5μL of master mix was added alongside 1μL each of forward and reverse primers, as identified in 3.3.7.5, and 5.5μL of UltraPure™ DNase/RNase-Free water. Finally, 5μL of standardised sample DNA was added. It should be noted, sample concentrations which did not meet the minimum 1ng/μL, as shown in Table 4-1, were instead added at neat concentrations. The tubes were gently flicked to mix then centrifuged, briefly, to remove residue from the caps using a ThermoFisher Fresco™ 21 Microcentrifuge with a 0.2mL PCR tube adapter plate (ThermoFisher, Renfrew, UK) before being transferred to a Blue-Ray Biotech TurboCycler Lite Thermal Cycler (SLS, Nottingham, UK) and amplified using the following thermal profile: Initial denaturation of 30 seconds at 95°C followed by 30 cycles of 15 seconds and 95°C, annealing for 15 seconds at 51°C and extension for 75 seconds at 65°C, with a final, prolonged, annealing step at 65°C. Samples were carried forward for DNA purification and continued processing for sequencing.

#### *4.3.3.2 AMPure XP DNA purification*

For all stages of the process for sample preparation for nanopore® sequencing, a bead-based DNA clean-up method was employed to purify DNA products. To begin with, samples were transferred to Eppendorf™ DNA Lo-bind™ RNase and DNase free tubes (ThermoFisher, Renfrew, UK). AMPure XP beads (Beckman-Coulter, Buckinghamshire, UK) were vortexed, briefly, to resuspend and added to the samples at a 1x ratio, or 25μL per sample, before being incubated at room temperature with

end-over-end rotation for 5 minutes. Samples were spun briefly in a microcentrifuge to pellet and transferred to a DynaMag magnetic rack (ThermoFisher, Renfrew, UK) until the samples were separated onto the magnet. With care not to disturb the pellet, the supernatant was removed and discarded from each sample before washing twice with 200μL of freshly prepared, ice-cold, 85% ethanol. The ethanol was removed, and samples were transferred to a microcentrifuge to spin for 1 minute at 13000RPM before being returned to the magnetic rack and pelleted again to remove any excess ethanol. Sample lids were left open to allow for evaporation of remaining ethanol for 60 seconds although care was taken to prevent samples from drying out completely which would result in cracking of the iron AMPure beads. Finally, beads were resuspended in 30μL of 10mM Tris-HCL with 50mM NaCl (Merck, Livingston, UK) and incubated for 2 minutes at room temperature before being replaced on the magnetic rack and pelleted until the sample was clear and colourless before being transferred to a clean 1.5mL DNA LoBind™ tube. Samples were then quantified via Qubit™ fluorometer as outlined in section 3.3.7.4 and standardised to 5ng/μL in Tris-EDTA buffer before being carried forward for PCR barcoding.

#### *4.3.3.3 PCR barcoding and sample pooling.*

As in the previous PCR amplification, in 0.2mL thin-walled PCR tubes, a master mix containing 50μL of LongAmp® *Taq* 2X master mix was added alongside 38μL of UltraPure™ DNase/RNase-Free water. To this, 2μL of specific barcodes from Oxford Nanopore® PCR Barcoding Expansion 1-96 (Oxford Nanopore®, Oxford, UK) were added to each sample. Care was taken to ensure that before addition, barcodes were spun, briefly, in a microcentrifuge fitted with a 96-well plate adapter, to ensure no residue was present on barcode lids before opening leading to potential cross contamination of barcodes. Given the unique nature of the barcodes as sample

identifiers post-pooling, it was essential that only one barcode be introduced to a sample. Finally, 10μL of input DNA was added to each tube. As previously, it should be stated that samples which were not identified as reaching the required DNA concentration were added to the sample neat. In some cases, where samples were below required concentration but still detectable, sample water ratio was adjusted and input DNA increased to accommodate for differences in concentration. Samples were, again, flicked to mix before transfer to a thermal cycler with the following thermal profile for amplification: Initial denaturation of 30 seconds at 95°C before 15 cycles of 15 seconds at 95°C, annealing for 15 seconds at 62°C and elongation for 75 seconds at 65°C with a follow up 10 minutes at 65°C. Samples were then transferred to 1.5mL LoBind™ tubes and purified via magnetic beads as outlined in 4.3.3.2 at a ratio of 0.5x beads to sample volume. Following clean-up, samples were diluted and pooled together to a weight of 1μg of DNA in 47μL of Tris-EDTA buffer.

#### *4.3.3.4 DNA repair and end-preparation*

To prepare the pooled sample for Nanopore® sequencing, a DNA repair and end-preparation step was employed using components from a NEBNext® companion module for Oxford Nanopore® (New England Biolabs, Buckinghamshire, UK). Reagents were thawed at room temperature and spun down briefly in a microcentrifuge to ensure sample contents were cleared from tube lids. In a 0.2mL thin-walled PCR tube, the following reagents from the companion moduel were combined to the 47μL of pooled DNA from the previous section: 3.5μL NEBNext® FFPE DNA Repair Buffer, 2μL of NEBNext FFPE Repair Mix, 3.5μL Ultra II End-prep reaction buffer, 3μL of Ultra II End-prep enzyme mix and 1μL of DNA CS. As with previous steps, samples were flicked to mix before being transferred to a thermal cycler and incubated at 20°C for 5 minutes followed by 65°C for 5 minutes. Again,

samples were briefly centrifuged to remove condensation from the cap before undergoing DNA clean-up as outlined in section 4.3.3.2 at a ratio of 1x AMPure beads to sample volume. If required, before final adapter ligation for Nanopore® sequencing, samples were stored at 4°C until prepared for use.

#### *4.3.3.5 Nanopore adapter ligation*

To prepare pooled DNA for sequencing, adapter ligation was prepared using reagents from the Ligation Sequencing Kit V14 (Oxford Nanopore®, Oxford, UK). Reagents were thawed at room temperature and spun briefly to ensure removal of sample residue from lids. To the 60μL of pooled DNA, 25μL of ligation buffer and 5μL of Adapter mix were added alongside 25μL NEBNext® Quick T4 DNA Ligase from the companion module identified in the previous section. The sample was flicked to mix and spun briefly in a microcentrifuge before incubation for 10 minutes at room temperature and subsequent clean-up with AMPure beads at a ratio of 0.4x to sample volume. It should be noted that rather than a second wash with ethanol, as indicated in the protocol in section 4.3.3.2, the beads were washed with 250μL of short fragment buffer from the ligation sequencing kit before returning to the previous protocol steps. Finally, the library was standardised to 50ng of DNA Tris-EDTA buffer.

#### *4.3.3.6 Nanopore flow cell priming*

The priming of the Nanopore® flow cell used reagents from the flow cell priming kit (Oxford Nanopore, Oxford, UK), and flow cell wash kit (Oxford Nanopore, Oxford, UK). All reagents were thawed at room temperature ahead of preparation, mixed via vortexing, and spun down to ensure even distribution of reagents. To produce a flow cell priming mix, 30μL of flush tether was added directly to a tube of flush buffer and mixed via pipetting. At this point, the Nanopore MinION flow cell R10.4.1 (Oxford Nanopore, Oxford, UK) was inserted into the MinION™ MK1C sequencing device

(Oxford Nanopore, Oxford, UK) to ensure a stable platform for sample addition and to undergo a pore health check to ensure the validity of the sequencing run ahead of time. The priming port on the flow cell was opened and buffer was very carefully drawn from the open channel by inserting a 1000μL pipette tip into the priming port and slowly adjusting the pipette volume by 20-30μL or until the buffer was visibly flush with the opening of the priming port. 800μL of the priming mix was then loaded into the priming port of the flow cells and incubated for five minutes while the loading library was prepared. To prepare the library, 12μL of the adapted library, as indicated in the previous section, was added to 37.5μL of sequencing buffer and 25.5μL of loading beads, which were mixed via pipette immediately prior to use, in a 0.2mL thin-walled PCR tube. To prep for loading, the SpotON sample port was lifted and an additional 200μL of the priming mix was added to the priming port to flush priming mix over the flow cell membrane. Just prior to loading, the library was mixed via pipetting and 75μL was added directly to the SpotOn sample port in a dropwise fashion. Once all liquid had been visibly taken into the sample port, both the SpotOn port and the priming port covers were replaced. It should be noted that a visually annotated version of this protocol can be obtained from the manufacturer.

#### *4.3.3.7 Sample sequencing and data analysis*

To begin sequencing, the MK1C MinION device was configured with the relevant sequencing kit (Ligation Sequencing Kit V14) and assigned for High-Accuracy Basecalling (HAC). Samples were sequenced to between 60,000 and 100,000 reads per sample. Run files were exported in .POD5 format before processing and analysis via MicrobiomeNanoplotApp generated by Christopher Delaney. Sample OTU and taxonomy files were subsequently exported and transferred to MicrobiomeAnalyst® for taxonomic assignment and statistical analyses (Dhariwal et al., 2017).

### *4.3.4 Study Design – Developing an ex-vivo biofilm model for microbiome analysis.*

In addition to the generation of analyses related to mock community data outlined in section 4.3.1, Nanopore® sequencing was undertaken to determine taxonomic distribution and organism diversity analyses for the experimental study design for *ex-vivo* biofilms in section 3.3.8. In addition to this, a study design identifying key factors in microbial development during the maturation of biofilms exposed to *C. albicans* strains SC5314, GSK22 and GSK107 was undertaken, outlined in Figure 4-1. Therein, *ex-vivo* saliva models, as outlined in 3.3.8.2, were grown in 6-well microtiter plates and assessed for growth over a period of 5-days (144 hours) to assess differentiation from the starting culture. Additionally, the study set out to assess the impact conventional antifungal therapies may have on this *ex-vivo* microbial population in a time-dependant manner. To this end, biofilms were challenged with either 1μg/mL of Amphotericin B (AMB) or 1mg/mL of Fluconazole (FLU), prepared daily, in 1mL of Dimethyl Sulfoxide (DMSO, [Merck, Livingston, UK]). Concentrations were chosen as outlined by Minimum Inhibitory Concentrations of *C. albicans* as outlined by Borman et al., in 2020 (Borman et al., 2020). These antifungal challenges were administered, daily, as part of regular media changes (T0-T5). As before, after each designated timepoint, samples were scraped and carried forward for DNA extraction and assessment as outlined in section 3.3.7.3.

It should be noted that many of the analyses generated in this section were done so as part of a wider experimental protocol carried out by the author and Hafsa S. A. Abduljalil. While the data presented here has been analysed separately, some of the same control samples containing *C. albicans* SC5314 were cross-analysed.

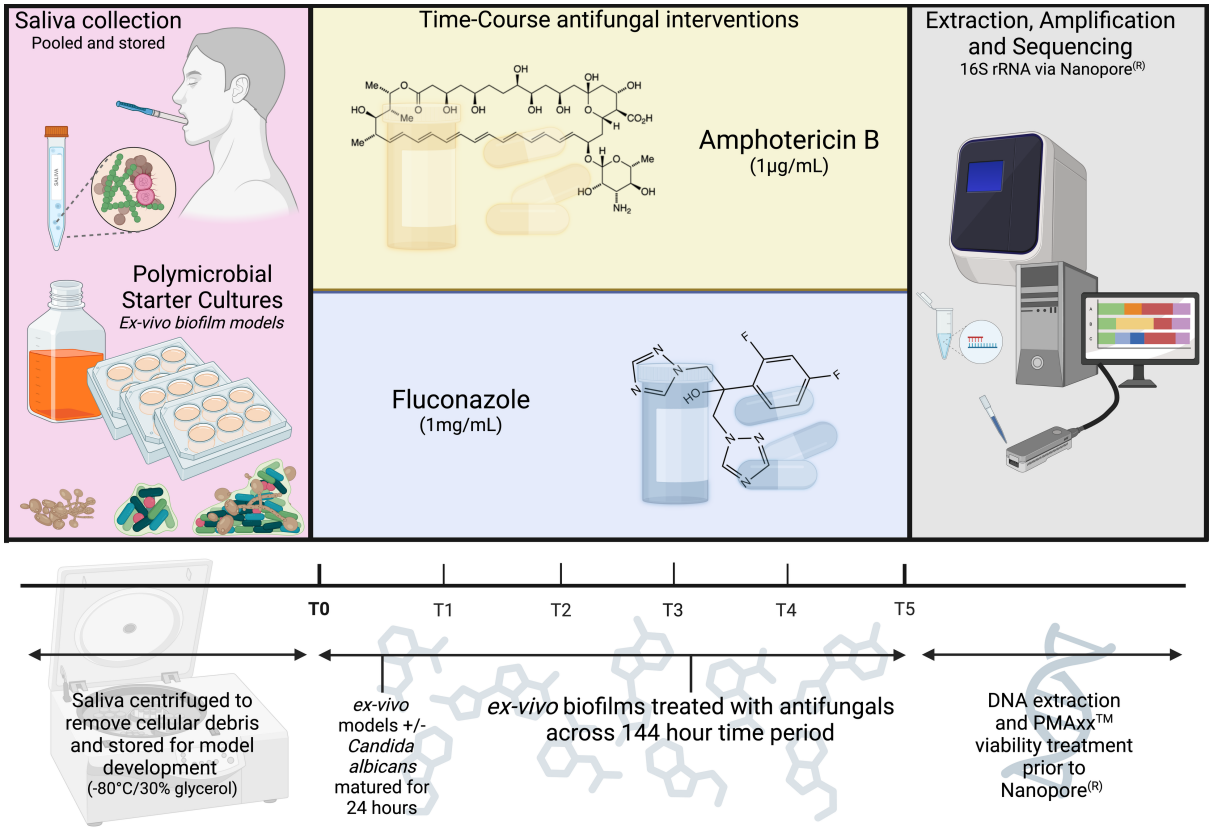


**Figure 4-1 – Development of a salivary ex-vivo biofilm model for microbiome analysis and impact of antifungal pressure.** Starter cultures were grown on Thermanox® cover-slips and developed over a period of 5 days (144 hours) with/without *C. albicans* strains SC5314, GSK22 and GSK107. Biofilms were exposed to antimicrobial agents Amphotericin B (AMB [1µg/mL]) and Fluconazole (FLU [1mg/mL]) at each timepoint and assessed via 16S rRNA amplicon sequencing.

## 4.4 Results

### *4.4.1 Bacterial mock community validation of Nanopore® protocol*

Having identified a lack of corroboration in the literature in section 2.5, in relation to methodologies ideal for 16S sequencing, the first aspect of this research was to observe potential impacts of extraction protocols. To best achieve this, it was essential to observe both the subjective simplicity of use in terms of extraction methodology as well as the quantifiable yield of DNA from each method. As this was a newly adopted methodology, with largely crowd-sourced directions, in the context of 16S rRNA sequencing, it was essential to examine multiple steps of the sequencing process to validate and address any potential issues that may have arisen in the downstream analysis.

To begin with, distributions of organisms in a bacterial mock community were observed to ascertain the success of primer amplification in replicating known quantities of organisms as well as to assess reproducibility of results when compared to a template control in sequencing pipelines. To enable this, pre-extracted DNA from a ZymoBiomics® Microbial Community Standard (Even distribution) was assessed for taxonomic distribution alongside three primer sequences to determine reproducibility of methodology and pipeline.

As shown, below in Figure 4-2, taxonomic distribution, in comparison to the theoretical standard provided by the manufacturer, achieved a very close resemblance across all 3 primer sequences (**Bact**), (**Kat**), and (**Ont**). While it was clear that there was some over-estimation of abundance of *Bacillus subtilis*, as well as an under-estimation of *Lactobacillus fermentum* and *Pseudomonas aeruginosa*. These marginal

inconsistencies appeared to be more than likely the result of inferred bias from the process of sequencing. As all expected species were observed within the mock community samples and given the apparent lack of distinguishing features between primer sequences, it was determined that the “bact” sequence of primers, being the most heavily cited in the literature, would be carried forward for determination of our own samples.

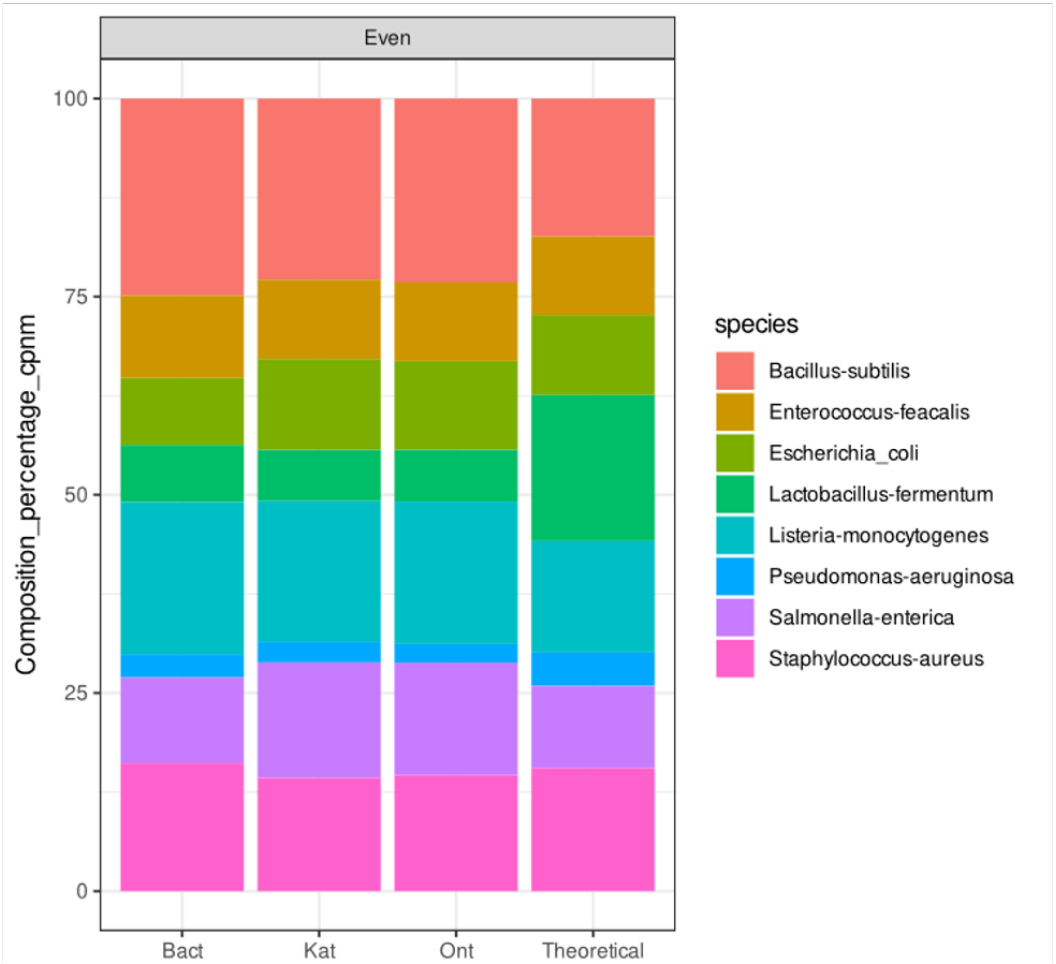


**Figure 4-2 - Distribution of organisms using 16S primers reveals comparable results to theoretical standard.** Percentage distribution of even distributed organisms from a ZymoBiomics® Microbial Community Standard. DNA amplified using 16S rRNA primers amplifying V1-V9 of the 16S gene region compared to a theoretical standard as provided by the manufacturer. Primers were derived from universal primers (**bact**) (Martin et al., 2002), developed in-house (**Kat)** or as included with the 16S sequencing kit from Oxford Nanopore® (**Ont**).

Next, having observed no obvious bias introduced through primer sequences, we sought to observe the potential deviation in sample content that may be introduced as the result of differing methodologies for DNA extraction.

As outlined below in Table 4-2 and Table 4-3, concentration of DNA retrieved from initial extraction methodologies was highly variable across kits. On average, all tested kits could extract amplifiable DNA for the purposes of sequencing.

In terms of initial extraction protocols, the Masterpure® Complete DNA and RNA kit (**MP**) yielded the greatest average concentration of DNA (19.3ng/μL) from the even distributed community, while the Purelink™ Microbiome DNA Purification Kit (**PLI**) produced the lowest average concentration of DNA (1.3ng/μL). Conversely, the Purelink™ kit yielded the highest average concentration of DNA (4.3ng/μL) in the log distributed microbial community, while the QIAamp® DNA Microbiome Kit (**QMB**) produced the lowest average concentration in the log distributed samples (0.18ng/μL). These results may indicate the introduction of bias across extraction methodologies in favour of certain organisms across the distributed list. Indeed, speculatively, the inclusion of certain Gram-positive bacteria, such as *Listeria* could result in uneven extraction of DNA depending on the precision and enzymatic inclusion for digestion in the protocol.

When observing the full-length amplified 16S product, results were seen to vary again with the QMB kit producing the highest concentration of amplified DNA in the even distribution. Interestingly, despite providing a poor yield in the even distribution, the PLI kit proved consistently the best in the amplification of DNA from the log distributed kits.

Overall, the variability in results for the even distribution of microbes left much to be desired in the context of choosing a kit for downstream analysis.

| Sample Name | DNA concentration (ng/μL) | 16S amplification (ng/μL) | Barcoding concentration (ng/μL) | Clean DNA (ng/μL) |
|---|---|---|---|---|
| **QIA E1** | 6 | OOR | 239 | 146 |
| **QIA E2** | 6 | 3.14 | 282 | 168 |
| **QIA E3** | 5 | 3.06 | 296 | 149 |
| **QIA BB E1** | 5 | 1.41 | 256 | 143 |
| **QIA BB E2** | 7 | 4.96 | 179 | 152 |
| **QIA BB E3** | 5 | 9.22 | 277 | 136 |
| **MP E1** | 24 | 1.1 | 14 | 148 |
| **MP E2** | 17 | 16.8 | 263 | 236 |
| **MP E3** | 17 | OOR | OOR | OOR |
| **MP-Y E1** | 14.1 | 1.1 | 260 | 126 |
| **MP-Y E2** | 9 | 6.73 | 308 | 270 |
| **MP-Y E3** | 9 | 5.31 | 330 | 258 |
| **QMB E1** | 2 | 2.72 | 287 | 220 |
| **QMB E2** | 2 | 12.2 | 316 | 270 |
| **QMB E3** | 2 | 15.3 | 271 | 326 |
| **PLI E1** | 5 | 16.9 | 319 | 276 |
| **PLI E2** | 4 | 19.5 | 339 | 280 |
| **PLI E3** | 4 | 6.35 | 293 | 173 |

**Table 4-2 – Quantitative assessment of DNA concentration throughput from an evenly distributed mock community.** DNA concentrations presented in ng/μL per given sample throughout extraction and amplification methodologies as determined via nanodrop® and Qubit® DNA quantification using ZymoBiomics® Microbial Community Standard (**Even distribution**). Samples unrecoverable during amplification for sequencing denoted as Out of Range (**OOR**). Bacterial DNA was recovered from all kits with a high degree of variability.

| Sample Name | DNA concentration (ng/μL) | 16S amplification (ng/μL) | Barcoding concentration (ng/μL) | Clean DNA (ng/μL) |
|---|---|---|---|---|
| **QIA L1** | 0.6 | 1.85 | 222 | 111 |
| **QIA L2** | 1.7 | 2.58 | 169 | 130 |
| **QIA L3** | 0.5 | 3.93 | 312 | 260 |
| **QIA BB L1** | 0.4 | 1.91 | 2 | OOR |
| **QIA BB L2** | 0.5 | OOR | 87 | 50 |
| **QIA BB L3** | 0.5 | 3.1 | 269 | 230 |
| **MP L1** | 0.3 | OOR | OOR | OOR |
| **MP L2** | 0 | OOR | 50 | 21 |
| **MP L3** | 0.4 | OOR | 194 | 91 |
| **MP-Y L1** | 0.5 | 5.63 | 11 | 268 |
| **MP-Y L2** | 0.14 | OOR | 18 | 10 |
| **MP-Y L3** | 0.5 | 5.14 | 24 | 19 |
| **QMB L1** | 0.15 | OOR | 136 | 45 |
| **QMB L2** | 0.2 | OOR | 10 | 5 |
| **QMB L3** | 0.2 | 1.38 | 196 | 93 |
| **PLI L1** | 1 | OOR | 87 | 44 |
| **PLI L2** | 2 | 3.38 | 255 | 202 |
| **PLI L3** | 1 | 2.01 | 152 | 96 |

**Table 4-3 - Quantitative assessment of DNA concentration throughput from a log distributed mock community.** DNA concentrations presented in ng/μL per given sample throughout extraction and amplification methodologies as determined via nanodrop® and Qubit® DNA quantification using ZymoBiomics® Microbial Community Standard (**Log distribution**). Samples unrecoverable during amplification for sequencing denoted as Out of Range (**OOR**). Bacterial DNA was recovered from all kits with a high degree of variability.

Having ascertained the yield of DNA extracted from kits, we next analysed the phylogenetic outline of each kit to compare how closely it matched that of the manufacturer's specifications from the bacterial mock community.

Depicted below, in Figure 4-3, percentage composition of organisms extracted using the MP, MP-Y, QIA, and QIA-BB all showed similar profiles to that displayed in the theoretical even distribution. Notably, the percentage of *Lactobacilli* were shown to be under-represented (<5%) across all kits, despite clear representation in the theoretical sample, indicating an inherent bias in these extraction protocols. A similar trend was observed for *Listeria* in the MP, MP-Y and QIA kit which, interestingly, was not observed when the QIA kit was accompanied by mechanical disruption through bead beating. As mentioned previously, the composition of the bacterial cell wall in species such as *Listeria* may contribute to difficulty in full digestion or extraction in kits that rely solely on lysis buffers without mechanical or enzymatic lysis steps. Conversely, the QIA-BB kit was shown to have an exaggerated representation of *Staphylococcus* species when compared with the others.

Both the PL and QMB kits were shown to have vastly different distributions of organisms, despite both kits being advertised as "Microbiome" kits. The PL kit heavily over-represented *Listeria* and *Staphylococcus* while heavily under-representing *E. coli, P. aeruginosa, L. fermentum* and *S. enterica*. Interestingly, the QMB kit, which displayed the lowest initial extraction concentration in both the log and even distributed communities, also had the poorest representation of organisms, vastly overestimating *E. coli* and *S. aureus* while having very low representation of *E. faecalis*, *L. fermentium* and *P. aeruginosa*.

In the log distributed community, given the very large (89.1%) representation of *Listeria* and otherwise smaller representation of other organisms, this community was selected

as a proxy for specificity in terms of successful amplification of very small starting quantities of DNA. This included 8.9% *P. aeruginosa* and 0.89% *B. subtilis*. As shown in the plot, *Listeria* was represented as the majority in all kits, with marginal differences in over representation of *B. subtilis.* Most notably, the MP kit had the most inconsistent abundance of organisms in comparison to the theoretical distribution, wildly over-estimating the presence of *S. enterica* and *E. coli*. It should be noted, however, that this may be the result of error or inconsistencies in sample recording producing an average which disperses organisms unfairly across the samples. Albeit the uniformity in the "Even" sample would indicate this may not be the case.

Having found that the methodologies for extraction had generated some clear bias in the context of DNA extracted as well as in mock community taxonomy, we selected the parameters for continued experiments on the following parameters:

- Accessibility of extraction kit
- Target extraction method
- Yield of DNA
- Similarity to mock community taxonomy

Predominantly, the inclusion of fungi and the resultant robustness of the extraction method to accommodate for this was a strong influence behind choice of extraction methodology, making the MP-Y or QIA-BB kits evident choices for this reason. This decision was reflected in the lack of fluctuation in DNA concentrations across parameters for these kits as well as their similarity to the mock community data. Ultimately, the accessibility and cost effectiveness of the Masterpure™ Yeast kit, as well as its overall specificity as a fungal kit, was selected for downstream applications.

Having identified these factors, it was next essential to observe how these decisions influenced the bacterial microbiome across study designs.

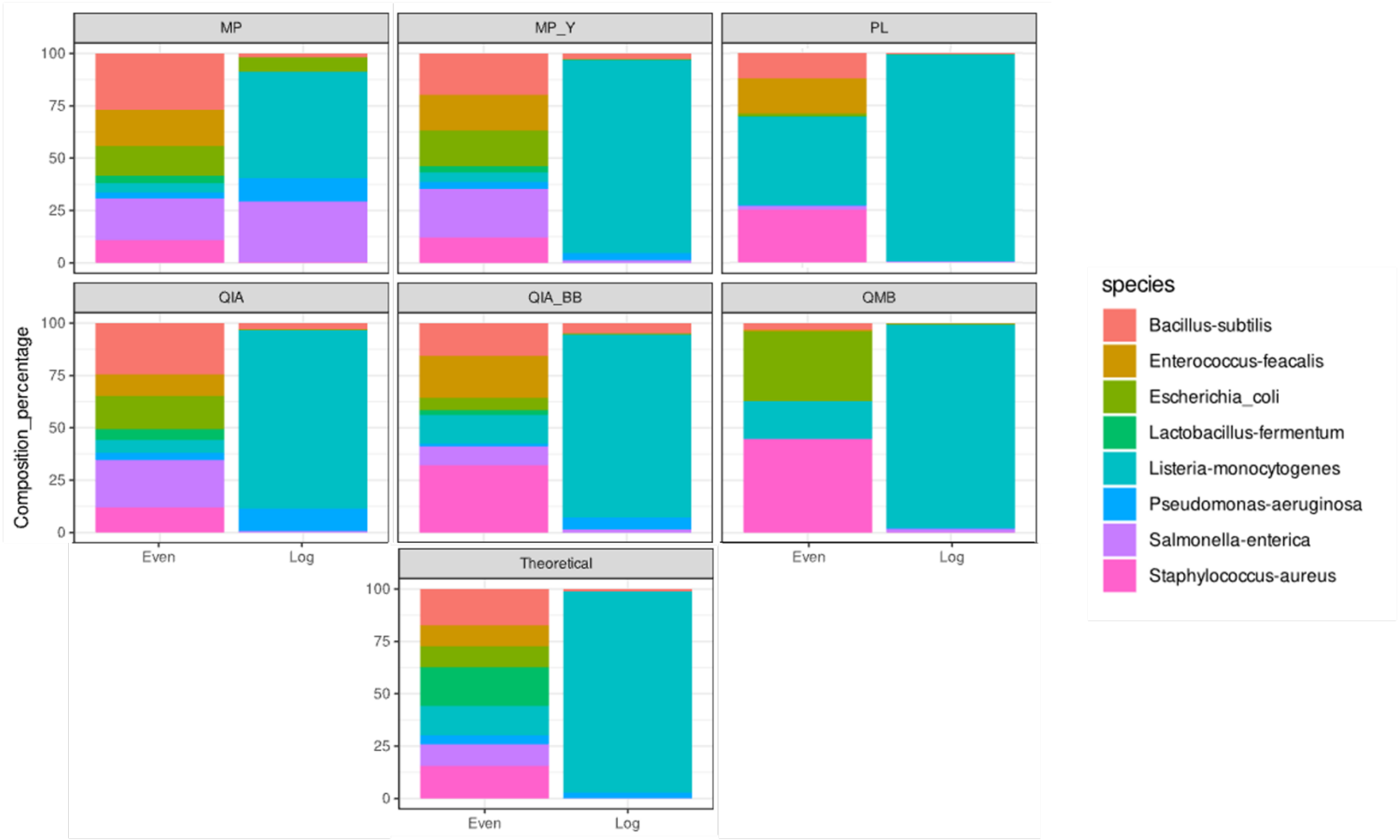


**Figure 4-3 - Mock community sequencing determines bias in represented organisms by extraction method.** Organism distribution comparing (**Even**) and (**Log**) distribution of ZymoBiomics® Microbial Community Standards as extracted by 6 different DNA extraction protocols: MP, MP-Y, PL (**Top**), QIA, QIA-BB, QMB (**Middle**) and the theoretical distribution of organisms (**Bottom**).

### *4.4.2 Observing microbial distribution as part of an ex-vivo biofilm model*

To observe the oral bacterial microbiota, we next observed the taxonomy of the organisms present in the initial saliva inoculum, as well as in our *ex-vivo* biofilm model and how they develop over a period of 5 days.

Figure 4-4, below, displayed the relative abundance of organisms associated with the saliva inoculum pre- and post-maturation at key timepoints across a 5-day period.

The DNA from the starting saliva culture displayed a wide array of organisms and was mostly heterogenous in aspect. The predominant organisms identified in the starting culture were *Streptococcus* (74%), *Haemophilus* (5%), *Veillonella* (6%), *Granulicatella* (3%), *Neisseria* (1%), with reads below 100 OTUs classified as “Other” (11%). Given the prevalence of these organisms within the literature concerning the oral cavity and upper respiratory tract, we were satisfied to see the heterogenous dispersal of organisms in our starting culture.

In the *ex-vivo* model after initial 24hr incubation (**D1**), the model is mostly dominated by *Streptococcus* species, making up 97% of the representative organisms in the biofilm with *Undibacterium* and *Granulicatella*, and “Others” making up the remainder. It should be noted that *Undibacterium* is a commonly identified contaminant that is known to be associated with reagents and laboratory conditions which is only commonly identified during low-biomass 16S sequencing (Salter et al., 2014). In the interest of complete representation of bacterial OTUs, *Undibacterium* was preserved in the sequencing results. After 72-hours the bacterial community had shifted considerably, including many low resolution OTUs, increasing the proportion of “other” to 15%, reducing *Streptococcus* to 53% and increasing abundance of *Klebsiella* species to 32%. Typically found in low abundance in the oral flora, *Klebsiella* presence could be indicative of altered development due to the nature of enriching organisms

via the *ex-vivo* model (Liu et al., 2023). Finally, after 120-hours, the samples had adjusted to 70% *Streptococcus*, 13% *Neisseria*, and 12% *Klebsiella*, and 5% “Other” species. This increase in *Neisseria* species could be indicative of differential metabolic needs which will indirectly shift in the biofilm over time as the community develops, allowing these typically low abundance organisms to develop within the niche.

Importantly, there appeared to be no major disruptions in the growth of the *ex-vivo* system to identify issues in consistency across the developmental timepoints, indicating that the system was stable enough to produce reliable replicates across a series of experiments.

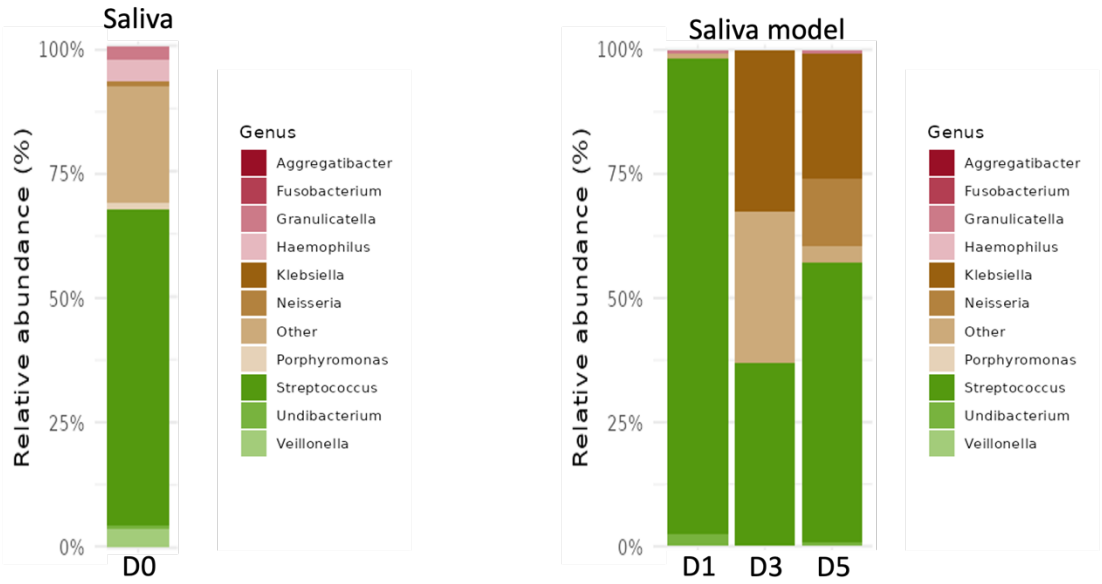


**Figure 4-4 - Optimised Nanopore sequencing model reveals development of saliva *ex-vivo*.** Relative abundance plot of bacteria observed in starter inoculum before growth (**D0**) in *ex-vivo* saliva models grown in 1:1 RPMI-THB as well as after 24 (**D1**), 72 (**D3**), and 120 (**D5**) hours maturation. Bacterial heterogeneity adjusts across the selected timepoints. Images constructed with NanoporeMicrobiomeApp.

### *4.4.3 Observing microbial distribution of ex-vivo biofilms under cariogenic conditions.*

To observe the potential cariogenic influence of *Candida* we looked to assess the shift in micro-organisms present in samples which had been influenced by the growth of *C. albicans* cultures with different capacity for biofilm growth, as well as the influence of 1% dietary sucrose, as well as under conditions which would emulate a “typical” oral hygiene regimen.

As shown below in Figure 4-5**,** there were many factors which influenced the development of the *ex-vivo* models within the study design. Most prominently, the distribution of organisms, even in the control samples, is vastly different to the of the original saliva samples. For example, we can see that the percentage distribution of organisms in the control samples for SC5314 is 96% *Pseudomonas*, an organism which was not clearly represented in the original data. However, this is not the case for the LBF and HBF strains of *C. albicans.* It is unclear if the inclusion of *Pseudomonas*, which was present in the smaller value OTUs in the saliva inoculum, is being bolstered by the inclusion of *Candida* or is being influenced by factors relating to the bovine enamel substrate.

GSK22, the LBF strain of *Candida*, identified a distribution of 32% *Lactobacillus*, 39% and 19% *Veillonella* in the control sample. As mentioned earlier, this presence of *Undibacterium* as a contaminant reflective of low biomass is understandable in the context of the more yeast-phenotype trait of the LBF *Candida*. Additionally, the abundance of *Lactobacillus* and *Veillonella* could also indicate a more carious biofilm being produced and additional acidification of the surrounding substrate.

Incidentally, GSK107, the HBF phenotype, also retained a high distribution of *Lactobacillus* (65%) and lower distribution of *Undibacterium* (25%) with 6% *Veillonella*. This is somewhat contradictory to the previous data, as the increased retention of

*Lactobacillus* would likely generate more carious conditions. However, the increased capacity of HBF *Candida* to buffer pH may contribute to a somewhat synergistic relationship between these two organisms which potentially reduces the impact on the substrate.

### *4.4.4 Amplification of off-target organisms indicates reduction in biomass post-treatment.*

The impact of oral hygiene regimen, through application of stannous fluoride and brushing of enamel substrates, is also displayed in Figure 4-5. Like the control sample, the distribution of organisms in the SC5314 sample remains with *Pseudomonas* (55%) and *Klebsiella* (45%). In the GSK107 and GSK22 samples, there is a marked increase in the abundance of *Undibacterium* at 63% and 72% respectively. This is indicative of a reduction in overall biomass recovered from the treated samples. In addition, the inclusion of *Caulobacter*, an organism widely identified in water samples and rarely in the oral microbiome, in the GSK22 (11%) and GSK107 (8%) samples could be indicative of parameters similar to *Undibacterium* and the amplification of off-target organisms introduced through the laboratory processes present during the study (Conrads et al., 2019). This is further compounded by the results observed after 24-hours post-treatment (**Re**) where the initial bacterial organisms were largely replaced by *Pseudomonas* and *Klebsiella* in all samples. Inclusion of *Pseudomonas* could be indicative of contamination from the disks, despite assurances that disks were sterile on receipt and additional decontamination regimen outlined in the methods section. Future reassurance of sterility from the provider should be sought upon receipt as well as attempting a trial run of sample sterility for sequencing ahead of planning a high volume experiment. Of additional note, there was a marginally increased presence of

*Veillonella* in the LBF samples in comparison to the other strains of *Candida*, again indicative of a potentially pathogenic outcome post-regrowth.

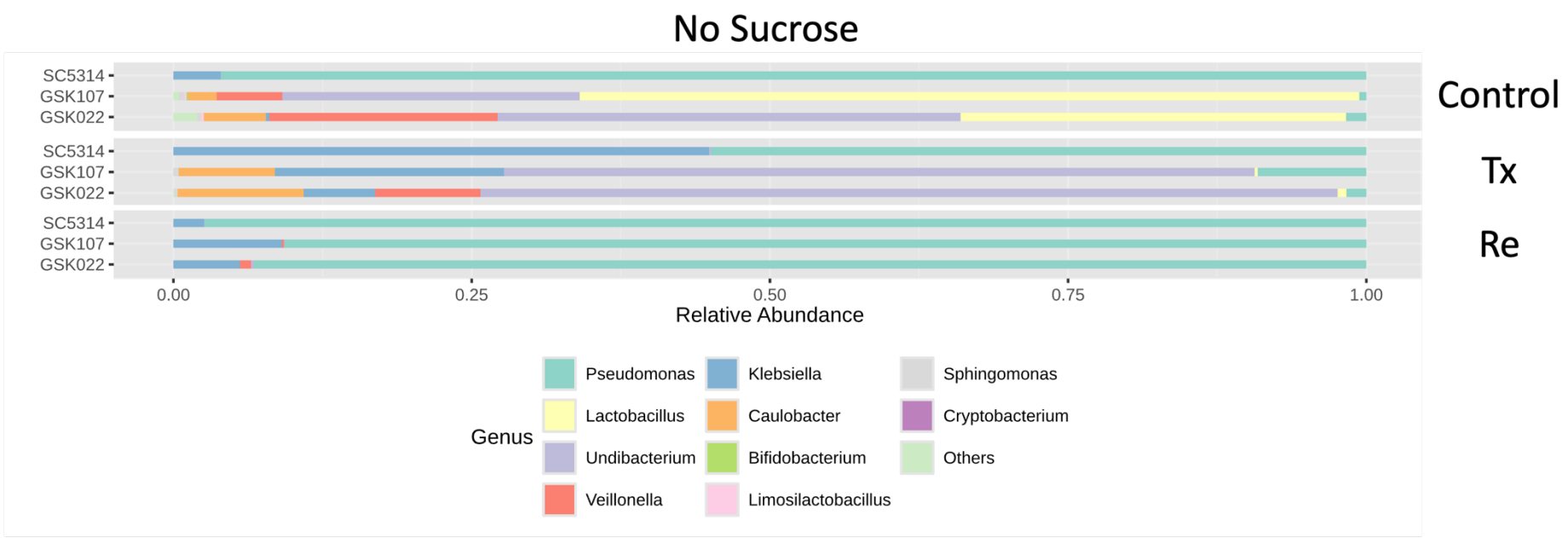


**Figure 4-5 – Bacterial taxonomy is affected by phenotype of *C. albicans* species in addition to oral hygiene regimen.** Relative abundance plots of bacteria distributed in an *ex-vivo* biofilm model using saliva as a starting substrate with the influence of *C. albicans* strains SC5314, GSK22, and GSK107. Organism distribution is influenced by *C. albicans* strain (**Top**), oral hygiene regimen (**Middle**) and subsequent regrowth of organisms (**Bottom**). Strain dependent influences appear largely independent of experimental variables. Images generated with MicrobiomeAnalyst®. Results representative of 9 replicates per sample type (n=9)

Having observed the effects of different strains of *C. albicans* on influencing the development of the *ex-vivo* model with and without treatment and subsequent regrowth, it was important to examine how these parameters were affected by the inclusion of dietary sucrose in the growth media. Previously, we had observed considerable differences in terms of cariogenicity of biofilms and the effect on the enamel substrate (3.3.8.5)

### *4.4.5 Dietary sucrose influences the oral microbiome independent of C. albicans*

As shown below, in Figure 4-6, and in comparison to the samples identified in Figure 4-5, the difference in organism diversity across samples when exposed to 1% sucrose was immediately apparent. This was perhaps best exemplified in the control sample for SC5314, previously having just *Pseudomonas* and *Klebsiella* within its most abundant taxa. When supplemented, this shifted to represent 74% *Lactobacillus*, 19% *Veillonella*, 5% *Bifidobacterium* and 3% *Limosilactobacillus*. Indeed, these organisms are reflective of those present in the non-sucrose samples containing GSK22, the LBF, and are commonly known for their capacity for sugar metabolism, as well as the production of lactic acid (Trindade et al., 2003, Hossain, 2022). This would indicate increased acidogenesis and cariogenic capacity of the *ex-vivo* biofilm model.

Interestingly, the LBF strain GSK22 also exhibited a notable shift in organism distribution, with 69% *Veillonella* present. Indeed, this overabundance of *Veillonella* could be indicative of enhanced pathogenesis similar to that induced by neglect of oral hygiene (Zhan et al., 2022). Although these organisms were present in the sample containing GSK107, *Pseudomonas* (83%) was seen to be the most abundant organism present.

### *4.4.6 Candida bolsters microbial heterogeneity in the presence of sucrose post-treatment.*

When considering the impact of the oral hygiene regimen (**Tx**), the microbial distribution was seen to parallel that of the samples without sucrose (Figure 4-5). Again, the presence of *Undibacterium* indicated that even as microbes were recovered, available biomass could have been diminished and led to subsequent over representation in the sequencing data. However, when biofilms were supplemented with sucrose, samples were able to retain a larger distribution of organisms. For example, in SC5314 samples, 48% of the represented taxa were *Lactobacillus* with GSK107 and GSK22 containing 43% and 20%, respectively. The larger representation of *Undibacterium* in samples containing GSK22 (52%) when compared to GSK107 (10%) and SC5314 (40%), may be indicative of the LBF strain of biofilm being more susceptible to the treatment, given the expected reduction in overall biomass.

Post-regrowth (**Re**), while SC5314 again conceded growth to the presence of *Pseudomonas* (96%), both GSK107 and GSK22 were seen to retain a wider distribution of organisms after 24 hours when compared to their non-sucrose counterparts.

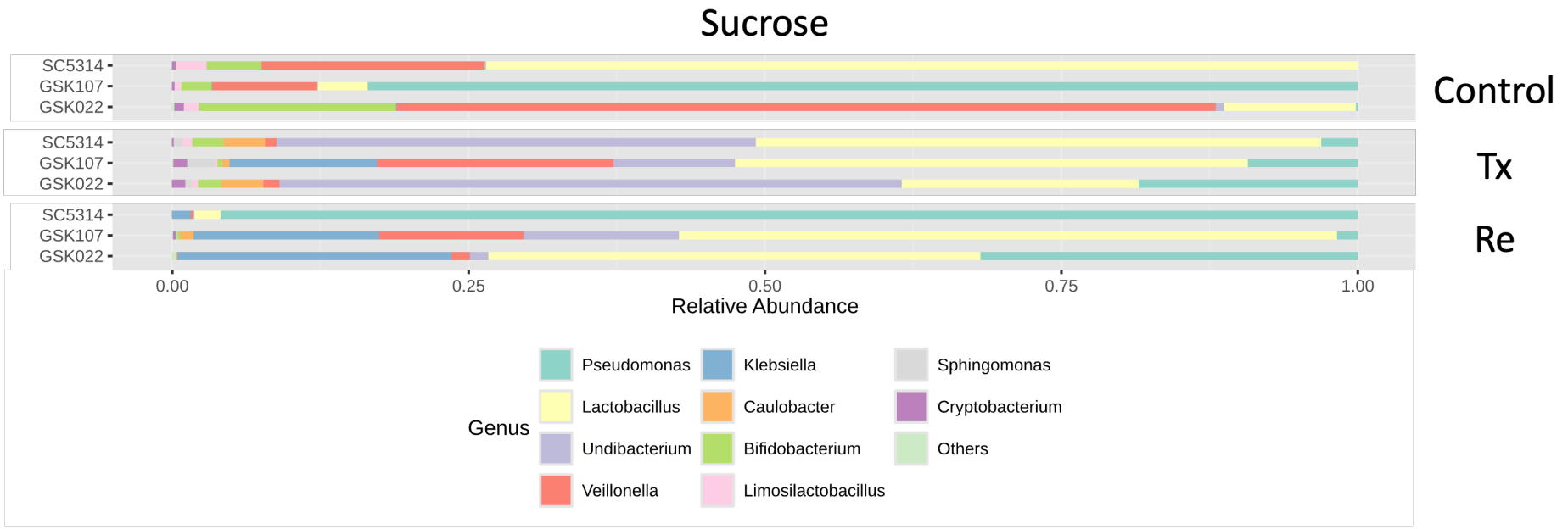


**Figure 4-6 - Bacterial heterogeneity in ex-vivo models is heavily influenced by dietary sucrose.** Relative abundance plots of bacteria distributed in an *ex-vivo* biofilm model using saliva as a starting substrate with the influence of *C. albicans* strains SC5314, GSK22, and GSK107. Organism distribution is influenced by *C. albicans* strain (**Top**), oral hygiene regimen (**Middle)** and subsequent regrowth of organisms (**Bottom**). Strain dependent influences, such as the abundance of *Veillonella* species observed in LBF *C. albicans* control samples, may be indicative of a more disease-associated micro-environment. This is reflected in the reduction of these organisms in regrowth samples.t

### *4.4.7 Diversity analyses reveal strain differences may be limited.*

Having observed the differences in terms of relative abundance of organisms in these samples, we next sought to look at the samples in terms of species richness within samples and between samples. Particularly, this would allow us to observe statistical differences between the HBF and LBF strains of *C. albicans* and assess based on the initial hypothesis that these were sustaining different communities of organisms.

Visualised in Figure 4-7, below, sample diversity was measured using Shannon diversity matrix to account for species richness and evenness across strains of *C. albicans* (**A**)**.** Overall, no statistical significance was inferred in terms of intra-sample organism diversity regardless of *C. albicans* strain (*P=0.333*). This trend continued when examining cross-sample diversity (**B**) using bray-curtis dissimilarity. Samples were not identified as statistically significant across strains (*P=0.087*).

While these results were not necessarily reflective of the initial hypothesis that strain dependency is important in influencing the microbiome, it is important to acknowledge the numerous potentially confounding factors in the analysis of the data such as the influence of sucrose vs. no sucrose or the inclusion of treatment and regrowth factors.

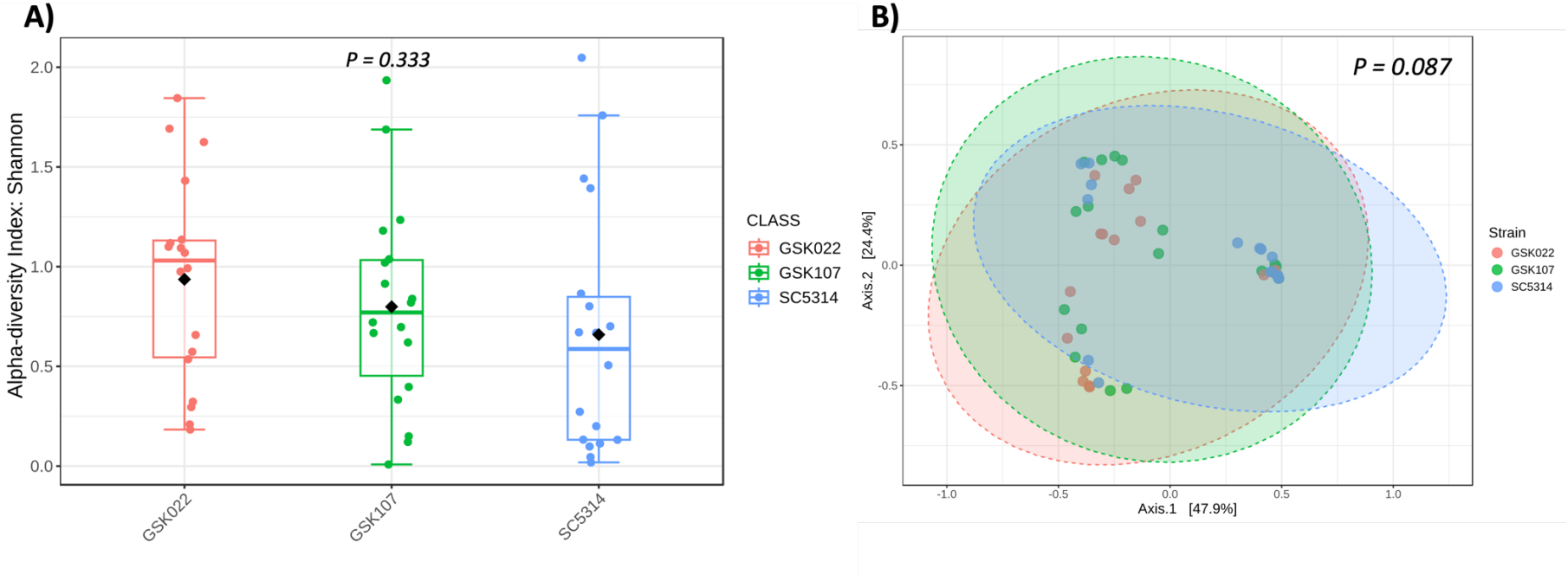


**Figure 4-7 - Diversity metrics indicate lack of statistical significance across strains.** Alpha- (**A**) and beta- (**B**) diversity plots of intra- and inter sample diversity used to account for differences across *C. albicans* strain SC5314, GSK107 and GSK22. No statistical significance observed for in-sample diversity (**A**) across strains (*P=0.333*) or between samples (**B**) (*P=0.087*).

### *4.4.8 Environmental factors significantly influence organism diversity.*

Having examined the lack of significant impact on strain diversity by strain type, it was important to understand how other factors in the experimental study design may influence sample diversity. To this end, the presence of environmental sucrose was compared in terms of alpha- and beta- diversity metrics to account for changes in organisms across samples.

As shown below, in Figure 4-8, statistical significance was observed in comparing samples using Shannon diversity matrix to observe in-sample diversity when samples were grown with or without sucrose (*P=0.0016*). Statistical significance was also observed, albeit not as strongly, in the assessment of cross-sample diversity (*P=0.019*). This would strongly reinforce the outcomes observed from the taxonomic plots in Figure 4-5 and Figure 4-6 where diversity of organisms was immediately more apparent in those samples which contained sucrose. Despite this significance in diversity, there was still an overall lack of defined overlap visually observable in the distance between samples on the PCoA plots, indicating that other factors in sample type may contribute more heavily to inter-sample differences, such as exposure to treatment or subsequent regrowth of organisms in a given sample.

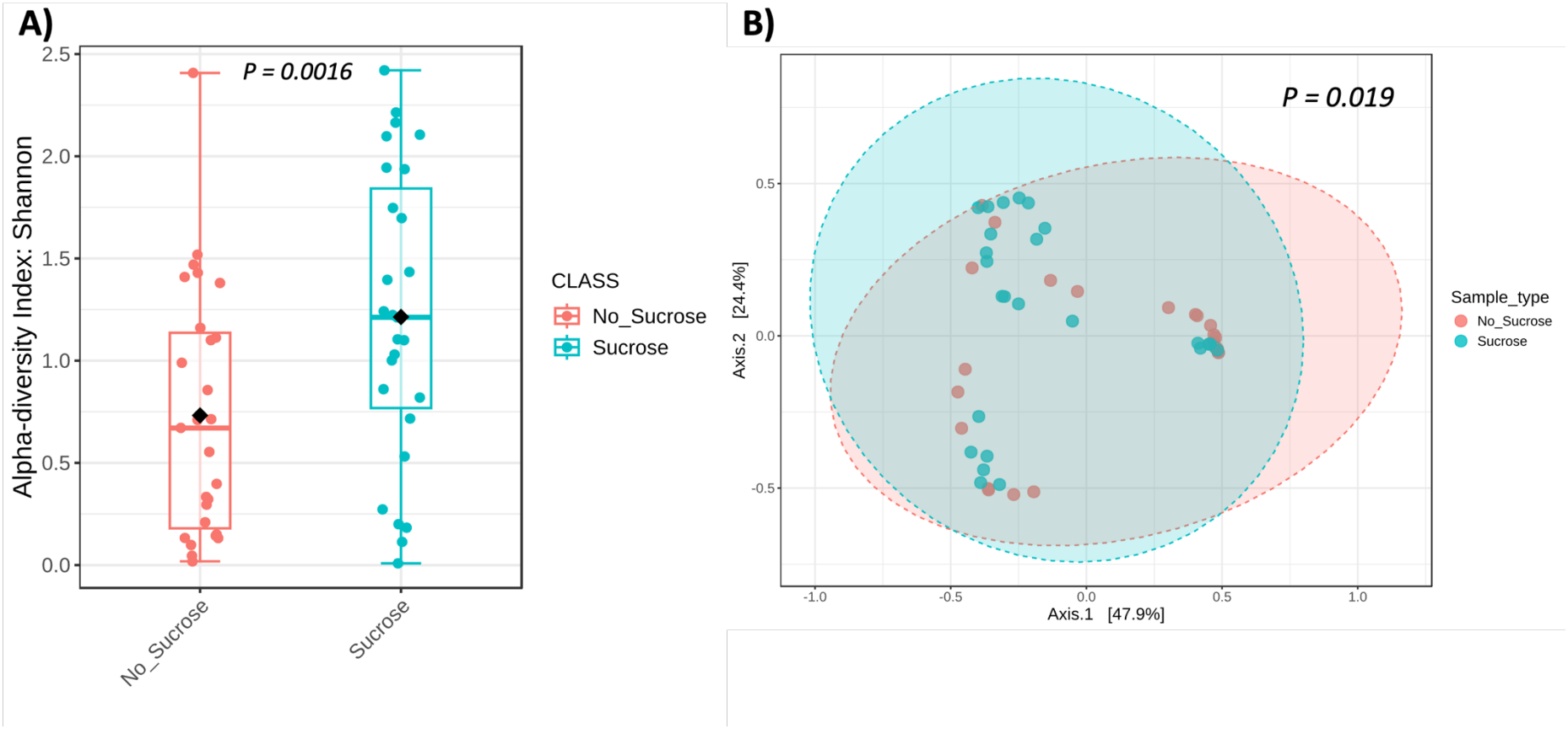


**Figure 4-8 - Diversity metrics reveal impact of sucrose on organism distribution.** Alpha- (**A**) and beta- (**B**) diversity plots of intra- and inter sample diversity used to account for differences between samples with, and without, 1% sucrose in the culture media. Statistical significance (*P=0.0016*) observed for alpha diversity (**A**) and beta diversity (*P=0.019*) (**B**).

In comparison to the results generated from the assessment of the bovine enamel in section 3.4.7, there was indication that the influence of *Candida* had a profound effect on the organisms present in the *ex-vivo* models and that these aspects, in unison with other experimental factors, were influencing cariogenic outputs in terms of organism selectivity and metabolic activity. Indeed, when *Candida* is overabundant in its environment, such as through conditions like denture stomatitis or oral thrush, there may be further implications for the oral microbiome either through altered organism distribution or through the impact of a planned antifungal intervention. As such, we next sought to investigate how these microbial systems may be affected by influencing *Candida* through antifungal intervention.

### *4.4.9 Microbiome analysis of ex-vivo models*

Having established the influence of *C. albicans* on the oral microbiome via the *ex-vivo* saliva models, we next embarked upon examining the dynamic shifting of organisms across samples with and without antimicrobial challenge.

#### *4.4.9.1 Examining saliva profile of ex-vivo models*

As previously considered in Figure 4-4, the initial objective of the study was to observe fundamental differences in saliva composition when exposed to antifungal challenge. Visualised below, in Figure 4-9, the distribution of organisms in each sample was observed to shift in accordance, not only with the timepoints observed but with the influence of each antimicrobial. The distribution of organisms in the unaltered saliva was comparable to that in the previous example of Figure 4-4**.** However, samples containing 1mg/mL fluconazole were observed to change across each timepoint. Initially, after 24-hours, samples were similar to the positive control (**PC**), being mostly

*Streptococcus* (97%). By 72-hours (**FLU_D3**), however, this distribution had shifted dramatically to represent 83% *Staphylococcus*, before returning to a majority *Streptococcus* (89%) and *Staphylococcus* (11%) by 120-hours (**FLU_D5**). Indeed, the abundance of other organisms detected in the saliva alone, such as *Neisseria* and *Klebsiella* were notably missing after these time points, indicating that fluconazole may be allowing *Staphylococcus* to overgrow in the biofilm.

When examining samples containing 1μg/mL of Amphotericin B (**AMB**), differences in organisms were even more noticeable. Again, the initial timepoint (**AMB_D1**) retained a high percentage of *Streptococcus* (97%), also observed by 72-hours (**AMB_D3**) which only mildly drifted (93%) to include more representative populations of *Neisseria* (4%) and *Aggregatibacter* (1%). However, by 120-hours of repeat exposure, samples appeared more diverse in organism distribution, now favouring *Neisseria* (43%), and including higher percentage of *Aggregatibacter* (13%), *Klebsiella* (12%), and *Haemophilus* (11%), with only 6% *Streptococcus*. While the retention of organisms more diverse than only *Streptococcus* was also observed in the later timepoint for the saliva only control (**PC_D5**) these proportions were vastly different, possibly indicating and off-target effect on bacteria being produced by Amphotericin B, either directly or indirectly through effect on unidentified fungal species within the original saliva sample which were not sequenced.

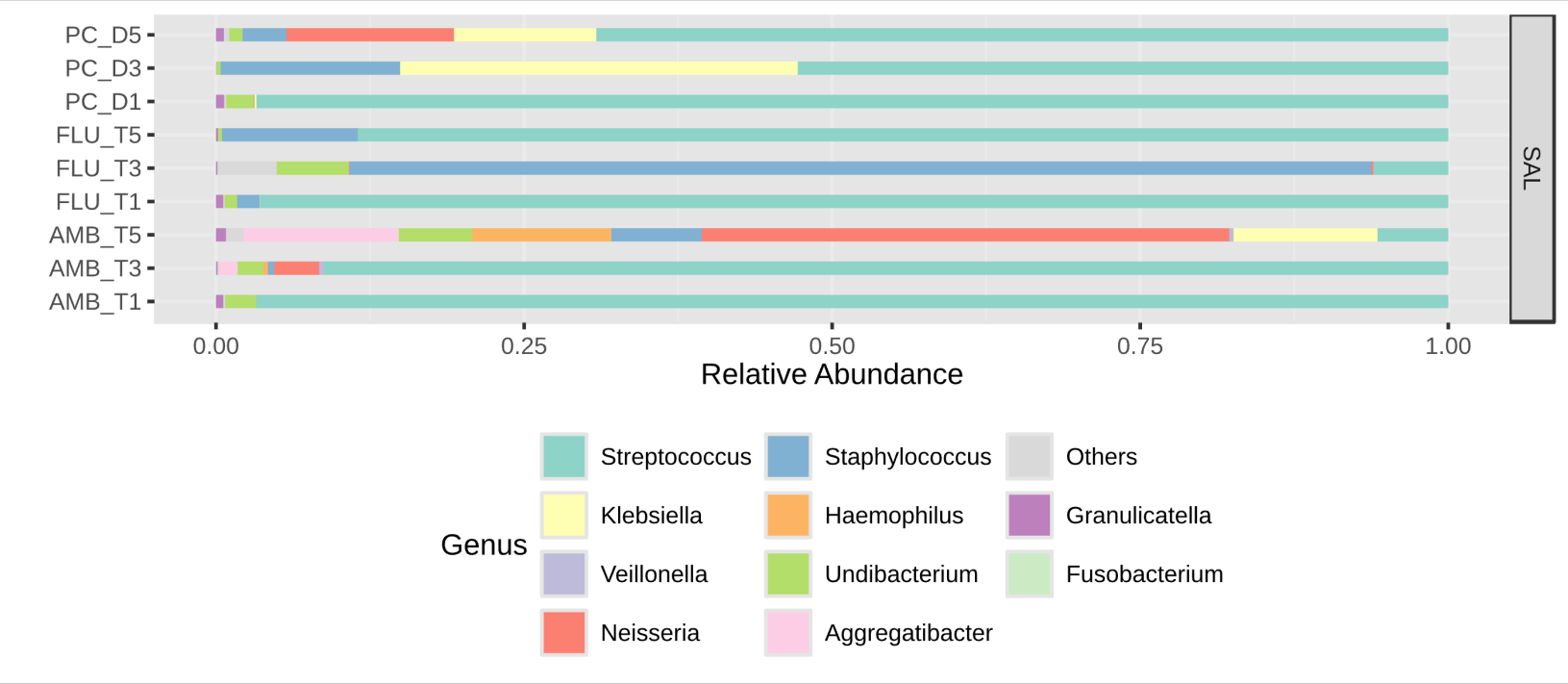


**Figure 4-9 - Phylogenetic analysis of *ex-vivo* samples reveal altered distribution of bacteria in presence of antifungals.** Relative abundance plots of bacteria distributed in an *ex-vivo* biofilm model using saliva as a starting substrate grown in RPMI:THB media (**PC**) and exposed to 1mg/mL Fluconazole (**FLU**) or 1μg/mL Amphotericin B (**AMB**) across timepoints of 24-hours (**D1**), 72-hours (**D3**), and 120-hours (**D5**) growth. Microbial distribution was seen to alter across timepoints and in a treatment-dependent manner.

#### *4.4.9.2 Examining HBF phenotype of C. albicans in ex-vivo models*

Having observed the direct effect of antifungal challenge on *ex-vivo* biofilms without the additional presence of *Candida*, it was essential to observe how the shifting phenotypes that have been implicated as having an effect on the organisms distribution (Figure 4-5 and Figure 4-6) may also contribute to the system when challenged with antimicrobials.

As below, in Figure 4-10, when compared with saliva only biofilms (Figure 4-9), it was immediately apparent that the distribution of organisms was affected by the inclusion of GSK107. In the initial control samples (**PC**) when compared to the abundance of *Streptococcus* in the saliva-only samples, the GSK 107 samples are more diverse at the initial timepoint (**PC_D1**), mostly being represented by *Veillonella* (55%), *Neisseria* (19%), and *Haemophilus* (12%). By 72-hours (**PC_D3**) these samples had adjusted to favour *Neisseria* (48%), *Streptococcus* (26%), and *Veillonella* (18%). At 120-hours (**PC_D5**), these species were still observed, but the biofilm had become dominated by *Klebsiella* (60%). Interestingly, compared to the biofilm grown using the bovine enamel, these samples were notably lacking *Lactobacillus* at the 72-hour timepoint, despite being derived from the same pooled saliva source, indicating a surface dictated difference in organism retention, perhaps being the result of increased surface area, sequestration of organisms within imperfections in the enamel, or improved microbial adhesion to the enamel.

When observing the inclusion of fluconazole, the initial (**FLU_T1**) sample diversity did not appear to differ greatly from the control samples, with 54% *Veillonella*, 21% *Neisseria*, and 8% *Haemophilus*. This would indicate that sample diversity in these samples is being affected by inclusion of HBF *C. albicans* than by antifungal challenge. However, by 72-hours (**FLU_T3**) organisms had shifted to a lower abundance of

*Veillonella* (19%) but an increased abundance of *Haemophilus* (30%) and *Neisseria* (26%) and *Aggregatibacter* (9%). Much like in the control sample (**PC_D5**), by 120-hours (**FLU_T5**), the biofilm was represented by *Klebsiella* (68%) and *Veillonella* (15%). These results could indicate a response to fluconazole at the 72-hour timepoint, after multiple exposures, but a potential loss of efficacy after 120-hours.

Finally, the inclusion of AMB in biofilm samples also affected the observed taxa within the phylogeny plots. In the initial control, (**AMB_D1**) *Klebsiella* (39%) was observed, unlike the other 24-hour timepoint samples which, by 72-hours (**AMB_D3**) had become the majority organism present (84%). The most diversity in bacteria present was observed after 120-hours (**AMB_T5**), with 34% *Neisseria*, 28% *Streptococcus*, and 27% *Veillonella*.

Given the previous evidence of taxonomic differences between strains of *C. albicans* it was important to expand on these parameters and examine the effect of antifungals on other strains of *C. albicans*.

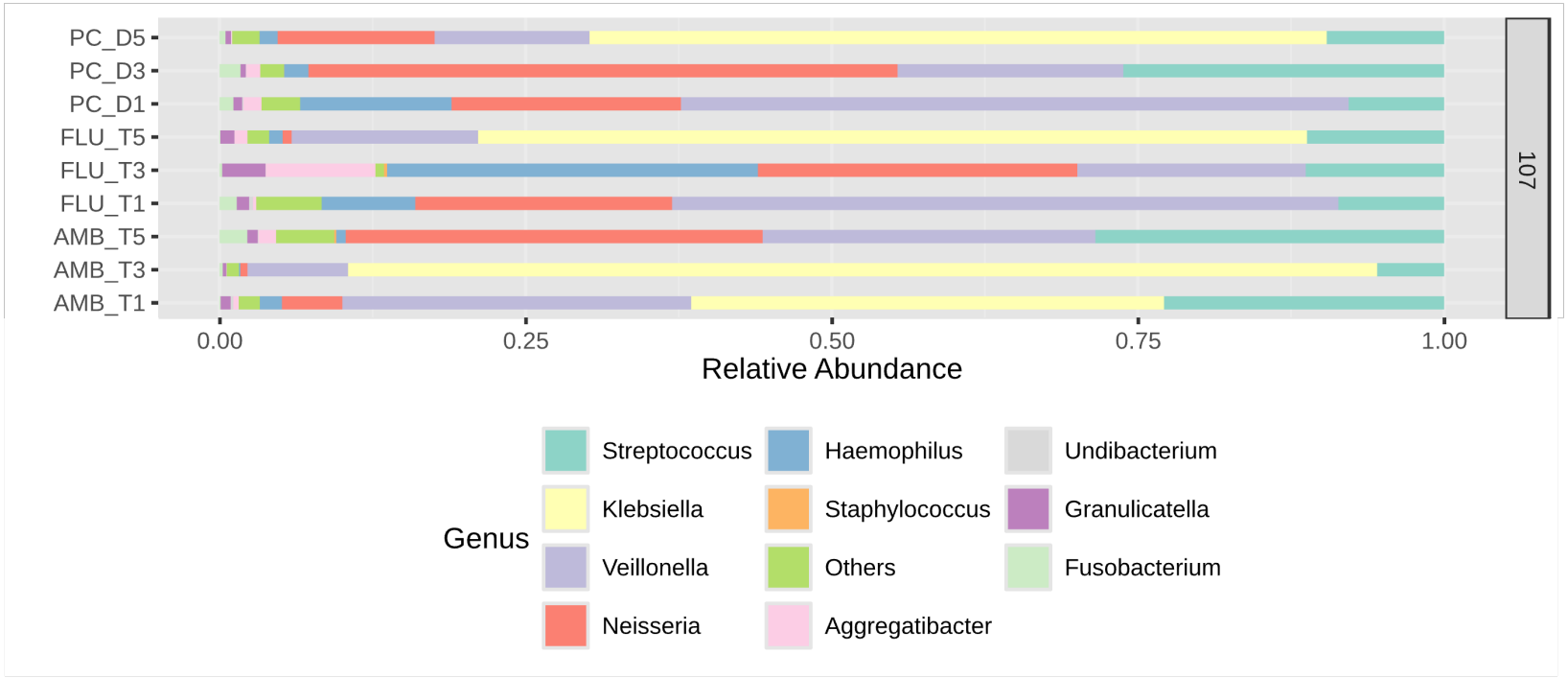


**Figure 4-10 - Introduction of *C.albicans* to *ex-vivo* systems produces shift in taxonomic profile.** Relative abundance plots of bacteria distributed in an *ex-vivo* biofilm model using saliva as a starting substrate grown with 1x10$^6$CFU/mL of *C. albicans* strain GSK107 in RPMI:THB media (**PC**) and exposed to 1mg/mL Fluconazole (**FLU**) or 1μg/mL Amphotericin B (**AMB**) across timepoints of 24-hours (**D1**), 72-hours (**D3**), and 120-hours (**D5**) growth. Microbial distribution was seen to alter with inclusion of GSK107, as well as alter across timepoints and in a treatment-dependent manner.

#### *4.4.9.3 Examining LBF phenotype of C. albicans in ex-vivo models*

Given the previously established understanding about antimicrobial resistance in *C. albicans* being heavily linked to biofilm development, it was important to observe changes in distribution of bacteria in samples inoculated with the LBF strain GSK22.

Visualised below, in Figure 4-11, when adjusting for LBF *C.albicans*, taxonomic diversity shift in comparison to saliva only controls and samples containing HBF GSK107. At the initial timepoint (**PC_D1**) *Neisseria* was the most represented organism (69%), a major contrast to the abundance of *Veillonella* and *Streptococcus* seen in the previous examples. These values shifted after 72-hours (**PC_D3**), to favour *Klebsiella* (60%), *Veillonella* (24%), and *Streptococcus* (9%), and retained a similar taxonomic profile after 120-hours (**PC_D5**) with 54% *Klebsiella*, 26% *Veillonella*, and 13%, *Streptococcus*. Interestingly, this taxological stability was not reflected in the previous samples and may be indicative of a unique trait to GSK22 *C. albicans*.

Following exposure to fluconazole (**FLU_T1**), taxonomic distribution shifts in favour of *Veillonella* (31%), *Neisseria* (26%), and *Klebsiella* (21%). After 72-hours (**FLU_D3**) *Veillonella* remains the majority organism within the biofilm (43%), with an increase in relative abundance of *Klebsiella* (30%), and *Streptococcus* (12%) with a reduction in *Neisseria* (4%). By 120-hours (**FLU_D5**) *Klebsiella* had become the majority organism (60%) with *Veillonella* (17%) and *Streptococcus* (13%). Interestingly, the abundance of *Klebsiella* identified in *C. albicans* samples, when compared with the saliva only samples, may implicate *Candida* as having a direct effect on the retention of this organism.

This potential analysis may be further emphasised by observing phylogeny data with samples challenged with amphotericin B (**AMB**). Taxonomic representation of these samples favoured *Neisseria* (51%), *Veillonella* (21%), and *Streptococcus* (11%) at the

initial timepoint (**AMB_T1**), which remained the majority represented organisms across the later timepoints. Interestingly, these samples did not identify any *Klebsiella*, which may indicate the phenotype of *C. albicans* as integral to retaining this organism. Additionally, the likely susceptibility of LBF *Candida* to AMB may also support the necessity for *Candida* presence to support abundant *Klebsiella*.

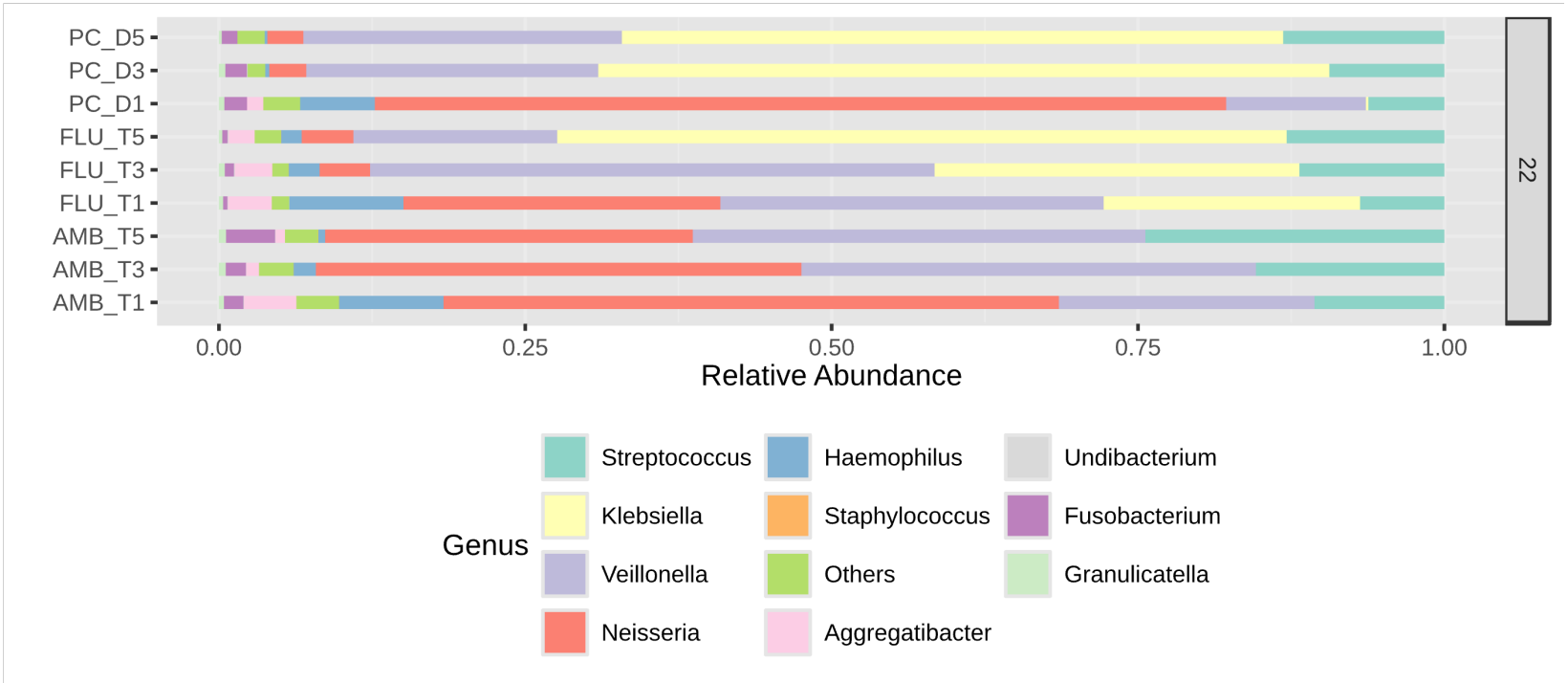


**Figure 4-11 – Shifts in taxonomic distribution respond to phenotype of *C. albicans*.** Relative abundance plots of bacteria distributed in an *ex-vivo* biofilm model using saliva as a starting substrate grown with 1x10$^6$CFU/mL of *C. albicans* strain GSK22 in RPMI:THB media (**PC**) and exposed to 1mg/mL Fluconazole (**FLU**) or 1μg/mL Amphotericin B (**AMB**) across timepoints of 24-hours (**D1**), 72-hours (**D3**), and 120-hours (**D5**) growth. Microbial distribution was seen to alter with inclusion of GSK22, as well as alter across timepoints and in a treatment-dependant manner.

#### *4.4.9.4 Examining type-strain SC5314 in ex-vivo models*

Having established the response of bacterial communities to the presence of clinical strains of *C. albicans* and subsequent antimicrobial challenge, it was important to next observe the same conditions with a well-researched type-strain of *C. albicans* SC5314.

Featured below, in Figure 4-12, the inclusion of SC5314 was accompanied by an increase in representation of *Klebsiella* across control samples from the initial timepoint (**PC_D1**) and remained the majority taxonomy across timepoints from 68% to 74% at 72-hours and 45% at 120-hours. *Veillonella* was also relatively abundant at the initial timepoint (22%), before dropping at 72-hours (9%) and then adjusting again at 120-hours (17%). There was also a steady increase in abundance of *Streptococcus* as the biofilm matured, initially representing only 2% of the taxa (**PC_D1**), which increased to 8% at 72-hours (**PC_D3**) and represented a quarter (25%) of the taxa by the 120-hour timepoint (**PC_D5**). A similar trend was noted in *Neisseria* which increased in abundance from 2% to 5% to 6% across timepoints. This continued support of *Klebsiella* and *Veillonella* in the presence of *Candida* species was further exemplified by these analyses.

Following fluconazole challenge, the initial timepoint (**FLU_T1**) followed a similar distribution to the control samples, having representative taxonomy high in *Klebsiella* (53%) and *Veillonella* (28%). Interestingly, this abundance of *Klebsiella* had completely diminished by 72-hours (**FLU_T3**) shifting to increase abundance of *Neisseria* (27%) and *Haemophilus* (23%), as well as *Streptococcus* (19%), while the proportion of *Veillonella* (24%) remained relatively unaffected. These results bore a similarity to the distribution of organisms present in the HBF strain samples under the same conditions (**Figure 4-10**) which, again, may be based on sensitivity to treatment outcome and the

effect on *C. albicans* impeding the sustainability of *Klebsiella*, allowing other organisms to develop. This could be reinforced again by the similarity of taxa in the 120-hour (**FLU_T5**) timepoint to those of the GSK107 strain, where *Klebsiella* becomes the majority taxa (66%) with *Streptococcus* (14%) and *Veillonella* (9%) while *Neisseria* and *Haemophilus* diminish to 3% and 2% of the representative abundance respectively.

Following examination of samples challenged with Amphotericin B, *Veillonella* was seen to be the majority taxa after 24-hours (**AMB_T1**) at 68%, followed by *Streptococcus* (13%), and *Neisseria* (9%). By 72-hours (**AMB_T3**), however, the represented taxa had shifted to favour *Neisseria* (37%) while also sustaining the highest abundance of *Aggregatibacter* (20%) seen in any of the samples. This, alongside sustained levels of *Veillonella* (16%) could indicate a unique potential for pathogenicity within the taxonomic profile of this sample. By 120-hours (**AMB_T5**), however, the taxonomic profile had returned to a profile like that of the mature control sample (**PC_D5**) with 55% *Klebsiella* and 22% *Veillonella*, albeit with smaller representative *Streptococcus* at 12%.

Throughout these analyses there was strong evidence of both dissimilarity and similarity between the measured conditions from the representative taxonomy. As such, it would be important to next assess what significance these findings may have in terms of organism diversity across key conditions within the study.

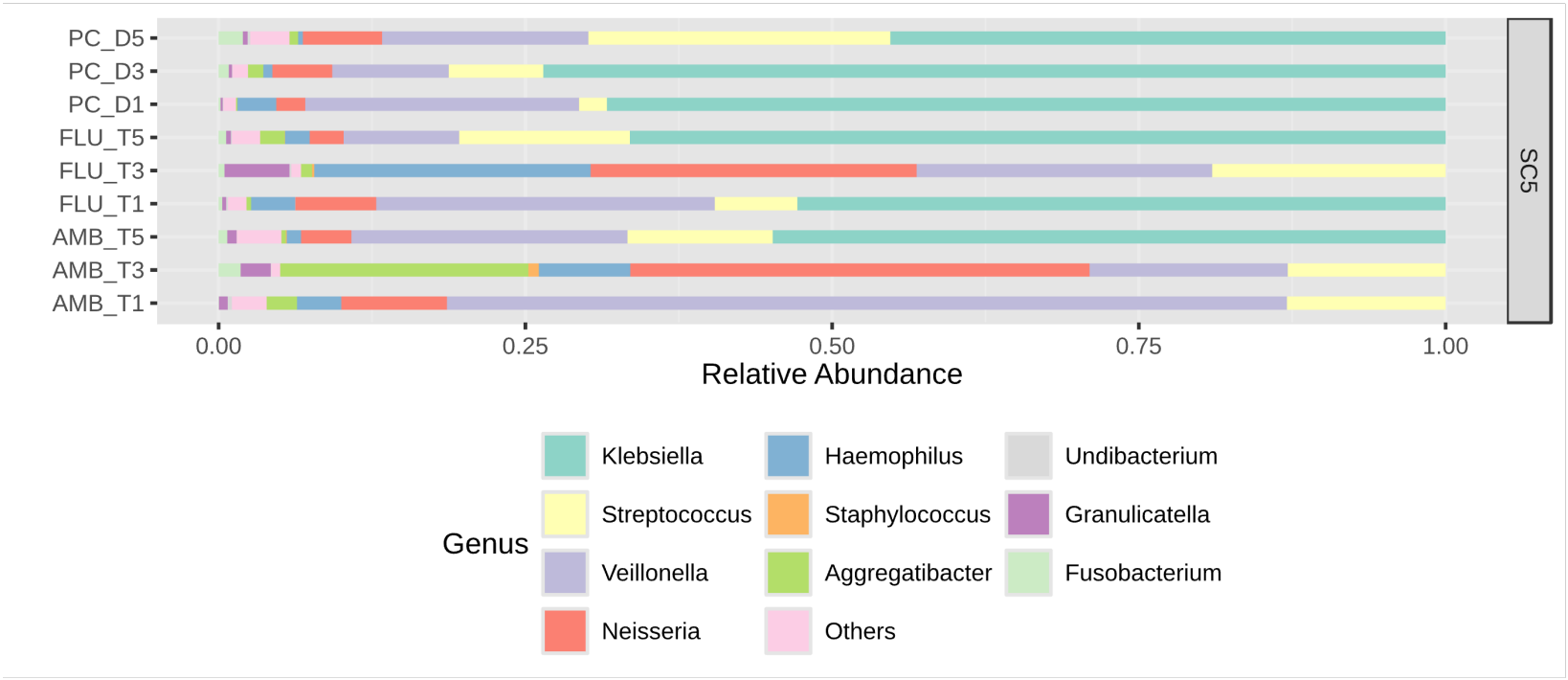


**Figure 4-12 - Taxonomic changes in *ex-vivo* biofilms are impacted by type-strain *C. albicans* SC5314.** Relative abundance plots of bacteria distributed in an *ex-vivo* biofilm model using saliva as a starting substrate grown with 1x10$^6$CFU/mL of *C. albicans* strain GSK22 in RPMI:THB media (**PC**) and exposed to 1mg/mL Fluconazole (**FLU**) or 1μg/mL Amphotericin B (**AMB**) across timepoints of 24-hours (**D1**), 72-hours (**D3**), and 120-hours (**D5**) growth. Microbial distribution was seen to alter with inclusion of SC5314, as well as alter across timepoints and in a treatment-dependent manner.

### *4.4.10 Diversity analysis of ex-vivo biofilm models.*

Having looked at the differences in sample taxa in detail, and having stated the objective comparisons between them, it was important to examine the impact of these differences in terms of quantifiable statistical output using key factors to consider intra- and inter- sample diversity.

#### *4.4.10.1 Diversity analysis of sample type*

Firstly, the key observation intended from the study design was to examine the influence of *C. albicans* in affecting the organisms distributed within the oral microbiome. Having confirmed this in a fixed model in section 3.4.4, we wished to examine its impact in a complex *ex-vivo* model. Visualised below, in Figure 4-13, sample diversity was seen to be heavily influenced by sample conditions and the inclusion of *Candida.* Indeed, pairwise comparison between samples revealed statistically significant differences ($P < 0.007$) in taxonomy between all parameters. These changes in taxonomy as well as the differences observed in the alpha and beta diversity plots would imply that the inclusion of *C. albicans*, regardless of strain, has a significant impact on the microbiome at these, biofilm relevant, inoculating concentrations.

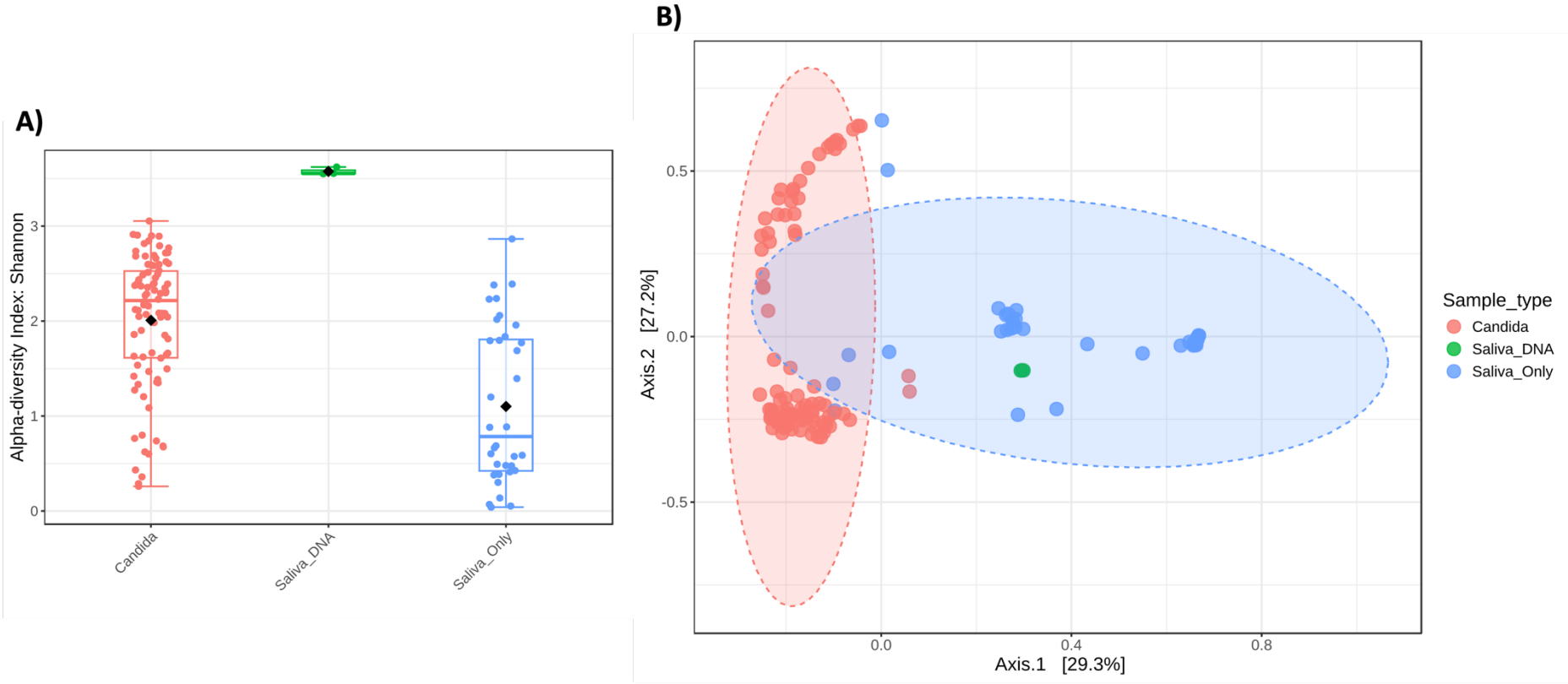


**Figure 4-13 - Diversity metrics reveal significant details across sample conditions.** Alpha- (**A**) and beta- (**B**) diversity plots of intra- and inter sample diversity used to account for differences between *ex-vivo* biofilm samples inoculated with $1x10^6$ *C. albicans* (**Candida**), derived wholly from saliva (**Saliva_Only**), or as a representation of organisms within the original saliva pool (**Saliva_Only**). Distinct clustering of samples was observed in both Shannon diversity and Bray-Curtis Dissimilarty based on sample conditions. Statistical significance was achieved across all pairwise comparisons ($P < 0.007$).

#### *4.4.10.2 Diversity analysis of Candida phenotype*

Having established the importance of *C.alibicans* in shaping the micro-environment, it was crucial to examine this in the context of our initial hypothesis that *C. albicans* phenotype is also heavily linked to the surrounding micro-environment.

As shown below, in Figure 4-14, intra-sample diversity in *C. albicans* strains revealed a tendency towards differences across strains, particularly in comparison between GSK22 and GSK 107 ($P = 0.09$), as determined via ANOVA. This result was reflected in the beta diversity between samples but was also lacking in statistical significance as determined by Bray-Curtis Dissimilarity test. Due to how microbiome samples are typically calculated, this lack of difference could also be indicative of a lack of power in sample size (Ferdous et al., 2022). As with the data analysed in the previous figure (Figure 4-13), differences between *C. albicans* strains and the unaltered *ex-vivo* model, across all pairwise parameters, were observed to be statistically significant ($P < 0.001$).

Given the complex study methodology in the context of longitudinal analysis of biofilm development as well as providing multiple treatment aspects, it was important to assess these factors for influence on the microbial diversity which may explain this lack of phenotypic distinction across *Candida* strains.

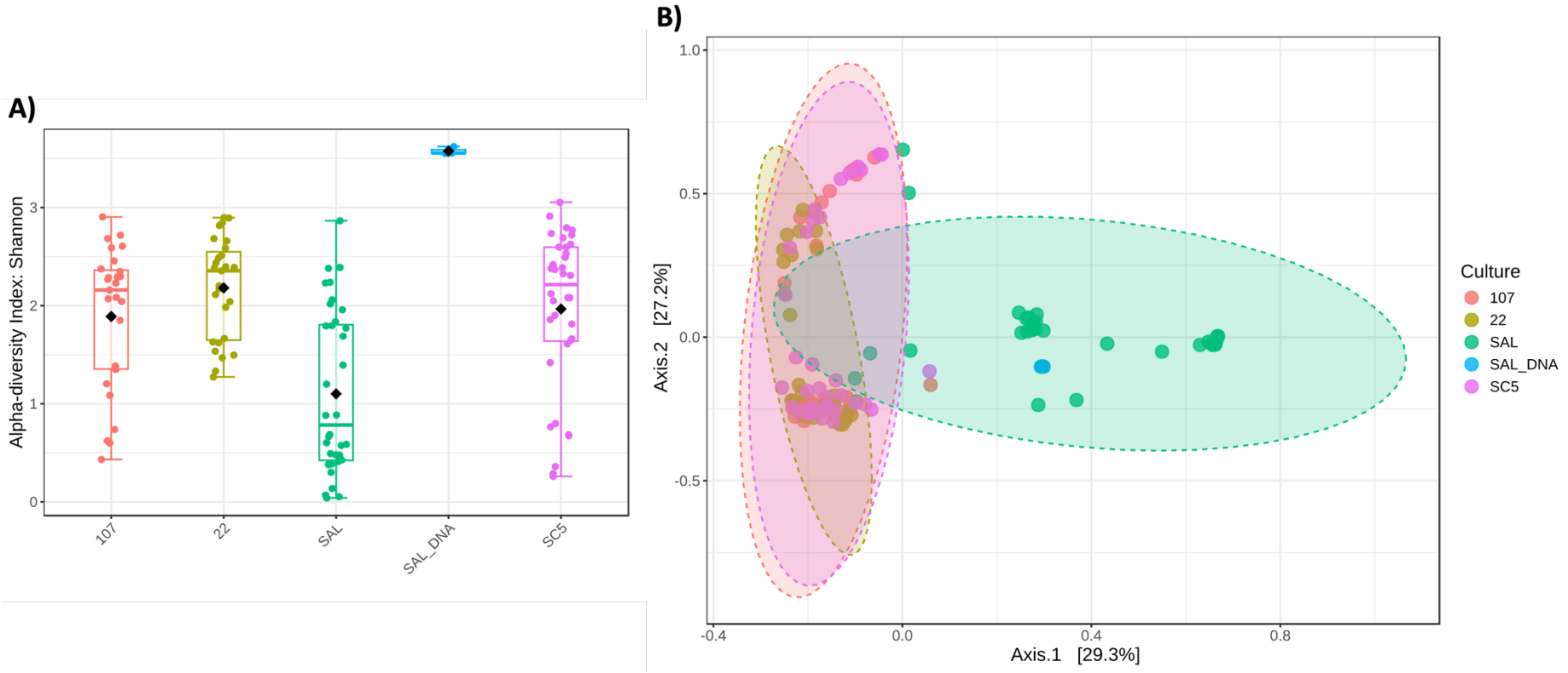


**Figure 4-14 - Diversity metrics reveal importance of *C. albicans* phenotype in taxonomic diversity.** Alpha- (**A**) and beta- (**B**) diversity plots of intra- and inter sample diversity used to account for differences between *ex-vivo* biofilm samples inoculated with $1x10^6$ *C. albicans* strains GSK107 (**107**), GSK22 (**22**), SC5314 (**SC5**) and in *ex-vivo* biofilm samples only (**SAL**) and the original sequenced saliva pool DNA (**SAL_DNA**). While there was an observable trend towards dissimilarity between sample types, this was not determined to be statistically significant. were observed across metrics for samples containing LBF *C. albicans*.

#### *4.4.10.3 Diversity analysis of antifungal challenge*

As stated previously, observing the potential influence of treatment types on the distribution of organisms in the *ex-vivo* system was essential to complete our understanding of the dynamic between *C. albicans*, antifungal challenge, and the potential impact on the oral microbiome.

Visualised below, in Figure 4-15, despite a lack of subjective clustering between samples in both diversity plots, statistical significance was observed between samples challenged with Amphotericin B and the control samples ($P < 0.05$). This would indicate that between the antifungal regimen, AMB may have the highest potential for inducing microbial dysbiosis in an *ex-vivo* setting.

Given that these samples were all observed longitudinally, diversity metrics were also observed across timepoints, however no significant difference was achieved across samples. Like analyses of phenotype in Figure 4-14, some non-significant differences were apparent regarding the latest timepoint (120-hours) across samples.

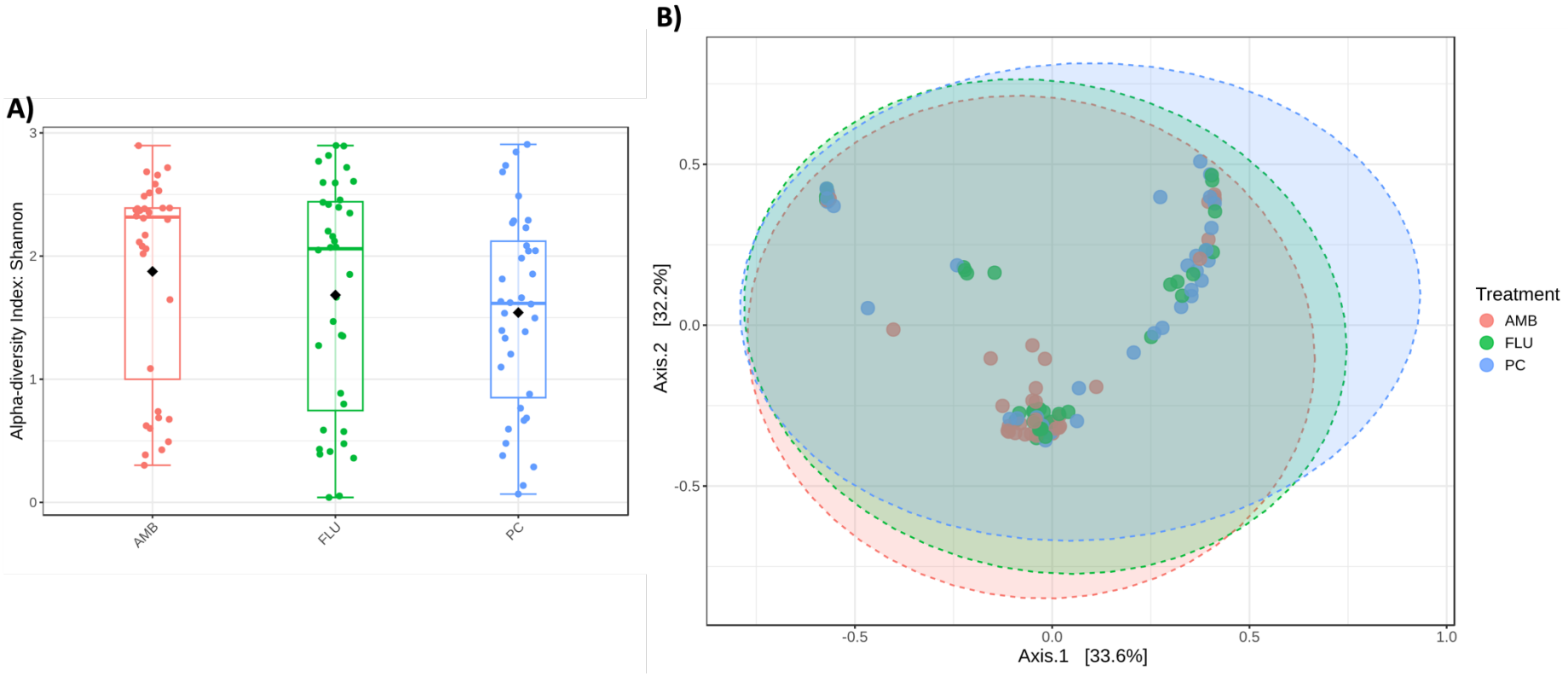


**Figure 4-15 - Diversity analysis of antifungal challenges emphasises sample differences.** Alpha- (**A**) and beta- (**B**) diversity plots of intra- and inter sample diversity used to account for differences between *ex-vivo* biofilm samples with and without *C. albicans* (**PC**) and those challenged with 1μg/mL Amphotericin B (**AMB**), 1mg/mL Fluconazole (**FLU**). Despite lack of visual disparity, statistical significance was observed in beta diversity when comparing samples challenged with AMB to control samples ($P < 0.05$).

## 4.5 Discussion

### *4.5.1 Overview*

We identified, in the previous chapter, the effect of strains of *C. albicans* on microbial diversity outcomes associated with sucrose, as well as related to antifungal influences on the bacterial microbiome. As a result, it was essential to understand the link between these organisms and the surrounding microbiome through examination of complex, undefined communities. This chapter investigated this as part of two distinct studies using saliva derived *ex-vivo* biofilm models.

### *4.5.2 Assessing disparity in techniques used in microbiome research*

As sequencing techniques have become more robust and widely available, the concept of moving beyond conventional biofilm models for testing specific bacterial communities has become more commonplace (Johnson et al., 2019, Greenman et al., 2024, Billington et al., 2022). While direct sequencing of clinical samples is advantageous, the accessibility, processing, and ethical considerations required for this research can lead to difficulty in maintaining consistency across studies (Gupta et al., 2019, Bharti and Grimm, 2019). In understanding this, this study sought to examine parameters for microbiome research which may adopt a “best-approach” methodology, an issue that has been highlighted for several reasons (Silva et al., 2022, Regueira-Iglesias et al., 2023, Pollock et al., 2018).

Firstly, we sought to examine the effects of DNA extraction protocols on a mock-community of organisms where we achieved results comparable to that of the expected template (Figure 4-2 and Figure 4-3) and observed distinct variation between samples based on extraction methods. The disparity between extraction protocols in the context of high-throughput sequencing has often been addressed (Teng et al.,

2018, Gand et al., 2023, Fouhy et al., 2016). Indeed, Elie et al., in 2023, highlighted significant differences in taxonomic outputs related to DNA extraction protocols (Elie et al., 2023). Moreover, studies such as those produced in 2022 by Tourlousse et al., highlight the use of microbial mock communities as a sense check for microbiome data and methodologies to overcome exactly this type of inconsistency, an opinion mirrored by the work produced by Galla et al., in 2023 (Tourlousse et al., 2022, Galla et al., 2023).

### *4.5.3 Surface matters in ex-vivo biofilm models*

Having established the methodology surrounding processing and sequencing of microbiome samples, the study sought to examine the complex relationship between the biofilm model and enamel surfaces. While the study was able to outline nuance between sample conditions under control conditions (Figure 4-4), some parameters remained obfuscated by unimpeded growth of off-target organisms such as *Pseudomonas* and *Undibacterium* (Figure 4-5 and Figure 4-6). It is well recognised in dental research that the formation of a dental pellicle is intrinsically linked plaque formation and to caries (Enax et al., 2023, Fischer and Aparicio, 2021). Without this pellicle formation, it is possible that non-specific organisms may adhere to sample surfaces, particularly where biomass is sparse, and lead to skewed results, which may explain the difference found in samples containing sucrose, a difference noted by Ayoub and colleagues, in 2020 (Ayoub et al., 2020).

### *4.5.4 Low biomass sequencing can influence microbiome analysis*

As outlined elsewhere, and observed in the taxonomic data in Figure 4-5 and Figure 4-6, as well as Figure 4-9 - Figure 4-11, the complexity of sequencing techniques and

the inclusion of multiple reagents throughout sample processing can easily introduce potential contaminants to a given system, as shown by Salter et al., in 2014 (Salter et al., 2014). This was evident during our testing of samples on enamel, where potential contamination from *Pseudomonas* had become a dominant organism despite not being represented in the sequenced saliva pool. Moreover, this potential is compounded by the inclusion of longitudinal aspects of biofilm growth which invite the risk of further exposure to contamination in the environment (Brown et al., 2022a, Zhu et al., 2020). This can be further influenced by the nature of contamination in sequencing being difficult to detect until the end-product (Karstens et al., 2019, Lao et al., 2023). Indeed, some research, such as that conducted by Dyrhovden, in 2021, highlight the necessity of cutoff scores particularly for low biomass samples with known off-target sequences being amplified (Dyrhovden et al., 2021). This may explain why samples rich in *C. albicans*, particularly HBF strains, showed less evidence of these potential off-target organisms.

### *4.5.5 Candida influencing complex microbial communities*

When observing the taxonomic differences in samples containing *Candida* across study parameters (Figure 4-5 and Figure 4-6 and Figure 4-9 - Figure 4-11) there was clear recorded differences in distribution of organisms between biofilm phenotypes. Indeed, reviews such as that by Peleg et al., in 2010, and Delaney et al., in 2018, have highlighted the influence of often under-appreciated fungal communities in a bacterial setting (Peleg et al., 2010, Delaney et al., 2018). While the framework is often based on the ability for bacteria to influence *C. albicans*, work such as that conducted by Mason et al., in 2012 examined the influence in reverse and noted that *C. albicans* persistence after antimicrobial challenge demonstrated faster recovery of bacteria

(Mason et al., 2012). Indeed, this could be reflective of the regrowth of organisms observed after oral hygiene intervention (Figure 4-6)

This implied recovery of organisms was key to the underlying hypothesis of *C. albicans* as a potential harbour of beneficial bacteria within the oral cavity and while its role as an opportunistically pathogenic organism is well understood, we found little support for our own hypotheses (Lemberg et al., 2022, Patel, 2022).

### *4.5.6 The usual suspects in oral microbial dysbiosis*

Throughout the examination of the microbiome in relation to *C. albicans* the predominant identified taxa displayed were *Klebsiella*, *Veillonella*, *Streptococcus*, *Neisseria*, *Haemophilus* and *Aggregatibacter*. (Figure 4-9 - 4-15). Indeed, most of these organisms have been identified in the literature in various formats from health to dysbiosis (Peng et al., 2022, Radaic and Kapila, 2021, Kreth et al., 2009, Donati et al., 2016, Gholizadeh et al., 2017). For example, research conducted by Falsetta et al., in 2014, highlighted the virulence of *Candida albicans* and *Streptococcus mutans* dual species biofilms, while *Veillonella* and *Aggregatibacter* have also been closely associated with *C. albicans* such as through work conducted by Fujinami et al., in 2021 (Fujinami et al., 2021, Falsetta et al., 2014). However, one key component with these studies is the influence of specific bacteria in the context of mucosal invasion and host immune response, as opposed to clear indications in oral caries and tooth decay. Moreover, the co-aggregation of commensal organisms with *C. albicans* may also lead to the occupation of the environmental niche associated with these organisms when removed from the context of the oral mucosa. Indeed, Kim et al., in 2017, identified a common phenotypic thread in relation to *C. albicans* as yeast being closely associated

with *S. mutans* (Kim et al., 2017b). This would potentially reinforce our assessment that *Candida* phenotype is closely related to caries outcomes.

### *4.5.7 Antifungal influence in oral models*

It was clear across all sequencing data relating to antifungal influence (Figure 4-9 - 4-15), that, despite lack of statistical significance in the findings, Fluconazole and Amphotericin B clearly influenced the distribution of organisms present in the *ex-vivo* models. As previously stated, it is possible that a lack of power in the study design when choosing the sample allocation has resulted in this lack of clear significance. Research into the influence of antifungals on the bacterial microbiome, such as that conducted by Heng et al., in 2021, have observed trends in altered distribution of bacteria after administration of oral fluconazole (Heng et al., 2021). Within that study, they highlighted that, despite no changes in overall abundance, the distribution of *Firmicutes* and *Proteobacteria* when compared to other organisms had greatly increased. This may also infer a question of suitability isn the context of using only diversity matrices as a measure of impact in the case of antimicrobial or hygiene interventions. This may validate some of the evidence of microbial distribution favouring *Klebsiella*, and *Veillonella* in the context of these antifungal treatments. These studies may highlight a potential risk in administration of antifungals in the bias they produce in the bacterial microbiome. Research such as that conducted by Rocco et al., in 2000, highlighted worsened outcomes in the critical care of patients after fluconazole administration (Rocco et al., 2000). While the impact of fluconazole in the context of intestinal fungal dysbiosis is relatively well understood, it is not as clear how it may impact the oral microbiome (Wheeler et al., 2016). While Amphotericin B was also implicated in the context of fungal dysbiosis in the gut by Wheeler et al., there is

an overall lack of research into its influence, likely due to its position as a “last-resort” in the treatment of fungal infections resulting in limited research on its off-target effects (Delhom et al., 2020). Overall, while antifungals elicit an effect on the oral microbiome, it is unclear how much that effect is mediated or exacerbated by the presence or absence of fungi without further research. Figure 4-16, below, depicts the potential influence that antimicrobials may have on existing polymicrobial communities, where the reduction of bacteria allow for the overgrowth of fungal species such as *C. albicans*, resulting in opportunistic thrush infections, a point mirrored in literature such as work by Hofer, in 2022., outlining this important consideration in the treatment of infections (Hofer, 2022)

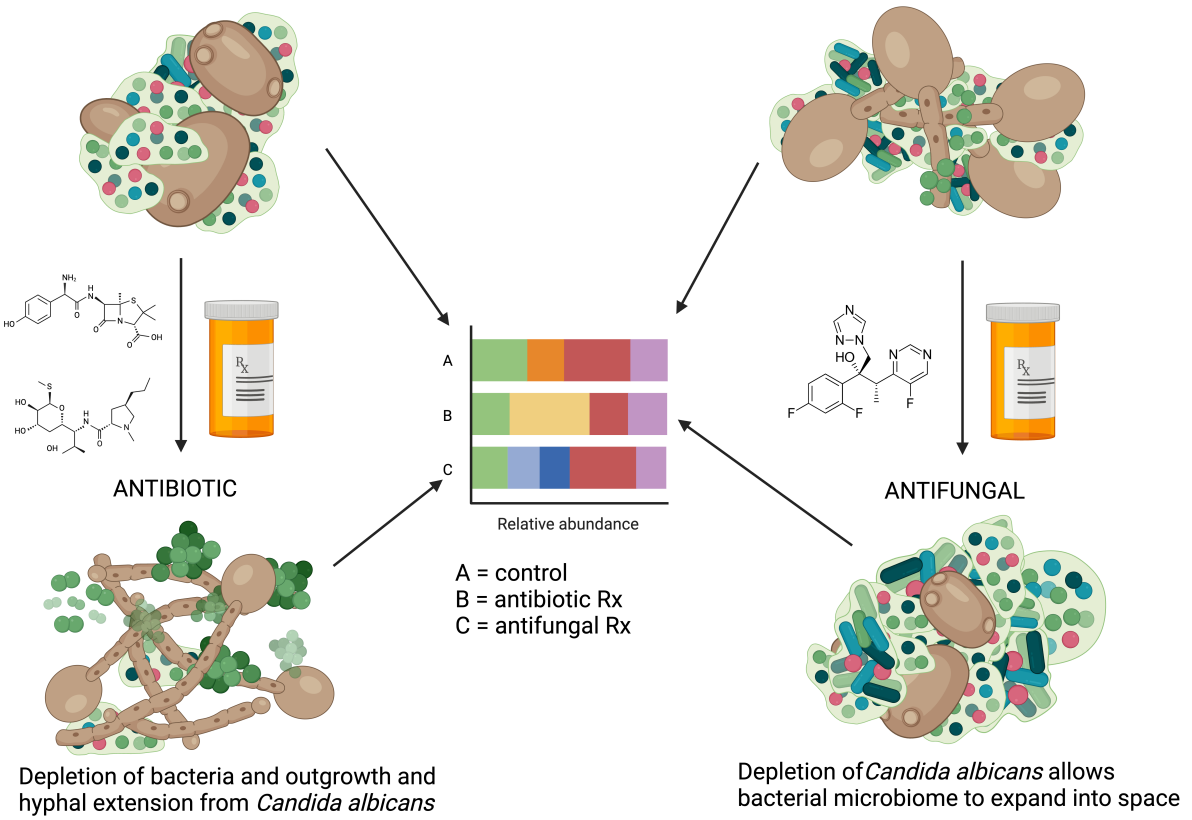


**Figure 4-16 – Collateral damage in antimicrobial use.** Visual representation of the potential unseen consequences brought about by antimicrobial usage in complex communities. Created with Biorender®.

### *4.5.8 Summary*

Through the data collected in this chapter, we were able to examine the effect of different phenotypes of *C. albicans* on an *ex-vivo* biofilm model to infer relationships in organisms associated with the oral microbiome in a format relevant to oral caries and relevant to antimicrobial challenge. We observed shifts in taxonomic features predominantly related to the presence of *C. albicans*, as well as significant effects on microbial diversity metrics based on the presence of *Candida*. Moreover, we were able to assess nuanced responses to antimicrobial challenge with Amphotericin B and Fluconazole which may imply the consequences of developing tolerance in polymicrobial communities across a timeframe of 5-days.

### *4.5.9 Key Findings*

In the interest of clarity and readability, the following points summarise key findings and outputs from this results chapter.

- DNA extraction methodology was critical in representing species present in a mock community of organisms for validation of 16S rRNA sequencing methods.
- *C. albicans* was associated with regrowth of more diverse taxonomic profiles of bacteria following a simulated oral health regimen.
- Presence of *Candida* was significantly associated with microbial diversity when compared with saliva in an *ex-vivo* biofilm model.
- Antifungal challenge with fluconazole and amphotericin displayed statistically significant diversity changes and altered organism profiles after 72-hours and 120-hours, implicating altered tolerance to antimicrobial compounds in complex systems.

# 5 General Discussion

## List of Publications

The following section contains work written by the author adapted from the following pre-published review:

Brown, J. L., W. Johnston, **M. C. Butcher**, M. Burleigh, and G. Ramage. 'The Butterfly Effect: Collateral Damage and Impacts of Antimicrobial Strategies on the Oral Microbiome.', *NPJ*, Pre-publication.

## 5.1 Overview

This thesis has shown that *C. albicans* influences the oral microbiome in a strain dependent manner. This has positive repercussions for the retention of organisms that are key to oral health in both the context of maintaining oral hygiene and in response to antifungal interventions. This has been evidenced through key methodological outputs such as microbial biomass, viability, microscopy, quantitative PCR, and 16S rRNA sequencing across each of the preceding chapters.

## 5.2 Considerations for "Big-Data" approaches

This thesis aimed, initially, to understand the literature of the oral microbiome related to caries in a meta-analytical approach and to identify if the microbiome could be leveraged as a predictive tool for defining caries (Chapter 2). Despite mixed results, the study made clear the necessity for more robust methodological approaches to the collection and management of microbiome data in the field. Moreover, this research, mirroring sentiments highlighted by Fabreau et al, in 2018, highlighted the necessity for robust study meta-data, such as external health, geographical or socio-economic factors, to paint a broader picture of how the progression or pre-disposition to certain disease states, such as oral caries can be better defined (Fabreau et al., 2018). The study revealed a lack of research related to how fungi impact the oral niche in this context. To begin with, the intent of this "Big-Data" approach to analysis was envisioned to include fungi as part of the search criteria, focusing on ITS sequencing. The lack of literature pertaining to fungal sequencing in the context of oral caries, however, as well as the same issues in terms of data accessibility, quickly identified a core issue with the landscape of microbial sequencing research at that time.

## 5.3 The critical nature of fungal research

Indeed, the lack of fungal research, not just in the space of microbiome sequencing, is a concern which has been highlighted on more than one occasion (Kong and Segre, 2020, Rodrigues and Nosanchuk, 2020). Recently, the call to attention of critical fungal pathogens by the WHO, in 2022, has bolstered this sentiment that fungi are of crucial importance in the landscape of disease (Fisher and Denning, 2023). This comes at a time when increasing global temperatures and global human displacement are contributing to the emergence of organisms out-with their typical geographical niche (Seidel et al., 2024, Ching and Zaman, 2023). Indeed, organisms such as *C. auris* are being increasingly identified in hospitals across Europe (Kohlenberg et al., 2022). This has given rise to awareness in the form of recommendations and protocols for *C. auris* screening, such as those produced by Leonhard et al., in 2024 (Leonhard et al., 2024). This comes only 3 years after recommendations in the UK advised against wide-scale screening for *C. auris* (Sharp et al., 2021). While healthcare issues such as these are nuanced, these studies highlight a rapidly changing shift in both the risk of fungal pathogens and the global attitude towards them.

## 5.4 *Candida* as a core component in caries

The caries meta-analysis revealed the lack of literature on, and the potentially critical importance of fungal research in the microbiome. The intent of the follow up chapter (Chapter 3) was to consider how *Candida albicans* may affect outcomes related to caries. As outlined previously, *C. albicans* has been considered as a biomarker in caries (Xiao et al., 2018, Menon et al., 2022). Often, this role has been associated as harmful, particularly in the context of early childhood caries. However, *Candida* has also previously been identified as a biological buffer of pH through phenotype

switching of yeast to hyphal morphology (Rane et al., 2019, Alshanta et al., 2022). Throughout the methodological approach in this chapter, this altered environment, and its effect on constituent organisms within a fixed model, was made clear. This highlights the same sentiments pronounced by Pitts et al., in 2021, where they make clear the notion of caries being a transmissible, bacterial disease caused by specific organisms should largely be reconsidered (Pitts et al., 2021). Indeed, as further suggested by Pitts et al, factors relating to pH management are of great importance in the context of exacerbating oral caries. While research outputs in fixed models and *in-vitro* systems agreed with the notion that *Candida* can be a protective influence by increasing micro-environmental pH in the context of caries, the influence of these microbial communities become somewhat less distinct.

## 5.5 Limitations of *ex-vivo* models

While the majority of biofilm research is carried out through *in-vitro* methodologies, the advancement of technology and access to techniques such as microbial sequencing has proven enticing in the development of new, more complex systems with which to bridge the gap between *in-vitro* and *in-vivo* research (Han and Lee, 2023). Work, such as that conducted by Li et al, in 2021, exemplified the positive influence of using a saliva-derived model for the development of an *ex-vivo* biofilm model (Li et al., 2021). However, as Li and colleagues also observed, these biofilms, much like their fixed model counterparts are heavily influenced by factors related to growth media and substrate. Indeed, despite our study using the same saliva pool for both the enamel study (3.3.8) and the antifungal study (4.3.4), and despite allowances for the same growth media, a stark difference could be observed between the representative organisms in either experiment, highlighting these key contrasts where sample

substrate is taken into account. Additionally, the study conducted by Li and colleagues used saliva from a single donor which may have impacted the uniformity of their overall results. This highlighted two potential areas of interest when contemplating study design, which include the complexity of the substrate examined and the inverse need for complexity in examining microbial samples for *in-vitro* research. Many studies, such as those highlighted by Darrene and Cecile, in 2016, focus specifically on the substrate and the development of less complex communities (Darrene and Cecile, 2016). While the pursuit of complex microbial research through OMICs driven research is of obvious value, there are still many facets to oral research using fixed methods to be examined.

## 5.6 Future work

This thesis has highlighted some potential avenues for the continuation of the work examined. Indeed, one of the core components of the meta-analysis of the literature was to examine novel candidate organisms in the microbiome for the development or adaptation of existing biofilm models. For example, some organisms such as *Selenomonas* and *Bifidobacterium* were highlighted as key in both caries and oral health and the study of these organisms in both mono- and multi-species formats could further assist in the profiling of bacterial dysbiosis in caries.

Additionally, while the impact of antifungals was examined in a sequencing format, more work could be undertaken to examine potential effects on constituent organisms of the microbiome. For instance, given the complex nature of the saliva pool, it was unclear if the influence of antifungals was direct on the bacteria or if it was the product of influencing other unidentified fungi within the system. This would, therefore, propose two avenues of investigation into the composition of fungi within these samples

through ITS sequencing or through the influence on gene expression in bacterial populations when exposed to Fluconazole or Amphotericin B.

## 5.7 Concluding remarks

The primary outcomes of this thesis have been summarised visually in Figure 5-1. The primary aim of this thesis was to explore the role of *C. albicans* in dental caries through a combination of literature meta-analysis and *in-vitro* modelling of complex communities.

In undertaking a systematic metanalysis of caries microbiome studies to assess their predictive value of the bacterial microbiome we identified a lack of reliable indication of caries development from bacterial microbiome data alone while highlighting a lack of methodological consistency and a lack of consideration of fungi within complex samples.

In developing defined and undefined models of cariogenic plaque, we identified the influence of *C. albicans* on key cariogenic outcomes such as pH and microbial composition in fixed models. We found that these outputs were influenced in a strain-dependent manner.

In examining a complex microbial culture derived from saliva we also observed the influence of candida, as well as the influence of substrate, dietary sucrose, and antifungal challenge, on the distribution of the core bacterial population. While the effects of *Candida* were observed, they were ultimately undistinguishable in the context of substrate influence and environmental factors.

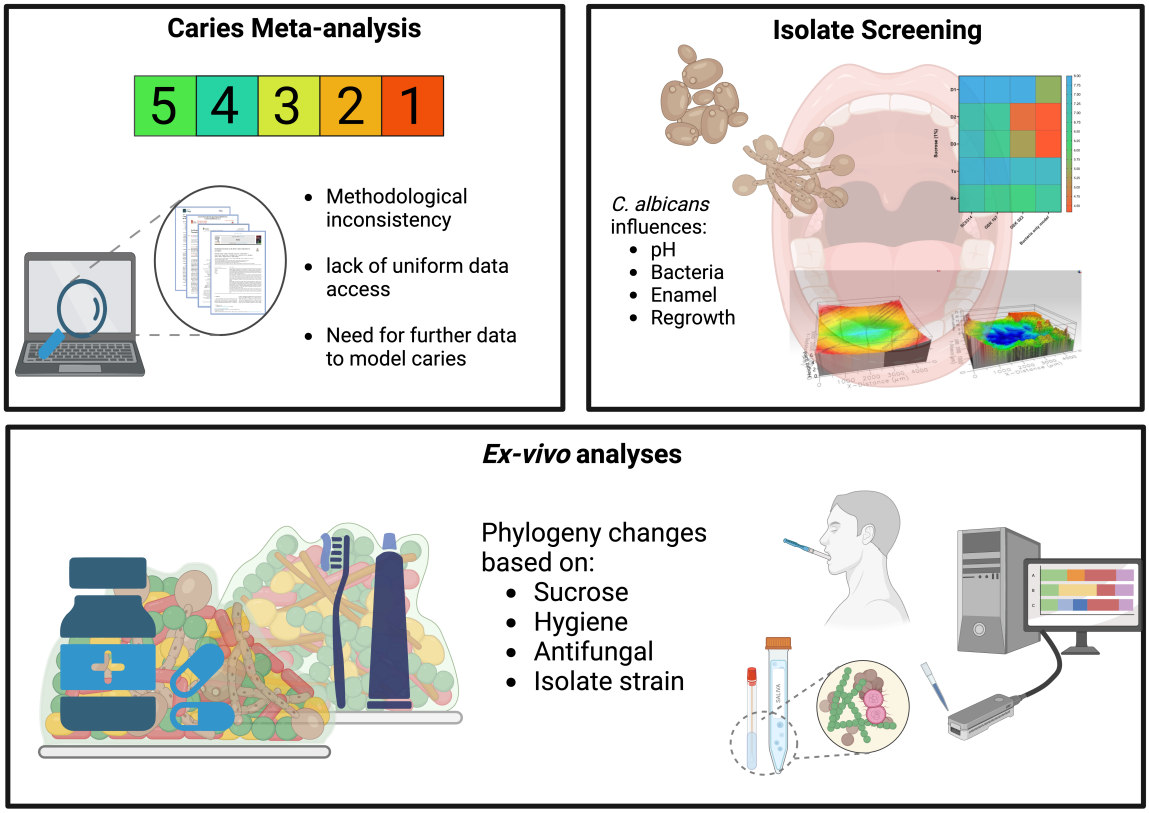


**Figure 5-1 – Graphical overview of Thesis outcomes.** A visual representation of key outcomes from study meta-analysis, Isolate screening and model development chapters. Created with Biorender®

# References


AAS, J. A., PASTER, B. J., STOKES, L. N., OLSEN, I. & DEWHIRST, F. E. 2005. Defining the normal bacterial flora of the oral cavity. *J Clin Microbiol,* 43**,** 5721-32.

ABOU NEEL, E. A., ALJABO, A., STRANGE, A., IBRAHIM, S., COATHUP, M., YOUNG, A. M., BOZEC, L. & MUDERA, V. 2016. Demineralization-remineralization dynamics in teeth and bone. *International journal of nanomedicine,* 11**,** 4743-4763.

ABUSREWIL, S., BROWN, J. L., DELANEY, C. D., BUTCHER, M. C., KEAN, R., GAMAL, D., SCOTT, J. A., MCLEAN, W. & RAMAGE, G. 2020. Filling the Void: An Optimized Polymicrobial Interkingdom Biofilm Model for Assessing Novel Antimicrobial Agents in Endodontic Infection. *Microorganisms,* 8.

ADAM, B., BAILLIE, G. S. & DOUGLAS, L. J. 2002. Mixed species biofilms of *Candida albicans* and *Staphylococcus epidermidis*. *J Med Microbiol,* 51**,** 344-9.

AKPAN, A. & MORGAN, R. 2002. Oral candidiasis. *Postgraduate Medical Journal,* 78**,** 455-459.

ALFA, M. J. 2019. Biofilms on instruments and environmental surfaces: Do they interfere with instrument reprocessing and surface disinfection? Review of the literature. *Am J Infect Control,* 47S**,** A39-A45.

ALLABAND, C., MCDONALD, D., VÁZQUEZ-BAEZA, Y., MINICH, J. J., TRIPATHI, A., BRENNER, D. A., LOOMBA, R., SMARR, L., SANDBORN, W. J., SCHNABL, B., DORRESTEIN, P., ZARRINPAR, A. & KNIGHT, R. 2019. Microbiome 101: Studying, Analyzing, and Interpreting Gut Microbiome Data for Clinicians. *Clinical gastroenterology and hepatology : the official clinical practice journal of the American Gastroenterological Association,* 17**,** 218-230.

ALSHANTA, O. A., ALBASHAIREH, K., MCKLOUD, E., DELANEY, C., KEAN, R., MCLEAN, W. & RAMAGE, G. 2022. *Candida albicans* and *Enterococcus faecalis* biofilm frenemies: When the relationship sours. *Biofilm,* 4**,** 100072.

ANDES, D., NETT, J., OSCHEL, P., ALBRECHT, R., MARCHILLO, K. & PITULA, A. 2004. Development and characterization of an *in-vivo* central venous catheter *Candida albicans* biofilm model. *Infect Immun,* 72**,** 6023-31.

APATZIDOU, D., LAPPIN, D. F., HAMILTON, G., PAPADOPOULOS, C. A., KONSTANTINIDIS, A. & RIGGIO, M. P. 2017. Microbiome of peri-implantitis affected and healthy dental sites in patients with a history of chronic periodontitis. *Arch Oral Biol,* 83**,** 145-152.

ARAÚJO, D., MIL-HOMENS, D., HENRIQUES, M. & SILVA, S. 2022. Anti-EFG1 2′-OMethylRNA oligomer inhibits *Candida albicans* filamentation and attenuates the candidiasis in *Galleria mellonella*. *Molecular Therapy - Nucleic Acids,* 27**,** 517-523.

AYOUB, H. M., GREGORY, R. L., TANG, Q. & LIPPERT, F. 2020. Influence of salivary conditioning and sucrose concentration on biofilm-mediated enamel demineralization. *J Appl Oral Sci,* 28**,** e20190501.

AZEVEDO, N. F., ALLKJA, J. & GOERES, D. M. 2021. Biofilms vs. cities and humans vs. aliens – a tale of reproducibility in biofilms. *Trends in Microbiology,* 29**,** 1062-1071.

BAENA-MONROY, T., MORENO-MALDONADO, V., FRANCO-MARTÍNEZ, F., ALDAPE-BARRIOS, B., QUINDÓS, G. & SÁNCHEZ-VARGAS, L. O. 2005. *Candida albicans*, *Staphylococcus aureus* and *Streptococcus mutans* colonization in patients wearing dental prosthesis. *Med Oral Patol Oral Cir Bucal,* 10 Suppl 1**,** E27-39.

BAHRAM, M. & NETHERWAY, T. 2021. Fungi as mediators linking organisms and ecosystems. *FEMS Microbiology Reviews,* 46.

BAKER, J. L., MORTON, J. T., DINIS, M., ALVAREZ, R., TRAN, N. C., KNIGHT, R. & EDLUND, A. 2021. Deep metagenomics examines the oral microbiome during dental caries, revealing novel taxa and co-occurrences with host molecules. *Genome Res,* 31**,** 64-74.

BAMFORD, C. V., D'MELLO, A., NOBBS, A. H., DUTTON, L. C., VICKERMAN, M. M. & JENKINSON, H. F. 2009. *Streptococcus gordonii* modulates *Candida albicans* biofilm formation through intergeneric communication. *Infection and immunity,* 77**,** 3696-3704.

BANDARA, H. M. H. N., PANDUWAWALA, C. P. & SAMARANAYAKE, L. P. 2019. Biodiversity of the human oral mycobiome in health and disease. *Oral Diseases,* 25**,** 363-371.

BANOS, S., LENTENDU, G., KOPF, A., WUBET, T., GLÖCKNER, F. O. & REICH, M. 2018. A comprehensive fungi-specific 18S rRNA gene sequence primer toolkit suited for diverse research issues and sequencing platforms. *BMC Microbiology,* 18**,** 190.

BARANIYA, D., CHEN, T., NAHAR, A., ALAKWAA, F., HILL, J., TELLEZ, M., ISMAIL, A., PURI, S. & AL-HEBSHI, N. N. 2020. Supragingival mycobiome and inter-kingdom interactions in dental caries. *J Oral Microbiol,* 12**,** 1729305.

BENITEZ-PAEZ, A., BELDA-FERRE, P., SIMON-SORO, A. & MIRA, A. 2014. Microbiota diversity and gene expression dynamics in human oral biofilms. *BMC Genomics,* 15**,** 311.

BHARDWAJ, R. G., ELLEPOLLA, A., DROBIOVA, H. & KARCHED, M. 2020. Biofilm growth and IL-8 & TNF-α-inducing properties of *Candida albicans* in the presence of oral gram-positive and gram-negative bacteria. *BMC Microbiol,* 20**,** 156.

BHARTI, R. & GRIMM, D. G. 2019. Current challenges and best-practice protocols for microbiome analysis. *Briefings in Bioinformatics,* 22**,** 178-193.

BILLINGTON, C., KINGSBURY, J. M. & RIVAS, L. 2022. Metagenomics Approaches for Improving Food Safety: A Review. *Journal of Food Protection,* 85**,** 448-464.

BISANZ, J. E., UPADHYAY, V., TURNBAUGH, J. A., LY, K. & TURNBAUGH, P. J. 2019. Meta-Analysis Reveals Reproducible Gut Microbiome Alterations in Response to a High-Fat Diet. *Cell Host Microbe,* 26**,** 265-272 e4.

BOLYEN, E., RIDEOUT, J. R., DILLON, M. R., BOKULICH, N. A., ABNET, C. C., AL-GHALITH, G. A., ALEXANDER, H., ALM, E. J., ARUMUGAM, M. & ASNICAR, F. 2019. Reproducible, interactive, scalable and extensible microbiome data science using QIIME 2. *Nature biotechnology,* 37**,** 852-857.

BONGOMIN, F., GAGO, S., OLADELE, R. O. & DENNING, D. W. 2017. Global and Multi-National Prevalence of Fungal Diseases-Estimate Precision. *J Fungi (Basel),* 3.

BORMAN, A. M., MULLER, J., WALSH-QUANTICK, J., SZEKELY, A., PATTERSON, Z., PALMER, M. D., FRASER, M. & JOHNSON, E. M. 2020. MIC distributions for amphotericin B, fluconazole, itraconazole, voriconazole, flucytosine and anidulafungin and 35 uncommon pathogenic yeast species from the UK determined using the CLSI broth microdilution method. *J Antimicrob Chemother,* 75**,** 1194-1205.

BRADSHAW, D. J., MARSH, P. D., SCHILLING, K. M. & CUMMINS, D. 1996. A modified chemostat system to study the ecology of oral biofilms. *J Appl Bacteriol,* 80**,** 124-30.

BRADSHAW, D. J., MARSH, P. D., WATSON, G. K. & ALLISON, C. 1998. Role of *Fusobacterium nucleatum* and coaggregation in anaerobe survival in planktonic and biofilm oral microbial communities during aeration. *Infect Immun,* 66**,** 4729-32.

BRADSHAW, D. J., MARSH, P. D, WATSON, G. K, ALLISON, C. 1997. Oral anaerobes cannot survive oxygen stress without interacting with faculTative/aerobic species as a microbial commmunity. *Lett Appl Microbiol,* 25**,** 385–387.

BRADSHAW, D. J., MCKEE, A. S. & MARSH, P. D. 1989. Effects of carbohydrate pulses and pH on population shifts within oral microbial communities *in-vitro*. *J Dent Res,* 68**,** 1298-302.

BREIMAN, L. 2001. Random Forests. *Machine Learning,* 45**,** 5-32.

BROWN, H. M., FARNSWORTH, C. W., BRYAN, A., GENZEN, J. R., GRONOWSKI, A., PHILIPS DEETER, J. & YARBROUGH, M. 2022a. One Bad Apple Can Spoil the Bunch: The Impact of Contamination in the Clinical Laboratory. *Clinical Chemistry,* 69**,** 9-16.

BROWN, J. L., BUTCHER, M. C., VEENA, C. L. R., CHOGULE, S., JOHNSTON, W. & RAMAGE, G. 2023. Generation of Multispecies Oral Bacteria Biofilm Models. *Methods Mol Biol,* 2588**,** 187-199.

BROWN, J. L., JOHNSTON, W., DELANEY, C., SHORT, B., BUTCHER, M. C., YOUNG, T., BUTCHER, J., RIGGIO, M., CULSHAW, S. & RAMAGE, G. 2019. Polymicrobial oral biofilm models: simplifying the complex. *J Med Microbiol,* 68**,** 1573-1584.

BROWN, J. L., YOUNG, T., MCKLOUD, E., BUTCHER, M. C., BRADSHAW, D., PRATTEN, J. R. & RAMAGE, G. 2022b. An *In-vitro* Evaluation of Denture Cleansing Regimens against a Polymicrobial Denture Biofilm Model. *Antibiotics (Basel),* 11.

BUDTZ JORGENSEN, E. 1974. The significance of *Candida albicans* in denture stomatitis. *Scandinavian Journal of Dental Research,* 82**,** 151-190.

BUDTZ-JØRGENSEN, E. 1981. Oral mucosal lesions associated with the wearing of removable dentures. *Journal of Oral Pathology & Medicine,* 10**,** 65-80.

BURCHAM, Z. M., GARNEAU, N. L., COMSTOCK, S. S., TUCKER, R. M., KNIGHT, R., METCALF, J. L., MIRANDA, A., REINHART, B., MEYERS, D., WOLTKAMP, D., BOXER, E., HUTCHENS, J., KIM, K., ARCHER, M., MCATEER, M., HUSS, P., DEFONSEKA, R., STAHLE, S., BABU, S., NUESSLE, T., SCHOWINSKY, V., COVERT, W., TRUMAN, W., REUSSER, W. & GENETICS OF TASTE LAB CITIZEN, S. 2020. Patterns of Oral Microbiota Diversity in Adults and Children: A Crowdsourced Population Study. *Scientific Reports,* 10**,** 2133.

BUTCHER, M. C., SHORT, B., VEENA, C. L. R., BRADSHAW, D., PRATTEN, J. R., MCLEAN, W., SHABAN, S. M. A., RAMAGE, G. & DELANEY, C. 2022. Meta-analysis of caries microbiome studies can improve upon disease prediction outcomes. *Apmis,* 130**,** 763-777.

CÁMARA, M., GREEN, W., MACPHEE, C. E., RAKOWSKA, P. D., RAVAL, R., RICHARDSON, M. C., SLATER-JEFFERIES, J., STEVENTON, K. & WEBB, J. S. 2022. Economic significance of biofilms: a multidisciplinary and cross-sectoral challenge. *NPJ Biofilms Microbiomes,* 8**,** 42.

CAMPOS, M. S., MARCHINI, L., BERNARDES, L. A. S., PAULINO, L. C. & NOBREGA, F. G. 2008. Biofilm microbial communities of denture stomatitis. *Oral Microbiology and Immunology,* 23**,** 419-424.

CANABARRO, A., VALLE, C., FARIAS, M., SANTOS, F., LAZERA, M. & WANKE, B. 2013. Association of subgingival colonization of *Candida albicans* and other yeasts with severity of chronic periodontitis. *Journal of periodontal research,* 48**,** 428-432.

CANGUI-PANCHI, S. P., ÑACATO-TOAPANTA, A. L., ENRÍQUEZ-MARTÍNEZ, L. J., SALINAS-DELGADO, G. A., REYES, J., GARZON-CHAVEZ, D. & MACHADO, A. 2023. Battle royale: Immune response on biofilms – host-pathogen interactions. *Current Research in Immunology,* 4**,** 100057.

CARLSSON, J., SÖDERHOLM, G. & ALMFELDT, I. 1969. Prevalence of *Streptococcus sanguis* and *Streptococcus mutans* in the mouth of persons wearing full-dentures. *Archives of Oral Biology,* 14**,** 243-249.

CAROLINE DE ABREU BRANDI, T., PORTELA, M. B., LIMA, P. M., CASTRO, G. F. B. D. A., MAIA, L. C. & FONSECA-GONÇALVES, A. 2016. Demineralizing potential of dental biofilm added with *Candida albicans* and *Candida parapsilosis* isolated from preschool children with and without caries. *Microbial Pathogenesis,* 100**,** 51-55.

CASAMASSIMO, P. S., THIKKURISSY, S., EDELSTEIN, B. L. & MAIORINI, E. 2009. Beyond the dmft: the human and economic cost of early childhood caries. *The Journal of the American Dental Association,* 140**,** 650-657.

CAVALHEIRO, M. & TEIXEIRA, M. C. 2018. Candida Biofilms: Threats, Challenges, and Promising Strategies. *Front Med (Lausanne),* 5**,** 28.

CHANDRA, J., KUHN, D. M., MUKHERJEE, P. K., HOYER, L. L., MCCORMICK, T. & GHANNOUM, M. A. 2001a. Biofilm formation by the fungal pathogen *Candida albicans*: development, architecture, and drug resistance. *J Bacteriol,* 183**,** 5385-94.

CHANDRA, J., MUKHERJEE, P. K., LEIDICH, S. D., FADDOUL, F. F., HOYER, L. L., DOUGLAS, L. J. & GHANNOUM, M. A. 2001b. Antifungal resistance of candidal biofilms formed on denture acrylic *in-vitro*. *J Dent Res,* 80**,** 903-8.

CHAWHUAVEANG, D. D., YU, O. Y., YIN, I. X., LAM, W. Y., MEI, M. L. & CHU, C. H. 2021. Acquired salivary pellicle and oral diseases: A literature review. *J Dent Sci,* 16**,** 523-529.

CHEN, C., HEMME, C., BELENO, J., SHI, Z. J., NING, D., QIN, Y., TU, Q., JORGENSEN, M., HE, Z., WU, L. & ZHOU, J. 2018. Oral microbiota of periodontal health and disease and their changes after nonsurgical periodontal therapy. *ISME J,* 12**,** 1210-1224.

CHEN, L., MA, L., PARK, N. H. & SHI, W. 2001. Cariogenic actinomyces identified with a beta-glucosidase-dependent green color reaction to *Gardenia jasminoides* extract. *Journal of clinical microbiology,* 39**,** 3009-3012.

CHEN, L., QIN, B., DU, M., ZHONG, H., XU, Q., LI, Y., ZHANG, P. & FAN, M. 2015. Extensive description and comparison of human supra-gingival microbiome in root caries and health. *PLoS One,* 10**,** e0117064.

CHEN, T., MARSH, P. D. & AL-HEBSHI, N. N. 2022. SMDI: An Index for Measuring Subgingival Microbial Dysbiosis. *J Dent Res,* 101**,** 331-338.

CHEN, X., DALIRI, E. B.-M., KIM, N., KIM, J.-R., YOO, D. & OH, D.-H. 2020. Microbial Etiology and Prevention of Dental Caries: Exploiting Natural Products to Inhibit Cariogenic Biofilms. *Pathogens (Basel, Switzerland),* 9**,** 569.

CHEN, Z., HUI, P. C., HUI, M., YEOH, Y. K., WONG, P. Y., CHAN, M. C. W., WONG, M. C. S., NG, S. C., CHAN, F. K. L. & CHAN, P. K. S. 2019. Impact of Preservation Method and 16S rRNA Hypervariable Region on Gut Microbiota Profiling. *mSystems,* 4.

CHERKASOV, S. V., POPOVA, L. Y., VIVTANENKO, T. V., DEMINA, R. R., KHLOPKO, Y. A., BALKIN, A. S. & PLOTNIKOV, A. O. 2019. Oral microbiomes in children with asthma and dental caries. *Oral Diseases,* 25**,** 898-910.

CHING, C. & ZAMAN, M. H. 2023. Infectious disease burden among forcibly displaced populations: considerations for effective research. *Pathog Glob Health,* 117**,** 435-436.

CLOONEY, A. G., FOUHY, F., SLEATOR, R. D., A, O. D., STANTON, C., COTTER, P. D. & CLAESSON, M. J. 2016. Comparing Apples and Oranges?: Next Generation Sequencing and Its Impact on Microbiome Analysis. *PLoS One,* 11**,** e0148028.

COCO, B. J., BAGG, J., CROSS, L. J., JOSE, A., CROSS, J. & RAMAGE, G. 2008. Mixed *Candida albicans* and *Candida glabrata* populations associated with the pathogenesis of denture stomatitis. *Oral Microbiol Immunol,* 23**,** 377-83.

COENYE, T., GOERES, D., VAN BAMBEKE, F. & BJARNSHOLT, T. 2018. Should standardized susceptibility testing for microbial biofilms be introduced in clinical practice? *Clin Microbiol Infect.,* 24**,** 570-572.

CONRADS, G., WENDT, L. K., HETRODT, F., DENG, Z. L., PIEPER, D., ABDELBARY, M. M. H., BARG, A., WAGNER-DÖBLER, I. & APEL, C. 2019. Deep sequencing of biofilm microbiomes on dental composite materials. *J Oral Microbiol,* 11**,** 1617013.

CORREIA, I., PRIETO, D., ROMÁN, E., WILSON, D., HUBE, B., ALONSO-MONGE, R. & PLA, J. 2019. Cooperative Role of MAPK Pathways in the Interaction of *Candida albicans* with the Host Epithelium. *Microorganisms,* 8.

COSTERTON, J. W., IRVIN, R. T. & CHENG, K. J. 1981. The role of bacterial surface structures in pathogenesis. *Crit Rev Microbiol,* 8**,** 303-38.

COSTERTON, J. W., LEWANDOWSKI, Z., CALDWELL, D. E., KORBER, D. R. & LAPPIN-SCOTT, H. M. 1995. Microbial biofilms. *Annu Rev Microbiol,* 49**,** 711-45.

COULTHWAITE, L. & VERRAN, J. 2007. Potential pathogenic aspects of denture plaque. *British Journal of Biomedical Science,* 64**,** 180-189.

COULTHWAITE, L. & VERRAN, J. 2008. Development of an *in-vitro* denture plaque biofilm to model denture malodour. *J Breath Res,* 2**,** 017004.

DARRENE, L. N. & CECILE, B. 2016. Experimental Models of Oral Biofilms Developed on Inert Substrates: A Review of the Literature. *Biomed Res Int,* 2016**,** 7461047.

DARWAZEH, A. M. & DARWAZEH, T. A. 2014. What makes oral candidiasis recurrent infection? A clinical view. *Journal of Mycology,* 2014.

DE JESUS, V. C., KHAN, M. W., MITTERMULLER, B. A., DUAN, K., HU, P., SCHROTH, R. J. & CHELIKANI, P. 2021. Characterization of Supragingival

Plaque and Oral Swab Microbiomes in Children With Severe Early Childhood Caries. *Front Microbiol,* 12**,** 683685.

DE JESUS, V. C., SHIKDER, R., ORYNIAK, D., MANN, K., ALAMRI, A., MITTERMULLER, B., DUAN, K., HU, P., SCHROTH, R. J. & CHELIKANI, P. 2020. Sex-Based Diverse Plaque Microbiota in Children with Severe Caries. *J Dent Res,* 99**,** 703-712.

DEFTA, C. L., ALBU, C. C., ALBU, S. D. & BOGDAN-ANDREESCU, C. F. 2024. Oral Mycobiota: A Narrative Review. *Dent J (Basel),* 12.

DELANEY, C., KEAN, R., SHORT, B., TUMELTY, M., MCLEAN, W. & RAMAGE, G. 2018. Fungi at the scene of the crime: innocent bystanders or accomplices in oral infections? *Current Clinical Microbiology Reports,* 5**,** 190-200.

DELANEY, C., O'DONNELL, L. E., KEAN, R., SHERRY, L., BROWN, J. L., CALVERT, G., NILE, C. J., CROSS, L., BRADSHAW, D. J., BRANDT, B. W., ROBERTSON, D. & RAMAGE, G. 2019. Interkingdom interactions on the denture surface: Implications for oral hygiene. *Biofilm,* 1**,** 100002.

DELHOM, R., NELSON, A., LAUX, V., HAERTLEIN, M., KNECHT, W., FRAGNETO, G. & WACKLIN-KNECHT, H. P. 2020. The Antifungal Mechanism of Amphotericin B Elucidated in Ergosterol and Cholesterol-Containing Membranes Using Neutron Reflectometry. *Nanomaterials (Basel),* 10.

DENHAM, S. T., WAMBAUGH, M. A. & BROWN, J. C. S. 2019. How Environmental Fungi Cause a Range of Clinical Outcomes in Susceptible Hosts. *J Mol Biol,* 431**,** 2982-3009.

DEO, P. N. & DESHMUKH, R. 2019. Oral microbiome: Unveiling the fundamentals. *Journal of oral and maxillofacial pathology : JOMFP,* 23**,** 122-128.

DESAI, A. R., SHAH, N. P. & POWELL, I. B. 2006. Discrimination of dairy industry isolates of the Lactobacillus casei group. *J Dairy Sci,* 89**,** 3345-51.

DESAI, J. V. & MITCHELL, A. P. 2015. *Candida albicans* Biofilm Development and Its Genetic Control. *Microbiol Spectr,* 3.

DEWHIRST, F. E., CHEN, T., IZARD, J., PASTER, B. J., TANNER, A. C., YU, W. H., LAKSHMANAN, A. & WADE, W. G. 2010. The human oral microbiome. *J Bacteriol,* 192**,** 5002-17.

DHARIWAL, A., CHONG, J., HABIB, S., KING, I. L., AGELLON, L. B. & XIA, J. 2017. MicrobiomeAnalyst: a web-based tool for comprehensive statistical, visual and meta-analysis of microbiome data. *Nucleic Acids Res,* 45**,** W180-w188.

DIAZ, P. I., STRAUSBAUGH, L. D. & DONGARI-BAGTZOGLOU, A. 2014. Fungal-bacterial interactions and their relevance to oral health: linking the clinic and the bench. *Front Cell Infect Microbiol,* 4**,** 101.

DODSON, T. A., CARLSON, E. A., WAMER, N. C., MORSE, C. N., GADIENT, J. N. & PRESTWICH, E. G. 2022. Characterization of Distinct Biofilm Cell

Subpopulations and Implications in Quorum Sensing and Antibiotic Resistance. *mBio,* 13**,** e0019122.

DOMINGUEZ, E., ZARNOWSKI, R., SANCHEZ, H., COVELLI, A. S., WESTLER, W. M., AZADI, P., NETT, J., MITCHELL, A. P. & ANDES, D. R. 2018. Conservation and Divergence in the Candida Species Biofilm Matrix Mannan-Glucan Complex Structure, Function, and Genetic Control. *mBio,* 9.

DONATI, C., ZOLFO, M., ALBANESE, D., TIN TRUONG, D., ASNICAR, F., IEBBA, V., CAVALIERI, D., JOUSSON, O., DE FILIPPO, C., HUTTENHOWER, C. & SEGATA, N. 2016. Uncovering oral Neisseria tropism and persistence using metagenomic sequencing. *Nature Microbiology,* 1**,** 16070.

DONLAN, R. M. 2002. Biofilms: microbial life on surfaces. *Emerg Infect Dis,* 8**,** 881-90.

DOUGLAS, L. J. 2003. Candida biofilms and their role in infection. *Trends Microbiol,* 11**,** 30-6.

DU, Q., REN, B., HE, J., PENG, X., GUO, Q., ZHENG, L., LI, J., DAI, H., CHEN, V., ZHANG, L., ZHOU, X. & XU, X. 2021a. *Candida albicans* promotes tooth decay by inducing oral microbial dysbiosis. *Isme j,* 15**,** 894-908.

DU, Q., REN, B., HE, J., PENG, X., GUO, Q., ZHENG, L., LI, J., DAI, H., CHEN, V., ZHANG, L., ZHOU, X. & XU, X. 2021b. *Candida albicans* promotes tooth decay by inducing oral microbial dysbiosis. *The ISME Journal,* 15**,** 894-908.

DUCKER, G. S. & RABINOWITZ, J. D. 2017. One-Carbon Metabolism in Health and Disease. *Cell metabolism,* 25**,** 27-42.

DUVALLET, C., GIBBONS, S. M., GURRY, T., IRIZARRY, R. A. & ALM, E. J. 2017. Meta-analysis of gut microbiome studies identifies disease-specific and shared responses. *Nat Commun,* 8**,** 1784.

DYRHOVDEN, R., RIPPIN, M., ØVREBØ, K. K., NYGAARD, R. M., ULVESTAD, E. & KOMMEDAL, Ø. 2021. Managing Contamination and Diverse Bacterial Loads in 16S rRNA Deep Sequencing of Clinical Samples: Implications of the Law of Small Numbers. *mBio,* 12**,** e0059821.

EDGERTON, M. & LEVINE, M. J. 1992. Characterization of acquired denture pellicle from healthy and stomatitis patients. *The Journal of prosthetic dentistry,* 68**,** 683-691.

EIDT, G., WALTERMANN, E. D. M., HILGERT, J. B. & ARTHUR, R. A. 2020. Candida and dental caries in children, adolescents and adults: A systematic review and meta-analysis. *Archives of Oral Biology,* 119**,** 104876.

ELIE, C., PERRET, M., HAGE, H., SENTAUSA, E., HESKETH, A., LOUIS, K., FRITAH-LAFONT, A., LEISSNER, P., VACHON, C., ROSTAING, H., REYNIER, F., GERVASI, G. & SALIOU, A. 2023. Comparison of DNA extraction methods for 16S rRNA gene sequencing in the analysis of the human gut microbiome. *Scientific Reports,* 13**,** 10279.

ENAUD, R., VANDENBORGHT, L. E., CORON, N., BAZIN, T., PREVEL, R., SCHAEVERBEKE, T., BERGER, P., FAYON, M., LAMIREAU, T. & DELHAES, L. 2018. The Mycobiome: A Neglected Component in the Microbiota-Gut-Brain Axis. *Microorganisms,* 6.

ENAX, J., GANSS, B., AMAECHI, B. T., SCHULZE ZUR WIESCHE, E. & MEYER, F. 2023. The composition of the dental pellicle: an updated literature review. *Front Oral Health,* 4**,** 1260442.

EPSTEIN, J. B. & POLSKY, B. 1998. Oropharyngeal candidiasis: a review of its clinical spectrum and current therapies. *Clinical therapeutics,* 20**,** 40-57.

EVANS, C. R., SMILEY, M. K., ASAHARA THIO, S., WEI, M., FLOREK, L. C., DAYTON, H., PRICE-WHELAN, A., MIN, W. & DIETRICH, L. E. P. 2023. Spatial heterogeneity in biofilm metabolism elicited by local control of phenazine methylation. *Proceedings of the National Academy of Sciences,* 120**,** e2313208120.

FABREAU, G. E., MINTY, E. P., SOUTHERN, D. A., QUAN, H. & GHALI, W. A. 2018. A Meta-Data Manifesto: The Need for Global Health Meta-Data. *Int J Popul Data Sci,* 3**,** 436.

FALSETTA, M. L., KLEIN, M. I., COLONNE, P. M., SCOTT-ANNE, K., GREGOIRE, S., PAI, C. H., GONZALEZ-BEGNE, M., WATSON, G., KRYSAN, D. J., BOWEN, W. H. & KOO, H. 2014. Symbiotic relationship between *Streptococcus mutans* and *Candida albicans* synergizes virulence of plaque biofilms *in-vivo*. *Infect Immun,* 82**,** 1968-81.

FARAH, C., LYNCH, N. & MCCULLOUGH, M. 2010. Oral fungal infections: an update for the general practitioner. *Australian dental journal,* 55**,** 48-54.

FECHNEY, J. M., BROWNE, G. V., PRABHU, N., IRINYI, L., MEYER, W., HUGHES, T., BOCKMANN, M., TOWNSEND, G., SALEHI, H. & ADLER, C. J. 2019. Preliminary study of the oral mycobiome of children with and without dental caries. *Journal of oral microbiology,* 11**,** 1536182.

FERDOUS, T., JIANG, L., DINU, I., GROIZELEAU, J., KOZYRSKYJ, A. L., GREENWOOD, C. M. T. & ARRIETA, M.-C. 2022. The rise to power of the microbiome: power and sample size calculation for microbiome studies. *Mucosal Immunology,* 15**,** 1060-1070.

FERNANDES, A., SKINNER, M. L., WOELFEL, T., CARPENTER, T. & HAGGERTY, K. P. 2013. Implementing Self-collection of Biological Specimens With a Diverse Sample. *Field methods,* 25.

FERRER, M. D., LÓPEZ-LÓPEZ, A., NICOLESCU, T., PEREZ-VILAPLANA, S., BOIX-AMORÓS, A., DZIDIC, M., GARCIA, S., ARTACHO, A., LLENA, C. & MIRA, A. 2020. Topic Application of the Probiotic *Streptococcus dentisani* Improves Clinical and Microbiological Parameters Associated With Oral Health. *Front Cell Infect Microbiol,* 10**,** 465.

FISCHER, N. G. & APARICIO, C. 2021. The salivary pellicle on dental biomaterials. *Colloids and Surfaces B: Biointerfaces,* 200**,** 111570.

FISHER, M. C. & DENNING, D. W. 2023. The WHO fungal priority pathogens list as a game-changer. *Nature Reviews Microbiology,* 21**,** 211-212.

FOUHY, F., CLOONEY, A. G., STANTON, C., CLAESSON, M. J. & COTTER, P. D. 2016. 16S rRNA gene sequencing of mock microbial populations- impact of DNA extraction method, primer choice and sequencing platform. *BMC Microbiology,* 16**,** 123.

FOX, E. P., BUI, C. K., NETT, J. E., HARTOONI, N., MUI, M. C., ANDES, D. R., NOBILE, C. J. & JOHNSON, A. D. 2015. An expanded regulatory network temporally controls *Candida albicans* biofilm formation. *Mol Microbiol,* 96**,** 1226-39.

FOXMAN, B., LUO, T., SRINIVASAN, U., RAMADUGU, K., WEN, A., GOLDBERG, D., SHEDDEN, K., CROUT, R., MCNEIL, D. W., WEYANT, R. & MARAZITA, M. L. 2016. The effects of family, dentition, and dental caries on the salivary microbiome. *Ann Epidemiol,* 26**,** 348-54.

FREIRE, M., MOUSTAFA, A., HARKINS, D. M., TORRALBA, M. G., ZHANG, Y., LEONG, P., SAFFERY, R., BOCKMANN, M., KUELBS, C., HUGHES, T., CRAIG, J. M. & NELSON, K. E. 2020. Longitudinal Study of Oral Microbiome Variation in Twins. *Scientific Reports,* 10**,** 7954.

FRIAS-LOPEZ, J. & DURAN-PINEDO, A. 2012. Effect of periodontal pathogens on the metatranscriptome of a healthy multispecies biofilm model. *J Bacteriol,* 194**,** 2082-95.

FUJINAMI, W., NISHIKAWA, K., OZAWA, S., HASEGAWA, Y. & TAKEBE, J. 2021. Correlation between the relative abundance of oral bacteria and *Candida albicans* in denture and dental plaques. *Journal of Oral Biosciences,* 63**,** 175-183.

GALLA, G., PRAEG, N., COLLA, F., RZEHAK, T., ILLMER, P., SEEBER, J. & HAUFFE, H. C. 2023. Mock community as an in situ positive control for amplicon sequencing of microbiotas from the same ecosystem. *Scientific Reports,* 13**,** 4056.

GAND, M., BLOEMEN, B., VANNESTE, K., ROOSENS, N. H. C. & DE KEERSMAECKER, S. C. J. 2023. Comparison of 6 DNA extraction methods for isolation of high yield of high molecular weight DNA suitable for shotgun metagenomics Nanopore sequencing to detect bacteria. *BMC Genomics,* 24**,** 438.

GARCIA, B. A., ACOSTA, N. C., TOMAR, S. L., ROESCH, L. F. W., LEMOS, J. A., MUGAYAR, L. R. F. & ABRANCHES, J. 2021. Association of *Candida albicans* and Cbp+ *Streptococcus mutans* with early childhood caries recurrence. *Scientific Reports,* 11**,** 10802.

GAUCH, L. M. R., PEDROSA, S. S., SILVEIRA-GOMES, F., ESTEVES, R. A. & MARQUES-DA-SILVA, S. H. 2018. Isolation of Candida spp. from denture-related stomatitis in Pará, Brazil. *Brazilian journal of microbiology : [publication of the Brazilian Society for Microbiology],* 49**,** 148-151.

GENDREAU, L. & LOEWY, Z. G. 2011. Epidemiology and Etiology of Denture Stomatitis. *Journal of Prosthodontics,* 20**,** 251-260.

GERÓS-MESQUITA, Â., CARVALHO-PEREIRA, J., FRANCO-DUARTE, R., ALVES, A., GERÓS, H., PAIS, C. & SAMPAIO, P. 2020. Oral *Candida albicans* colonization in healthy individuals: prevalence, genotypic diversity, stability along time and transmissibility. *Journal of Oral Microbiology,* 12**,** 1820292.

GHANNOUM, M. A., JUREVIC, R. J., MUKHERJEE, P. K., CUI, F., SIKAROODI, M., NAQVI, A. & GILLEVET, P. M. 2010a. Characterization of the Oral Fungal Microbiome (Mycobiome) in Healthy Individuals. *PLOS Pathogens,* 6**,** e1000713.

GHOLIZADEH, P., PORMOHAMMAD, A., ESLAMI, H., SHOKOUHI, B., FAKHRZADEH, V. & KAFIL, H. S. 2017. Oral pathogenesis of *Aggregatibacter actinomycetemcomitans. Microbial Pathogenesis,* 113**,** 303-311.

GIENTKA, I., BZDUCHA-WRÓBEL, A., STASIAK-RÓŻAŃSKA, L., BEDNARSKA, A. A. & BŁAŻEJAK, S. 2016. The exopolysaccharides biosynthesis by Candida yeast depends on carbon sources. *Electronic Journal of Biotechnology,* 22**,** 31-37.

GLEIZNYS, A., ZDANAVIČIENĖ, E. & ŽILINSKAS, J. 2015. *Candida albicans* importance to denture wearers. A literature review. *Stomatologija,* 17**,** 54-66.

GOMEZ, A. & NELSON, K. E. 2017. The Oral Microbiome of Children: Development, Disease, and Implications Beyond Oral Health. *Microb Ecol,* 73**,** 492-503.

GREENMAN, N., HASSOUNEH, S. A.-D., ABDELLI, L. S., JOHNSTON, C. & AZARIAN, T. 2024. Improving Bacterial Metagenomic Research through Long-Read Sequencing. *Microorganisms,* 12**,** 935.

GRIFFEN, A. L., BEALL, C. J., CAMPBELL, J. H., FIRESTONE, N. D., KUMAR, P. S., YANG, Z. K., PODAR, M. & LEYS, E. J. 2012. Distinct and complex bacterial profiles in human periodontitis and health revealed by 16S pyrosequencing. *ISME J,* 6**,** 1176-85.

GROSS, E. L., LEYS, E. J., GASPAROVICH, S. R., FIRESTONE, N. D., SCHWARTZBAUM, J. A., JANIES, D. A., ASNANI, K. & GRIFFEN, A. L. 2010. Bacterial 16S sequence analysis of severe caries in young permanent teeth. *Journal of clinical microbiology,* 48**,** 4121-4128.

GUERRA, F., MAZUR, M., NDOKAJ, A., CORRIDORE, D., LA TORRE, G., POLIMENI, A. & OTTOLENGHI, L. 2018. Periodontitis and the microbiome: a systematic review and meta-analysis. *Minerva Stomatol,* 67**,** 250-258.

GUGGENHEIM, B., GUGGENHEIM, M., GMÜR, R., GIERTSEN, E. & THURNHEER, T. 2004. Application of the Zürich biofilm model to problems of cariology. *Caries Res,* 38**,** 212-22.

GULATI, M. & NOBILE, C. J. 2016. *Candida albicans* biofilms: development, regulation, and molecular mechanisms. *Microbes Infect,* 18**,** 310-21.

GUPTA, S., MORTENSEN, M. S., SCHJØRRING, S., TRIVEDI, U., VESTERGAARD, G., STOKHOLM, J., BISGAARD, H., KROGFELT, K. A. & SØRENSEN, S. J. 2019. Amplicon sequencing provides more accurate microbiome information in healthy children compared to culturing. *Communications Biology,* 2**,** 291.

GUZMÁN-SOTO, I., MCTIERNAN, C., GONZALEZ-GOMEZ, M., ROSS, A., GUPTA, K., SUURONEN, E. J., MAH, T.-F., GRIFFITH, M. & ALARCON, E. I. 2021. Mimicking biofilm formation and development: Recent progress in *in-vitro* and *in-vivo* biofilm models. *iScience,* 24**,** 102443.

GUZZO, G. L., ANDREWS, J. M. & WEYRICH, L. S. 2022. The Neglected Gut Microbiome: Fungi, Protozoa, and Bacteriophages in Inflammatory Bowel Disease. *Inflamm Bowel Dis,* 28**,** 1112-1122.

HAFFAJEE, A. D., SOCRANSKY, S. S., PATEL, M. R. & SONG, X. 2008. Microbial complexes in supragingival plaque. *Oral Microbiol Immunol,* 23**,** 196-205.

HAJISHENGALLIS, G., DARVEAU, R. P. & CURTIS, M. A. 2012. The keystone-pathogen hypothesis. *Nat Rev Microbiol,* 10**,** 717-25.

HAMADA, S., KOGA, T. & OOSHIMA, T. 1984. Virulence Factors of *Streptococcus mutans* and Dental Caries Prevention. *Journal of Dental Research,* 63**,** 407-411.

HAN, A. & LEE, S. Y. 2023. An overview of various methods for *in-vitro* biofilm formation: a review. *Food Sci Biotechnol,* 32**,** 1617-1629.

HARRISON, X. A., MCDEVITT, A. D., DUNN, J. C., GRIFFITHS, S. M., BENVENUTO, C., BIRTLES, R., BOUBLI, J. P., BOWN, K., BRIDSON, C., BROOKS, D. R., BROWETT, S. S., CARDEN, R. F., CHANTREY, J., CLEVER, F., COSCIA, I., EDWARDS, K. L., FERRY, N., GOODHEAD, I., HIGHLANDS, A., HOPPER, J., JACKSON, J., JEHLE, R., DA CRUZ KAIZER, M., KING, T., LEA, J. M. D., LENKA, J. L., MCCUBBIN, A., MCKENZIE, J., DE MORAES, B. L. C., O'MEARA, D. B., PESCOD, P., PREZIOSI, R. F., ROWNTREE, J. K., SHULTZ, S., SILK, M. J., STOCKDALE, J. E., SYMONDSON, W. O. C., DE LA PENA, M. V., WALKER, S. L., WOOD, M. D. & ANTWIS, R. E. 2021. Fungal microbiomes are determined by host phylogeny and exhibit widespread associations with the bacterial microbiome. *Proc Biol Sci,* 288**,** 20210552.

HASIN, Y., SELDIN, M. & LUSIS, A. 2017. Multi-omics approaches to disease. *Genome Biology,* 18**,** 83.

HAVSED, K., STENSSON, M., JANSSON, H., CARDA-DIÉGUEZ, M., PEDERSEN, A., NEILANDS, J., SVENSÄTER, G. & MIRA, A. 2021. Bacterial Composition

and Metabolomics of Dental Plaque From Adolescents. *Front Cell Infect Microbiol,* 11**,** 716493.

HAWSER, S. 1996. Adhesion of different Candida spp. to plastic: XTT formazan determinations. *J Med Vet Mycol,* 34**,** 407-10.

HAWSER, S. P. & DOUGLAS, L. J. 1994. Biofilm formation by Candida species on the surface of catheter materials *in-vitro*. *Infect Immun,* 62**,** 915-21.

HE, J., KIM, D., ZHOU, X., AHN, S. J., BURNE, R. A., RICHARDS, V. P. & KOO, H. 2017. RNA-Seq Reveals Enhanced Sugar Metabolism in *Streptococcus mutans* Co-cultured with *Candida albicans* within Mixed-Species Biofilms. *Front Microbiol,* 8**,** 1036.

HE, J., TU, Q., GE, Y., QIN, Y., CUI, B., HU, X., WANG, Y., DENG, Y., WANG, K., VAN NOSTRAND, J. D., LI, J., ZHOU, J., LI, Y. & ZHOU, X. 2018. Taxonomic and Functional Analyses of the Supragingival Microbiome from Caries-Affected and Caries-Free Hosts. *Microbial Ecology,* 75**,** 543-554.

HEDGES, A. J., SHANNON, R. & HOBBS, R. P. 1978. Comparison of the precision obtained in counting viable bacteria by the spiral plate maker, the droplette and the Miles & Misra methods. *J Appl Bacteriol,* 45**,** 57-65.

HENG, X., JIANG, Y. & CHU, W. 2021. Influence of Fluconazole Administration on Gut Microbiome, Intestinal Barrier, and Immune Response in Mice. *Antimicrob Agents Chemother,* 65.

HOFER, U. 2022. How antibiotics predispose to candidiasis. *Nature Reviews Microbiology,* 20**,** 382-382.

HOLMAN, L., HEAD, M. L., LANFEAR, R. & JENNIONS, M. D. 2015. Evidence of Experimental Bias in the Life Sciences: Why We Need Blind Data Recording. *PLoS Biol,* 13**,** e1002190.

HONG, B. Y., FURTADO ARAUJO, M. V., STRAUSBAUGH, L. D., TERZI, E., IOANNIDOU, E. & DIAZ, P. I. 2015. Microbiome profiles in periodontitis in relation to host and disease characteristics. *PLoS One,* 10**,** e0127077.

HOSIDA, T. Y., CAVAZANA, T. P., HENRIQUES, M., PESSAN, J. P., DELBEM, A. C. B. & MONTEIRO, D. R. 2018. Interactions between *Candida albicans* and *Candida glabrata* in biofilms: Influence of the strain type, culture medium and glucose supplementation. *Mycoses,* 61**,** 270-278.

HOSSAIN, T. J. 2022. Functional genomics of the lactic acid bacterium *Limosilactobacillus fermentum* LAB-1: metabolic, probiotic and biotechnological perspectives. *Heliyon,* 8**,** e11412.

HURLEY, E., BARRETT, M. P. J., KINIRONS, M., WHELTON, H., RYAN, C. A., STANTON, C., HARRIS, H. M. B. & O'TOOLE, P. W. 2019. Comparison of the salivary and dentinal microbiome of children with severe-early childhood caries to the salivary microbiome of caries-free children. *BMC Oral Health,* 19**,** 13.

JABRA-RIZK, M. A., FALKLER, W. A. & MEILLER, T. F. 2004. Fungal biofilms and drug resistance. *Emerg Infect Dis,* 10**,** 14-9.

JACKSON, S., COULTHWAITE, L., LOEWY, Z., SCALLAN, A. & VERRAN, J. 2014. Biofilm development by blastospores and hyphae of *Candida albicans* on abraded denture acrylic resin surfaces. *J Prosthet Dent,* 112**,** 988-93.

JACOB-DUBUISSON, F., MECHALY, A., BETTON, J.-M. & ANTOINE, R. 2018. Structural insights into the signalling mechanisms of two-component systems. *Nature Reviews Microbiology,* 16**,** 585-593.

JANUS, M. M., WILLEMS, H. M. & KROM, B. P. 2016. *Candida albicans* in Multispecies Oral Communities; A Keystone Commensal? *Adv Exp Med Biol,* 931**,** 13-20.

JASWAL, K., TODD, O. A. & BEHNSEN, J. 2023. Neglected gut microbiome: interactions of the non-bacterial gut microbiota with enteric pathogens. *Gut Microbes,* 15**,** 2226916.

JENKINSON, H. F. 2011. Beyond the oral microbiome. *Environ Microbiol,* 13**,** 3077-87.

JEONG, J., YUN, K., MUN, S., CHUNG, W.-H., CHOI, S.-Y., NAM, Y.-D., LIM, M. Y., HONG, C. P., PARK, C., AHN, Y. J. & HAN, K. 2021. The effect of taxonomic classification by full-length 16S rRNA sequencing with a synthetic long-read technology. *Scientific Reports,* 11**,** 1727.

JIANG, Q., LIU, J., CHEN, L., GAN, N. & YANG, D. 2018. The Oral Microbiome in the Elderly With Dental Caries and Health. *Front Cell Infect Microbiol,* 8**,** 442.

JIN, P., WANG, L., CHEN, D. & CHEN, Y. 2024. Unveiling the complexity of early childhood caries: *Candida albicans* and *Streptococcus mutans* cooperative strategies in carbohydrate metabolism and virulence. *Journal of Oral Microbiology,* 16**,** 2339161.

JOHNSON, J. S., SPAKOWICZ, D. J., HONG, B.-Y., PETERSEN, L. M., DEMKOWICZ, P., CHEN, L., LEOPOLD, S. R., HANSON, B. M., AGRESTA, H. O., GERSTEIN, M., SODERGREN, E. & WEINSTOCK, G. M. 2019. Evaluation of 16S rRNA gene sequencing for species and strain-level microbiome analysis. *Nature Communications,* 10**,** 5029.

KALAN, L. & GRICE, E. A. 2018. Fungi in the Wound Microbiome. *Adv Wound Care (New Rochelle),* 7**,** 247-255.

KALPANA, B., PRABHU, P., BHAT, A. H., SENTHILKUMAR, A., ARUN, R. P., ASOKAN, S., GUNTHE, S. S. & VERMA, R. S. 2020. Bacterial diversity and functional analysis of severe early childhood caries and recurrence in India. *Scientific Reports,* 10**,** 21248.

KARINE MARCOMINI, E. & NEGRI, M. 2023. Fungal quorum-sensing molecules and antiseptics: A promising strategy for biofilm modulation? *Drug Discovery Today,* 28**,** 103624.

KARSTENS, L., ASQUITH, M., DAVIN, S., FAIR, D., GREGORY, W. T., WOLFE ALAN, J., BRAUN, J. & MCWEENEY, S. 2019. Controlling for Contaminants in Low-Biomass 16S rRNA Gene Sequencing Experiments. *mSystems,* 4**,** 10.1128/msystems.00290-19.

KASIMOGLU, Y., KORUYUCU, M., BIRANT, S., KARACAN, I., TOPCUOGLU, N., TUNA, E. B., GENCAY, K. & SEYMEN, F. 2020. Oral microbiota and dental caries data from monozygotic and dizygotic twin children. *Scientific Data,* 7**,** 348.

KHU, S.-T., CHANGCHUN, X. & WANG, T. 2023. Effects of flow velocity on biofilm composition and microbial molecular ecological network in reclaimed water distribution systems. *Chemosphere,* 341**,** 140010.

KILIAN, M., CHAPPLE, I. L. C., HANNIG, M., MARSH, P. D., MEURIC, V., PEDERSEN, A. M. L., TONETTI, M. S., WADE, W. G. & ZAURA, E. 2016. The oral microbiome – an update for oral healthcare professionals. *British Dental Journal,* 221**,** 657-666.

KIM, B. R., SHIN, J., GUEVARRA, R., LEE, J. H., KIM, D. W., SEOL, K. H., LEE, J. H., KIM, H. B. & ISAACSON, R. 2017a. Deciphering Diversity Indices for a Better Understanding of Microbial Communities. *J Microbiol Biotechnol,* 27**,** 2089-2093.

KIM, B. S., HAN, D. H., LEE, H. & OH, B. 2018a. Association of Salivary Microbiota with Dental Caries Incidence with Dentine Involvement after 4 Years. *J Microbiol Biotechnol,* 28**,** 454-464.

KIM, D., LIU, Y., BENHAMOU, R. I., SANCHEZ, H., SIMON-SORO, A., LI, Y., HWANG, G., FRIDMAN, M., ANDES, D. R. & KOO, H. 2018b. Bacterial-derived exopolysaccharides enhance antifungal drug tolerance in a cross-kingdom oral biofilm. *ISME J,* 12**,** 1427-1442.

KIM, D., SENGUPTA, A., NIEPA, T. H. R., LEE, B.-H., WELJIE, A., FREITAS-BLANCO, V. S., MURATA, R. M., STEBE, K. J., LEE, D. & KOO, H. 2017b. *Candida albicans* stimulates *Streptococcus mutans* microcolony development via cross-kingdom biofilm-derived metabolites. *Scientific Reports,* 7**,** 41332.

KIM, J., PARK, H. D. & CHUNG, S. 2012. Microfluidic approaches to bacterial biofilm formation. *Molecules,* 17**,** 9818-34.

KIRST, M. E., LI, E. C., ALFANT, B., CHI, Y. Y., WALKER, C., MAGNUSSON, I. & WANG, G. P. 2015. Dysbiosis and alterations in predicted functions of the subgingival microbiome in chronic periodontitis. *Appl Environ Microbiol,* 81**,** 783-93.

KOHLENBERG, A., MONNET, D. L. & PLACHOURAS, D. 2022. Increasing number of cases and outbreaks caused by *Candida auris* in the EU/EEA, 2020 to 2021. *Euro Surveill,* 27.

KOLJALG, U., NILSSON, R. H., ABARENKOV, K., TEDERSOO, L., TAYLOR, A. F., BAHRAM, M., BATES, S. T., BRUNS, T. D., BENGTSSON-PALME, J.,

CALLAGHAN, T. M., DOUGLAS, B., DRENKHAN, T., EBERHARDT, U., DUENAS, M., GREBENC, T., GRIFFITH, G. W., HARTMANN, M., KIRK, P. M., KOHOUT, P., LARSSON, E., LINDAHL, B. D., LUCKING, R., MARTIN, M. P., MATHENY, P. B., NGUYEN, N. H., NISKANEN, T., OJA, J., PEAY, K. G., PEINTNER, U., PETERSON, M., POLDMAA, K., SAAG, L., SAAR, I., SCHUSSLER, A., SCOTT, J. A., SENES, C., SMITH, M. E., SUIJA, A., TAYLOR, D. L., TELLERIA, M. T., WEISS, M. & LARSSON, K. H. 2013. Towards a unified paradigm for sequence-based identification of fungi. *Mol Ecol,* 22**,** 5271-7.

KOMMEREIN, N., STUMPP, S. N., MUSKEN, M., EHLERT, N., WINKEL, A., HAUSSLER, S., BEHRENS, P., BUETTNER, F. F. & STIESCH, M. 2017. An oral multispecies biofilm model for high content screening applications. *PLoS One,* 12**,** e0173973.

KONG, H. H. & SEGRE, J. A. 2020. Cultivating fungal research. *Science,* 368**,** 365-366.

KOPYLOVA, E., NOÉ, L. & TOUZET, H. 2012. SortMeRNA: fast and accurate filtering of ribosomal RNAs in metatranscriptomic data. *Bioinformatics,* 28**,** 3211-3217.

KRANEVELD, E. A., BUIJS, M. J., BONDER, M. J., VISSER, M., KEIJSER, B. J. F., CRIELAARD, W. & ZAURA, E. 2012. The relation between oral Candida load and bacterial microbiome profiles in Dutch older adults. *PloS one,* 7**,** e42770-e42770.

KRETH, J., MERRITT, J. & QI, F. 2009. Bacterial and host interactions of oral streptococci. *DNA Cell Biol,* 28**,** 397-403.

KUIPERS, A., STAPELS, D. A. C., WEERWIND, L. T., KO, Y. P., RUYKEN, M., LEE, J. C., VAN KESSEL, K. P. M. & ROOIJAKKERS, S. H. M. 2016. The S*taphylococcus aureus* polysaccharide capsule and Efb-dependent fibrinogen shield act in concert to protect against phagocytosis. *Microbiology (Reading),* 162**,** 1185-1194.

KURZ, D. L., SECCHI, E., CARRILLO, F. J., BOURG, I. C., STOCKER, R. & JIMENEZ-MARTINEZ, J. 2022. Competition between growth and shear stress drives intermittency in preferential flow paths in porous medium biofilms. *Proceedings of the National Academy of Sciences,* 119**,** e2122202119.

LAGREE, K., DESAI, J. V., FINKEL, J. S. & LANNI, F. 2018. Microscopy of fungal biofilms. *Curr Opin Microbiol,* 43**,** 100-107.

LAMONT, R. J., KOO, H. & HAJISHENGALLIS, G. 2018. The oral microbiota: dynamic communities and host interactions. *Nature reviews. Microbiology,* 16**,** 745-759.

LANGILLE, M. G. I., RAVEL, J. & FRICKE, W. F. 2018. “Available upon request”: not good enough for microbiome data! *Microbiome,* 6**,** 8.

LANGILLE, M. G. I., ZANEVELD, J., CAPORASO, J. G., MCDONALD, D., KNIGHTS, D., REYES, J. A., CLEMENTE, J. C., BURKEPILE, D. E., VEGA THURBER, R. L., KNIGHT, R., BEIKO, R. G. & HUTTENHOWER, C. 2013. Predictive

functional profiling of microbial communities using 16S rRNA marker gene sequences. *Nature Biotechnology,* 31**,** 814-821.

LANNI, F., LAGREE, K., HUANG, M. Y., YAN, L., WOOLFORD, C. A. & MITCHELL, A. P. 2020. Clarifying and Imaging *Candida albicans* Biofilms. *J Vis Exp*.

LAO, H. Y., WONG, L. L., HUI, Y., NG, T. T., CHAN, C. T., LO, H. W., YAU, M. C., LEUNG, E. C., WONG, R. C., HO, A. Y., YIP, K. T., LAM, J. Y., CHOW, V. C., LUK, K. S., QUE, T. L., CHOW, F. W. N. & SIU, G. K. 2023. The clinical utility of Nanopore 16S rRNA gene sequencing for direct bacterial identification in normally sterile body fluids. *Front Microbiol,* 14**,** 1324494.

LEMBERG, C., MARTINEZ DE SAN VICENTE, K., FRÓIS-MARTINS, R., ALTMEIER, S., TRAN, V. D. T., MERTENS, S., AMORIM-VAZ, S., RAI, L. S., D'ENFERT, C., PAGNI, M., SANGLARD, D. & LEIBUNDGUT-LANDMANN, S. 2022. *Candida albicans* commensalism in the oral mucosa is favoured by limited virulence and metabolic adaptation. *PLoS Pathog,* 18**,** e1010012.

LEONHARD, S. E., CHONG, G. M., FOUDRAINE, D. E., BODE, L. G. M., CROUGHS, P., POPPING, S., SCHAFTENAAR, E., KLAASSEN, C. H. W. & SEVERIN, J. A. 2024. Proposal for a screening protocol for *Candida auris* colonization. *J Hosp Infect,* 146**,** 31-36.

LI, X., SHANG, L., BRANDT, B. W., BUIJS, M. J., ROFFEL, S., VAN LOVEREN, C., CRIELAARD, W., GIBBS, S. & DENG, D. M. 2021. Saliva-derived microcosm biofilms grown on different oral surfaces *in-vitro*. *npj Biofilms and Microbiomes,* 7**,** 74.

LI, X. V., LEONARDI, I., PUTZEL, G. G., SEMON, A., FIERS, W. D., KUSAKABE, T., LIN, W.-Y., GAO, I. H., DORON, I., GUTIERREZ-GUERRERO, A., DECELIE, M. B., CARRICHE, G. M., MESKO, M., YANG, C., NAGLIK, J. R., HUBE, B., SCHERL, E. J. & ILIEV, I. D. 2022. Immune regulation by fungal strain diversity in inflammatory bowel disease. *Nature,* 603**,** 672-678.

LIF HOLGERSON, P., ESBERG, A., SJÖDIN, A., WEST, C. E. & JOHANSSON, I. 2020. A longitudinal study of the development of the saliva microbiome in infants 2 days to 5 years compared to the microbiome in adolescents. *Scientific Reports,* 10**,** 9629.

LIU, J., SPENCER, N., UTTER, D. R., GROSSMAN, A., SANTOS, N. C. D., SHI, W., BAKER, J. L., HASTURK, H., HE, X. & BOR, B. 2023. Persistent enrichment of multidrug resistant Klebsiella in oral and nasal communities during long-term starvation. *bioRxiv*.

LOESCHE, W. J. 1976. Chemotherapy of dental plaque infections. *Oral Sci Rev,* 9**,** 65-107.

LOO, C. Y., CORLISS, D. A. & GANESHKUMAR, N. 2000. *Streptococcus gordonii* biofilm formation: identification of genes that code for biofilm phenotypes. *J Bacteriol,* 182**,** 1374-82.

LOOZEN, G., BOON, N., PAUWELS, M., QUIRYNEN, M. & TEUGHELS, W. 2011. Live/dead real-time polymerase chain reaction to assess new therapies against dental plaque-related pathologies. *Mol Oral Microbiol,* 26**,** 253-61.

LU, Y., LIN, Y., LI, M. & HE, J. 2023. Roles of *Streptococcus mutans-Candida albicans* interaction in early childhood caries: a literature review. *Frontiers in Cellular and Infection Microbiology,* 13.

LV, X., WANG, L., ZHANG, J., ZENG, H., CHEN, X., SHI, L., CUI, H., HE, X. & ZHAO, L. 2020. Rapid and sensitive detection of VBNC *Escherichia coli* O157: H7 in beef by PMAxx and real-time LAMP. *Food Control,* 115**,** 107292.

MAH, T.-F. C. & O'TOOLE, G. A. 2001. Mechanisms of biofilm resistance to antimicrobial agents. *Trends in Microbiology,* 9**,** 34-39.

MALONE, M., GOERES, D. M., GOSBELL, I., VICKERY, K., JENSEN, S. & STOODLEY, P. 2017. Approaches to biofilm-associated infections: the need for standardized and relevant biofilm methods for clinical applications. *Expert Rev Anti Infect Ther,* 15**,** 147-156.

MANOS, J. 2022. The human microbiome in disease and pathology. *APMIS,* 130**,** 690-705.

MARK WELCH, J. L., ROSSETTI, B. J., RIEKEN, C. W., DEWHIRST, F. E. & BORISY, G. G. 2016. Biogeography of a human oral microbiome at the micron scale. *Proc Natl Acad Sci U S A,* 113**,** E791-800.

MARSH, P. D. 1991. Sugar, fluoride, pH and microbial homeostasis in dental plaque. *Proc Finn Dent Soc,* 87**,** 515-25.

MARSH, P. D. 1994. Microbial ecology of dental plaque and its significance in health and disease. *Adv Dent Res,* 8**,** 263-71.

MARSH, P. D., HUNTER, J. R., BOWDEN, G. H., HAMILTON, I. R., MCKEE, A. S., HARDIE, J. M. & ELLWOOD, D. C. 1983. The influence of growth rate and nutrient limitation on the microbial composition and biochemical properties of a mixed culture of oral bacteria grown in a chemostat. *J Gen Microbiol,* 129**,** 755-70.

MARSH, P. D., MARSH, P., LEWIS, M. A. O., ROGERS, H., WILLIAMS, D. & WILSON, M. 2016. *Marsh and Martin's Oral Microbiology*, Elsevier.

MARSH, P. D., PERCIVAL, R. S. & CHALLACOMBE, S. J. 1992. The influence of denture-wearing and age on the oral microflora. *J Dent Res,* 71**,** 1374-81.

MARSH, P. D., WILLIAMSON, M. I., KEEVIL, C. W., MCDERMID, A. S. & ELLWOOD, D. C. 1982. Influence of sodium and potassium ions on acid production by washed cells of *Streptococcus mutans* ingbritt and *Streptococcus sanguis* NCTC 7865 grown in a chemostat. *Infect Immun,* 36**,** 476-83.

MARSH, P. D. & ZAURA, E. 2017. Dental biofilm: ecological interactions in health and disease. *J Clin Periodontol,* 44 Suppl 18**,** S12-S22.

MARTIN, F. E., NADKARNI, M. A., JACQUES, N. A. & HUNTER, N. 2002. Quantitative microbiological study of human carious dentine by culture and real-time PCR: association of anaerobes with histopathological changes in chronic pulpitis. *J Clin Microbiol,* 40**,** 1698-704.

MASON, K. L., ERB DOWNWARD, J. R., MASON, K. D., FALKOWSKI, N. R., EATON, K. A., KAO, J. Y., YOUNG, V. B. & HUFFNAGLE, G. B. 2012. *Candida albicans* and bacterial microbiota interactions in the cecum during recolonization following broad-spectrum antibiotic therapy. *Infect Immun,* 80**,** 3371-80.

MATSUO, Y., KOMIYA, S., YASUMIZU, Y., YASUOKA, Y., MIZUSHIMA, K., TAKAGI, T., KRYUKOV, K., FUKUDA, A., MORIMOTO, Y., NAITO, Y., OKADA, H., BONO, H., NAKAGAWA, S. & HIROTA, K. 2021. Full-length 16S rRNA gene amplicon analysis of human gut microbiota using MinION™ nanopore sequencing confers species-level resolution. *BMC Microbiology,* 21**,** 35.

MCCALL, A. & EDGERTON, M. 2017. Real-Time Approach to Flow Cell Imaging of *Candida albicans* Biofilm Development. *J Fungi (Basel),* 3.

MCCALL, A. D., PATHIRANA, R. U., PRABHAKAR, A., CULLEN, P. J. & EDGERTON, M. 2019. *Candida albicans* biofilm development is governed by cooperative attachment and adhesion maintenance proteins. *npj Biofilms and Microbiomes,* 5**,** 21.

MCDERMID, A. S., MCKEE, A. S., ELLWOOD, D. C. & MARSH, P. D. 1986. The effect of lowering the pH on the composition and metabolism of a community of nine oral bacteria grown in a chemostat. *J Gen Microbiol,* 132**,** 1205-14.

MCKEE, A. S., MCDERMID, A. S., ELLWOOD, D. C. & MARSH, P. D. 1985. The establishment of reproducible, complex communities of oral bacteria in the chemostat using defined inocula. *J Appl Bacteriol,* 59**,** 263-75.

MCMURDIE, P. J. & HOLMES, S. 2013. phyloseq: an R package for reproducible interactive analysis and graphics of microbiome census data. *PLoS One,* 8**,** e61217.

MENON, L. U., SCOFFIELD, J. A., JACKSON, J. G. & ZHANG, P. 2022. *Candida albicans* and Early Childhood Caries. *Frontiers in Dental Medicine,* 3.

MILLHOUSE, E., JOSE, A., SHERRY, L., LAPPIN, D. F., PATEL, N., MIDDLETON, A. M., PRATTEN, J., CULSHAW, S. & RAMAGE, G. 2014. Development of an *in-vitro*periodontal biofilm model for assessing antimicrobial and host modulatory effects of bioactive molecules. *BMC Oral Health,* 14**,** 80.

MINICH, J. J., HUMPHREY, G., BENITEZ, R. A. S., SANDERS, J., SWAFFORD, A., ALLEN, E. E. & KNIGHT, R. 2018. High-Throughput Miniaturized 16S rRNA Amplicon Library Preparation Reduces Costs while Preserving Microbiome Integrity. *mSystems,* 3.

MIRA, A., BUETAS, E., ROSIER, B., MAZUREL, D., VILLANUEVA-CASTELLOTE, A., LLENA, C. & FERRER, M. D. 2019. Development of an *in-vitro* system to study

oral biofilms in real time through impedance technology: validation and potential applications. *J Oral Microbiol,* 11**,** 1609838.

MIRZAYI, C., RENSON, A., FURLANELLO, C., SANSONE, S.-A., ZOHRA, F., ELSAFOURY, S., GEISTLINGER, L., KASSELMAN, L. J., ECKENRODE, K., VAN DE WIJGERT, J., LOUGHMAN, A., MARQUES, F. Z., MACINTYRE, D. A., ARUMUGAM, M., AZHAR, R., BEGHINI, F., BERGSTROM, K., BHATT, A., BISANZ, J. E., BRAUN, J., BRAVO, H. C., BUCK, G. A., BUSHMAN, F., CASERO, D., CLARKE, G., COLLADO, M. C., COTTER, P. D., CRYAN, J. F., DEMMER, R. T., DEVKOTA, S., ELINAV, E., ESCOBAR, J. S., FETTWEIS, J., FINN, R. D., FODOR, A. A., FORSLUND, S., FRANKE, A., FURLANELLO, C., GILBERT, J., GRICE, E., HAIBE-KAINS, B., HANDLEY, S., HERD, P., HOLMES, S., JACOBS, J. P., KARSTENS, L., KNIGHT, R., KNIGHTS, D., KOREN, O., KWON, D. S., LANGILLE, M., LINDSAY, B., MCGOVERN, D., MCHARDY, A. C., MCWEENEY, S., MUELLER, N. T., NEZI, L., OLM, M., PALM, N., PASOLLI, E., RAES, J., REDINBO, M. R., RÜHLEMANN, M., BALFOUR SARTOR, R., SCHLOSS, P. D., SCHRIML, L., SEGAL, E., SHARDELL, M., SHARPTON, T., SMIRNOVA, E., SOKOL, H., SONNENBURG, J. L., SRINIVASAN, S., THINGHOLM, L. B., TURNBAUGH, P. J., UPADHYAY, V., WALLS, R. L., WILMES, P., YAMADA, T., ZELLER, G., ZHANG, M., ZHAO, N., ZHAO, L., BAO, W., CULHANE, A., DEVANARAYAN, V., DOPAZO, J., FAN, X., FISCHER, M., JONES, W., KUSKO, R., MASON, C. E., MERCER, T. R., SANSONE, S.-A., SCHERER, A., SHI, L., THAKKAR, S., TONG, W., WOLFINGER, R., HUNTER, C., et al. 2021. Reporting guidelines for human microbiome research: the STORMS checklist. *Nature Medicine,* 27**,** 1885-1892.

MIZUGAI, H., ISOGAI, E., HIROSE, K. & CHIBA, I. Effect of denture wearing on occurrence of Candida species in the oral cavity.

MONTELONGO-JAUREGUI, D., SRINIVASAN, A., RAMASUBRAMANIAN, A. K. & LOPEZ-RIBOT, J. L. 2016. An *In-vitro* Model for Oral Mixed Biofilms of *Candida albicans* and *Streptococcus gordonii* in Synthetic Saliva. *Front Microbiol,* 7**,** 686.

MORALES, D. K. & HOGAN, D. A. 2010. *Candida albicans* interactions with bacteria in the context of human health and disease. *PLoS Pathog,* 6**,** e1000886.

MOYE, Z. D., ZENG, L. & BURNE, R. A. 2014. Fueling the caries process: carbohydrate metabolism and gene regulation by *Streptococcus mutans*. *Journal of oral microbiology,* 6**,** 10.3402/jom.v6.24878.

MUKAI, Y., TORII, M., URUSHIBARA, Y., KAWAI, T., TAKAHASHI, Y., MAEDA, N., OHKUBO, C. & OHSHIMA, T. 2020. Analysis of plaque microbiota and salivary proteins adhering to dental materials. *Journal of Oral Biosciences,* 62**,** 182-188.

MUKAREMERA, L., LEE, K. K., MORA-MONTES, H. M. & GOW, N. A. R. 2017. *Candida albicans* Yeast, Pseudohyphal, and Hyphal Morphogenesis Differentially Affects Immune Recognition. *Front Immunol,* 8**,** 629.

NAGLIK, J. R., MOYES, D. L., WÄCHTLER, B. & HUBE, B. 2011. *Candida albicans* interactions with epithelial cells and mucosal immunity. *Microbes and Infection,* 13**,** 963-976.

NANCE, W. C., DOWD, S. E., SAMARIAN, D., CHLUDZINSKI, J., DELLI, J., BATTISTA, J. & RICKARD, A. H. 2013. A high-throughput microfluidic dental plaque biofilm system to visualize and quantify the effect of antimicrobials. *J Antimicrob Chemother,* 68**,** 2550-60.

NAZIR, M., AL-ANSARI, A., AL-KHALIFA, K., ALHAREKY, M., GAFFAR, B. & ALMAS, K. 2020. Global prevalence of periodontal disease and lack of its surveillance. *The Scientific World Journal,* 2020.

NETT, J. & ANDES, D. 2006. *Candida albicans* biofilm development, modeling a host-pathogen interaction. *Curr Opin Microbiol,* 9**,** 340-5.

NETT, J. E. & ANDES, D. R. 2020. Contributions of the Biofilm Matrix to Candida Pathogenesis. *J Fungi (Basel),* 6.

NETT, J. E. & D, R. A. 2015. Fungal Biofilms: *In-vivo* Models for Discovery of Anti-Biofilm Drugs. *Microbiol Spectr,* 3**,** E30.

NIKAWA, H., HAMADA, T. & YAMAMOTO, T. 1998. Denture plaque — past and recent concerns. *Journal of Dentistry,* 26**,** 299-304.

NILSSON, R. H., RYBERG, M., ABARENKOV, K., SJÖKVIST, E. & KRISTIANSSON, E. 2009. The ITS region as a target for characterization of fungal communities using emerging sequencing technologies. *FEMS Microbiology Letters,* 296**,** 97-101.

NOBILE, C. J., FOX, E. P., NETT, J. E., SORRELLS, T. R., MITROVICH, Q. M., HERNDAY, A. D., TUCH, B. B., ANDES, D. R. & JOHNSON, A. D. 2012. A recently evolved transcriptional network controls biofilm development in *Candida albicans*. *Cell,* 148**,** 126-38.

NOBILE, C. J. & MITCHELL, A. P. 2006. Genetics and genomics of *Candida albicans* biofilm formation. *Cell Microbiol,* 8**,** 1382-91.

NYVAD, B. & TAKAHASHI, N. 2020. Integrated hypothesis of dental caries and periodontal diseases. *J Oral Microbiol,* 12**,** 1710953.

O'DONNELL, L. E., ALALWAN, H. K. A., KEAN, R., CALVERT, G., NILE, C. J., LAPPIN, D. F., ROBERTSON, D., WILLIAMS, C., RAMAGE, G. & SHERRY, L. 2017. *Candida albicans* biofilm heterogeneity does not influence denture stomatitis but strongly influences denture cleansing capacity. *J Med Microbiol,* 66**,** 54-60.

O'DONNELL, L. E., MILLHOUSE, E., SHERRY, L., KEAN, R., MALCOLM, J., NILE, C. J. & RAMAGE, G. 2015a. Polymicrobial Candida biofilms: friends and foe in the oral cavity. *FEMS Yeast Res,* 15.

O'DONNELL, L. E., ROBERTSON, D., NILE, C. J., CROSS, L. J., RIGGIO, M., SHERRIFF, A., BRADSHAW, D., LAMBERT, M., MALCOLM, J., BUIJS, M. J., ZAURA, E., CRIELAARD, W., BRANDT, B. W. & RAMAGE, G. 2015b. The Oral Microbiome of Denture Wearers Is Influenced by Levels of Natural Dentition. *PLoS One,* 10**,** e0137717.

O'DONNELL, L. E., SMITH, K., WILLIAMS, C., NILE, C. J., LAPPIN, D. F., BRADSHAW, D., LAMBERT, M., ROBERTSON, D. P., BAGG, J., HANNAH, V. & RAMAGE, G. 2016. Dentures are a Reservoir for Respiratory Pathogens. *Journal of Prosthodontics,* 25**,** 99-104.

O'TOOLE, G. A. 2011. Microtiter dish biofilm formation assay. *J Vis Exp*.

OHTA, A., NISHI, K., HIROTA, K. & MATSUO, Y. 2023. Using nanopore sequencing to identify fungi from clinical samples with high phylogenetic resolution. *Scientific Reports,* 13**,** 9785.

OLMS, C., YAHIAOUI-DOKTOR, M., REMMERBACH, T. W. & STINGU, C. S. 2018. Bacterial Colonization and Tissue Compatibility of Denture Base Resins. *Dentistry journal,* 6**,** 20.

ONYANGO, S. O., CLERCQ, N. D., BEERENS, K., CAMP, J. V., DESMET, T., WIELE, T. V. D. & ERCOLINI, D. 2020. Oral Microbiota Display Profound Differential Metabolic Kinetics and Community Shifts upon Incubation with Sucrose, Trehalose, Kojibiose, and Xylitol. *Applied and Environmental Microbiology,* 86**,** e01170-20.

PANARIELLO, B. H. D., KLEIN, M. I., PAVARINA, A. C. & DUARTE, S. 2017. Inactivation of genes TEC1 and EFG1 in *Candida albicans* influences extracellular matrix composition and biofilm morphology. *J Oral Microbiol,* 9**,** 1385372.

PARADIS, E. & SCHLIEP, K. 2018. ape 5.0: an environment for modern phylogenetics and evolutionary analyses in R. *Bioinformatics,* 35**,** 526-528.

PASTER, B. J., OLSEN, I., AAS, J. A. & DEWHIRST, F. E. 2006. The breadth of bacterial diversity in the human periodontal pocket and other oral sites. *Periodontol 2000,* 42**,** 80-7.

PATEL, M. 2022. Oral Cavity and *Candida albicans*: Colonisation to the Development of Infection. *Pathogens,* 11.

PELEG, A. Y., HOGAN, D. A. & MYLONAKIS, E. 2010. Medically important bacterial–fungal interactions. *Nature Reviews Microbiology,* 8**,** 340-349.

PENESYAN, A., PAULSEN, I. T., KJELLEBERG, S. & GILLINGS, M. R. 2021. Three faces of biofilms: a microbial lifestyle, a nascent multicellular organism, and an incubator for diversity. *npj Biofilms and Microbiomes,* 7**,** 80.

PENG, X., CHENG, L., YOU, Y., TANG, C., REN, B., LI, Y., XU, X. & ZHOU, X. 2022. Oral microbiota in human systematic diseases. *International Journal of Oral Science,* 14**,** 14.

PEREIRA-CENCI, T., DEL BEL CURY, A. A., CRIELAARD, W. & TEN CATE, J. M. 2008. Development of Candida-associated denture stomatitis: new insights. *J Appl Oral Sci,* 16**,** 86-94.

PEREZ-CHAPARRO, P. J., GONCALVES, C., FIGUEIREDO, L. C., FAVERI, M., LOBAO, E., TAMASHIRO, N., DUARTE, P. & FERES, M. 2014. Newly identified pathogens associated with periodontitis: a systematic review. *J Dent Res,* 93**,** 846-58.

PERIASAMY, S., CHALMERS, N. I., DU-THUMM, L. & KOLENBRANDER, P. E. 2009. Fusobacterium nucleatum ATCC 10953 requires *Actinomyces naeslundii* ATCC 43146 for growth on saliva in a three-species community that includes *Streptococcus oralis* 34. *Appl Environ Microbiol,* 75**,** 3250-7.

PETERS, B. A., WU, J., HAYES, R. B. & AHN, J. 2017. The oral fungal mycobiome: characteristics and relation to periodontitis in a pilot study. *BMC Microbiology,* 17**,** 157.

PIERCE, C. G., UPPULURI, P., TRISTAN, A. R., WORMLEY, F. L., JR., MOWAT, E., RAMAGE, G. & LOPEZ-RIBOT, J. L. 2008. A simple and reproducible 96-well plate-based method for the formation of fungal biofilms and its application to antifungal susceptibility testing. *Nat Protoc,* 3**,** 1494-500.

PITTS, N. B., TWETMAN, S., FISHER, J. & MARSH, P. D. 2021. Understanding dental caries as a non-communicable disease. *British Dental Journal,* 231**,** 749-753.

POLLOCK, J., GLENDINNING, L., WISEDCHANWET, T. & WATSON, M. 2018. The Madness of Microbiome: Attempting To Find Consensus “Best Practice” for 16S Microbiome Studies. *Applied and Environmental Microbiology,* 84**,** e02627-17.

PONDE, N. O., LORTAL, L., RAMAGE, G., NAGLIK, J. R. & RICHARDSON, J. P. 2021. *Candida albicans* biofilms and polymicrobial interactions. *Critical Reviews in Microbiology,* 47**,** 91-111.

PREMARAJ, T. S., VELLA, R., CHUNG, J., LIN, Q., PANIER, H., UNDERWOOD, K., PREMARAJ, S. & ZHOU, Y. 2020. Ethnic variation of oral microbiota in children. *Scientific Reports,* 10**,** 14788.

PRICE, M. N., DEHAL, P. S. & ARKIN, A. P. 2010. FastTree 2 – Approximately Maximum-Likelihood Trees for Large Alignments. *PLOS ONE,* 5**,** e9490.

QUAN, K., HOU, J., ZHANG, Z., REN, Y., PETERSON, B. W., FLEMMING, H.-C., MAYER, C., BUSSCHER, H. J. & VAN DER MEI, H. C. 2022. Water in bacterial biofilms: pores and channels, storage and transport functions. *Critical Reviews in Microbiology,* 48**,** 283-302.

RADAIC, A. & KAPILA, Y. L. 2021. The oralome and its dysbiosis: New insights into oral microbiome-host interactions. *Computational and Structural Biotechnology Journal,* 19**,** 1335-1360.

RAJA, M., HANNAN, A. & ALI, K. 2010a. Association of oral candidal carriage with dental caries in children. *Caries Res,* 44**,** 272-6.

RAMAGE, G. 2016. Comparing apples and oranges: considerations for quantifying candidal biofilms with XTT [2,3-bis(2-methoxy-4-nitro-5-sulfo-phenyl)-2H-tetrazolium-5-carboxanilide] and the need for standardized testing. *J Med Microbiol,* 65**,** 259-260.

RAMAGE, G. & LOPEZ-RIBOT, J. L. 2005. Techniques for antifungal susceptibility testing of *Candida albicans* biofilms. *Methods Mol Med,* 118**,** 71-9.

RAMAGE, G., MARTINEZ, J. P. & LOPEZ-RIBOT, J. L. 2006. Candida biofilms on implanted biomaterials: a clinically significant problem. *FEMS Yeast Res,* 6**,** 979-86.

RAMAGE, G., O'DONNELL, L., SHERRY, L., CULSHAW, S., BAGG, J., CZESNIKIEWICZ-GUZIK, M., BROWN, C., MCKENZIE, D., CROSS, L., MACINNES, A., BRADSHAW, D., VARGHESE, R., GOMEZ PEREIRA, P., JOSE, A., SANYAL, S. & ROBERTSON, D. 2019. Impact of frequency of denture cleaning on microbial and clinical parameters - a bench to chairside approach. *J Oral Microbiol,* 11**,** 1538437.

RAMAGE, G., SAVILLE, S. P., THOMAS, D. P. & LOPEZ-RIBOT, J. L. 2005. Candida biofilms: an update. *Eukaryot Cell,* 4**,** 633-8.

RAMAGE, G., SHORT, B., MCKLOUD, E., ALSHANTA, O., BUTCHER, M., MCLEAN, W. & BROWN, J. L. 2022. Clinical Management of Fungal Biofilm Infections. *In:* RICHTER, K. & KRAGH, K. N. (eds.) *Antibiofilm Strategies. Springer Series on Biofilms.* Springer.

RAMAGE, G., TOMSETT, K., WICKES, B. L., LÛPEZ-RIBOT, J. L. & REDDING, S. W. 2004. Denture stomatitis: a role for Candida biofilms. *Oral Surgery, Oral Medicine, Oral Pathology, Oral Radiology, and Endodontology,* 98**,** 53-59.

RAMAGE, G., VANDE WALLE, K., WICKES, B. L. & LOPEZ-RIBOT, J. L. 2001a. Standardized method for *in-vitro* antifungal susceptibility testing of *Candida albicans* biofilms. *Antimicrob Agents Chemother,* 45**,** 2475-9.

RAMAGE, G., VANDEWALLE, K., BACHMANN, S. P., WICKES, B. L. & LOPEZ-RIBOT, J. L. 2002. *In-vitro* pharmacodynamic properties of three antifungal agents against preformed *Candida albicans* biofilms determined by time-kill studies. *Antimicrob Agents Chemother,* 46**,** 3634-6.

RAMAGE, G., VANDEWALLE, K., WICKES, B. L. & LÓPEZ-RIBOT, J. L. 2001b. Characteristics of biofilm formation by *Candida albicans*. *Rev Iberoam Micol,* 18**,** 163-70.

RAMAGE, G., WICKES, B. L. & LOPEZ-RIBOT, J. L. 2008. A seed and feed model for the formation of *Candida albicans* biofilms under flow conditions using an improved modified Robbins device. *Rev Iberoam Micol,* 25**,** 37-40.

RANE, H. S., HAYEK, S. R., FRYE, J. E., ABEYTA, E. L., BERNARDO, S. M., PARRA, K. J. & LEE, S. A. 2019. *Candida albicans* Pma1p Contributes to Growth, pH Homeostasis, and Hyphal Formation. *Front Microbiol,* 10**,** 1012.

RAO, X., HUANG, X., ZHOU, Z. & LIN, X. 2013. An improvement of the 2ˆ(-delta delta CT) method for quantitative real-time polymerase chain reaction data analysis. *Biostat Bioinforma Biomath,* 3**,** 71-85.

RASMUSSEN, T. B. & GIVSKOV, M. 2006. Quorum sensing inhibitors: a bargain of effects. *Microbiology,* 152**,** 895-904.

RAUTEMAA, R. & RAMAGE, G. 2011. Oral candidosis--clinical challenges of a biofilm disease. *Crit Rev Microbiol,* 37**,** 328-36.

REDFERN, J., TOSHEVA, L., MALIC, S., BUTCHER, M., RAMAGE, G. & VERRAN, J. 2022. The denture microbiome in health and disease: an exploration of a unique community. *Lett Appl Microbiol,* 75**,** 195-209.

REGUEIRA-IGLESIAS, A., BALSA-CASTRO, C., BLANCO-PINTOS, T. & TOMÁS, I. 2023. Critical review of 16S rRNA gene sequencing workflow in microbiome studies: From primer selection to advanced data analysis. *Mol Oral Microbiol,* 38**,** 347-399.

RICHARDSON, M. & LASS-FLÖRL, C. 2008. Changing epidemiology of systemic fungal infections. *Clin Microbiol Infect,* 14 Suppl 4**,** 5-24.

ROBIN, X., TURCK, N., HAINARD, A., TIBERTI, N., LISACEK, F., SANCHEZ, J. C. & MÜLLER, M. 2011. pROC: an open-source package for R and S+ to analyze and compare ROC curves. *BMC Bioinformatics,* 12**,** 77.

ROBINSON, S., PETERSON, C. B., SAHASRABHOJANE, P., AJAMI, N. J., SHELBURNE, S. A., KONTOYIANNIS, D. P. & GALLOWAY-PEÑA, J. R. 2020. Observational Cohort Study of Oral Mycobiome and Interkingdom Interactions over the Course of Induction Therapy for Leukemia. *mSphere,* 5.

ROCCO, T. R., REINERT, S. E. & SIMMS, H. H. 2000. Effects of Fluconazole Administration in Critically Ill Patients: Analysis of Bacterial and Fungal Resistance. *Archives of Surgery,* 135**,** 160-165.

RODGER, G., TAYLOR, R. L., PEARSON, G. J. & VERRAN, J. 2010. *In-vitro* colonization of an experimental silicone by *Candida albicans*. *J Biomed Mater Res B Appl Biomater,* 92**,** 226-35.

RODRIGUES, M. L. & NOSANCHUK, J. D. 2020. Fungal diseases as neglected pathogens: A wake-up call to public health officials. *PLoS Negl Trop Dis,* 14**,** e0007964.

ROMANO, S., SAVVA, G. M., BEDARF, J. R., CHARLES, I. G., HILDEBRAND, F. & NARBAD, A. 2021. Meta-analysis of the Parkinson's disease gut microbiome suggests alterations linked to intestinal inflammation. *npj Parkinson's Disease,* 7**,** 27.

ROSIER, B. T., DE JAGER, M., ZAURA, E. & KROM, B. P. 2014. Historical and contemporary hypotheses on the development of oral diseases: are we there yet? *Front Cell Infect Microbiol,* 4**,** 92.

RUMBAUGH, K. P. & BJARNSHOLT, T. 2023. Microbial Primer: *In-vivo* biofilm. *Microbiology,* 169.

SALERNO, C., PASCALE, M., CONTALDO, M., ESPOSITO, V., BUSCIOLANO, M., MILILLO, L., GUIDA, A., PETRUZZI, M. & SERPICO, R. 2011. Candida-associated denture stomatitis. *Med Oral Patol Oral Cir Bucal,* 16**,** e139-43.

SALTER, S. J., COX, M. J., TUREK, E. M., CALUS, S. T., COOKSON, W. O., MOFFATT, M. F., TURNER, P., PARKHILL, J., LOMAN, N. J. & WALKER, A. W. 2014. Reagent and laboratory contamination can critically impact sequence-based microbiome analyses. *BMC Biology,* 12**,** 87.

SAMARANAYAKE, L. P. & MACFARLANE, T. W. 1980. An *in-vitro* study of the adherence of *Candida albicans* to acrylic surfaces. *Archives of Oral Biology,* 25**,** 603-609.

SAMARIAN, D. S., JAKUBOVICS, N. S., LUO, T. L. & RICKARD, A. H. 2014. Use of a high-throughput *in-vitro* microfluidic system to develop oral multi-species biofilms. *J Vis Exp*.

SÁNCHEZ-VARGAS, L. O., ESTRADA-BARRAZA, D., POZOS-GUILLEN, A. J. & RIVAS-CACERES, R. 2013. Biofilm formation by oral clinical isolates of Candida species. *Arch Oral Biol,* 58**,** 1318-26.

SANTOSH, A. B. R., MUDDANA, K. & BAKKI, S. R. 2021. Fungal infections of oral cavity: diagnosis, management, and association with COVID-19. *SN comprehensive clinical medicine***,** 1-12.

SAUER, K., STOODLEY, P., GOERES, D. M., HALL-STOODLEY, L., BURMOLLE, M., STEWART, P. S. & BJARNSHOLT, T. 2022. The biofilm life cycle: expanding the conceptual model of biofilm formation. *Nat Rev Microbiol,* 20**,** 608-620.

SAVILLE, S. P., LAZZELL, A. L., CHATURVEDI, A. K., MONTEAGUDO, C. & LOPEZ-RIBOT, J. L. 2008. Use of a genetically engineered strain to evaluate the pathogenic potential of yeast cell and filamentous forms during *Candida albicans* systemic infection in immunodeficient mice. *Infect Immun,* 76**,** 97-102.

SCHERZ, V., GREUB, G. & BERTELLI, C. 2022. Building up a clinical microbiota profiling: a quality framework proposal. *Crit Rev Microbiol,* 48**,** 356-375.

SCHINABECK, M. K., LONG, L. A., HOSSAIN, M. A., CHANDRA, J., MUKHERJEE, P. K., MOHAMED, S. & GHANNOUM, M. A. 2004. Rabbit model of *Candida albicans* biofilm infection: liposomal amphotericin B antifungal lock therapy. *Antimicrob Agents Chemother,* 48**,** 1727-32.

SCHLAFER, S., RAARUP, M. K., MEYER, R. L., SUTHERLAND, D. S., DIGE, I., NYENGAARD, J. R. & NYVAD, B. 2011. pH landscapes in a novel five-species model of early dental biofilm. *PLoS One,* 6**,** e25299.

SCHULZ-WEIDNER, N., WEIGEL, M., TURUJLIJA, F., KOMMA, K., MENGEL, J. P., SCHLENZ, M. A., BULSKI, J. C., KRÄMER, N. & HAIN, T. 2021. Microbiome

Analysis of Carious Lesions in Pre-School Children with Early Childhood Caries and Congenital Heart Disease. *Microorganisms,* 9**,** 1904.

SCORNEAUX, B., ANGULO, D., BORROTO-ESODA, K., GHANNOUM, M., PEEL, M. & WRING, S. 2017. SCY-078 is fungicidal against Candida species in time-kill studies. *Antimicrobial agents and chemotherapy,* 61**,** e01961-16.

SEIDEL, D., WURSTER, S., JENKS, J. D., SATI, H., GANGNEUX, J. P., EGGER, M., ALASTRUEY-IZQUIERDO, A., FORD, N. P., CHOWDHARY, A., SPRUTE, R., CORNELY, O., THOMPSON, G. R., 3RD, HOENIGL, M. & KONTOYIANNIS, D. P. 2024. Impact of climate change and natural disasters on fungal infections. *Lancet Microbe,* 5**,** e594-e605.

SERRANO-FUJARTE, I., LÓPEZ-ROMERO, E., REYNA-LÓPEZ, G. E., MARTÍNEZ-GÁMEZ, M. A., VEGA-GONZÁLEZ, A. & CUÉLLAR-CRUZ, M. 2015. Influence of culture media on biofilm formation by Candida species and response of sessile cells to antifungals and oxidative stress. *Biomed Res Int,* 2015**,** 783639.

SHARMA, D., MISBA, L. & KHAN, A. U. 2019. Antibiotics versus biofilm: an emerging battleground in microbial communities. *Antimicrobial Resistance & Infection Control,* 8**,** 76.

SHARP, A., MULLER-PEBODY, B., CHARLETT, A., PATEL, B., GORTON, R., LAMBOURNE, J., CUMMINS, M., ALCOLEA-MEDINA, A., WILKS, M., SMITH, R., MACK, D., HOPKINS, S., DODGSON, A., BURNS, P., PERERA, N., LIM, F., RAO, G., KHANNA, P., JOHNSON, E., BORMAN, A., SCHELENZ, S., GUY, R., CONNEELY, J., MANUEL, R. J. & BROWN, C. S. 2021. Screening for *Candida auris* in patients admitted to eight intensive care units in England, 2017 to 2018. *Euro Surveill,* 26.

SHERRY, L., LAPPIN, G., O'DONNELL, L. E., MILLHOUSE, E., MILLINGTON, O. R., BRADSHAW, D. J., AXE, A. S., WILLIAMS, C., NILE, C. J. & RAMAGE, G. 2016. Viable Compositional Analysis of an Eleven Species Oral Polymicrobial Biofilm. *Front Microbiol,* 7**,** 912.

SHERRY, L., MILLHOUSE, E., LAPPIN, D. F., MURRAY, C., CULSHAW, S., NILE, C. J. & RAMAGE, G. 2013. Investigating the biological properties of carbohydrate derived fulvic acid (CHD-FA) as a potential novel therapy for the management of oral biofilm infections. *BMC Oral Health,* 13**,** 47.

SHERRY, L., RAJENDRAN, R., LAPPIN, D. F., BORGHI, E., PERDONI, F., FALLENI, M., TOSI, D., SMITH, K., WILLIAMS, C., JONES, B., NILE, C. J. & RAMAGE, G. 2014. Biofilms formed by *Candida albicans* bloodstream isolates display phenotypic and transcriptional heterogeneity that are associated with resistance and pathogenicity. *BMC Microbiology,* 14**,** 182.

SHI, B., WU, T., MCLEAN, J., EDLUND, A., YOUNG, Y., HE, X., LV, H., ZHOU, X., SHI, W., LI, H. & LUX, R. 2016. The Denture-Associated Oral Microbiome in Health and Stomatitis. *mSphere,* 1.

SHI, M., WEI, Y., HU, W., NIE, Y., WU, X. & LU, R. 2018a. The Subgingival Microbiome of Periodontal Pockets With Different Probing Depths in Chronic and Aggressive Periodontitis: A Pilot Study. *Front Cell Infect Microbiol,* 8**,** 124.

SHI, W., TIAN, J., XU, H., ZHOU, Q. & QIN, M. 2018b. Distinctions and associations between the microbiota of saliva and supragingival plaque of permanent and deciduous teeth. *PLoS One,* 13**,** e0200337.

SHOKRALLA, S., SPALL, J. L., GIBSON, J. F. & HAJIBABAEI, M. 2012. Next-generation sequencing technologies for environmental DNA research. *Mol Ecol,* 21**,** 1794-805.

SHREINER, A. B., KAO, J. Y. & YOUNG, V. B. 2015. The gut microbiome in health and in disease. *Curr Opin Gastroenterol,* 31**,** 69-75.

SIDDIQUI, R., BADRAN, Z., BOGHOSSIAN, A., ALHARBI, A. M., ALFAHEMI, H. & KHAN, N. A. 2023. The increasing importance of the oral microbiome in periodontal health and disease. *Future Sci OA,* 9**,** FSO856.

SILVA, D. P., EPSTEIN, H. E. & VEGA THURBER, R. L. 2022. Best practices for generating and analyzing 16S rRNA amplicon data to track coral microbiome dynamics. *Front Microbiol,* 13**,** 1007877.

SILVERMAN, J. D., WASHBURNE, A. D., MUKHERJEE, S. & DAVID, L. A. 2017. A phylogenetic transform enhances analysis of compositional microbiota data. *eLife,* 6**,** e21887.

SIMON-SORO, A., SHERRIFF, A., SADIQUE, S., RAMAGE, G., MACPHERSON, L., MIRA, A., CULSHAW, S. & MALCOLM, J. 2018. Combined analysis of the salivary microbiome and host defence peptides predicts dental disease. *Scientific Reports,* 8**,** 1484.

SING, T., SANDER, O., BEERENWINKEL, N. & LENGAUER, T. 2005. ROCR: visualizing classifier performance in R. *Bioinformatics,* 21**,** 3940-3941.

SLUTSKY, B., BUFFO, J. & SOLL, D. R. 1985. High-frequency switching of colony morphology in *Candida albicans*. *Science,* 230**,** 666-9.

SOCRANSKY, S. S., HAFFAJEE, A. D., CUGINI, M. A., SMITH, C. & KENT, R. L., JR. 1998. Microbial complexes in subgingival plaque. *J Clin Periodontol,* 25**,** 134-44.

SRIDHAR, S., SUPRABHA, B. S., SHENOY, R., SUMAN, E. & RAO, A. 2020. Association of *Streptococcus mutans*, *Candida albicans* and Oral Health Practices with Activity Status of Caries Lesions Among 5-Year-Old Children with Early Childhood Caries. *Oral Health Prev Dent,* 18**,** 911-919.

STALEY, J. T. & KONOPKA, A. 1985. Measurement of *in situ* activities of nonphotosynthetic microorganisms in aquatic and terrestrial habitats. *Annu Rev Microbiol,* 39**,** 321-46.

STANISZEWSKA, M., BONDARYK, M., SWOBODA-KOPEC, E., SIENNICKA, K., SYGITOWICZ, G. & KURZATKOWSKI, W. 2013. *Candida albicans* morphologies revealed by scanning electron microscopy analysis. *Braz J Microbiol,* 44**,** 813-21.

STRUZYCKA, I. 2014. The oral microbiome in dental caries. *Pol J Microbiol,* 63**,** 127-35.

SURESH UNNIACHAN, A., KRISHNAVILASOM JAYAKUMARI , N. & SETHURAMAN, S. 2020. Association between Candida species and periodontal disease: A systematic review. *Currenyt Medical Mycology,* 6**,** 63-68.

SZTUKOWSKA, M. N., DUTTON, L. C., DELANEY, C., RAMSDALE, M., RAMAGE, G., JENKINSON, H. F., NOBBS, A. H. & LAMONT, R. J. 2018. Community Development between Porphyromonas gingivalis and *Candida albicans* Mediated by InlJ and Als3. *mBio,* 9.

TAKAHASHI, N., WASHIO, J. & MAYANAGI, G. 2012. Metabolomic approach to oral biofilm characterization—A future direction of biofilm research. *Journal of Oral Biosciences,* 54**,** 138-143.

TALAPKO, J., JUZBAŠIĆ, M., MATIJEVIĆ, T., PUSTIJANAC, E., BEKIĆ, S., KOTRIS, I. & ŠKRLEC, I. 2021. *Candida albicans*-The Virulence Factors and Clinical Manifestations of Infection. *J Fungi (Basel),* 7.

TANNER, A. C. R., KRESSIRER, C. A., ROTHMILLER, S., JOHANSSON, I. & CHALMERS, N. I. 2018. The Caries Microbiome: Implications for Reversing Dysbiosis. *Adv Dent Res,* 29**,** 78-85.

TELLEZ, M., ZINI, A. & ESTUPIÑAN-DAY, S. 2014. Social Determinants and Oral Health: An Update. *Current Oral Health Reports,* 1**,** 148-152.

TELLIER, R., KRAJDEN, M., GRIGORIEW, G. A. & CAMPBELL, I. 1992. Innovative endpoint determination system for antifungal susceptibility testing of yeasts. *Antimicrob Agents Chemother,* 36**,** 1619-25.

TENG, F., DARVEEKARAN NAIR, S. S., ZHU, P., LI, S., HUANG, S., LI, X., XU, J. & YANG, F. 2018. Impact of DNA extraction method and targeted 16S-rRNA hypervariable region on oral microbiota profiling. *Scientific Reports,* 8**,** 16321.

TENG, F., YANG, F., HUANG, S., BO, C., XU, Z. Z., AMIR, A., KNIGHT, R., LING, J. & XU, J. 2015. Prediction of Early Childhood Caries via Spatial-Temporal Variations of Oral Microbiota. *Cell Host Microbe,* 18**,** 296-306.

THACKER, P. D. 2003. Understanding Fungi through Their Genomes. *BioScience,* 53**,** 10-15.

THEILADE, E. 1986. The non-specific theory in microbial etiology of inflammatory periodontal diseases. *J Clin Periodontol,* 13**,** 905-11.

THEILADE, E. & BUDTZ-JØRGENSEN, E. 1988. Predominant cultivable microflora of plaque on removable dentures in patients with denture-induced stomatitis. *Oral Microbiology and Immunology,* 3**,** 8-13.

THEILADE, E., BUDTZ-JØRGENSEN, E. & THEILADE, J. 1983. Predominant cultivable microflora of plaque on removable dentures in patients with healthy oral mucosa. *Arch Oral Biol,* 28**,** 675-80.

THEIN, Z. M., SAMARANAYAKE, Y. H. & SAMARANAYAKE, L. P. 2006. Effect of oral bacteria on growth and survival of *Candida albicans* biofilms. *Arch Oral Biol,* 51**,** 672-80.

THEIN, Z. M., SAMARANAYAKE, Y. H. & SAMARANAYAKE, L. P. 2007. *In-vitro* biofilm formation of *Candida albicans* and non-albicans Candida species under dynamic and anaerobic conditions. *Arch Oral Biol,* 52**,** 761-7.

THROWER, Y., PINNEY, R. J. & WILSON, M. 1997. Susceptibilities of *Actinobacillus actinomycetemcomitans* biofilms to oral antiseptics. *J Med Microbiol,* 46**,** 425-9.

THURNHEER, T., GMUR, R. & GUGGENHEIM, B. 2004. Multiplex FISH analysis of a six-species bacterial biofilm. *J Microbiol Methods,* 56**,** 37-47.

TIWARI, S., JAMAL, S. B., HASSAN, S. S., CARVALHO, P. V. S. D., ALMEIDA, S., BARH, D., GHOSH, P., SILVA, A., CASTRO, T. L. P. & AZEVEDO, V. 2017. Two-Component Signal Transduction Systems of Pathogenic Bacteria As Targets for Antimicrobial Therapy: An Overview. *Frontiers in Microbiology,* 8.

TOURLOUSSE, D. M., NARITA, K., MIURA, T., OHASHI, A., MATSUDA, M., OHYAMA, Y., SHIMAMURA, M., FURUKAWA, M., KASAHARA, K., KAMEYAMA, K., SAITO, S., GOTO, M., SHIMIZU, R., MISHIMA, R., NAKAYAMA, J., HOSOMI, K., KUNISAWA, J., TERAUCHI, J., SEKIGUCHI, Y. & KAWASAKI, H. 2022. Characterization and Demonstration of Mock Communities as Control Reagents for Accurate Human Microbiome Community Measurements. *Microbiol Spectr,* 10**,** e0191521.

TOURNU, H. & VAN DIJCK, P. 2012. Candida biofilms and the host: models and new concepts for eradication. *Int J Microbiol,* 2012**,** 845352.

TRINDADE, M. I., ABRATT, V. R. & REID, S. J. 2003. Induction of sucrose utilization genes from *Bifidobacterium lactis* by sucrose and raffinose. *Appl Environ Microbiol,* 69**,** 24-32.

TUMBARELLO, M., POSTERARO, B., TRECARICHI, E. M., FIORI, B., ROSSI, M., PORTA, R., DE GAETANO DONATI, K., LA SORDA, M., SPANU, T., FADDA, G., CAUDA, R. & SANGUINETTI, M. 2007. Biofilm production by Candida species and inadequate antifungal therapy as predictors of mortality for patients with candidemia. *J Clin Microbiol,* 45**,** 1843-50.

URUÉN, C., CHOPO-ESCUIN, G., TOMMASSEN, J., MAINAR-JAIME, R. C. & ARENAS, J. 2020. Biofilms as Promoters of Bacterial Antibiotic Resistance and Tolerance. *Antibiotics (Basel),* 10.

URZÚA, B., HERMOSILLA, G., GAMONAL, J., MORALES-BOZO, I., CANALS, M., BARAHONA, S., CÓCCOLA, C. & CIFUENTES, V. 2008. Yeast diversity in the oral microbiota of subjects with periodontitis: *Candida albicans* and *Candida dubliniensis* colonize the periodontal pockets. *Sabouraudia,* 46**,** 783-793.

VALM, A. M., MARK WELCH, J. L., RIEKEN, C. W., HASEGAWA, Y., SOGIN, M. L., OLDENBOURG, R., DEWHIRST, F. E. & BORISY, G. G. 2011. Systems-level analysis of microbial community organization through combinatorial labeling and spectral imaging. *Proc Natl Acad Sci U S A,* 108**,** 4152-7.

VALM, A. M., OLDENBOURG, R. & BORISY, G. G. 2016. Multiplexed Spectral Imaging of 120 Different Fluorescent Labels. *PLoS One,* 11**,** e0158495.

VAN CHARANTE, F., WIEME, A., RIGOLE, P., DE CANCK, E., OSTYN, L., GRASSI, L., DEFORCE, D., CRABBE, A., VANDAMME, P., JOOSSENS, M., VAN NIEUWERBURGH, F., DEPUYDT, P. & COENYE, T. 2022. Microbial diversity and antimicrobial susceptibility in endotracheal tube biofilms recovered from mechanically ventilated COVID-19 patients. *Biofilm,* 4**,** 100079.

VENTURA, T. M. D. S., CASSIANO, L. D. P. S., SOUZA E SILVA, C. M. D., TAIRA, E. A., LEITE, A. D. L., RIOS, D. & BUZALAF, M. A. R. 2017. The proteomic profile of the acquired enamel pellicle according to its location in the dental arches. *Archives of Oral Biology,* 79**,** 20-29.

VERMA, D., GARG, P. K. & DUBEY, A. K. 2018. Insights into the human oral microbiome. *Archives of microbiology,* 200**,** 525-540.

VERRAN, J. 1988. Preliminary Studies on Denture Plaque Microbiology and Acidogenicity. *Microbial Ecology in Health and Disease,* 1**,** 51-55.

VERRAN, J. 1998. Denture plaque, denture stomatitis and the adhesion of *Candida albicans* to inert materia. *In:* H J BUSSCHER & EVANS., L. V. (eds.) *Oral Biofilms and Plaque Control.* Harwood Academic Publishers.

VERRAN, J., JACKSON, S., COULTHWAITE, L., SCALLAN, A., LOEWY, Z. & WHITEHEAD, K. 2014. The effect of dentifrice abrasion on denture topography and the subsequent retention of microorganisms on abraded surfaces. *The Journal of Prosthetic Dentistry,* 112**,** 1513-1522.

VERRAN, J. & MARYAN, C. J. 1997. Retention of *Candida albicans* on acrylic resin and silicone of different surface topography. *J Prosthet Dent,* 77**,** 535-9.

VERRAN, J., SHAKESPEARE, A. P., WILLCOX, M. D. P. & KNOX, K. W. 1991. The Effect of pH on Adhesion and Hyphal Formation by Strains of *Candida albicans*. *Microbial Ecology in Health and Disease,* 4**,** 73-80.

VOS, T., FLAXMAN, A. D., NAGHAVI, M., LOZANO, R., MICHAUD, C., EZZATI, M., SHIBUYA, K., SALOMON, J. A., ABDALLA, S. & ABOYANS, V. 2012. Years lived with disability (YLDs) for 1160 sequelae of 289 diseases and injuries 1990–2010: a systematic analysis for the Global Burden of Disease Study 2010. *The lancet,* 380**,** 2163-2196.

VYAS, H. K. N., XIA, B. & MAI-PROCHNOW, A. 2022. Clinically relevant *in-vitro* biofilm models: A need to mimic and recapitulate the host environment. *Biofilm,* 4**,** 100069.

WALTER, B. & FRANK, R. M. 1985. Ultrastructural relationship of denture surfaces, plaque and oral mucosa in denture stomatitis. *Journal de biologie buccale,* 13**,** 145-166.

WANG, D., ZENG, N., LI, C., LI, Z., ZHANG, N. & LI, B. 2024. Fungal biofilm formation and its regulatory mechanism. *Heliyon,* 10**,** e32766.

WEERASEKERA, M. M., WIJESINGHE, G. K., JAYARATHNA, T. A., GUNASEKARA, C. P., FERNANDO, N., KOTTEGODA, N. & SAMARANAYAKE, L. P. 2016. Culture media profoundly affect *Candida albicans* and Candida tropicalis growth, adhesion and biofilm development. *Mem Inst Oswaldo Cruz,* 111**,** 697-702.

WHEELER, MATTHEW L., LIMON, JOSE J., BAR, AGNIESZKA S., LEAL, CHRISTIAN A., GARGUS, M., TANG, J., BROWN, J., FUNARI, VINCENT A., WANG, HANLIN L., CROTHER, TIMOTHY R., ARDITI, M., UNDERHILL, DAVID M. & ILIEV, ILIYAN D. 2016. Immunological Consequences of Intestinal Fungal Dysbiosis. *Cell Host & Microbe,* 19**,** 865-873.

WIEDERHOLD, N. P., NAJVAR, L. K., OLIVO, M., MORRIS, K. N., PATTERSON, H. P., CATANO, G. & PATTERSON, T. F. 2021. Ibrexafungerp Demonstrates *In-vitro* Activity against Fluconazole-Resistant *Candida auris* and *In-vivo* Efficacy with Delayed Initiation of Therapy in an Experimental Model of Invasive Candidiasis. *Antimicrob Agents Chemother,* 65.

WILLEMS, H. M., KOS, K., JABRA-RIZK, M. A. & KROM, B. P. 2016. *Candida albicans* in oral biofilms could prevent caries. *Pathogens and Disease,* 74.

WOJCIECHOWSKA, D., SALAMON, S. & WROBLEWSKA-SENIUK, K. 2024. It's time to shed some light on the importance of fungi in neonatal intensive care units: what do we know about the neonatal mycobiome? *Front Microbiol,* 15**,** 1355418.

WRIGHT, T. L., ELLEN, R. P., LACROIX, J. M., SINNADURAI, S. & MITTELMAN, M. W. 1997. Effects of metronidazole on *Porphyromonas gingivalis* biofilms. *J Periodontal Res,* 32**,** 473-7.

WU, T., HU, E., XU, S., CHEN, M., GUO, P., DAI, Z., FENG, T., ZHOU, L., TANG, W., ZHAN, L., FU, X., LIU, S., BO, X. & YU, G. 2021a. clusterProfiler 4.0: A universal enrichment tool for interpreting omics data. *The Innovation,* 2**,** 100141.

WU, T. T., XIAO, J., SOHN, M. B., FISCELLA, K. A., GILBERT, C., GRIER, A., GILL, A. L. & GILL, S. R. 2021b. Machine Learning Approach Identified Multi-Platform Factors for Caries Prediction in Child-Mother Dyads. *Front Cell Infect Microbiol,* 11**,** 727630.

XIAO, C., RAN, S., HUANG, Z. & LIANG, J. 2016. Bacterial Diversity and Community Structure of Supragingival Plaques in Adults with Dental Health or Caries Revealed by 16S Pyrosequencing. *Front Microbiol,* 7**,** 1145.

XIAO, J., HUANG, X., ALKHERS, N., ALZAMIL, H., ALZOUBI, S., WU, T. T., CASTILLO, D. A., CAMPBELL, F., DAVIS, J., HERZOG, K., BILLINGS, R., KOPYCKA-KEDZIERAWSKI, D. T., HAJISHENGALLIS, E. & KOO, H. 2018. *Candida albicans* and Early Childhood Caries: A Systematic Review and Meta-Analysis. *Caries Res,* 52**,** 102-112.

XU, H., TIAN, J., HAO, W., ZHANG, Q., ZHOU, Q., SHI, W., QIN, M., HE, X. & CHEN, F. 2018. Oral Microbiome Shifts From Caries-Free to Caries-Affected Status in 3-Year-Old Chinese Children: A Longitudinal Study. *Front Microbiol,* 9**,** 2009.

YASUNAGA, A., YOSHIDA, A., MORIKAWA, K., MAKI, K., NAKAMURA, S., SOH, I., AWANO, S. & ANSAI, T. 2013. Monitoring the prevalence of viable and dead cariogenic bacteria in oral specimens and *in-vitro* biofilms by qPCR combined with propidium monoazide. *BMC Microbiol,* 13**,** 157.

YITZHAKI, S., RESHEF, L., GOPHNA, U., ROSENBERG, M. & STERER, N. 2018. Microbiome associated with denture malodour. *Journal of Breath Research,* 12**,** 027103.

YOUNG, T., ALSHANTA, O. A., KEAN, R., BRADSHAW, D., PRATTEN, J., WILLIAMS, C., WOODALL, C., RAMAGE, G. & BROWN, J. L. 2020. *Candida albicans* as an Essential "Keystone" Component within Polymicrobial Oral Biofilm Models? *Microorganisms,* 9.

YOUNG, V. B. 2017. The role of the microbiome in human health and disease: an introduction for clinicians. *BMJ,* 356**,** j831.

ZANDONA, F., SOINI, H. A., NOVOTNY, M. V., SANTIAGO, E., ECKERT, G. J., PREISSER, J. S., BENECHA, H. K., ARTHUR, R. A. & ZERO, D. T. 2015. A Potential Biofilm Metabolite Signature for Caries Activity - A Pilot Clinical Study. *Metabolomics (Los Angel),* 5.

ZAURA, E., BRANDT, B. W., PRODAN, A., TEIXEIRA DE MATTOS, M. J., IMANGALIYEV, S., KOOL, J., BUIJS, M. J., JAGERS, F. L., HENNEQUIN-HOENDERDOS, N. L., SLOT, D. E., NICU, E. A., LAGERWEIJ, M. D., JANUS, M. M., FERNANDEZ-GUTIERREZ, M. M., LEVIN, E., KROM, B. P., BRAND, H. S., VEERMAN, E. C., KLEEREBEZEM, M., LOOS, B. G., VAN DER WEIJDEN, G. A., CRIELAARD, W. & KEIJSER, B. J. 2017. On the ecosystemic network of saliva in healthy young adults. *ISME J,* 11**,** 1218-1231.

ZHAN, L. 2018. Rebalancing the Caries Microbiome Dysbiosis: Targeted Treatment and Sugar Alcohols. *Advances in Dental Research,* 29**,** 110-116.

ZHAN, Z., LIU, W., PAN, L., BAO, Y., YAN, Z. & HONG, L. 2022. Overabundance of *Veillonella parvula* promotes intestinal inflammation by activating macrophages via LPS-TLR4 pathway. *Cell Death Discov,* 8**,** 251.

ZHANG, F., ASCHENBRENNER, D., YOO, J. Y. & ZUO, T. 2022a. The gut mycobiome in health, disease, and clinical applications in association with the gut bacterial microbiome assembly. *Lancet Microbe,* 3**,** e969-e983.

ZHANG, J. S., CHU, C. H. & YU, O. Y. 2022b. Oral Microbiome and Dental Caries Development. *Dent J (Basel),* 10.

ZHANG, L., SUN, T., ZHU, P., SUN, Z., LI, S., LI, F., ZHANG, Y., TAN, K., LU, J., YUAN, R., CHEN, Z., GUO, D., GUO, Q., TENG, F. & YANG, F. 2020. Quantitative Analysis of Salivary Oral Bacteria Associated with Severe Early Childhood Caries and Construction of Caries Assessment Model. *Scientific Reports,* 10**,** 6365.

ZHANG, L., ZHAN, H., XU, W., YAN, S. & NG, S. C. 2021. The role of gut mycobiome in health and diseases. *Therap Adv Gastroenterol,* 14**,** 17562848211047130.

ZHENG, D., LIWINSKI, T. & ELINAV, E. 2020. Interaction between microbiota and immunity in health and disease. *Cell Research,* 30**,** 492-506.

ZHENG, X., HE, J., WANG, L., ZHOU, S., PENG, X., HUANG, S., ZHENG, L., CHENG, L., HAO, Y., LI, J., XU, J., XU, X. & ZHOU, X. 2017. Ecological Effect of Arginine on Oral Microbiota. *Scientific Reports,* 7**,** 7206.

ZHOU, Y., MILLHOUSE, E., SHAW, T., LAPPIN, D. F., RAJENDRAN, R., BAGG, J., LIN, H. & RAMAGE, G. 2018. Evaluating *Streptococcus mutans* Strain Dependent Characteristics in a Polymicrobial Biofilm Community. *Front Microbiol,* 9**,** 1498.

ZHU, C., YUAN, C., AO, S., SHI, X., CHEN, F., SUN, X. & ZHENG, S. 2018. The Predictive Potentiality of Salivary Microbiome for the Recurrence of Early Childhood Caries. *Front Cell Infect Microbiol,* 8**,** 423.

ZHU, X., LI, X., WANG, W. & NING, K. 2020. Bacterial contamination screening and interpretation for biological laboratory environments. *Medicine in Microecology,* 5**,** 100021.

ZLATARIĆ, D. K., CELEBIĆ, A. & VALENTIĆ-PERUZOVIĆ, M. 2002. The effect of removable partial dentures on periodontal health of abutment and non-abutment teeth. *J Periodontol,* 73**,** 137-44.

ZOMORODIAN, K., HAGHIGHI, N. N., RAJAEE, N., PAKSHIR, K., TARAZOOIE, B., VOJDANI, M., SEDAGHAT, F. & VOSOGHI, M. 2011. Assessment of Candida species colonization and denture-related stomatitis in complete denture wearers. *Medical Mycology,* 49**,** 208-211.